UNIVERSITY OF LIVERPOOL

# Using label free proteomics and RNA sequencing to investigate the human respiratory syncytial virus and the effects of the antiviral ribavirin

Thesis submitted in accordance with the requirements of the University of Liverpool for the degree of

Doctor in Philosophy by

**Waleed A. Aljabr**

November 2016

## AUTHOR'S DECLARATION

Apart from the help and advice acknowledged, this thesis represents the unaided work of the author

.....

Waleed Abdurhaman Suliman Aljabr

November 2016

This research was carried out in the Department of Infection Biology and Institute of Infection and Global Health, University of Liverpool

## DEDICATION

I dedicate this work to my parents who pray me constantly and inspire me. A dedication also goes to my brothers, sisters and my daughters (Leen, Almas and Yara) and my son (Luay) who were always encouraging and supportive throughout my PhD. Finally, special thanks go to my wife (Amal) for her encouragement and support during this time and for looking after my children.

# ACKNOWLEDGEMENTS

In the name of Allah, the Most Gracious, the Most Merciful. All Thanks to Allah the Creator of the universe and the mastermind of everything.

I would like to express my sincere gratitude to my supervisor Prof Julian Hiscox for the continuous support of my PhD study and research, for his motivation, enthusiasm, patience and wide knowledge. This work would not have been possible without the help and support of my principle supervisor. Very special thanks to my second supervisor Prof James Stuart for his support and encouragement.

I am also indebted to my PhD advisors, Prof Stuart Carter and Dr Jane Hodgkinson who have been invaluable on both an academic and a personal level, for which I am extremely grateful. Appreciation also goes out to Dr Olivier for his technical support and the assistance he provided at all levels during this thesis. I must acknowledge Dr Weining Wu and Dr Diane Monday for all the instances in which their assistance helped me along the way. I would like to thank Mrs Catherine Hartley and Jenna Dawson for their support in the laboratory. Special thanks for Dr Stuart Armstrong for his help on MS-proteomic analysis. I wish to thank Centre for Genomic Research, University of Liverpool for RNA sequencing. I am also grateful to all members of the staff of Department of Infection Biology and all people in IGH, Liverpool University for being helpful during this course. I would like to thank all my colleagues back home and in the UK for encouragements. Also, I wish to thanks Hiscox's group mates, Dr Simon Clegg and all members in Infection of Biology for being supportive and encouragements. Thanks to my sponsorship, Prince Mohammed Medical City, Ministry of Health, the Ministry of Education, in Saudi Arabia for financial support to complete the project. I appreciate the kindness for all members of the Saudi Arabia Cultural Bureau and Saudi Embassy for guidance.

I would like to thanks parents, brothers and sisters for their love, care and encouragement. All my successes would not have been possible without the prayers of my mother and may Allah bless her and I ask Allah for her the paradise. Last but not least, unlimited thanks go to my wife, daughters and son for all your love, encouragement and constant support throughout this PhD journey. I would never have got through it without you.

# ABSTRACT

**Using label free proteomics and RNA sequencing to investigate the human respiratory syncytial virus and the effects of the antiviral ribavirin**

Waleed A. Aljabr

Human respiratory syncytial virus (HRSV) is a known cause of severe lower respiratory tract infection (LRTI) in infants and young children worldwide. HRSV can cause illness in all ages especially those people at high risk including the immunocompromised and the elderly. Globally, HRSV infection leads to a significant healthcare and economic burden due to the lack of an approved vaccine and costly antiviral therapies that are potentially ineffective in some cases. Ribavirin is the only therapeutic licensed for the treatment of severe HRSV infection. It is a synthetic nucleoside with broad spectrum of antiviral activity encompassing both DNA and RNA viruses. The mechanism of action of ribavirin is unclear. It is thought to inhibit the replication of HRSV and lead to a reduction in viral load. How it does this is unknown and the subject of this thesis. This study focused on investigating the effect of the anti-viral ribavirin on cells in general and then infected with HRSV using both label free quantitative proteomics and transcriptomics. This allowed the investigation of the mutation frequency in HRSV and cellular protein abundance, which encompass several mechanisms by which ribavirin is postulated to work. This study was demonstrated that treatment of cells with ribavirin resulted in the increased transcription of selected cellular mRNAs including those involved in mediating anti-viral signalling. Additionally, ribavirin treatment caused a decrease in viral mRNA and proteins. In the absence of ribavirin, HRSV specific transcripts accounted for up to one third of total RNA reads from the infected cell RNA population. Ribavirin treatment resulted in a greater than 90% reduction in reads mapping to viral mRNA, while at the same time no such drastic reduction was detected for the abundance of cellular transcripts. The presented data revealed that ribavirin significantly increased the frequency of HRSV-specific RNA mutations in the viral genome, suggesting direct influence on the fidelity of the HRSV polymerase. The presented data shows transition and transversion substitutions occur during HRSV replication, and that these changes occurred in ‘hot spots’ along the HRSV genome. Examination of nucleotide substitution rates in the viral genome indicated an increase in the frequency of transition but not transversion mutations in the presence of ribavirin. In addition, the data indicated that in the continuous cell types used, and at the time points analyzed, the abundance of some HRSV mRNAs did not reflect the order in which the mRNAs were transcribed. Overall, the work describes a mechanism of action for ribavirin in the context of viral infection, that has not previously been elucidated for HRSV.

# TABLE OF CONTENTS

## LIST OF FIGURES

## LIST OF TABLES

## LIST OF ABBREVIATIONS

| | |
|---|---|
| 17-AAG | 17-N-Allylamino-17-demethoxygeldamycin |
| AMPV | Avian metapneumovirus |
| APS | Ammonium persulphate |
| ALRI | Acute lower respiratory infection |
| A549 | Adenocarcinmic human alveolar basal epithelial cells |
| bp | Base pairs |
| BRSV | Bovine respiratory syncytial virus |
| BSA | Bovine serum albumin |
| CHD | Congenital heart disease |
| Cdc2 | Cell division control protein 2 homolog |
| cDNA | Complementary DNA |
| CLD | Chronic lung disease |
| cm | Centimetre |
| CPE | Cytopathic effect |
| DAPI | 4'-6-Diamidino-2-phenylindole |
| 17-DMAG | 17-Dimethylaminoethylamino17-demethoxygeldanamycin |
| DMEM | Dulbecco's Modified Eagles Medium |
| DMSO | Dimethyl sulfoxide |
| DNA | Deoxyribonucleic acid |
| dNTP | Deoxyribonucleotide |
| DNase | Deoxyribonuclease |
| DTT | Dithiothreitol |
| EC | Effective concentration |
| ECACC | European Collection of Authenticated Cell Cultures |

| | |
|---|---|
| ECL | Enhanced chemiluminescence |
| EDTA | Ethylenediaminetetraacetic acid |
| EM | Electron microscopy |
| EtBr | Ethidium bromide |
| F | HRSV fusion protein |
| FBL | Fibrillarin protein |
| FBS | Foetal bovine serum |
| FDA | Food and Drug Administration of the USA |
| FITC | Fluorescein isothiocyanate |
| G | HRSV attachment glycoprotein |
| g | Gram |
| GAPDH | Glyceraldehyde 3-phosphate dehydrogenase |
| GTP | Guanosine triphosphate |
| hrs | Hours |
| HBEpC | Human bronchial epithelial cell |
| HCV | Hepatitis C virus |
| HEp-2 | Human epidermoid cancer cells |
| HIV | Human immunodeficiency virus |
| HRP | Horseradish peroxidise |
| HPIVs | Human parainfluenza viruses HPIVs |
| HMPV | Human metapneumovirus |
| HRSV | Human respiratory syncytial virus |
| Hsp | Heat shock protein |
| ICTV | International Committee on Taxonomy of Viruses |
| IF | Immunofluorescence |

| | |
|---|---|
| IFN | Interferon |
| IκB | NFκB inhibitor protein |
| IMPDH | Inosine monophosphate dehydrogenase |
| IPA | Ingenuity Pathways Analysis |
| IRF3 | Interferon regulatory factor 3 |
| ISG15 | Interferon stimulated gene 15 kDa protein |
| JAK | Janus kinase |
| kDa | kilo-Dalton |
| L | HRSV large polymerase protein |
| LC | Liquid chromatography |
| LC-MS | Liquid chromatography-mass spectrometry |
| LDC | Lithium dodecyl sulfate |
| LRT | Lower respiratory tract |
| LRTI | Lower respiratory tract infection |
| M | HRSV matrix protein, also molar |
| mAb | Monoclonal antibody |
| mg | Milligram |
| min | Minutes |
| ml | Millilitre |
| mM | Micro molar |
| MOI | Multiplicity of infection |
| MPC | Magnetic Particle Concentrator |
| mRNA | Messenger RNA |
| MS | Mass spectrometry |
| MTT | 3-(4,5-Dimethylthiazol-2-yl)-2,5-diphenyltetrazolium |

| | |
|---|---|
| | bromide |
| m/z | Mass to charge ratio |
| N | HRSV nucleocapsid protein |
| NA | Not available |
| ng | Nanograms |
| NK | Natural killer |
| NS | HRSV non-structural protein |
| Nm | Nanometre |
| NT | Neutralize Tagment Buffer |
| OAS3 | 2’5’ oligoadenylate synthase 3 |
| P | HRSV phosphoprotein |
| PBS | Phosphate buffered saline |
| PCR | Polymerase chain reaction |
| PEG | Polyethylene glycol |
| PBS-T | Phosphate buffered saline-0.5% tween |
| PVDF | Poly-vinylidine fluoride |
| PFU | Plaque forming unit |
| p.i. | Post infection |
| PIS | Penicillin-Streptomycin |
| qRT-PCR | Quantatitive real-time PCR |
| RBV | Ribavirin |
| RdRp | RNA-dependent RNA polymerase |
| RIN | RNA integrity number |
| RIPA | Radio immunoprecipitation assay |
| RNA | Ribonucleic acid |

| | |
|---|---|
| RNP | Ribonucleoprotein |
| RNase | Ribonuclease |
| RRM2 | Ribonucleoside-diphosphate reductase subunit M2 |
| rRNA | Ribosomal RNA |
| rpm | Rotations per minute |
| RT | Reverse transcription |
| RTP | Ribavirin 5’-triphosphate |
| SDS-PAGE | Sodium dodecyl sulphate polyacrylamide gel electrophoresis |
| Sec | Second |
| SH | Small hydrophobic protein |
| SOD2 | Superoxide dismutase 2 |
| -ssRNA | Negative single-stranded RNA |
| +ssRNA | Positive single-stranded RNA |
| Stat1 | Signal transducer and activator of transcription 1-alpha/ beta |
| TBST | Tris-buffered saline-0.1% tween |
| TEMED | Tetramethylethylenediamine |
| $TCID_{50}$ | Tissue culture infectious dose 50% |
| TFA | Trifluoroacetic acid |
| TLR | Toll-like receptor |
| TNF | Tumour necrosis factor |
| TRIM25 | Tripartite motif-containing protein 25 |
| URTI | Upper respiratory tract infection |
| V | Voltage |

| | |
|---|---|
| VDAC | Voltage-dependent anion channel |
| v/v | Volume to volume |
| WHO | World Health Organisation |
| w/v | Weight to volume |
| x *g* | Times *g* (gravity) |
| ˚C | Degrees Celsius |
| µl | Microlitres |
| µM | Micro molar |
| µg | Micrograms |
| UTP14A | U3 small nucleolar RNA-associated protein 14 homog A |

# CHAPTER 1: INTRODUCTION

## 1.1. CLASSIFICATION, DISCOVERY AND EPIDEMIOLOGY

### 1.1.1 CLASSIFICATION

Human respiratory syncytial virus (HRSV) is a negative strand RNA virus belong to the genus *Pneumovirus,* of the subfamily *Pneumovirinae,* of the family *Paramyxoviridae,* of the order *Mononegavirales* according to the International Committee on Taxonomy of Viruses (ICTV) (Table 1.1). *Paramyxoviridae* has two subfamilies: *Paramyxovirinae*, which includes several important human pathogens, e.g. human parainfluenza viruses (HPIVs), mumps, and measles; and the subfamily of *Pneumovirinae* has two genera: *Pneumovirus* which includes HRSV, bovine respiratory syncytial virus (BRSV); and the *Metapneumovirus* genus which includes human metapneumovirus (HMPV) and avian *metapneumovirus* (AMPV). Moreover, The *Mononegavirales* are classified under group V according to Baltimore classification system based on the method of viral mRNA synthesis. This class are all single-stranded negative sense RNA viruses (Baltimore, 1971).

The properties of the *Paramyxoviridae* family are enveloped non-segmented negative-stranded RNA (-ssRNA) viruses and are defined as having a protein (F) that causes viral cell membrane fusion. Members of the *Paramyxoviridae* causes disease in humans and animals; e.g. measles virus (which is one of the most infectious viruses), parainfluenza viruses (PIVs), mumps virus, respiratory syncytial virus (RSV) (are the most prevalent viruses). The *Paramyxoviridae* included Hendra and Nipah viruses, which causes deadly

diseases (Collins, 2013). Moreover, other unique features of the *Paramyxoviridae* family is that all viruses are transmitted through the respiratory route and that virus replication occurs in the cytoplasm (Enders, 1996).

**Table 1.1**. Classification of HRSV from the virus Taxonomy of the International Committee on Taxonomy of Viruses (ICTV) released in 2012.

http://ictvonline.org/virusTaxonomy.asp?version=2012

| Order | Family | Subfamily | Genus | Type Species |
|---|---|---|---|---|
| *Mononegavirales* | *Bornaviridae* | | *Bornavirus* | Borna disease virus |
| | *Filoviridae* | | *Ebolavirus* | Zaire Ebolavirus |
| | | | *Marburgvirus* | Marburg marburgvirus |
| | *Paramyxoviridae* | *Paramyxovirinae* | *Aquaparamyxovirus* | Atlantic salmon paramyxovirus |
| | | | *Avulavirus* | Newcastle disease virus |
| | | | *Ferlavirus* | Fer-de-Lance paramyxovirus |
| | | | *Henipavirus* | Hendra virus |
| | | | *Morbillivirus* | Measles virus |
| | | | *Respirovirus* | Sendai virus |
| | | | *Rubulavirus* | Mumps virus |
| | | *Pneumovirinae* | *Metapneumovirus* | Avian Metapneumovirus |
| | | | *Pneumovirus* | **Human respiratory syncytial virus** |

| | | | | |
|---|---|---|---|---|
| | *Rhabdoviridae* | | *Cytorhabdovirus* | Lettuce necrotic yellow virus |
| | | | *Ephemerovirus* | Bovine ephemeral fever virus |
| | | | *Lyssavirus* | Rabies virus |
| | | | *Novrirhabdovirus* | Infectious hematopoietic necrosis virus |
| | | | *Nucleorhabdovirus* | Potato yellow dwarf virus |
| | | | *Perhabdovirus* | Perch rhabdovirus |
| | | | *Sigmavirus* | *Drosophila melanogaster sigmavirus* |
| | | | *Tibrovirus* | Tibrogargan virus |
| | | | *Vesiculovirus* | Vesicular stomatitis Indiana virus |

### 1.1.2. DISCOVERY AND EPIDEMIOLOGY

HRSV was first isolated from chimpanzees in 1956 and a year later was recovered from infants who had severe lower respiratory tract disease (Blount Jr *et al.*, 1956). Most children are infected with HRSV by the age two years and re-infection occurs throughout life. HRSV can cause acute upper respiratory tract infection in people of all ages; but can also cause severe lower respiratory tract infection (such as acute bronchiolitis and pneumonia)

in young children (Borchers *et al.*, 2013). Generally, mortality from HRSV is very low in developed countries, whereas, in developing countries it can be quite high. The highest case fatality rate is found among those who have chronic lung disease, immune deficiency or congenital heart disease and elderly patients (Navas *et al.*, 1992; Stensballe *et al.*, 2003).

HRSV has a single serotype with two major antigenic subgroups; A and B and although both subtypes usually co-circulate, one of the subtypes predominates (Gilca *et al.*, 2006; Imaz *et al.*, 2000). In temperate countries, HRSV infections demonstrates a distinct seasonality with onset in late autumn or early winter and a peak between mid-December and early February, before a fall in cases around late spring. The seasons of HRSV epidemics are difficult to predict because they typically depend on geographic location and the climate (Borchers *et al.*, 2013).

According to the World Health Organization, HRSV infects approximately 60 million people and causes an estimated 160,000 deaths every year (MacLellan *et al.*, 2007). Also, from a recent study, it has been estimated that HRSV caused about 34 million cases of acute lower respiratory tract infection (ALRI) in children younger than 5 years old in 2005 and 10% of those cases requiring hospitalization (Nair *et al.*, 2010).

## 1.2. HRSV STRUCTURE, GENOME ORGANISATION AND GENOMIC RNA

### 1.2.1 HRSV STRUCTURE

The HRSV ribonucleocapsid is found inside the virion, surrounded by a lipid bilayer derived from the host cell plasma membrane through virus budding (Figure 1.1) and comprises of virally encoded transmembrane surface glycoproteins (Collins, 2013). The viral genome of HRSV has 10 genes and encodes 11 different proteins. The genomic RNA of HRSV has five structural proteins which consist of the viral nucleoprotein (N), phosphoprotein (P), the large polymerase protein (L), matrix (M), and M2-1 and two non-structural proteins (NS1 and NS2). The characteristic spikes of HRSV virions are formed by the glycoprotein (G), the fusion protein (F) and the small hydrophobic (SH) protein. Syncytia formed during viral infection, are necessary for cell-to-cell viral transmission and are the hallmark of the HRSV cytopathic effect (McNamara & Smyth, 2002).

The structure of the virions of HRSV are heterogeneous, both in shape and size, which can be observed using electron microscopy (EM) (Figure 1.2). Two types of viral particles can be identified: virus filaments that are membrane-bound progeny viruses up to 10 $\mu$m in length and round- or kidney shaped viruses which are around 150 to 250 nm thick (Bachi & Howe, 1973). Using sucrose gradient centrifugation, these two particles can be separated (Gower *et al.*, 2005).

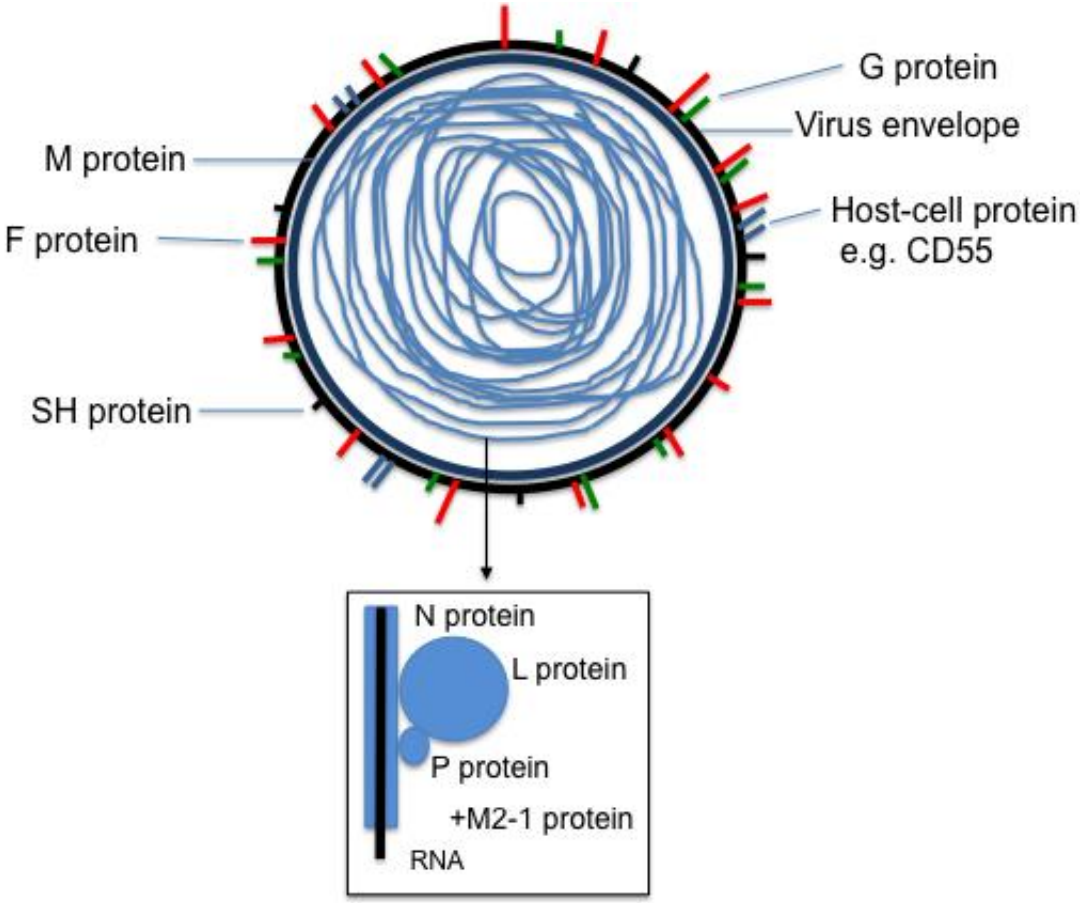


***Figure 1.1*** *Schematic diagram of HRSV virion structure. The inset shows viral genomic RNA that composes the nucleocapsid with the ribonucleoprotein (RNP)s complex, including N, P, L and M2-1 proteins. The nucleocapsid is encapsuled into the viral envelope structure; external which is made of the glycosylated G, F and SH protein and internal non-glycosylated M protein.*

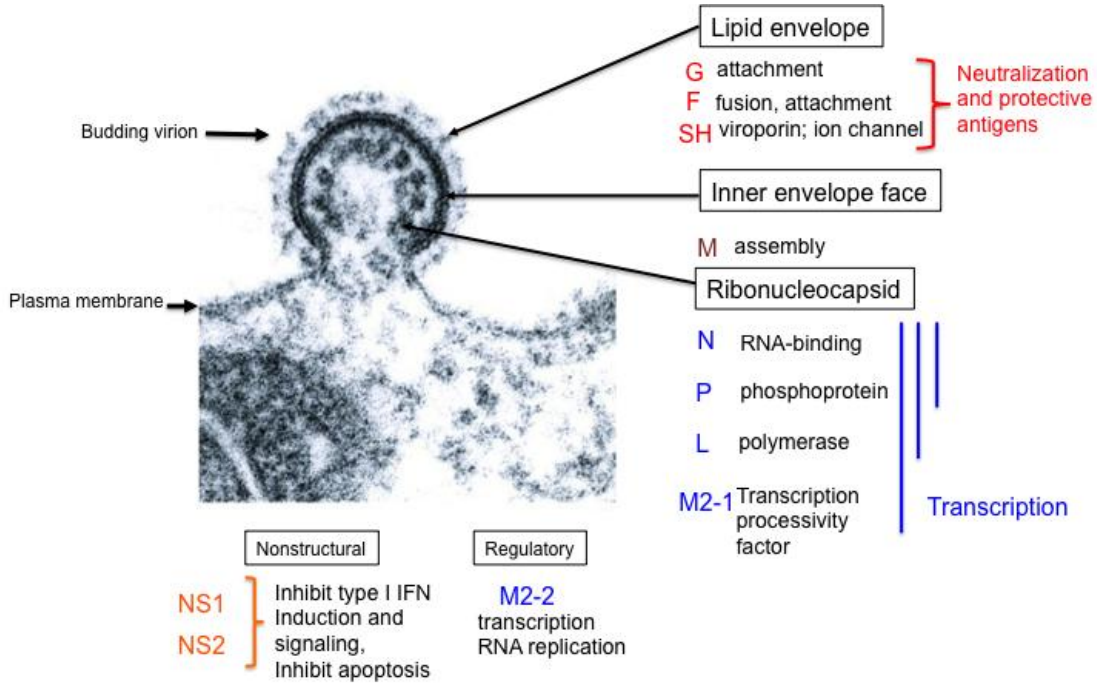


***Figure 1.2*** *Electron micrograph showing an RSV budding virion through the plasma membrane of an infected cell, RNA genome and encoded proteins. The viral protein functions in the virion and their locations are indicated. This electron micrograph image was adapted from Garofalo et al., 2013.*

### 1.2.2. *PARAMYXOVIRIDAE* GENOMIC ORGANISATION

Both sub-families *Paramyxoviridae* and *Pneumovirinae* in the family *Paramyxoviridae* encode N, P, M, F and L genes (Figure 1.3), however, they have limited sequence relatedness (Collins, 2013). Members of *Pneumovirinae* subfamily express a G protein, which has an attachment function, to facilitate cell entry, whereas members of *Paramyxoviridae* subfamily express the attachment proteins hemagglutinin (H) or hemagglutinin-neuraminidase (HN) for a similar function. Moreover, the M2

gene encodes M2-1 and M2-2, which is unique to the *Pneumovirinae* subfamily. The NS1 and NS2 non-structural (NS) proteins are only expressed by HRSV.

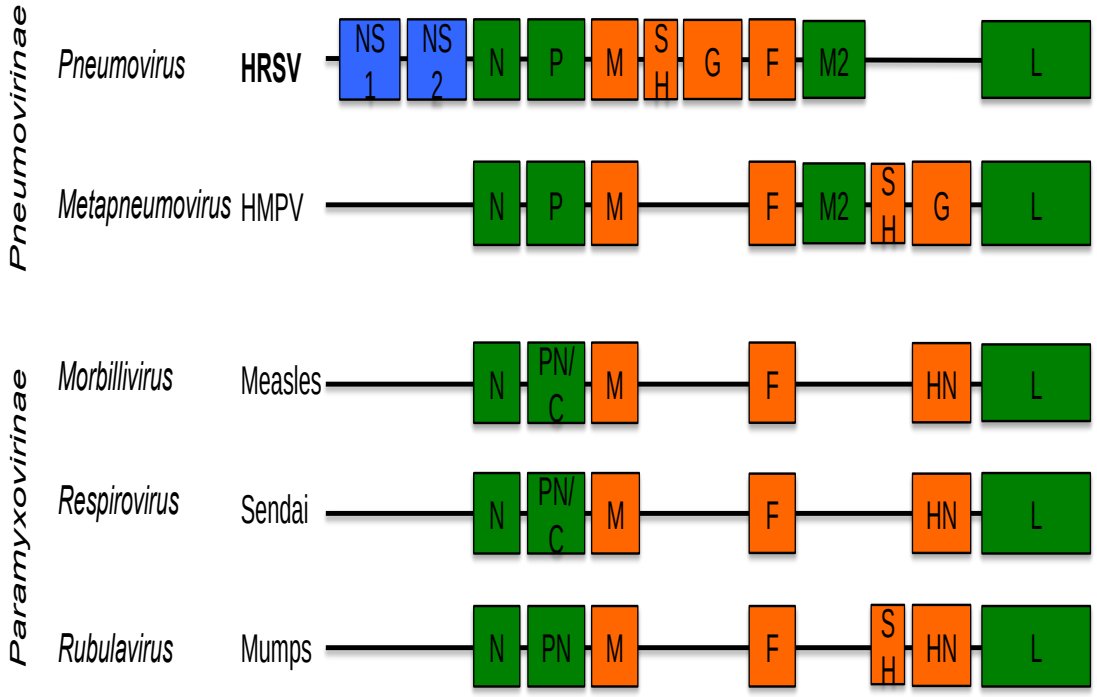


***Figure 1.3*** *A genetic map of the genomic organization of viruses in Paramyxoviridae family. The gene encodes viral proteins matching their function. Genes highlighted in green colour encode proteins that are essential for viral replication. Genes shown in orange colour encode proteins that form the viral envelops. Genes in blue colour encode proteins that are unique to HRSV.*

### 1.2.3. THE HRSV GENOME

HRSV genome is a negative-sense, single strand and non-segmented RNA of approximately 15.2 kb in length. The HRSV genome has ten non-

segmented genes that follow a linear order from 3' (leader region) to 5' (trailer region) along the genome (Collins, 2013). These genes encode eleven viral proteins (Figure 1.4). The 3' end of the genome contains the 44-nt leader (Le) promoter region which is responsible for directing initiation of mRNA transcription and anti-genome synthesis. Also, at the 3' end of the anti-genome contains a 155-nt trailer complement (TrC) promoter that directs genome RNA synthesis. To perform transcription and genome replication, the RNA dependent RNA polymerase RdRp engages with the promoter sequences that lie at the 3' ends of the genome and anti-genome RNAs (Collins *et al.*, 1991). The ten viral genes are arranged sequentially, NS1, NS2, N, P, M, SH, G, F, M2 and L, and each (except the overlapping L and M2-1 genes) is flanked by conserved gene-start (GS) and gene-end (GE) sequences, which control the polymerase during transcription. Each gene is separated from the preceding one by an intergenic region of variable length. The polymerase initiates RNA synthesis at the leader promoter and then progresses along the length of the genome. When it reaches a GE signal, the polymerase polyadenylates and releases the nascent mRNA. It then reinitiates RNA synthesis at the next GS signal. By responding to the GE and GS signals in this fashion, the polymerase is able to transcribe viral mRNAs (Barik, 1992).

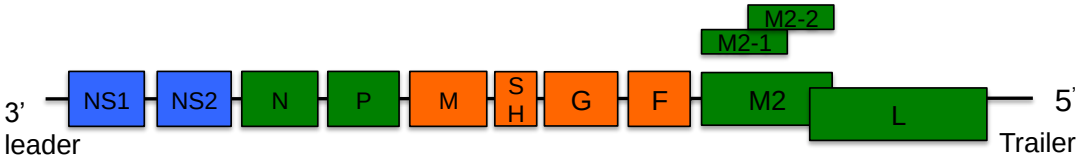


***Figure 1.4*** *Schematic of the HRSV negative-sense, single strand and non-segmented enveloped RNA virus ~15 kb. From the 3'-end, HRSV genomic RNA is transcribed into 10 mRNAs genes, however, the M2 gene encodes two proteins, M2-1 and M2-2, which have slightly overlapping open reading frames (ORFs).*

## 1.3 PROTEINS

### 1.3.1 ENVELOPE PROTEINS: G, F, SH AND M

The HRSV virion consists of a RNP that is packaged in a lipid bilayer envelope derived from the host cell plasma membrane through budding (Collins, 2013). HRSV particles are surrounded by a lipid layer where three transmembrane surface (outside the virion) glycoproteins are integrated; the attachment (G) protein that functions in binding the virus to the host cell surface (Lamb, 2013), fusion (F) protein which mediates fusion of the viral and cell membranes (Collins, 2013), and small hydrophobic (SH) protein. All of these glycoproteins form the characteristic spikes of HRSV virions. Also, the non-glycosylated matrix (M) protein is thought to form a layer on the inner surface of the envelope (Collins & Mottet, 1993).

#### 1.3.1.1 G PROTEIN

The G protein is a major attachment glycoprotein that is expressed in two different forms in the infected cells; soluble protein (Gs) that is excreted by the infected cells and trans-membrane protein (Gm) that is incorporated into virions (Hendricks *et al.*, 1987; Hendricks *et al.*, 1988). The length of this protein is 282-319 amino acids but this depends on the strain of HRSV (Johnson *et al.*, 1987). The HRSV has the ability to re-infect individuals repeatedly may be due to immunological pressure changing certain areas of the G protein (Cane *et al.*, 1991). The G protein is important for viral replication and was initially expected to play a role in viral attachment, however, it was later found that even when deleted from recombinant HRSV, there was no significant reduction in replication in HEp-2 cells or mice (Tengt & Collins, 2002). The ectodomain of the G protein comprises a CX3C motif that has sequence relatedness with the CX3C domain of the chemokine fractalkine (Tripp *et al.*, 2001). Also this ectodomain of the G protein has been shown to have activity in modulating host defence and inhibiting the host innate immune response to HRSV by inhibiting activation of the NF-kB transcription factor and secretion of inflammatory cytokines by monocytes (Polack *et al.*, 2005).

#### 1.3.1.2 F PROTEIN

The F glycoprotein mediates viral penetration by fusion between the virion envelope and the infected cell plasma membrane. This protein, through infection, passed on the cell surface can mediate fusion with neighbouring cells to make syncytia (giant cell formation) (Lamb, 2013; Techaarpornkul *et*

*al.*, 2001). The F protein is a transmembrane protein that is synthesized as an inactive precursor ($F_0$) and then cleaved by cellular proteases during maturation to yield two disulfide-linked polypeptides, F1 from the C-terminus and F2 from N-terminus, and a small p24 fragment (Collins & Mottet, 1991). The HRSV F protein can efficiently mediate fusion independent of the other viral glycoproteins, however, unlike for most members of *Paramyxovirinae,* they promote fusion require for interaction between both (G) and (F) proteins, however, *in vivo* HRSV which is lacking the G protein is highly attenuated, and results in formation of small sized of syncytia (Techaarpornkul *et al.*, 2001; Teng *et al.*, 2001). The F protein has been demonstrated to initiate an innate immune response by two cellular pattern recognition receptors, a cluster of differentiation 14 (CD14) and the Toll-like receptor (TLR) (Kurt-Jones *et al.*, 2000). The F protein can also induce caspase-dependent cell apoptosis and activation protein 53 (p53) in epithelial cells (Eckardt-Michel *et al.*, 2008).

#### 1.3.1.3 SH PROTEIN

The function of the SH protein in the HRSV infectious cycles is unknown (Carter *et al.*, 2010), which is only the viral gene that still remains without an allocated activity for viral replication in cell culture, or within the human host (Melero, 2007). However, the SH viral protein was slightly attenuated in mice and chimpanzees (Bukreyev *et al.*, 1997) and deletion of SH from a highly attenuated vaccine candidate did not increase the level of attenuation in small infants (Karron *et al.*, 2005). Earlier studies demonstrated that SH could enhance cell-to-cell fusion (Heminway *et al.*, 1994) or act as a channel-

forming viroporin (Carter *et al.*, 2010; Techaarpornkul *et al.*, 2001), however, the function as an ion channel activity in HRSV biology is uncertain.

#### 1.3.1.4 M PROTEIN

The HRSV M matrix protein is a non-glycosylated protein which accumulates at the inner surface of envelope face (Figure 1.2) and interacts with the F protein and other factors during the process of virion morphogenesis (Henderson *et al.*, 2002; Teng & Collins, 1998). It has been reported that the M protein interacts with cell membranes during the later phase of the HRSV replication cycle (Marty *et al.*, 2004). The M protein also plays a major role in coordinating the assembly, budding process and release of new HRSV virions particles by; the interacting of nucleocapsids proteins N, P and M2-1 protein and the viral envelope proteins G and P at specific sites of the cell membrane (Förster *et al.*, 2015; Liljeroos *et al.*, 2013; Melero, 2007). It was demonstrated that at an early phase of HRSV infection, the M protein is localized in the nucleus of infected cells and may have the ability to inhibit host cell transcription (Ghildyal *et al.*, 2003). Since the HRSV M protein is essential for virion morphogenesis and can bind RNA, it has been predicted that its activity may shut off RNA synthesis by the viral nucleocapsid (Rodríguez *et al.*, 2004).

### 1.3.2 NUCLEOCAPSID PROTEINS: N, P, L AND M2 PROTEINS

HRSV has four proteins N, P, L and M2-1 associated with RNP formulation which are involved in RNA synthesis (Melero, 2007). The N protein tightly

binds the genomic RNA and forms a helical nucleocapsid for viral RNA (MacLellan *et al.*, 2007; Tawar *et al.*, 2009). The P protein is the major phosphorylated HRSV protein and is a part of the polymerase complex (Collins, 2013). The L protein is the viral RdRp (Stec *et al.*, 1991). The M2-1 protein is known as a transcription factor important for viral viability and allowing the synthesis of full-length mRNAs (Collins *et al.*, 1995; Collins *et al.*, 1996; Hardy & Wertz, 1998).

The N, P and L proteins are essential for sufficient direct RNA replication (Collins *et al.*, 1996; Melero, 2007; Turner *et al.*, 2014). Moreover, the N, P and L proteins have transcription functions, however, complete transcription requires the M2-1 protein (Collins, 2007; Collins, 2013; Melero, 2007) (Figure 1.2). The N protein interact with the P protein in the nucleocapsid (Collins, 2013), the P protein also binds to the L (Khattar *et al.*, 2001) and M2-1 (Asenjo *et al.*, 2006) proteins and can mediate the interactions of these with the nuclopcapsid. Thus, the P protein has some roles in the viral genome; it is important for promoter clearance (Dupuy *et al.*, 1999) and chain elongation by the viral polymerase, and in separating the M protein from the nucleocapsid during the un-coating stage to initiate the infection (Asenjo *et al.*, 2008).

Although the HRSV M2-1 protein is necessary for sufficient viral transcription, without this protein, the viral polymerase terminates prematurely and non-specifically within several hundred nucleotides and downstream genes are

not transcribed (Collins *et al.*, 1999; Collins *et al.*, 1996; Fearns & Collins, 1999). In addition, the HRSV M2-1 has the ability to decline the termination efficiency at the gene-end signals (GE) transcription signals causing increased production of read-through mRNA's (Burke *et al.*, 1998). The M2-1 protein binds RNA and it has been indicated that the P protein deliver to the RNA template (Cartee & Wertz, 2001; Tran *et al.*, 2009). The M2-2 protein has been indicated to play a function in shifting RNA synthesis from the transcription stage to the RNA replication stage. Also, the M2-2 protein can inhibit RNA synthesis, however, the inhibition activity can happen when protein M2-2 expression is increased (Collins, 2013).

### 1.3.3 ACCESSORY PROTEINS: NS1 AND NS2

NS1 and NS2 proteins (139 and 124 amino acid, respectively) were characterized as non-structural proteins due to the difficulty to detect them in the purified HRSV virion (Huang *et al.*, 1985). Hence, they are not essential for viral growth in cell culture (Melero, 2007). HRSV NS1 and NS2 are non-structural proteins that suppress the induction of interferon IFN-$\alpha/\beta$ in HRSV infection (Ramaswamy *et al.*, 2004). This occurs by inhibiting the phosphorylation and nuclear translocation of interferon regulatory factor 3 (IRF3) (Spann *et al.*, 2005). In addition, it has been reported that there was inhibition of the interferon-induced JAK/STAT signalling pathway and targeting STAT2 for proteasome-mediated degradation (Bakre *et al.*, 2015), however, thus can be mediated primarily by both NS1 and NS2 together (Ramaswamy *et al.*, 2004). It has been suggested that both NS1 and NS2

play a vital function in inhibition of premature apoptosis and thus enhances viral replication in the HRSV infected cell (Bitko *et al.*, 2007; Wu *et al.*, 2012).

## 1. 4. INFECTIOUS CYCLE

### 1.4.1. BINDING AND ENTRY

HRSV can infect cells and replicate *in vitro* in both human and animal cells, however, it has been identified that *in vivo*, the respiratory ciliated epithelial cells of the respiratory tract are the main sites of virus replication. There are extensive ranges of epithelial cultured cells that are permissible to growth of HRSV, for example; human larynx carcinoma cell (HEp-2), human lung alveolar basal epithelial cells (A549), and African green monkey kidney epithelial cell (Vero). However, the efficient infection and viral propagation are different on these cell lines. Moreover, efficient HRSV binding (attachment) occurs through interaction between the G and F proteins and cellular glycosaminoglycans (GAGs), mainly heparin sulphate and chondroitin sulphate B (Hallak *et al.*, 2000; Techaarpornkul *et al.*, 2002). There are also some cellular surface proteins receptors which have been reported to assist binding, including, RhoA (Pastey *et al.*, 1999), annexin II (Malhotra *et al.*, 2003), intracellular adhesion molecule (ICAM)-1(Behera *et al.*, 2001), and the CX3CR1 chemokine receptor (Tripp *et al.*, 2001). However, it has been reported that the same virus might use different receptor combinations based on the cell type being infected (Melero, 2007). The HRSV replication cycle occurs in the cytoplasm and requires clathrin-mediated endocytosis at neutral pH (Kolokoltsov *et al.*, 2007) (Figure 1.5).

The viral entry route starts by fusion of the virion and the cell plasma membrane (Srinivasakumar *et al.*, 1991) and insertion of the RNP complex into the host cell (Figure 1.5 a and b). Some elements are required for HRSV replication including cytoskeletal proteins, whereas, efficient RNA synthesis requires actin that is packaged in the virion and profilin (Burke *et al.*, 1998; Burke *et al.*, 2000).

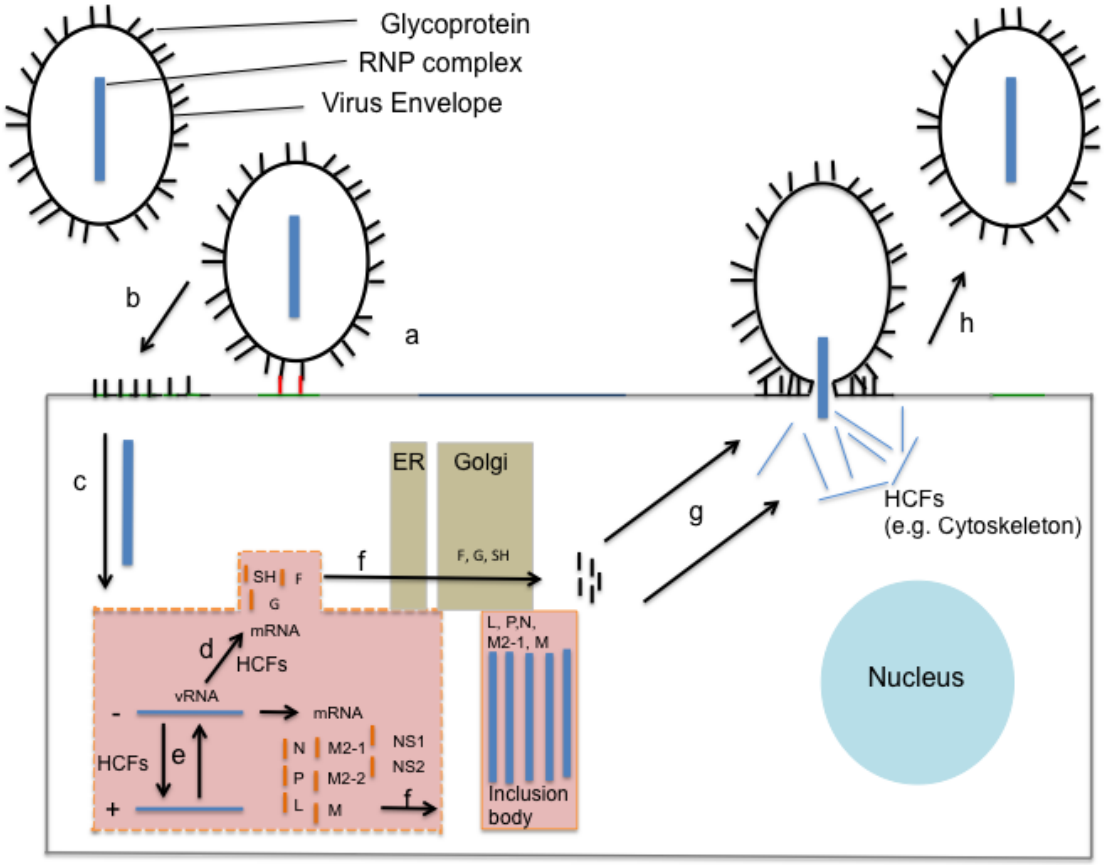


***Figure 1.5*** *Overview of the HRSV replication cycle. (a) Shows the interaction of the virus with the host cell. The virus interaction is localised in a lipid* bilayer *(green) with the host-cell receptor (red) and is mediated by the G protein (dark blue). (b) Fusion step, the lipid* bilayer *derived from the virus enveloped and the cell membrane, mixed on cell surface, the virus glycoproteins are embedded in the cell membrane. (c) The RNP complex*

*was transported in the host cell to the site of mRNA transcription and replication. (d) The vRNA transcription step, the virus polymerase generates mRNA species (orange) from each virus gene and then subsequently translated into the various virus proteins. (e)The vRNA replication step which is linked with the viral genes expression which is subsequently used as a template to produce more vRNA by the virus polymerase. (f) Accumulation of viral particles. (g) Virus assembly where new virus glycoproteins are synthesised and RNP complexes are targeted to specific sites on the cell surface membrane. (h) The virus maturation where the virus are release from the cell, to go infect another cell where the process begins again.*

### 1.4.2. TRANSCRIPTION AND REPLICATION OF THE VIRAL GENOME

HRSV mRNAs transcription and protein synthesis can be detected in the cell cytoplasm 4-6 hr post-infection (and reach a peak at approximately 15 to 20 hr post-infection) (Collins, 2013). Because the Group V viruses in the Baltimore classification system, (*Paramyxoviruses,* including HRSV) have –ssRNA genomes which are not directly readable by the host cell ribosomes, therefore, they encode their own RdRp (present in the virion) which transcribe the –ssRNA genome into a readable, monocistronic positive sense mRNAs form (Figure 1.5). HRSV transcription proceeds from the 3’ to 5’ end of the viral gene (vRNA) in a sequential stop-start manner (Dickens *et al.*, 1984). However, there are several factors that affect the relative levels of HRSV gene expression, thus genes closer to the 3’ end of genome are expressed more efficiently because the polymerase (RdRP) falls-off at the sequential transcription (intergenic) regions (Collins & Wertz, 1983; Krempl *et*

*al.*, 2002). Another factor that has effects on the relative levels of gene expression are alterations in the efficiency of transcription at the gene end (GE) signals in a specific site in the L polymerase (Harmon & Wertz, 2002; Moudy *et al.*, 2004). When the polymerase has reached a GE signal, polyadenylation of the RNA occurs, releasing the nascent mRNA and allows reinitiation of the transcription from the next GS single promoter at 3' end, capping and cap methylation. The transcription process is repeated for each gene to generate different mRNAs (Melero, 2007).

There are four proteins required for the transcription step; (1) the L polymerase protein which stimulates the polymerization stages of RNA synthesis as well as the capping and polyadenylation process of the mRNAs, (2) the N protein that forms the nucleocapsid template recognised by the polymerase, (3) the P protein known to be a co-factor of the L polymerase and (4) the M2-2 protein, an anti-termination factor that promotes completion of mRNA synthesis. Also, the M2-2 protein has been reported to be responsible for shifting RNA synthesis from transcription to RNA replication and ensuring a balance during the infection (Bermingham & Collins, 1999).

### 1.4.3 ASSEMBLY AND BUDDING

The mature HRSV virions begins to be released by 10-12 hr post-infection and reaches a peak after 24 hr and continues until the cells are destroyed by 30-48 hr post-infection (Collins, 2013). The mature viruses bud only from the apical surface in polarized epithelial cells during the infection (Lamb, 2013).

The assembly and budding of HRSV virions involves the viral components, including the viral surface (enveloped proteins) and the M protein and the RNP complexes at the cell plasma membrane. Two steps are required for assembly: first, free N protein and the P-L protein complex associates with the viral genome or template RNA to form the helical RNP structure in the cytoplasm (Collins, 2013), secondly the assembly of the RNP complex within the envelope occurs at the regions of the host cell surface enriched by caveolin-1 (CAV-1) (Brown *et al.*, 2002). Moreover, it has been reported that the M protein plays a major role in the assembly of new virions by bridging the interaction with specific sites on the cell membrane (Marty *et al.*, 2004; Teng & Collins, 1998).

## 1.5. DISEASE PATHOGENESIS AND HOST-CELL INTERACTIONS

### 1.5.2 DISEASE PATHOGENESIS

HRSV is the most common human pathogen that causes illnesses with symptoms similar to the common cold in most healthy adults and children. It causes lower respiratory tract infection (LRTI), pneumonia and bronchiolitis in infants and young children (Van Drunen Littel-Van Den Hurk & Watkiss, 2012) HRSV also can cause many diseases such as asthma (Mailaparambil *et al.*, 2009) and otitis media (middle ear infection) (Gomaa *et al.*, 2012). HRSV is the most common respiratory virus and can be isolated from patients hospitalized for bronchiolitis during the HRSV season (Hall *et al.*, 2009). The peak season of HRSV infections in temperate climates of the Northern hemisphere are the months of November to April, while HRSV

outbreaks occur regularly during the rainy season in tropical climates. In 2005, around 34 million cases of LRTI in children were caused by HRSV, the 10% required hospitalization. The mortality in the same year was 66000-199000 worldwide, of which 99% occurred in developing countries (Nair *et al.*, 2010). Humans are the only host for HRSV infection and it spreads rapidly through close contact with infected individuals or through contact with hands contaminated with nasal or conjunctival mucosa. Viral replication starts in the nasopharynx and the incubation period from infection time to symptoms onset is 4 to 5 days (Collins, 2013). Common clinical signs of HRSV include rhinorrhea, cough and low grade fever. HRSV can cause morbidity and mortality in infants, immunocompromised and elderly people, and this required a better understanding of the mechanisms of HRSV pathogenesis to allow for effective treatments (Collins & Graham, 2008).

#### 1.5.2.1 FACTORS PLAYING A ROLE IN HRSV PATHOGENESIS AND DISEASE OUTCOME

It is thought that there are many factors which drives the pathogenesis of HRSV; genetic polymorphisms, viral, environmental and host factors which contribute to severe disease especially in infants (Figure 1.6).

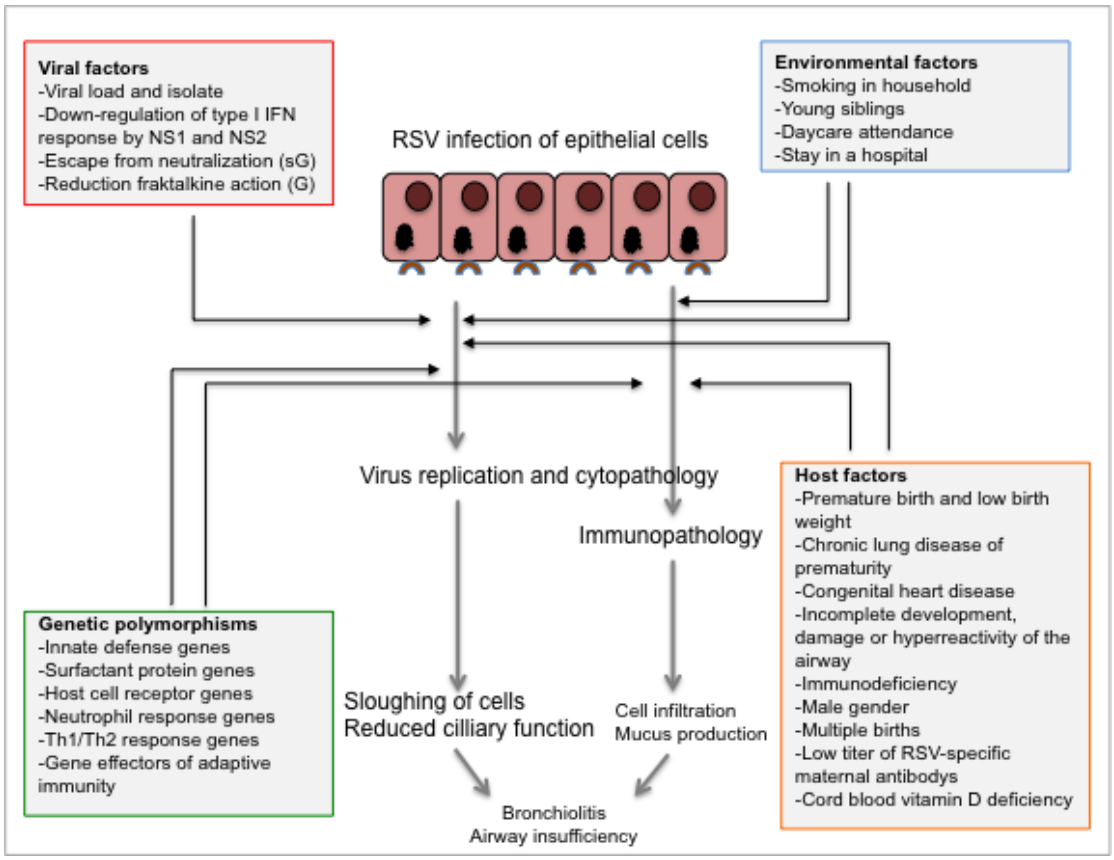


***Figure 1.6*** *Factors influencing the pathogenesis and clinical disease caused by HRSV infection in infants and young children. adapted from HRSV pathogenesis van Drunen Littel-van den Hurk and Watkiss (2012)*

#### 1.5.2.1.1 ENVIRONMENTAL AND SOCIAL FACTORS

Several factors may play a role and increase the risk of serious infection with HRSV such as the presence of members of the household who smoke or young siblings, day care attendance, stay in a nursing home or hospital (Bocchini Jr *et al.*, 2009). In general, exposure to smoke from cigarettes has a detrimental impact on respiratory health. There is a significant link illustrated between smoking in the household, and the incidence and severity of HRSV infection (Bradley *et al.*, 2005).

#### 1.5.2.1.2 VIRAL FACTORS

HRSV is not a very cytopathic virus, but targeting nonbasilar airway epithelial cells and type I alveolar (Johnson *et al.*, 2007). This results in damage to the ciliary function and removal of infected epithelial cells (Wright *et al.*, 2005). In general, HRSV does not stop cell transcription; nevertheless, there was a change in abundance of cell cycle regulatory proteins investigated in A549 and human primary HBEpC cells, and this leads to enrichment of cells in the G0/G1 population and doubled the number of progeny virus (Wu *et al.*, 2011). Viral load is not the only factor determining disease severity and the correlation remains controversial. In spite of HRSV low cytopathicity, there is clear evidence that the level of HRSV replication relates to the severity of disease (El Saleeby *et al.*, 2011). Consequently, HRSV in clinical isolations was found to induce variable pathogenesis (Van Drunen Littel-Van Den Hurk & Watkiss, 2012).

There are many HRSV proteins that play a role in alteration of the host response to infection. NS1 and NS2 proteins stop IFN regulatory factor 3 activation and prevent the type I IFN induced signalling during the JAK/STAT pathway. Therefore, this leads to an effective block of IFN$\alpha/\beta$ production by the infected host allowing increased virus replication without killing. HRSV also down regulates the production and function of IFN by inhibiting toll-like receptor (TLR) signalling during mitochondrial antiviral signalling protein (Bhoj *et al.*, 2008). Moreover, a reduced apoptosis and enhanced survival of the infected cells results from activation of the phosphoinositidide 3-kinase pathway by NS1 and NS2 (Bitko *et al.*, 2007).

The transmembrane attachment glycoprotein G plays an important function in immune evasion in HRSV. Firstly, the G protein is a highly glycosylated protein, which may impede immune recognition. Secondly, it is highly variable, with only 53% amino acid identity and 1–7% antigenic relatedness between subgroups, and, as a result, leads to easy escape from specific neutralizing antibodies. Thirdly, the G protein also has limited sequence homology to fraktalkine (CX3CL1), therefore, decreasing the action of host fraktalkine and the influx of CXCR1 leukocytes, for instance CD4, CD8 T and cells natural killer (NK) cells (Tripp *et al.*, 2001).

#### 1.5.2.1.3 HOST FACTORS

Host risk factors for more severe LRTI HRSV infections and hospitalization are correlated to premature birth, immunodeficiency, chronic lung disease (CLD) of prematurity and hemodynamically congenital heart disease (CHD). In addition, immunodeficiency, immunosuppression or old age may lead to prolonged viral replication and more severe illness. Further risk factors for children include male gender, low birth weight, multiple births and low titer of HRSV-specific maternal antibodies (Groothuis *et al.*, 2011; Kristensen *et al.*, 2012; Resch *et al.*, 2002).

#### 1.5.2.1.4 GENETIC FACTORS

Many genetic polymorphisms, including innate defence genes, host cell receptor genes, neutrophil response genes surfactant protein genes, Th1/Th2 response genes and gene effectors of adaptive immunity (Figure

1.6) have been reported as significant factors in the severity of human RSV disease (Miyairi & DeVincenzo, 2008).

Macrophages and epithelial cells were predictably involved in the innate immune response to HRSV. Therefore, many cytokines and chemokines including IL-8/ CXCL8, IP-10/CXCL10, MCP-1/CCL2, MIP-1$\alpha$, CCL3, MIP-1b/CCL4, RANTES/CCL5, IL-6, TNF-$\alpha$, IL-1$\alpha/\beta$, and IFN-$\alpha/\beta$ are produced by macrophages and epithelial cells in response to HRSV infection, and can be detected in enhanced amounts in respiratory secretions of children, hospitalized for HRSV infection (McNamara *et al.*, 2005).

## 1.6 TREATMENTS AND PREVENTION

While there has been a lot of research into the clinical manifestation, diagnostic approaches and animal models of HRSV, there is currently no vaccine or general anti-viral therapy and the infection causes large economical and health care burdens every year.

### 1.6.1. TREATMENT

#### 1.6.1.1 RIBAVIRIN

Ribavirin (1-b-D-ribofuranosyl-1, 2, 4-triazole-3-carboxamide) is the only antiviral drug licensed by the FDA for the treatment of severe HRSV infection. It is a synthetic nucleoside with a broad spectrum of antiviral activity that affects a diverse range of DNA and RNA viruses *in vivo* and *in vitro*

(Sidwell *et al.*, 1972). Ribavirin has become a standard therapy for the treatment of hepatitis C virus infection in combination with pegylated interferon (Pawlotsky, 2003) and has been used experimentally against Lassa fever virus infection (McCormick *et al.*, 1986) and other haemorrhagic virus infections, for instance, ebola (Alfson KJ, 2015; Bronze & Greenfield, 2003). Moreover, the doses of ribavirin for HRSV patients are administered as a little-particle aerosol for two to five days and usually for 12 or more hours per day. However, ribavirin is not in routine use for management of infants/children with HRSV infection because the drug is expensive, difficult to administrating and produced conflicting results for long-term treatments (Wright & Piedimonte, 2011). For these reasons, the drug is used for those patients at high risk of developing severe disease and the decision depends on the individual stations (Lieberthal *et al.*, 2006).

Since ribavirin was discovered, its mechanism of action *in vivo* is still unknown (Crotty *et al.*, 2002). However, it is thought to inhibit the replication of HRSV throughout the active replication phase (Jafri, 2003). There are many mechanisms thought to be responsible for the antiviral activity of ribavirin (Figure 1.7), depending on the particular virus being studied (Paeshuyse *et al.*, 2011). And there are five primary mechanisms of action suggested for ribavirin, three direct mechanisms contain direct inhibition of the viral polymerase, inhibition of RNA capping activity and reproduced mutation frequency throughout incorporation of ribavirin into newly synthesized genomes resulting to error catastrophe. Two indirect mechanisms compose an immunomodulatory effect in which a T-helper type

1 (antiviral) immune response is maintained and a decrease in cellular guanosine triphosphate (GTP) pools through inosine monophosphate dehydrogenase (IMPDH) inhibition (Crotty *et al.*, 2001; Graci & Cameron, 2006; Hofmann *et al.*, 2008). However, the predominant mechanism of antiviral activity of ribavirin against *Paramyxoviruses* such as HRSV and parainfluenza *in vitro* is based on inhibition of IMPDH activity (Leyssen *et al.*, 2005).

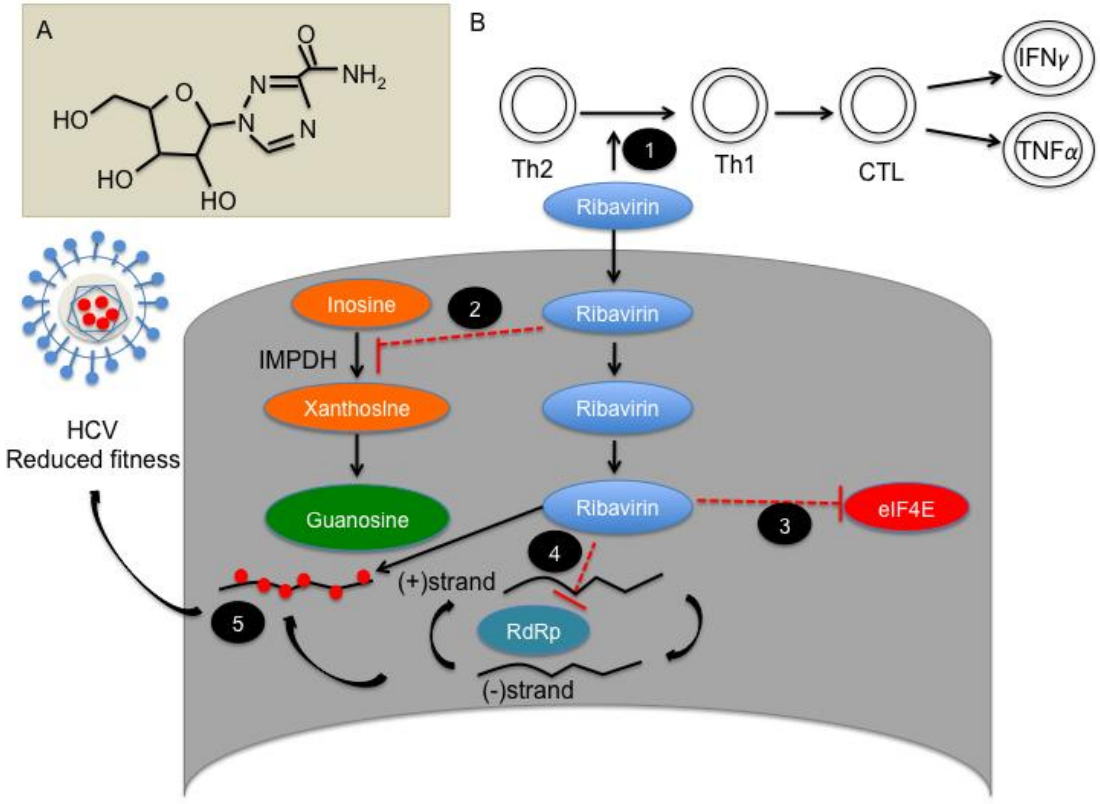


***Figure 1.7*** *A. structural formula of ribavirin. B. The five mechanisms of action: (1) modulation of Th1 and Th2 immune response, (2) Inhibition of IMPDH, (3) Direct inhibition of translation initiation factor eIF4E, (4) Direct inhibition of viral polymerase, (5) Viral lethal mutagenesis. However, the precise mechanism of action of ribavirin is still unknown for HRSV. Adapted from (Chung et al., 2008; Paeshuyse et al., 2011).*

### 1.6.1.2 MECHANISM OF ACTION (FIVE MECHANISMS)

The mechanism of action of ribavirin in many cases is unknown. Several hypotheses for a mode of action have been suggested and are discussed below:

#### 1.6.1.2.1 IMMUNOMODULATORY EFFECT

Immunomodulation of antiviral cellular responses are an indirect mechanism of action of ribavirin, for instance the ability to induce a Th2 to Th1 shift in the immune response (Shah *et al.*, 2010) (Figure 1.7 B). It has been suggested that the cytokine profile of CD4 cells may determine whether HCV infection results in a chronic, failure of the immune system to amount an active cellular response needed to clear the virus from the liver (Rehermann, 2009; Rehermann & Nascimbeni, 2005), or clearance to clear HCV following an acute infection which is associated with production of Th1 cytokine, interleukin 2 and interferon gamma (Rehermann & Nascimbeni, 2005). Therefore, ribavirin is thought to preserve or enhance the Th1 responses that are needed to clear HCV infection, Th2 responses that associated with tolerance and chronic infection (Fang *et al.*, 2000) and for HRSV (DeVincenzo, 2000).

#### 1.6.1.2.2 INHIBITION OF IMPDH

Intracellular pools of GTP are depleted in ribavirin treated cells through inhibition of cellular inosine monophosphate dehydrogenase (IMPDH) (Figure 1.7 B). This has been suggested to be correlated with the inhibition of

flavivirus (including yellow fever virus) and paramyxovirus replication. Inhibition of IMPDH is an indirect mechanism of action of ribavirin, which is a host enzyme that specific for the *de novo* synthesis of guanosine triphosphate (GTP) and has a key role in guanine nucleotide biosynthesis (Leyssen *et al.*, 2005; Leyssen *et al.*, 2006; Malinoski & Stollar, 1981; Shu & Nair, 2008; Streeter *et al.*, 1973). Also, IMPDH has been reported to modulate intracellular guanine (deoxy)nucleotide pools and thus has a vital impact on many of cellular processes, composing the control of cell proliferation. Intracellular pools of GTP are an essential building block for viral RNA synthesis and have been reported to be reduced by up to 60% in cells infected with influenza or those which are treated with ribavirin (Wray *et al.*, 1985). Moreover, inhibition of IMPDH by ribavirin results in inhibition of the replication of many RNA viruses, including HCV and flavivirus (Leyssen *et al.*, 2005; Leyssen *et al.*, 2006).

#### 1.6.1.2.3 INHIBITION OF RNA CAPPING ACTIVITY

Inefficient translation of viral transcripts occurs as a result of ribavirin which prevent the capping of mRNA (Figure 1.7 B). Ribavirin can also affect the translation of eukaryotic mRNAs and has been proposed as a therapeutic for acute myeloid leukemia (Tamburini *et al.*, 2009). It has also been shown to act as a competitive inhibitor of the methyl 7-guanosine (m(7)G) cap, the natural ligand of the translation initiation factor eIF4E (Volpon *et al.*, 2013). Moreover, ribavirin has been reported to have an effect on HCV replication by inhibition of eIF4E (Paeshuyse *et al.*, 2011).

#### 1.6.1.2.4 INHIBITION OF VIRAL POLYMERASE

It has been reported that ribavirin can lead to a direct inhibition of viral RdRp (Figure 1.7 B), which is responsible for the replication of the viral genome, such as in influenza virus (Eriksson *et al.*, 1977) and vesicular stomatitis virus (Toltzis *et al.*, 1988). This leads to inhibition of viral transcription and replication. For HCV infection, ribavirin 5'-triphosphate (RTP) can function as a substrate for the HCV RdRP, interacting with the viral polymerase and inhibiting nucleic acid synthesis (Graci & Cameron, 2006). Ribavirin was demonstrated to act as a competitive inhibitor of either GTP or ATP (i.e act as an analoge) suggesting that ribavirin might be an RNA virus mutagen *in vivo*. However, RTP has been suggested to inhibit predominantly the RNA transcription of reovirus (Rankin Jr *et al.*, 1989). In addition, ribavirin was investigated to act as inhibitor to HIV-1 reverse transcription (Fernandez-Larsson & Patterson, 1990).

#### 1.6.1.2.5 LOSS OF FITNESS OF RNA VIRUS GENOMES

RNA virus error catastrophe is a direct mechanism of action of ribavirin (Figure 1.7 B). Ribavirin is a base analogue of either adenine or guanine and thus can base pair with cytosine or uracil. For RNA viruses, ribavirin might be incorporated into genomic RNA by the RdRp during replication. The result is termed hyper-mutation that can cause ''lethal mutagenesis'' to virus biology through error catastrophe. This mechanism of action has been proposed and supported by experimental data *in vitro* for poliovirus (Crotty *et al.*, 2001) and HCV and *in vivo* for HCV (Dietz *et al.*, 2013).

Multiple mechanisms of action, GTP depletion by ribavirin may act in concert to increase its incorporation into viral genomes, thus increasing error prone replication as has been suggested for West Nile virus (Day *et al.*, 2005). Furthermore, up-regulation of anti-viral gene products, micro-array analysis suggested that ribavirin can directly up-regulate antiviral gene expression including STAT-1$\alpha$ and STAT-1$\beta$ in HRSV-infected cells (Zhang *et al.*, 2003). In summary, all mechanisms of action of ribavirin discussed above were different from virus one to other, whether the virus causes an acute or chronic infection and the accumulation of ribavirin, *in vivo*, in some tissues (such as liver when administered orally or an aerosol) (Crotty *et al.*, 2002).

### 1.6.2. PREVENTATIVE THERAPY

Palivizumab (Syngis: MedImmune) prophylaxis is a monoclonal antibody (MAB) that was developed against the F protein of HRSV. It is the main drug approved by the FDA for the prevention of serious LRTI caused by HRSV in young children and infants at high-risk. Also, it has been proven to be safe, effective and reduces the risk of hospitalization for HRSV LRTI in high-risk infants (Connor, 1998). Palivizumab can be used in hematopoietic stem cell recipients making it useful for immunocompromised people (Boeckh *et al.*, 2001). Therefore, the FDA approval was based on the reduction in HRSV hospitalization by 45% (Feltes *et al.*, 2003). Palivizumab was recommended at 5 monthly doses of 15mg/kg body weight in the start of the HRSV season, which occurs differently from country to country (Bocchini Jr *et al.*, 2009). However, many studies have unsuccessfully attempted to develop modules that predict which infants at high risk would benefit most from using

palivizuamb prophylaxis (Sampalis *et al.*, 2008; Simões *et al.*, 2008). Overall, no drug will completely prevent HRSV infection, but they can limit replication sufficiently to reduce disease (Zhu *et al.*, 2011).

Vaccination is the most effective way to prevent virus infection. However, there are currently no licensed HRSV vaccine available (Gomez *et al.*, 2014). Vaccines and new antiviral drugs are in pre-clinical and clinical development, however, until these are complete controlling HRSV still remains a formidable challenge (Collins & Melero, 2011; Zhu *et al.*, 2011). Therefore, the major challenges to develop improved antivirals and vaccines include; elucidating the basis of the pathology associated with HRSV infection and understanding the effects that HRSV has on the host immune response (Collins & Melero, 2011; Dapat & Oshitani, 2016).

## 1.7. HIGH THROUGHPUT APPROACHES

### 1.7.1 AN INTRODUCTION TO LABEL FREE PROTEOMICS

Label- free quantitative proteomics approaches have become highly popular in mass spectrometer-based proteomics. It is a technique in MS that have two main concepts to compare two or more samples. This method is providing an excellent resource for studying host cell proteomes and can be applied for the study of virus infection (Cox & Mann, 2011; Otto *et al.*, 2014). In order to have successful quantitative proteomics, its important to perform excellent experimental design and appropriate sample preparation. Also,

having statistical analysis and validation of the MS data through the use of independent techniques and functional analysis (Podwojski *et al.*, 2012).

Label-free quantification aim to compare two or more different experiments by (i) associating the direct mass spectrometric signal intensity for any given peptide or (ii) comparing the number of fragment spectra matching to a peptide/protein as an indicator for their respective amounts in a given protein (Otto *et al.*, 2014). However, there are three important experimental parameters affect the analytical accuracy of quantification by ion intensities for proteomic analysis of very complex peptide mixture; (i) It is useful to employ a high mass accuracy mass spectrometer because the influence of interfering signals of similar but distinct mass can be minimized. (ii) The peptide chromatographic profile should be optimized for reproducibility in order to ease finding corresponding peptides between different experiments. (iii) The good balance between acquisition of survey and fragment spectra has to be found. MS has no longer cycles between MS and MS/MS mode but aims to detect and fragment all peptides in a chromatographic window simultaneously by rapidly alternating between high-and low-energy conditions in the MS (Bantscheff *et al.*, 2007; Cox & Mann, 2011). Label-free approaches are the least accurate technique among the MS quantification techniques when considering the overall experimental process since all the systemic and non-systemic variations between experiments are reflected in the obtained data. Also, in term of simple practical, the time-consuming steps of introducing a label into proteins or peptides can be neglected and there are no costs for labelling reagents (Bantscheff *et al.*, 2007).

Advantages of label-free quantification over stable isotope labelling by amino acids in cell culture (SILAC): In terms of analytical strategy, there are some important advantages over SILAC: (a) label free has no principle limit to the number of experiments that can be compared whereas SILAC are typically limited to 2-8 experiments. (b) Label-free methods give higher dynamic range of quantification than SILAC. (C) Label-free different for SILAC techniques, mass spectral complexity is not increased that might provide for more analytical depth as the MS is not occupied with fragmenting all forms of the labelled peptide (Bantscheff *et al.*, 2007; Cox *et al.*, 2014; Cox & Mann, 2011). Previous studies of HRSV infection have been studied using SILAC technique (Munday *et al.*, 2010a; Munday *et al.*, 2012a).

Another high throughout quantitative proteomic approach utilises isobaric tagging, where chemical isotope incorporation is based on tags with an identical chemical labelling structure and same total mass (Dayon & Sanchez, 2012). The two key platforms are isobaric tags for absolute and relative quantitation (iTRAQ) and Tandem mass tags (TMT). Both platforms represent a method for differentiating between multiple conditions and determining relative protein levels in 4 or 8 samples (iTRAQ) or 6 or 10 samples (TMT) simultaneously (Amaya *et al.*, 2014). This approach lends itself to the labelling of *in vivo* samples and/or primary cells (Wiese *et al.*, 2007) as such labels are applied post-sample preparation. For example, iTRAQ has been used to investigate influenza virus infection in primary human macrophages (Lietzén *et al.*, 2011). However, the disadvantages of

such techniques include; incomplete labelling, complex sample preparation and the requirement for high sample concentration (Munday *et al.*, 2012b).

One of label free proteomics applications in this thesis is to study the effect of ribavirin on the host cell in the absence and presence of HRSV using high throughput quantitative proteomic techniques but focused on label free rather than SILAC. This includes using antiviral drugs such as ribavirin, and determining the viral and cellular proteome changes that occur during virus infection.

### 1.7.2 AN INTRODUCTION TO RNA-SEQ

RNA-seq is high-throughput technique, also known whole transcription of RNA molecules including the messenger RNA (mRNA), provides a complete set and precise measurement of the changing expression levels of each transcript in cells and tissues during development and under different conditions (McGettigan, 2013). Transcriptomics also focused on the gene expression at the RNA level and provides the genome information of gene structure and function in specific biological processes (Dong & Chen, 2013; Ozsolak & Milos, 2011). Understanding the transcriptome is necessary for interpreting the functional elements of the viral genome and exposing the molecular constituents of cells and understanding diseases (Wang *et al.*, 2009).

RNA-seq has generally replaced traditional approach such as microarray techniques by providing the ability to visualise gene expression in sequence form (Grada & Weinbrecht, 2013; Liu *et al.*, 2014). Previous studies of host cell gene expression, after HRSV infection, have been studied using microarray analysis (Dapat & Oshitani, 2016; Martínez *et al.*, 2007; Zhang *et al.*, 2003). However, the RNA-seq approach allows sequencing and quantification of mRNA expression levels on a small or large scale (Wang *et al.*, 2009). Moreover, RNA-seq has advantages over microarray, for instance, RNA-seq can identify novel transcripts because it is not limited to detecting transcripts that correspond to existing gene sequences (Marioni *et al.*, 2008; Wang *et al.*, 2009). Another advantage is that RNA-seq has a larger dynamic range to quantify gene expression level accurately (Wang *et al.*, 2009). Finally, RNA-seq has a much lower cost than microarrays for gene expression profiling in model organisms (Mantione *et al.*, 2014).

RNA-seq approach is now common use in biology and in detecting cellular pathway changes during viral infection, for example, on West Nile virus (Qian *et al.*, 2013), human adenovirus (Evans *et al.*, 2012) and Hendra virus (Wynne *et al.*, 2014). However, RNA-seq has not been used for HRSV in the published literature, thus using such this high-resolution approach making a novelty in this thesis. Therefore, this will allow determination of the genetic sequence of the virus to great depth of coverage and to better understanding the mechanism of action of the antiviral ribavirin.

## 1.8. RESEARCH OBJECTIVES

The main aims of this study were to investigate the potential mechanism of ribavirin and study its effect on the host cell in the absence and presence of HRSV by using high throughput techniques; quantitative proteomics and RNA-seq. The findings of this study will provide a better understanding of the mechanism of action on HRSV and the host cell. This thesis is composed three parts: the first part focuses on establishing appropriate experimental and assay conditions to study the effect of ribavirin in the following chapters. HEp-2 and A549 cell lines, derived from human lung carcinomas, were used in this study. The results generated from this work were presented in Chapter 3 and have contributed to a publication (Aljabr *et al*., 2015) (see appendix).

The second part of this study aimed to investigate the action of ribavirin on the host cell and HRSV biology in general, using a combined high-resolution RNA-seq and deep discovery label free quantitative proteomics. The results based on this work are presented in Chapter 4. Some of this work (mainly the chaperone proteins which were detected in mock verses HRSV infected cells) contributed to another publication (Munday *et al*., 2015) (see appendix). A manuscript is currently in preparation using the most data in Chapter 4.

The third part of this study investigates the effect of ribavirin on HRSV infected cells and identifying a potential direct mutagenic effect of ribavirin on HRSV. The results based on this work were presented in Chapter 5, and has

contributed to several publications (Aljabr *et al*., 2015; Noton *et al*., 2014) (see appendix).

# CHAPTER 2: MATERIALS AND METHODS

## 2.1. TISSUE CELL CULTURE METHODS

### 2.1.1. CONTINUOUS CELL CULTURE

HEp-2 and A549 cells were purchased from the European Collection of Authenticated Cell Cultures (ECACC) (held by Public Health England) and were maintained at 37°C with 5% $CO_2$. Both continuous cell lines, HEp-2 and A549, were grown in Dulbecco's modified Eagle's medium (DMEM) (Sigma [D6429]) and supplemented with 10% foetal bovine serum (FBS) (Sigma [F9665]) and 100% penicillin and streptomycin antibiotics (Sigma [P4333]). All cell lines were passaged using trypsin EDTA ([Sigma [T3924]) for normal cell maintenance, or using a phosphate-buffer saline (PBS) (Sigma). For different infection experiments, cells were seeded at the following densities 24 hr prior to infection to achieve a 60-70% confluent cell layer (Table 2.1). The cell monolayers were washed with PBS and 2 ml of (1X) Trypsin/EDTA was added release adherent cells from culture surfaces for 2 min at 37°C. Following detachment, 10 ml growth medium were added to the flask containing cells to prevent further tryptic activity. The cell suspension was transferred to a 50 ml conical tube and centrifuged at 220 x g for 5 min at room temperature. Without disturbing the cell pellet, the supernatant was aspirated from the tube and the tip of the conical tube was flicked by finger to loosen the cell pellet. Then the cells were re-suspended in 2 ml of growth medium by pipetting the cells up and down to break up cell collections. For quick growth in a 75 $cm^2$ flask, 7.5 $x10^3$ cells per $cm^2$ were seeded, however, for regular sub-culturing 5 $x10^3$ cells per $cm^2$ were seeded. For IF

experiments, 19 mm glass coverslips were dipped in methanol and left to dry before the coverslips were washed in sterile PBS (137 mM NaCl, 2.7 mM KCl, 10 mM Na2HPO$_4$, 1.8 mM KH$_2$PO$_4$ pH adjusted to 7.4) then transferred to dishes or 6 well plates prior to seeding using methanol sterilised forceps.

***Table 2.1*** *The seeding density of HEp-2 and A549 cells. 24 hr post-seeding required growing cells at a layer 60-70% confluent. The amount of diluted virus per ml during the virus incubation.*

| **Cell Culture Vessels** | **Seeding Density** | **Diluted virus in Serum Free Media (ml)** | **Growth Medium (ml)** |
|---|---|---|---|
| **Dishes** | | | |
| 60 mm | $8x10^5$ | 1-1.5 | 3 |
| **Cluster Plates** | | | |
| 6-well | $2X10^5$ | 0.5-1 | 2 |
| 12-well | $2X10^5$ | 0.5-1 | 1-2 |
| 24-well | $2X10^5$ | 0.5 | 1 |
| 96-well | $1X10^4$ | 0.05 | 0. 2 |
| **Flasks** | | | |
| T-25 | $5.2X10^6$ | 2.5 | 5 |
| T-75 | $1.5X10^6$ | 4-5 | 10 |
| T-175 | $3X10^6$ | 5-7 | 25 |

### 2.1.2. FREEZING AND THAWING CELLS

In order to have a continual supply of cells, cells were frozen in liquid nitrogen; $10^6$ cells/per vial were washed three times in ice-cold PBS and centrifuged at 1000 x g for 3 min at 4°C. To prevent ice crystal formation, the cell pellet was re-suspended in pre-prepared ice cold FBS supplemented with 10% (v/v) DMSO and 1 ml/vial of cell suspension was transferred to labelled cryovials. The cryovial tubes were stored at least 24 hr at -80°C in an isopropanol chamber or a rate freezing chamber before being transferred to liquid nitrogen storage. Frozen cells were rapidly thawed at 37°C (in incubator or water bath) and transferred to a conical tube containing growth media and centrifuged at 1000 x g for 3 min at room temperature. The cell pellet was washed three times in room temperature with PBS to remove all traces of DMSO and was re-suspended in an appropriate volume of complete cell culture media and transferred to a 25 $\mathrm{cm}^2$ flask. Another way to eliminate DMSO from frozen cells was to transfer the cells directly to a 25 $cm^2$ flask that has culture media with a dilution 1:10. Once cells were 80% confluent, cell cultures were expanded and sub-cultured in 75 $cm^2$ flasks.

### 2.1.3 INHIBITOR STUDY

#### 2.1.3.1 RIBAVIRIN

The antiviral ribavirin was obtained from Sigma (R9644). A 1 mM stock was pre-prepared in dimethyl sulfoxide (DMSO) and added at either 6 hr or 24 hr post-infection. From the stock, aliquots were made (in order to avoid thaw and freeze cycles) and stored at -20°C.

### 2.1.3.2 17-AAG & 17-DMAG

17-N-Allylamino-17-demethoxygeldamycin (17-AAG) was obtained from Calbiochem/EMD Millipore (100068) and was diluted in DMSO and a 10 mM stock solution was made. 17-Dimethylaminoethylamino-17-demethoxygeldanamycin (17-DMAG) was obtained from Santa Cruz (CAS 467214-20-6), diluted in water and a 10 mM stock solution was made. Both were aliquoted and stored at -20°C.

### 2.1.3.3 ETOPOSIDE

Etoposide was purchased from Sigma (E1383) and dissolved in DMSO. A 1 M stock solution was made, aliquoted, covered with foil and stored at -20°C.

### 2.1.4 MTT ASSAY

Cell viability was determined by using a colorimetric 3-(4,5-Dimethylthiazol-2-yl)-2,5-diphenyltetrazolium bromide assay (MTT) from Sigma (MKBH9792V). A549 and HEp-2 cells were seeded in triplicate in 96-well plates at a density of $1x10^4$ cells/well to ensure 70% confluency 24 hr later. After which, all wells were washed twice with 1x phosphate buffered saline (PBS). Ribavirin (or other inhibitors e.g. 17-AAG or 17-DMAG) were then added to wells at different concentrations (low to high concentration) and incubated for 24 hr at 37°C. 24 hr later, wells were washed twice with 1x PBS. Then 0.024 g of MTT was prepared in 10 ml of media (DMEM plus 10% FBS) and warmed at 37°C for 15 min. The MTT was dissolved and filtered and 100 µl added to each well and the plate incubated for 45 min at 37°C. The MTT was then

removed and 100 µl of DMSO added and mixed. The optical density was measured by spectrophotometer at 570 nm on a Tecan (Infinite® F50/Robotic-Absorbance microplate reader). A curve was then created to assess cell viability.

### 2.1.5 HRSV STRAINS

In this study the HRSV-A2 strain was used and it was kindly provided by Dr Patricia Cane and Dr Brian Dove (Public Health England, UK). HRSV-A2 undergoes productive infection in A549 and HEp-2 cells, and was passaged and propagated through the latter. The full-length cDNA sequence of the A2 strain has been published on GenBank: http://www.ncbi.nlm.nih.gov/nuccore/M74568.

### 2.1.6 VIRUS PROPAGATION: SUPERNATANT

HRSV was propagated in HEp-2 cells and seeded in four 175 $cm^2$ flasks at a density of $3x10^6$ cells/flask, 24 hr prior to infection. HRSV at low MOI (MOI 0.1) was diluted in 10 ml serum-free media, applied to the cells and incubated for 2 hr at 37°C with shaking every 10 min to ensure coverage of the whole flask. New culture media (supplemented with 10% [v/v] FBS) was added to each flask (20 ml) before further incubation at 37°C. After five days post-infection, virus was harvested by cell disruption with autoclaved glass beads and the supernatant (80 ml) was collected and clarified by centrifugation at 3200 x g for 10 min at 4°C. The supernatant was either passed through a 0.45 µm filter, aliquotted, snap-frozen in an ethanol/dry ice

bath or liquid nitrogen and stored at -80°C, or additional virus concentrated by using a sucrose density gradient.

### 2.1.7 VIRUS PURIFICATION BY SUCROSE GRADIENT

Sucrose gradient centrifugation was performed to purify HRSV supernatant in order to remove the culture media and the majority of cellular components, that can act as contaminants and effect follow on experiments (Wu *et al*., 2012). Two sucrose gradients; discontinuous and continuous were prepared 24 hr prior to use: the discontinuous gradient was prepared by three sequential layers of 2.5 ml of 60%, 45% and 30% (w/v) sucrose (dissolved in autoclaved NT buffer [50 mM Tris-HCl (pH 7.5), 100 mM $MgSO_4$, 1mM EDTA, 150 mM NaCl] and filter sterilised) into each of two, 14x89 mm centrifuge tubes (Sefton). Between each layer step, the gradient was frozen at -20°C. After adding the final layer the gradient was left overnight at -20°C and thawed immediately before use. The continuous gradient was prepared by two sequential layers of 3 ml of 60% and 30% sucrose into each of two, 14x89 mm centrifuge tubes. Also, between each layer step, the sucrose gradient was frozen at -20°C. After the application of the final layer, the continuous gradient was kept overnight at 4°C to let the layers to disperse into one another. Polyethylene glycol (PEG)-6000 powder was dissolved in NT buffer to make a 50% (w/v) solution and 20 ml was added to the clarified virus suspension to dilute the final PEG concentration to 10%. Virus was precipitated for 90 min at 4°C (inside a cold room) with moderate stirring, transferred into 50 ml conical tubes and centrifuged at 3200 x g for 10 min at

4°C. The pelleted virus was re-suspended in 5 ml of cold NT buffer and added equally to the tops of the discontinuous sucrose gradients prior to centrifugation at 35,000 rpm for 90 min at 4°C in a TH-641 swinging rotor. The middle opalescent band observed at the 30-45% sucrose interface (~2 ml) gently was removed from each centrifuge tube by using a 5 ml syringe and carefully a 25 gauge needle, and diluted with 2 ml of cold NT buffer. Diluted virus was added equally to the top of the two continuous sucrose gradients tubes before centrifugation at 35,000 rpm for 90 min at 4°C in a TH-641 swinging rotor. The white opalescent band observed at ~45% sucrose density was carefully removed using a 5 ml syringe and a 25 gauge needle (~1.5 ml), mixed gently, aliquoted and snap-frozen in an ethanol-dry ice bath for long term storage at -80°C. If needed, a sample of the undiluted middle band from the discontinuous gradient was kept for a concentration comparison to the final continuous gradient band by $TCID_{50}$ or plaque assay. Furthermore, the bottom bands observed at the 45-60% interface of the discontinuous gradient were extracted for $TCID_{50}$ or plaque assay comparison to the middle band.

### 2.1.8 HRSV TITRE DETERMINATION

#### 2.1.8.1 PLAQUE ASSAY

HRSV titre was calculated for HEp-2 and A549 cells by using an antibody based methylcellulose plaque assay procedure based on previous studies (McKimm-Breschkin, 2004; Murphy *et al*., 1990). Before using this technique, 1.6% (w/v) high viscosity carboxymethyl-cellulose (Sigma [M0555]) was

made in $ddH_2O$. In separate bottles $ddH_2O$ and the carboxymethyl-cellulose powder (plus a stir bar) were autoclaved before adding hot water to the powder immediately after autoclaving and allowing the powder to dissolve with stirring. Cells were seeded at density 1 x $10^5$ / well in a 24-well plate 24 hr before infection to achieve 70-80% confluency. 50 µl of HRSV stock (that need to titrated) was serial diluted in 450 µl of DMEM ranging from $10^{-1}$ to $10^{-8}$ in duplicate for each dilution. Growth culture media was removed and the monolayers were washed with sterile 1x PBS before adding 400 µl of each virus dilution to the cells. Additionally, in duplicate wells, 400 µl serum- and antibiotic-free DMEM was added and acted as a mock-infected control. 24 well plates were incubated for 2 hr at 37°C with intermittent 10-15 min rocking periods to ensure coverage of the entire wells. 2 hr later, the virus inoculum was aspirated and the cell monolayer washed with sterile 1x PBS three times to ensure that unbound virus was removed. High viscosity carboxymethyl-cellulose (1.6%) (already prepared) and DMEM (plus 10% FBS and 1% penicillin-streptomycin) were mixed 1:1 and 1 ml of this mixture was applied to each well. With a minimal movement, plates were incubated at 37°C from 3 to 6 days or until syncytia were observed. The carboxymethyl-cellulose overlay was aspirated using an aspirator and the wells were washed four times with 1x PBS in order to remove the overlay. Cells were fixed in 80% (v/v) of cold methanol (already prepared and stored at -20°C) and the plates stored at -20°C for 1 hr. Alternative fixative applications were used including, 4% (v/v) ice cold formalin fixative was incubated at room temperature for 10 min or cold 100% acetone (-20°C storage) for 30 sec. Cells were then washed with PBS-0.1% tween (PBST) three times and 200

µl in each well of blocking buffer solution (5% [w/v] dried skimmed milk in PBS). The plates were incubated with rocking overnight at 4°C or for 1 hr at room temperature. Goat anti-HRSV primary antibody (Abcam [ab20745]) was diluted 1:200 in blocking buffer (~100 to 200 µl/well) and kept overnight at 4°C (inside the cold room) on a rocker. To visualized the plaques, a horseradish peroxidise (HRP) conjugated anti-goat secondary antibody (Abcam [ab6741]) diluted 1:1000 in blocking buffer (~100 to 200 µl/well) was applied and incubated overnight at 4°C or 1 hr at room temperature with rocking. The secondary antibody was detected using the peroxidise substrate, 4-Chloro-1-naphthol (4-CN) (Pierce [Thermo Scientific-34010]) prepared in either ethanol or methanol and diluted 1/10 in 10 ml PBS. Before using the diluted 4-CN directly, it was supplement with 30% (v/v) hydrogen peroxide ($H_2O_2$) (10 µl $H_2O_2$ /10 ml PBS) and added to the wells. Plates were incubated with rocking for 10 min at room temperature or shaking every 2 min, after which time the grey/purple colour development was detected and the reaction was stopped with water. Duplicate wells containing between 10 and 100 colour stained plaques were only counted and using this formula to calculate the titration of virus:

HRSV titre (PFU/ml) was calculated by (number of plaques) / (dilution factor x volume of diluted virus added to the well). For making virus stocks, cells were infected at MOI 0.1. For all the experiments discussed in Chapter 3, 4 and 5 (unless otherwise specified) cells were infected with HRSV-A2 at MOI 0.5.

### 2.1.8.2 TISSUE CULTURE INFECTIOUS DOSE 50 ($TCID_{50}$)

HEp-2 cells were trypsinized as explained above and the cell suspensions were counted. The density for the $TCID_{50}$ in 24-well plates was 5 x $10^4$ of HEp-2 cells per well in 1 ml growth medium in order to achieve a ~80% confluence following overnight incubation. Then 900 µl of HEp-2 infection medium (2% FBS, 1% PIS) were added to 5 ml tubes, using eight tubes to test each viral stock. The virus stocks were quickly thawed in a 37°C water bath and put immediately on ice. 100 µl of virus stock were added on the first dilution tube and 7-fold serial dilutions were undertaken for each sample by sequentially adding 100 µl of virus sample to the 5 ml tubes, vortexing before continuing to the next dilution. Therefore, virus stock was diluted to $10^{-8}$ and all dilutions were kept on ice until they were used to infect the cell cultures in 6 well plates. However, before infecting the cells, most of the medium was removed from wells and the cells were washed twice with 500 µl of PBS. 200 µl of each sample dilution was added to four wells in the same order that were washed in order to avoid the possibility of the well drying out. The plates were incubated at 37°C for 1.5 – 2 hr with shaking every 15 min. Virus dilution were removed and the cells were washed three time with 1x PBS and 1 ml of maintenance medium added and kept all plates at 37°C for seven days. In days five and seven post-infection, the plates were tested and the number of wells of each dilution which were positive for typical HRSV cytopathic effects CPE (syncytia formation) was counted. Virus titres were calculated using the method of Kärber algorithm in units noted as ($TCID_{50}$), as described below:

$$Log_{10}\ TCID_{50} = D + d(S-0.5)$$

Where:

D, $Log_{10}$ of the last dilution demonstrating 100 % CPE, i.e., all wells of the dilution are positive for viral CPE. d, $Log_{10}$ of the dilution factor (in this case the dilution factor is 10). S, the sum of the fraction of all the wells inoculated for each dilution, including and beyond the last dilution with 100 % CPE, that are positive for viral CPE (as 4 wells are inoculated, the fraction beyond the 100 % CPE row will be 0.25, 0.5, 0.75 or 1.0).

The titre was calculated according to the above formula and corresponds to a volume of 0.2 ml (the volume added per well). To adjust this titre to $log_{10}$ $TCID_{50}$ per ml, 0.7 was added to the $Log_{10}$ value calculated. This corresponds to $log_{10}$ 5, with 5 being the multiplication factor necessary to adjust 0.2 ml to 1 ml. To have the titre as PFU/ml, the value needs to multiply the $TCID_{50}$ by 0.7.

## 2.2 MOLECULAR BIOLOGICAL TECHNIQUES

### 2.2.1 RNA EXTRACTION

Total RNA from HEp-2 cells (different conditions) was extracted using the RNeasy Mini Kit (Qiagen) based on the manufacturer's instructions. The reagents were provided by Qiagen and the components of the buffers supplied were not disclosed, however, these kit components are marked with an asterisk (*) in the text. All centrifugation steps in this technique were done at room temperature for 15 sec at 8000 x g ($\geq 10{,}000\mathrm{rpm}$). Cell pellets

(<5x$10^6$ cells) were thawed (if they were in -80°C) and re-suspended by vortexing in 350 µl RLT buffer* (plus 1.43 mM β-mercaptoethanol [BME]) for 1 min. 1 volume of 70% ethanol was added to each sample (700 µl in total) and mixed by pipetting. The samples were then transferred to an RNeasy mini column, placed in a 2 ml collection tube, centrifuged and discard the flow through (RLT buffer). Then another centrifugation after 350 µl buffer RW1* was added to each column. Following centrifugation, genomic DNA contamination was removed by using the RNase-Free DNase Set. Once placed in a clean collection tube, master mix pre-prepared depends on number of samples (each sample has 10 µl DNase I solution was added to 70 µl buffer RDD* mixed gently) and the mixture was transferred to the column prior to incubation at room temperature for 15 min. After incubation, 350 µl buffer RW1* was added followed by centrifugation. Once centrifuged the flow through (buffer RW1) was discarded before adding 500 µl buffer RPE* to each column sample, followed by centrifugation. The last step was repeated by thoroughly washing the column, followed by centrifugation for 2 min, ensuring that no ethanol is carried over for RNA elution. Prior to the RNA elution step, a new 1.5 ml collection tube* was used, 30-50 µl RNase-free water was added and centrifuged for 1 min. If required at a high concentration, RNA elution was repeated and followed by centrifugation for 1 min. The concentration of RNA was then quantified by Qubit®RNA BR Assay Kit (from Life technologies). Standards and samples were vortexed for 2-3 sec and incubated at room temperature for 2 min. The RNA broad range assay was selected on Qubit ®fluorometer to calibrate with standards. Alternatively, the RNA concentration was determined using a NanoDrop 1000

spectrophotometry and the purity was estimated to meet this criteria (OD260/280 ~2.0, OD260/230 > 2.0). To ascertain RNA integrity and observe and distinguished the 28S and 18S rRNA bands, 0.5 µg RNA was run on a 1% agarose gel for 45 min at 100V. A good indication of purified total cellular RNA is that the 28S rRNA band should be approximately twice as intense as the 18S rRNA band (with a ratio of band intensity ~2:1). RNA samples were stored at -80°C.

### 2.2.2 First-strand cDNA synthesis and reverse transcription

cDNA was synthesised from 1 µg of total RNA using the ThermoScript RT-PCR System (Invitrogen) according to the manufacturer's instructions: using an RNase-free 0.2 or 0.5 ml tube, 1 µg of total RNA, 500 ng oligo (dT)20 and 2 µl of 10 mM deoxyribonucleotide triphosphate dNTP were mixed and DEPC-treated water or RNase-free di$H_2O$ were used to adjust the final volume to 12 µl. RNA and primer was denatured by incubating at 65°C for 5 min and placed on ice for 1 min. Following incubation, a master reaction mix was prepared on ice (depending on the number of samples) from 4 µl 5X cDNA Synthesis Buffer, 1 µl 0.1 M DTT and 1 µl RNaseOUT (40 units/µl), 1 µl DEPC-treated water and 1 µl ThermoScript RT (15 U/µl) and added into each reaction tube on ice. Then this was incubated at 50°C for 1 hr. To terminate the reaction, samples were incubated at 85°C for 5 min and 1 µl of RNase H was added. This was incubated at 37°C for 20 min. Following incubation, 20 µl of cDNA product was diluted in 80 µl of nuclease-free water to produce 100 µl in total. Successful reverse transcription was confirmed by

PCR amplifying the HRSV G gene (923 bp) and a human GAPDH gene fragment (240 bp).

### 2.2.3 OLIGONUCLEOTIDES

All of the DNA primers in Table 2.2 were designed and purchased from MWG Biotech (Germany) with HPLC purification, whereas, the human GAPDH gene primers were purchased from Enzo Life Sciences. The lyophilised primers were resuspended in nuclease-free water to a final concentration of 100 µM (stock solution) and aliquoted and further diluted to 10 µM (working solution) and all of them were stored at -20°C.

***Table 2.2*** *Primers used for PCR and qRT-PCR*

| **Oligo Name** | **Sequence (5' → 3')** |
|---|---|
| HRSV-A2 G-fwd | CTCGAGCCATGTCCAAAAACAAGGACC |
| HRSV-A2 G-rev | GGATCCCTACTGGCGTGGTGTGTTGGG |
| HRSV-A2 G-fwd | ATGTCCAAA AACAAG GACCAACG |
| HRSV-A2 G-rev | CTACTGGCGTGGTGTGTTGGGTG |
| HRSV-A2 NS1-fwd | TTGGCTAAGGCAGTGATA |
| HRSV-A2 NS1-rev | AGGTTGAGAGCAATGTGT |
| HRSV-A2 NS2-fwd | CCCTCGAGATGGACACAACCCACAATGATAATA |

| | |
|---|---|
| HRSV-A2 NS2-rev | CCGGATCCCGTGGATTGAGATCATACTTGTATATTATG |
| HRSV A2 N-fwd | CTCGAGCCATGGCTCTTAGCAAAGTCAAG |
| HRSV-A2 N-rev | GGATCCTCAAAGCTCTACATCATTATC |
| HRSV-A2 P-fwd | CTCGAGCCATGGAAAAGTTTGCTCCTG |
| HRSV-A2 P-rev | GGATCCTCAGAAATCTTCAAGTGATG |
| HRSV-A2 M-fwd | CTCGAGCCATGGAAACATACGTGAACAAG |
| HRSV-A2 M-rev | GGATCCATCTTCCATGGGTTTGATTGC |
| HRSV-A2 F-fwd | CTCGAGCCATGGAGTTGCTAATCCTCAAAG |
| HRSV-A2 F-rev | GGATCCTTAGTTACTAAATGGAATATTATTTAT |
| HRSV-A2 SH-fwd | CTCGAGCCATGGAAAATACATCCATAAC |
| HRSV-A2 SH-rev | GGATCCCTATGTGTTGACTCGAGCTC |
| HRSV-A2 M21-fwd | CTCGAGCCAGTGGAGCTGCAGAGTTGGAC |
| HRSV-A2 M21-rev | GGATCCTCAGGTAGTATCATTATTTTTG |
| HRSV-A2 L- fwd | CTCGAGCCATGACCATGCCAAAAATAATG |
| HRSV-A2 L-rev | GGATCCTTATGACACTAATATATATATTG |

### 2.2.4 MEASUREMENT OF DNA CONCENTRAION

The concentration of DNA were measured using a Qubit® dsDNA BR Assay Kit (Life technologies). Standards and samples were vortexed for 2-3 sec and incubated at room temperature for 2 min. A DNA broad range assay was selected on Qubit ®fluorometer to calibrate with standards. Alternatively the DNA concentration was determined using a NanoDrop, and the purity was estimated to meet this criteria (OD260/280 ~1.8, OD260/230 ≥ 2.0).

### 2.2.5 POLYMERASE CHAIN REACHTION (PCR) FOR HRSV-G AND GAPDH DETECTION

PCR (referred to general PCR not 'qRT-PCR' which is described below) was used to detect HRSV infection by amplifying the HRSV G gene. PCR was performed in thin-walled 0.2 ml PCR tubes and reaction volumes of 25 µl typically comprised the following; 2.5 µl of 10X PCR buffer minus Mg, 1 of 10mM (dNTP) mix (Invitrogen [18427013]), 0.5 µl of 10 µM of appropriate forward and reverse primers, 1 µl of template cDNA (created as described in section 2.2.2), 0.5 µl unit of Taq DNA polymerase and DEPC-treated water bringing 25 µl in total. PCR cycling was carried out in a thermocycler (Primus, MWG Biotech) typically using the conditions shown in Table 2.3. PCR products (5 µl) then were analysed by agarose gel electrophoresis as described in section 2.2.7.

***Table 2.3.*** *PCR conditions used for detection of HRSV genes*

| No. of cycles | Duration | Temperature |
|---|---|---|
| 1 | 2 min | 94°C |
| 30 | 30 sec | 94°C |
| | 30 sec | 60°C (55°C GAPDH) |
| | 1.5 min (30 sec GAPDH) | 72°C |
| 1 | 2 min | 72°C |

### 2.2.6 QUANTITATIVE REAL-TIME RT-PCR

Following confirmation of successful RT via PCR reactions with primers of human GAPDH or HRSV G gene from a 100 µl of cDNA that made according to section 2.2.2. Using iTaq ™ Universal SYBR® Green Supermix (BIO-RAD), a PCR master mix was made up with each primer set for each reaction according to the manufacture's instructions; for each reaction, 1 µl of diluted cDNA and 10 µl iTaq ™ Universal SYBR® Green Supermix mixed with 1 µl of the appropriate primer pairs (0.5 µl of each forward primer and reverse primer) and made up the final reaction volume to 20 µl with nuclease-free water. The mixture was equally loaded into each well (20 µl /well) of the 96-well array plate. Quantitative Real-Time PCR (qRT_PCR) arrays were performed on DNA Engine Opticon 2 Real-Time Cycler (BioRad) with the following program settings (Table 2.4). The data results from three independent experiments were averaged and normalized using a human GAPDH gene as control.

***Table 2.4*** *qPCR program setting using DNA Engine Opticon 2 Real-Time Cycler*

| No. of cycles | Duration | Temperature |
|---|---|---|
| 1 | 10 min | 95°C |
| 40 | 15 sec | 95°C |
| | 30 sec | 55°C |
| | 30 sec | 72°C |
| 1 | Melt Curve (Default Setting) | |

### 2.2.7 AGAROSE GEL ELECTROPHORESIS

Agarose gel electrophoresis with ethidium bromide (EtBr) staining was used to visualize DNA or RNA, digestion analysis and purification. Electrophoresis grade agarose (AGTC Bioproducts) (1% [w/v]) was melted in 1X TAE buffer (40 mM Tris-acetate, 1 mM EDTA, pH 8.0) or 1x TBE (89 mM Tris-borate, 0.5 M EDTA, pH 8.0) by heating, and EtBr was added to molten agarose to a final concentration of 0.5 µg/ml. Molten agarose was then added into a gel-casting tray containing an appropriate comb, and allowed to set. Once the gel had set the tray was transferred to a gel running tank and submerged with sufficient 1X TAE or 1x TBE buffer. An appropriate volume of DNA was diluted in 5x DNA loading buffer (Bioline) and 5 µl of Hyperladder I DNA ladder (Bioline) were loaded in the wells of gel. The electrophoresis was then run until the indicator dye migrated to about the three quarters length of the gel.

### 2.2.8 PURIFICATION OF DNA FROM GEL

The bands were separated on a 2% agarose gel corresponding to correct DNA fragments were excised by visualization with a UV transilluminator. Purification of DNA from agarose gel was performed using the QIAquick® Gel Extraction Kit (Qiagen) according to the manufacture's instruction. All centrifugation steps in this technique were done at room temperature for 1 min at 17,900 x g ($13{,}000\ \mathrm{rpm}$). The DNA fragments were excised from the agarose gel with a clean and sharp scalpel. DNA gel slices were weighed in a 1.5 ml (Eppendorf tubes) and 3 volumes buffer QG were added to 1 volume gel. Tubes were incubated at 50°C until the gel slice had completely dissolved with vortex steps every 2-3 min to help dissolve gels. Once the gel slices had dissolved, the colour of the mixture was checked and compared to Buffer QG. If the colour was not yellow, 10 µl of 3 M sodium acetate were added and mixture turned yellow. One gel volume of isopropanol 100% was added to the samples and mixed. The mixtures were transferred in a QIAquick spin column and centrifuged. After centrifugation, the flow through was discarded before 0.5 ml of buffer QG was added and centrifuge. Following centrifugation, the flow through was discarded; 0.75 ml Buffer PE (prepared in 100% of ethanol) was added and centrifuged. A new 1.5 ml tubes were placed after centrifugation, purified DNA was eluted in 30-50 µl of buffer EB or free water and centrifuged. The concentration of DNA was then determined according to section 2.2.4.

### 2.2.9 TOTAL RNA-SEQ

After assessing the quality extracted total RNA from the RNA integrity number RIN values, the samples were subjected to poly A selection using the Dynabead mRNA purification kit (Life Technologies). In this case, 15 µl of beads per sample were washed with binding buffer (2X) and re-suspended in 30 µl of 2x bead buffer. RNA samples were made up to 30 µl and heated to 65°C for 5 min to remove any secondary structure. Samples were then mixed with the beads on a rotator for 5 min at room temperature. After collecting the beads on a Magnetic Particle Concentrator (MPC), the beads were washed 2x with wash buffer, removing all traces after each washing step. 12 µl of water was added to the beads for elution, which was achieved by heating at 70 degrees for 2 min and immediately placing on the MPC to retrieve the supernatant containing the RNA. This was assessed for rRNA on a RNA pico chip. The twice poly A-selected material was all used as input for Scriptseq (Epicentre). Samples were treated as the protocol indicated. Samples were mixed with primer and fragmentation buffer, and heated at 85°C for 5 min and placed on ice. Samples were converted to cDNA and purified with Ampure XP. Samples were mixed with barcoded primers and amplified with 15 cycles PCR. The libraries were purified with Ampure XP and assessed by bioanalyser using HS DNA kit and the quantity was determined by Qubit DNA HS kit. Samples were pooled on an equimolar basis for a single lane.

The quantity and quality of the final pool were assessed using Qubit (Invitrogen) and Bioanalyzer (Agilent) and subsequently qPCR using the

Illumina Library Quantification Kit from Kapa on a Roche Light Cycler LC480II according to manufacturer's instructions. The template DNA was denatured according to the protocol described in the Illumina cBot User guide and loaded at 9 pM concentration. To improve sequencing quality control, 1% PhiX was spiked-in. The sequencing was carried out on one lane of an Illumina HiSeq 2500 with version 3 chemistry generating 2 × 100 bp paired end reads. For each time point, the sequence reads were mapped to the HRSV A2 genome using Bowtie2. For each alignment to the HRSV genome, the output BAM files were further analysed using QuasiRecomb. Where Bowtie2 aligned more than 1 million reads to the HRSV genome, 1 million alignments were selected at random. The coverage option for QuasiRecomb was used (command line: java -XX:NewRatio=9 -Xms2G -Xmx10G -jar QuasiRecomb.jar –i reads.sam -coverage) and then parsed the output files with in house software written in PERL that determined the most abundant nucleotide for each position (i.e. the consensus nucleotide) and reported the frequency of use for the other three nucleotides. The RNA-seq was carried out by the Centre for Genomic Research CGR, University of Liverpool.

## 2.3 PROTEIN METHODS

### 2.3.1 PREPARATION OF WHOLE CELL LYSATES

For different applications; Coomassie stain, silver-stain or western blot analysis of whole cell lysate, RIPA buffer (50 mM Tris, [pH 7.5], 150 mM NaCl, 1% (v/v) NP40 alternative, 0.5% (w/v) sodium deoxycholate, 0.1% sodium dodecyl-sulphate [SDS], supplemented with 1 EDTA-free complete

protease inhibitor mixture [Roche Applied Science] per 50 ml buffer) was applied directly to the washed cell monolayer and incubated for 20 min at 4°C before cell scraping. Alternatively, cell pellets were re-suspended in RIPA buffer and incubated for 30 min at 4°C. Both procedures of lysis were followed by 3 min incubation in a sonicating water bath at 4°C to complete lysis. The whole cell lysate was centrifugated at 13,000 x g for 20 min at 4°C, the supernatant containing total protein was collected and stored at -80°C.

### 2.3.2 DETERMINING PROTEIN CONCENTRATION BY BCA ASSAY

**DETERMINING PROTEIN CONCENTRATION BY BCA ASSAY**

The whole cell lysates were obtained as explained above (section 2.3.1) and total protein concentrations were determined using the Micro BCA (bicinchoninic acid) protein assay system (Pierce [23227]) according to the manufacture's 96-well plate instructions. Bovine serum albumin (BSA) standards were used in order to create a standard curve. Protein lysates were first diluted in either distal water or their respective buffer to give a 100 µl volume. Whole cell lysate was diluted 1/20. In duplicate or triplicate, 10 µl of each sample and standard were then mixed with 200 µl assay standard reagent (prepared by diluting reagent B 1:50 into reagent A) and transferred to a 96 well plate (200 µl / well) and incubated at 37°C for 30 min. Absorbance was then measured at 570 nm on a Tecan microplate reader (Infinite F50/Robotic-Absorbance). The mean was calculated and a standard curve was created using the BCA standards to which the test samples could be compared. The protein concentration was determined at the same time as taking the dilution factor into account.

### 2.3.3. SODIUM-DODECYL SULPHATE POLYACRYLAMIDE GEL ELECTROPHORESIS (SDS-PAGE)

Protein samples (size 5-10 µg) were resolved using a Bio-Rad Mini-Protein system and appropriate concentration of SDS-polyacrylamide gel electrophoresis (SDS-PAGE) was made. Resolving (7.5%, 10% or 12%) and stacking gel (5%) were made as described in (Table 2.5). The resolving gel solution was placed between two clean glass plates and a small volume of distilled water or water -saturated butanol was added to provide a smooth gel interface. After the resolving gel was set and the water removed, the stacking gel solution was added on top of the resolving gel and a comb was added. Following stacking gel polymerisation the comb was removed, the glass plate and wells were placed inside the tank with 1x SDS-PAGE running buffer (25 mM Tris-HCl [pH 8.3], 250 mM glycine, 0.1 % [w/v] SDS). Protein samples were then prepared using 4x LDS sample buffer (Invitrogen) and supplemented with 50 mM DTT reducing agent and denatured at 80°C for 10 min (when using 5x LDS no DTT was added and the denaturation temperature was 95°C and incubated for 10 min). 5 µl SeeBlue plus 2 pre-stained standard (Invitrogen: 250-4 kDa [LC5925]) or ColorPlus prestained protein ladder (NEB: 11-245 kDa [P7712S]) was loaded as a reference for a molecular weight ladder. The SDS-PAGE gel was run at 15V/cm in 1x SDS-PAGE running buffer and the gel run at 100-150V, the current 200-400mA for ~30-45 min) until the optimum separation of marker proteins was achieved. Gels were analyzed by staining with coomassie blue or continued to western blot analysis.

***Table 2.5.*** *SDS-PAGE resolving and stacking gel reagents with different concentrations. The acrylamide materials were used to cast 2 mini-gels for the Bio-Rad Mini-Protein II system, and the volume doubled if a 26 thick gel casting set was used.*

| **Resolving Gel (10 ml)** | | | | | **Stacking Gel (5 ml)** | |
|---|---|---|---|---|---|---|
| **% Gel** | **15%** | **12%** | **10%** | **7.5%** | **% Gel** | **5%** |
| 30% Acrylamide | 5 ml | 4 ml | 3.3 ml | 2.5 | 30 % Acrylamide | 830 µl |
| 1.5M Tris-HCl pH8.8 | 2.5 ml | | | | 1M Tris-HCl pH6.8 | 630 µl |
| $H_2O$ | 2.3 ml | 3.3 ml | 4 ml | 4.8 ml | H2O | 3.4 ml |
| 10% (w/v) SDS | 100 µl | | | | 10% (w/v) SDS | 50 µl |
| 10% (w/v) APS | 100 µl | | | | 10% (w/v) APS | 50 µl |
| TEMED | 10 µl | | | | TEMED | 5 µl |
| Resolution (Protein kDa) | 10-40 | 20-100 | 30-100 | 25-200 | | |

### 2.3.4. WESTERN IMMUNOBLOT

Once SDS-PAGE was completed, poly-vinylidine fluoride (PVDF) membranes (Millipore [IPVH00010]) were kept in 100% methanol for 30 sec and placed on the bottom of the gel using Towbin transfer buffer (25 mM Tris-HCl [pH8.3], 192 mM glycine, 20% [v/v] methanol). Also, two thick pieces of filter paper were soaked in the transfer buffer and placed with this order (from bottom to the top); one of filter paper was placed on the surface of a

Bio-Rad semi-dry transfer instrument, the soaked PVDF membrane, the complete gel, finally, the second piece of soaked filter paper was placed on top of the gel. Transfers were carried out according to the manufacturer's instructions, at 15 V for 1.5 hr. After the transfer, the membranes were blocked in 5%-10% (w/v) fat free skimmed milk powder (Sigma) dissolved in Tris-buffered saline (50 mM Tris-HCl [pH 8.3], 150 mM NaCl) containing 0.5% (v/v) Tween-20 (TBST) at room temperature on a rocker for 1 hr at 4°C (cold room) overnight. Blocking buffer was then discarded and membranes were washed three times in TBST. Primary antibodies (listed in Table 2.6) were diluted in blocking buffer and 4-8 ml applied for either overnight at 4°C (cold room) or 1 hr at room temperature on rocker. Unbound antibody was then washed from PVDF membranes by three washes in 1X TBST for 5 min for each wash. The primary antibodies were detected with the horse radish peroxidase HRP-conjugated secondary antibodies listed in (Table 2.7) which were diluted in blocking buffer and 4-8 ml added onto the membranes for 1 hr at room temperature with rocking. Unbound antibody was removed with three washes in 1X TBST for 5 min of each wash. The target protein(s) bound to antibodies were visualised by using either enhanced chemiluminescence (ECL) or SuperSignal West Femto Substrate (Thermo Scientific). The blots were reused by striping and restoring a maximum of three times using a blot restore membrane rejuvenation kit (Millipore [2520]) according to the manufacturer's instructions.

# 2.4 IMMUNOFLUORESCENCE-BASED TECHNIQUES

## 2.4.1 CELL FIXATION

Prior to fixation, cells grown on coverslips were washed three times with PBS to remove traces of growth media and fixed using either 4% (V/V) paraformaldehyde [37% of formaldehyde stock solution [BDH Chemicals] diluted in 1x PBS) and incubated for 10 min at room temperature or 100% cold acetone (stored in -20°C before used) and incubated for 20 min at 4°C. The fixation solution was removed and the monolayer was washed three times with PBS. PBS containing 0.1% (v/v) sodium azide could be used for fixed coverslip-adhered monolayers as long-term storage at 4°C.

## 2.4.2 CELL PERMEABILISATION AND IMMUNOFLUORESCENCE STAINING

Following fixation, cells were permeabilised in order to take the antibodies into cells using 0.1% (v/v) Triton X-100 made up in PBS for 10 min at room temperature. The permeabilisation buffer was then removed and the monolayer was washed three times with PBS. Primary antibodies diluted in PBS containing 2% (v/v) FBS (Table 2.6), 50-100 µl were added onto coverslips and incubated either 1 hr at room temperature or overnight at 4°C (cold room). Unbound primary antibody was washed off using three rinses in PBS-0.5% Tween-20 (PBST) for 5 min per wash on a rocker. The fluorescently-conjugated secondary antibody (Table 2.8) was diluted in PBS containing 2% FBS and incubated in the dark either 1 h at room temperature or overnight at 4°C. Coverslips were washed three times in PBST to remove the unbound secondary antibody.

### 2.4.3 MOUNTING OF FIXED CELLS SAMPLES

Coverslips were removed from dishes by clean forceps, inverted and placed on glass microscope slides spotted with Prolong Gold mounting media either contain DAPI (Invitrogen) counter stain to allow visualisation of cell nuclei or not and incubated overnight in the dark at room temperature. Mounted coverslips were sealed with clear nail varnish and stored at 4°C with protection from light.

### 2.4.4 MICROSCOPY

Immunofluorescence images were captured on an Axio imager M2 microscope (Carl Zeiss).

## 2.5 MASS SPECTROMETRY

### 2.5.1 PREPARATION OF WHOLE CELL LYSATE FOR LABEL FREE QUANTITATIVE PROTEOMICS

HEp-2 cells at 70% confluency were infected with HRSV A2 at a MOI of 0.5 while uninfected cells were used as controls (mock). At 6 hr post-infection uninfected and infected cells were treated with Ribavirin (RBV), the (DMSO) or left untreated. At 24 hr post-infection, cells that were uninfected-untreated (mock), uninfected-treated (DMSO or RBV), infected-untreated (HRSV) and infected-treated (HRSV + DMSO or HRSV + RBV) were harvested in triplicates and re-suspended in an equal volume of 0.1% RapiGest diluted in fresh 25 mM ammonium bicarbonate (pH 7.8). Three freeze-thaw cycles (10 sec in liquid nitrogen), including 5 min vortexing between each cycle were

carried out followed by two cycles of 15 min sonication to allow for maximum solubilization efficiency. Samples were then heated at 80℃ for 10 min before the soluble fraction was transferred to low adhesion micro-centrifuge (Eppendorf) tubes. Finally, total protein concentration was measured by BCA assay (Pierce).

### 2.5.2 SAMPLE PREPARATION FOR PROTEOMICS

Sample protein content and volume was normalised with 25 mM ammonium bicarbonate. Samples were then heated at 80ºC for 10 minutes, reduced with 3 mM dithiothreitol (Sigma) at 60ºC for 10 minutes then alkylated with 9 mM iodoacetimde (Sigma) at room temperature for 30 min in the dark. Proteomic grade trypsin (Sigma) was added at a protein: trypsin ratio of 50:1 and samples incubated at 37ºC for 12 hr. Rapigest (Waters) was removed by adding TFA to a final concentration of 1% (v/v) and incubating at 37ºC for 2 hr. Peptide samples were centrifuged at 12,000 g for 60 min (at 4ºC) to remove the precipitated Rapigest.

### 2.5.3 NANOLC MS ESI MS/MS ANALYSIS

Peptide mixtures (2 µl) were analyzed by on-line nanoflow liquid chromatography (LC) using the nanoACQUITY-nLC system (Waters MS technologies, Manchester, UK) coupled to an LTQ-Orbitrap Velos

(ThermoFisher Scientific, Bremen, Germany) mass spectrometer equipped with the manufacturer's nanospray ion source. The analytical column (nanoACQUITY UPLCTM BEH130 C18 15 cm x 75 µm, 1.7 µm capillary column) was maintained at 35ºC and a flow-rate of 300 nl/min. The gradient consisted of 3-40% acetonitrile in 0.1% formic acid for 150 min then a ramp of 40-85% acetonitrile in 0.1% formic acid for 5 min. Full scan MS spectra (m/z range 300-2000) were acquired by the Orbitrap at a resolution of 30,000. Analysis was performed in data dependant mode. The top 20 most intense ions from MS1 scan (full MS) were selected for tandem MS by collision induced dissociation (CID) and all product spectra were acquired in the LTQ ion trap.

Thermo RAW files were imported into Progenesis LC–MS (version 4.1, Nonlinear Dynamics). Runs were time aligned using default settings and using an auto selected run as reference. Peaks were picked by the software and filtered to include only peaks with a charge state of between +2 and +6. Peptide intensities were normalised against the reference run by Progenesis LC-MS and these intensities are used to highlight differences in protein expression between control and treated samples with supporting statistical analysis (ANOVA p-values) calculated by the Progenesis LC-MS software. Spectral data were transformed to .mgf files with Progenesis LC–MS and exported for peptide identification using the Mascot (version 2.3.02, Matrix Science) search engine. Tandem MS data were searched against the human (20,253 sequences; 11,332,942 residues) and human respiratory syncytial

virus HRSV A (strain A2) predicted proteomes (Uniprot release 2013_04). Mascot search parameters were as follows; precursor mass tolerance set to 10ppm and fragment mass tolerance set to 0.5 Da. One missed tryptic cleavage was permitted. Carbamidomethylation (cysteine) was set as a fixed modification and oxidation (methionine) set as a variable modification. Mascot search results were further processed using the machine learning algorithm Percolator. The false discovery rate was < 1%. Individual ion scores > 13 indicated identity or extensive homology ($p < 0.05$). Protein identification results were imported into Progenesis LC–MS as .xml files.

## 2.6 DATA PROCESS

### 2.6.1 STATISTICAL ANALYSIS

Prism 5 was used to compare two independent dataset of different time points with different conditions for growth curves. Student's t-test was used to analysis the cell viability with different concentrations of ribavirin. Statistical analysis of three datasets of data (MOCK, DMSO, RBV, HRSV, HRSV plus DMSO and HRSV plus RBV) when harvesting in two different time points were performed using the (ANOVA *p*-values) test. For all tests, a *p*-value<0.05 was considered statistically significant.

### 2.6.2 BIOINFORMATICS ANALYSIS USING STRING AND INGENUITY PATHWAY ANALYSIS (IPA)

The String 9.05 programme was used to identify protein-protein interaction networks and the pathways, however, only proteins were uploaded which

were identified and quantified with two or more peptides and a cut-off ≥ 2 fold change. Also, data were analyzed by the use of Ingenuity Pathway Analysis software (Ingenuity® Systems, www.ingenuity.com). Networks were generated using data sets containing gene identifiers and corresponding expression values, which were uploaded into the application. Each gene identifier was mapped to its corresponding gene object in the Ingenuity Pathways Knowledge Base. A cut-off of ≥2.0 or greater was set to identify the genes whose expression in abundance may have different functional relevance. These genes, named focus genes, were overlaid onto a global molecular network developed from information contained in the Ingenuity Pathways Knowledge Base. Focus genes networks were then algorithmically generated based on their connectivity. Graphical representations of the molecular relationships between genes/gene products were generated. Genes or gene products are represented as nodes, and the biological relationship between two nodes is represented as an edge (line). All edges are supported by at least one published reference from the literature, from a textbook, or from canonical information stored in the Ingenuity Pathways Knowledge Base. Human, mouse, and rat orthologs of a gene are stored as separate objects in the Ingenuity Pathways Knowledge Base but are represented as a single node in the network. The intensity of the node color indicates the relative change in expression level; the increased (red) or decreased (green) abundance, whereas, grey nodes represent no change in abundance. Nodes are displayed using numerous shapes that represent the functional class of the gene product. Canonical pathway analysis utilizes well characterized metabolic and cell signaling pathways which are generated

prior to data input and on which identified proteins are overlaid. From various datasets, some of interesting cellular proteins and genes, that identified and quantified by mass spectrometry and RNA-seq, were searched in Uniprot identification database (http://www.uniprot.org) in order to ascertain their functions and gain further information. Some analysis on RNA-seq and label free proteomics has already been described above in Sections, 2.2.9 and 2.5.3, respectively.

## 2.7 LIST OF ANTIBODIES

### 2.7.1 PRIMARY ANTIBODIES

***Table 2.6*** *Primary antibodies used in this study for western blot and/or immunofluorescence staining.*

| Target antigen | Vendor | Product No. | Species | WB dilution | IF dilution |
|---|---|---|---|---|---|
| HRSV | Abcam | Ab20745 | Goat polyclonal | 1:1000 | 1:50 |
| GAPDH | Abcam | Ab8245 | Mouse Monoclonal | 1:5000 | NA |
| OAS3 | Santa Cruz | Sc-99100 | NA | 1:200-1:1000 | 1:50 |
| ISG15 | Santa Cruz | Sc-50366 | NA | 1:200-1:1000 | 1:50 |
| HRSV FITC | Abcam | Ab20391 | Goat ploYclonal | NA | 1:50 |
| FBL | Abcam | Ab153862 | Rabbit polyclonal | NA | NA |
| UTP14A | Abcam | Ab138278 | Rabbit | NA | NA |

| | | | | | |
|---|---|---|---|---|---|
| | | | polyclonal | | |
| RRM2 | Abcam | Ab154964 | Rabbit ploYclonal | NA | NA |
| TRIM25 | Abcam | Ab167154 | Rabbit monoclonal | NA | NA |
| Stat1 | Santa Cruz | Sc-346 | NA | NA | NA |
| SOD2 | Abcam | Ab13533 | NA | 1:5000 | NA |
| Actin | Abcam | Ab3280 | NA | 1:1000 | NA |
| VDAC2 | Abcam | Ab77160 | NA | NA | NA |
| Cdc2 | Abcam | Ab18 | Mouse monoclonal | 1:1000 | 1:50 |

### 2.7.2 SECONDARY ANTIBODIES FOR WESTERN BLOT

***Table 2.7*** *Secondary HRP-conjugated antibodies used for western blot were diluted at 1:2500 in 5% milk TBST.*

| **Target antigen** | **Vendor** | **Product No.** | **Species** |
|---|---|---|---|
| Rabbit | Sigma | A6154 | Goat |
| Goat | Abcam | Ab6741 | Rabbit |
| Mouse | Sigma | A4116 | Goat |
| Rat | Sigma | A5795 | Rabbit |

### 2.7.3 SECONDARY ANTIBODIES FOR IMMUNOFLUORESCENCE

***Table 2.8*** *Secondary fluorochrome-conjugated antibodies used for immunofluorescence were diluted at 1:200 in 1x PBS.*

| **Target antigen** | **Vendor** | **Fluorophore** | **Product No** | **Species** |
|---|---|---|---|---|
| Goat | Abcam | FITC | Ab6881 | Donkey |
| Mouse | Invitrogen | Alexa Fluor 568 | A10037 | Donkey |
| Rabbit | Invitrogen | Alexa Fluor 546 | A10040 | Donkey |

# CHAPTER 3: OPTIMISING THE APPLICATION OF RIBAVIRIN AND VIRAL INFECTION

## 3.1 INTRODUCTION

Acute infection with HRSV is treated therapeutically with ribavirin, i.e. the drug is applied post-infection (Shah *et al.*, 2010; Zhang *et al.*, 2003). In order to characterize the effect of ribavirin on the host cell, and dissect the potential anti-viral activity, in more detail, a high-resolution approach was used to elucidate the interaction between ribavirin, the host cell and HRSV in a cell culture system. Two independent but over lapping methods, RNA-seq and quantitative label free proteomics, were used to assess whether both cellular and viral gene expression were changed in the presence of ribavirin in uninfected and HRSV-infected cells. RNA-seq was used to quantify changes in the abundance of cellular and viral transcripts, and to evaluate whether the mutational frequency during HRSV RNA synthesis was increased. Quantitative label free proteomics was used to quantify changes in the abundance of cellular and viral proteins. Both approaches had the potential to identify the same gene product to study regulation and generally transcriptomic approaches provide the greater coverage, and thus if the proteomic approach did not identify or quantify a gene product, then RNA-seq may have done. However, before these approaches were used, the optimal experimental conditions were defined including; the concentration of ribavirin, MOI and the time points to be assayed post-infection. This has to be balanced with maximising data output with a realistic cost of the proteomics and transcriptomic assays.

The objective of the current study was to establish appropriate experimental and assay conditions to study the effect of ribavirin in the following chapters. HEp-2 and A549 cell lines, derived from human lung carcinomas, were used in this study. Both cell lines are permissive for HRSV (Hughes *et al.*, 1988; Xatzipsalti & Papadopoulos, 2007) and have been used extensively in the study of this virus and other respiratory pathogens using high-resolution approaches (Coombs *et al.*, 2010; Dove *et al.*, 2012; Evans *et al.*, 2012; Lam *et al.*, 2010; Munday *et al.*, 2010a; van Diepen *et al.*, 2010). In general, the HEp-2 cells line was used in this analysis to study the effect of ribavirin and in some cases the A549 cell line was used to validate the results and investigate whether data was cell line specific. It is worth noting that previously, the A549 cell line, was reported to show some resistances to ribavirin (Morfin *et al.*, 2005). For this reason the HEp-2 cell line was used predominately in this study.

The A2 strain of HRSV was used as researchers in the laboratory had previously characterised the biology of this virus in cell culture using proteomics and other assays (Munday *et al.*, 2010a; Wu *et al.*, 2011) and therefore would provide a basis of comparison to historical data sets, and validate the approaches used in this thesis. It is important to study the viability of the cells in the presence of any compound without the virus (Mosmann, 1983) as many inhibitors can also be toxic to the cell at certain concentrations. In order to assess cell viability; different concentrations of the drug can be added in a dose dependent manner. Previous studies have also

investigated optimising the addition of ribavirin in cell culture to disrupt virus replication and these can be used as a starting point (Hruska *et al.*, 1980; Shah *et al.*, 2010). The data in this chapter defining the affect of ribavirin on cell viability and optimisation of HRSV were used as a starting point for the high-resolution approaches described in subsequent chapters.

Some of the work described in this chapter has recently been published in the Journal of Virology. **Waleed Aljabr**, Olivier Touzelet, Georgios Pollakis, Weining Wu, Diane C. Munday, Margaret Hughes, Christiane Hertz-Fowler, John Kenny, Rachel Fearns, John N. Barr, David A. Matthews and Julian A. Hiscox, (2015). Investigating the influence of ribavirin on human respiratory syncytial virus RNA synthesis using a high-resolution RNA-seq approach 10.1128/JVI.02349-15. (See appendix).

The candidate confirms that the work submitted is his own, except where work which has formed part of jointly-authored publications has been included. The contribution of the candidate and the other authors to this work has been explicitly indicated below. The candidate confirms that appropriate credit has been given within the thesis where reference has been made to the work of others.

**Chapter 3** of this thesis was based on the work from jointly-authored publication:

- Waleed Aljabr planned and performed all experiments, prepared samples for RNA-seq, western blot, immunofluorescence, data analyses, and jointly wrote the manuscript.
- Rachel Fearns and John Barr provided advice regarding manuscript structure.
- Oliver Touzelet, Weining Wu and Diane Munday provided technical support.
- Georgios Pollakis provided minor variant analysis.
- John Kenny, Margaret Hughes and Christiane Hertz-Fowler run RNA-seq.
- David Matthews provided viral transcriptomic analysis.
- Julian Hiscox provided supervision and jointly wrote the manuscript.

## 3.2. RESULTS

### 3.2.1 DETERMINING THE CELL VIABILITY IN THE PRESENCE OF RIBAVIRIN

To establish an optimal therapeutic regime for ribavirin in cell culture, the toxicity of ribavirin was first established in HEp-2 cells (Figure 3.1). An MTT assay was used to determine the proportion of viable cells in the presence of different concentrations of ribavirin, ranging from 100 µM to 30 mM, based on an analysis of published concentrations of ribavirin used *in vitro* (Player *et al.*, 1998; Shah *et al.*, 2010; Zhang *et al.*, 2003). Untreated cells were used to measure the total viable cell population and this was fixed at 100%, for comparison of the ribavirin treatments. Etoposide, which promotes apoptosis, was used as a positive control for cell death, and hence loss of cell viability (Barry *et al.*, 1993; Day *et al.*, 2009). The data indicated that at concentrations above 500 µM of ribavirin less than 50% of cells were viable. However, at concentrations less than 500 µM more viable cells were observed.

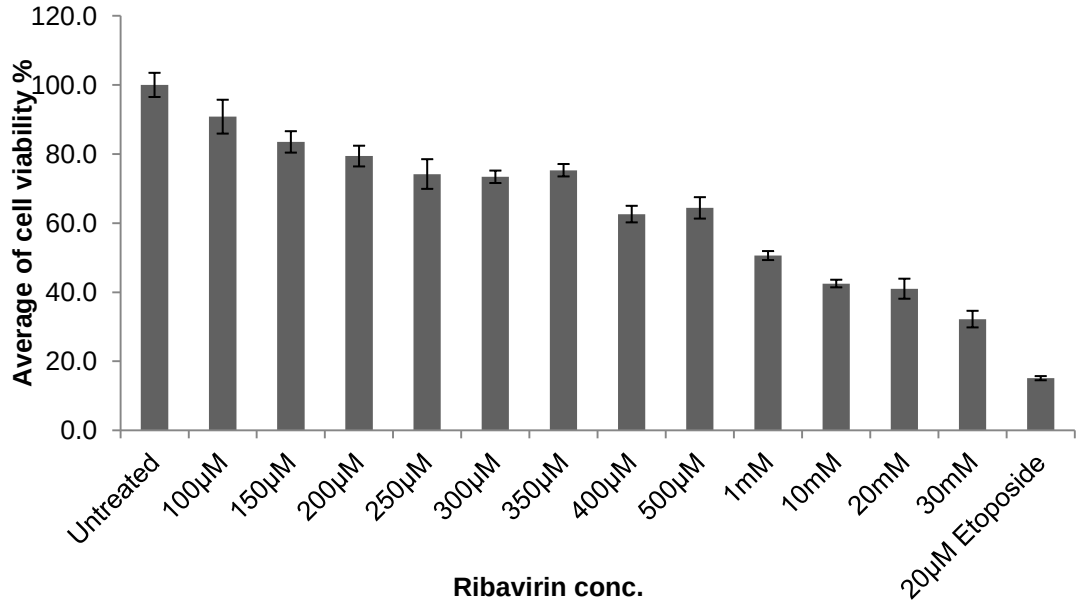


***Figure 3.1*** *Cell viability at 48h post treatment with different concentrations of ribavirin on HEp-2 cells using 3-(4,5-dimethylthiazol-2-yl)-2, 5-diphenyltetrazolium bromide (MTT) colorimetric assay on 96-well microplate* (in triplicates)*. MTT a yellow tetrazole is reduced by mitochondrial dehydrogenases in living cells to purple formazan. Absorbance at 570 nm was measured by spectrophotometer on Tecan reader to calculate cell viability in order to determine the half maximal effective concentration (EC50) of ribavirin. 500 μM of ribavirin becomes the EC50. Etoposide, at 20 μM, was used as positive control for defining minimum cell viability.*

### 3.2.2 ASSESSING RIBAVIRIN ON DIFFERENT MULTPLICITIES OF INFECTION (MOI)

The optimum multiplicity of infection (MOI – the theoretical number of viruses that will infect each cell) of HRSV was then established in either untreated cells or cells treated with 500 μM ribavirin. Both the RNA-seq and quantitative label free proteomic approaches are comparative, i.e. the abundances of mRNA/protein prepared from mock-infected cells can be compared to the abundance of the same mRNA/protein from HRSV-infected cells. Therefore the proportion of infected cells was maximised relative to the control cell layer. Also, this had to be balanced with the effective concentration of ribavirin (500 μM) being able to reduce infection. Based on previous experience (Jairath *et al.*, 1997; Munday *et al.*, 2015; Zhang *et al.*, 2002), four different MOIs were used, 0.005, 0.05, 0.5 and 5. Cells were then treated with 500 μM ribavirin and infected cells were visualized using indirect immunofluorescence (Figure 3.2).

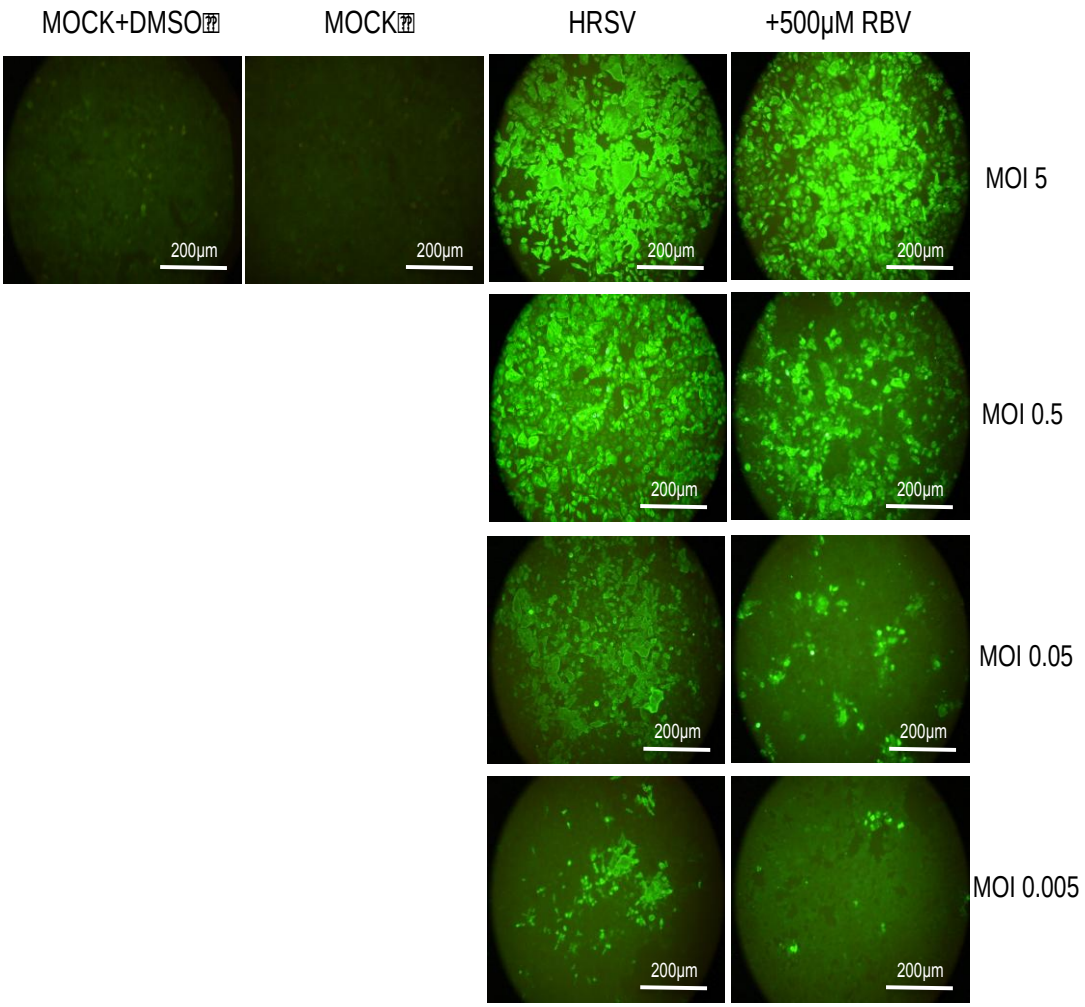


***Figure 3.2*** *Indirect immunofluorescence was used to determine the proportion of cells infected. Shown are Mock, HRSV and different MOIs with 500 μM of ribavirin (RBV). Mock cells without HRSV/RBV, HRSV infected cells only at different MOI (MOI 5, 0.5, 0.05 and 0.005 respectively) at 48 hr post-infection. HRSV+RBV infected cells at different MOI (MOI 5, 0.5, 0.05 and 0.005 respectively) at 48 hr post-infection and treated with 500 μM of ribavirin at 24 hr post-infection. HRSV viral proteins were labeled with goat anti-HRSV antibody and conjugated with donkey anti-goat FITC fluorescent antibody (Green). For each of the IF picture the scale bar is shown.*

The data indicated that using an MOI of 0.005 and 0.05, the number of infected cells was significantly decreased with 500 μM ribavirin, however, very few cells were infected. While using an MOI of 5, the majority of cells were infected, but there was no apparent difference at the number of infected cells between ribavirin treated and untreated cells. In contrast, at an MOI of 0.5, the majority of cells were positive for fluorescence, but 500 μM ribavirin resulted in a decrease in the proportion of stained cells. Taken together, this study suggested that infection cells with MOI 0.5 would be a good distinguishable MOI to study the infected cells with and without ribavirin treatment (Figure 3.2). Further, more quantitative assays were used to investigate this.

### 3.2.3 TIME COURSE OF INFECTION VERSUS TREATMENT WITH RIBAVIRIN

After identifying the appropriate concentration of ribavirin (Figure 3.1) and the optimum MOI (Figure 3.2) it was important to know which time points to perform the antiviral ribavirin in this study. To determine assay points for high- resolution analysis, the affect of ribavirin on HRSV infection was investigated at different time points post-infection (Figure 3.3). The virus was added at time zero and 500 μM ribavirin added at; -6hpi, 0hpi, +6hpi, +12hpi and +18hpi.

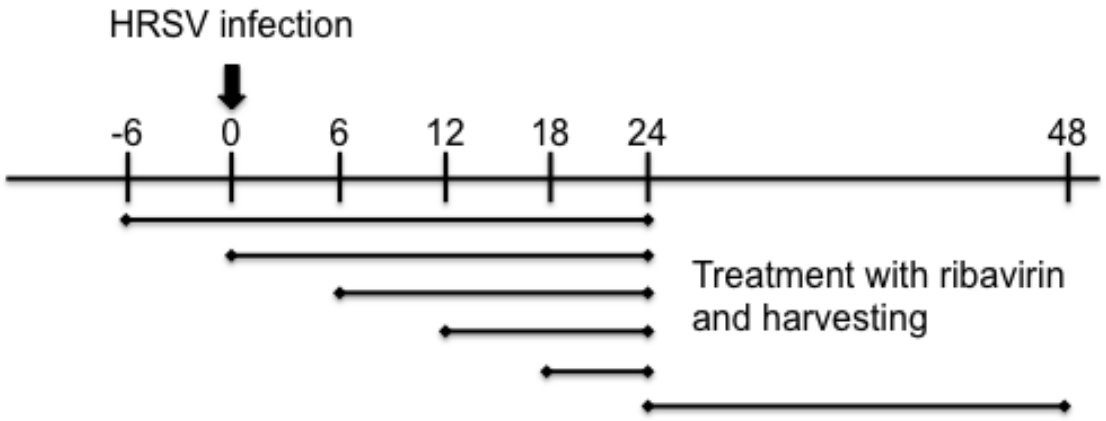


***Figure 3.3*** *Scale of adding ribavirin at different time points post-infection. This scale shows the time course of adding ribavirin drug before the infection as prophylaxis (-6hpi), at the same time of infection (0hpi) and after the infection as a therapeutic (6, 12, 18hpi) and harvest after 24 hr post-infection. Also, adding the drug after 24 hr post-infection and harvest after 48 hr post-infection. Cells infected with HRSV-A2 at MOI 0.5 and the concentration of ribavirin was 500 μM.*

For these time points virus biology was assayed at +24 hr post-infection by extracting either total RNA for RNA-seq and qRT-PCR or whole cell lysate for quantitative proteomics described in subsequent chapters. Ribavirin (500 μM) was also added at +24 hr post-infection and virus biology assayed at +48 hr post-infection by extracting either total RNA for RNA-seq or cell lysate for quantitative proteomics described in subsequent chapters. Virus biology and progeny virus production was determined by indirect immunofluorescence (Figure 3.4), viral proteins abundance was measured using western blot (Figure 3.5), and $TCID_{50}$ was used to determine progeny virus production (Figure 3.6). All these approaches were used to evaluate virus-infected cells. These factors were compared in untreated infected cells at +24 hr post-infection and +48 hr post-infection.

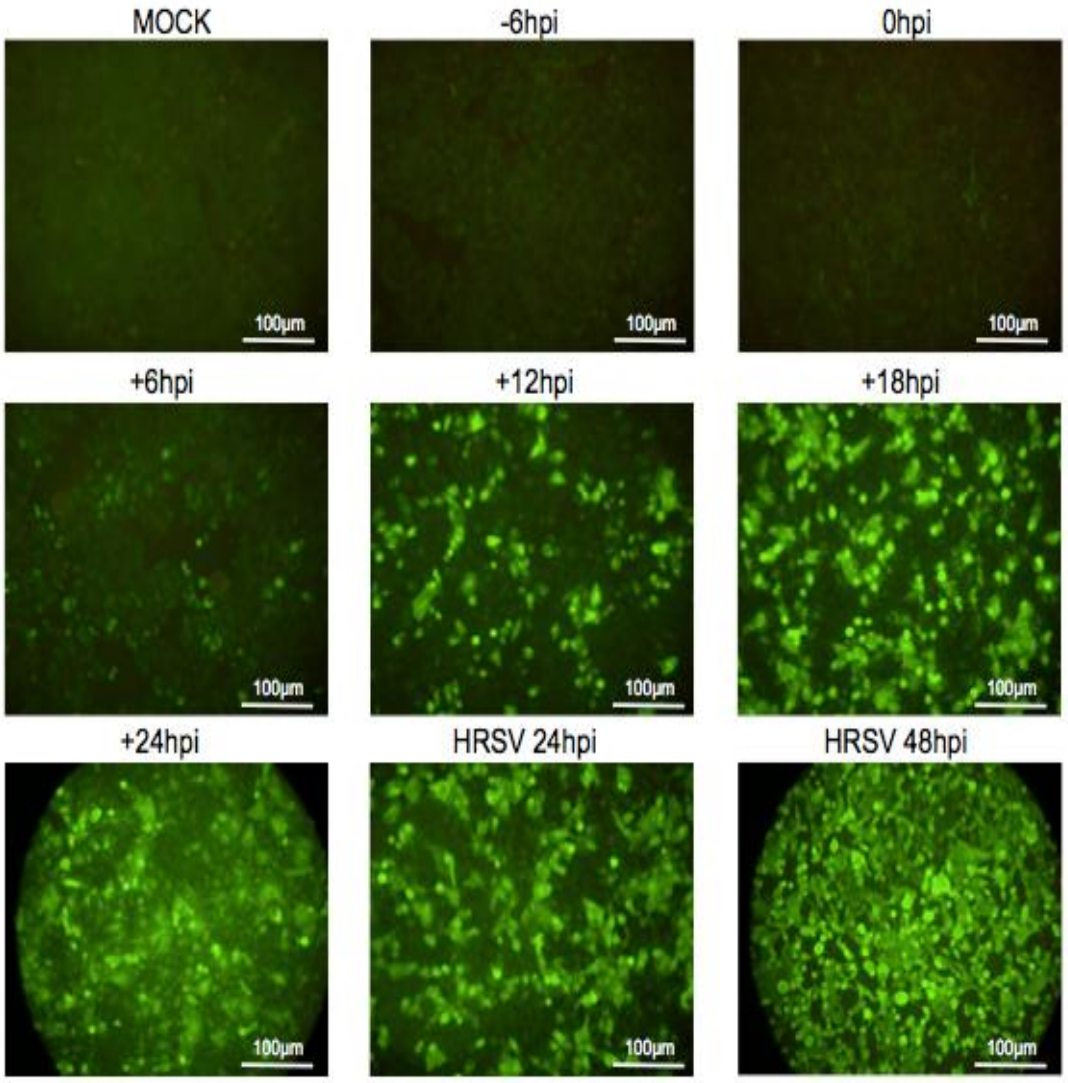


***Figure 3.4*** *Indirect Immunofluorescence showing the time points tested in HEp-2 cells. Mock (cells only), -6 hr post-infection (treated 6 h before infection), 0 hr post-infection (treated and infected at the same time), +6 hr post-infection (treated after 6 hr of infection), +12 hr post-infection (treated after 12 hr of infection), +18 hr post-infection (treated after 18 hr of infection), HRSV (positive control harvested at 24 hr post-infection), +24 hr post-infection (treated after 24 hr post infection) and HRSV 48 hr (positive control harvested at 48 hr post- infection). Ribavirin, at 500 µM, was used in all treated time points and HRSV-A2 at MOI 0.5 in all infected time points. The*

*IF analysis demonstrated that no virus was able to grow at -6 and 0 hr post-infection, hence ribavirin stoppeded replication. At +6, +12, +18 and 24 hr post-infection virus grew with varying degrees. HRSV viral proteins were labeled with goat ant-HRSV antibody and conjugated with donkey anti-goat FITC fluorescent antibody. For each of the IF picture the scale bar is shown.*

Indirect immunofluorescence was demonstrated (Figure 3.4) at all time points which were explained in Figure 3.3. Mock (cells only), -6hpi (treated 6 hr before infection) as a model for prophylaxis, 0 hr post-infection (treated and infected at the same), +6 hr post-infection (treated after 6 h of infection), +12 hr post-infection (treated after 12 h of infection), +18 hr post-infection (treated after 18 hr of infection), HRSV (positive control harvested at 24 hr post-infection), +24 hr post-infection (treated after 24 hr post infection) and HRSV 48 hr (positive control harvested at 48 hr post infection). As can be seen from (Figure 3.4) adding ribavirin 6 hr before infections prevented the infection; also adding the ribavirin and infection at the same time (0 hr post-infection) appeared to prevent viral growth (as determined by fluorescence). However, there was a small amount of fluorescence when ribavirin was added 6 hr post-infection and it appeared that some cells stained with green were infected with the virus. Whereas, at later time points; 12, 18, 24 hr post-infection, most of the cells were infected and these indicated that the addition of ribavirin 500 µM at late times points did not appear to inhibit the virus – as determined by fluorescence. Therefore, an alternative technique, western blot (Figure 3.5) was used to investigate this inhibition in more depth to compare viral proteins in the presence and absence of ribavirin.

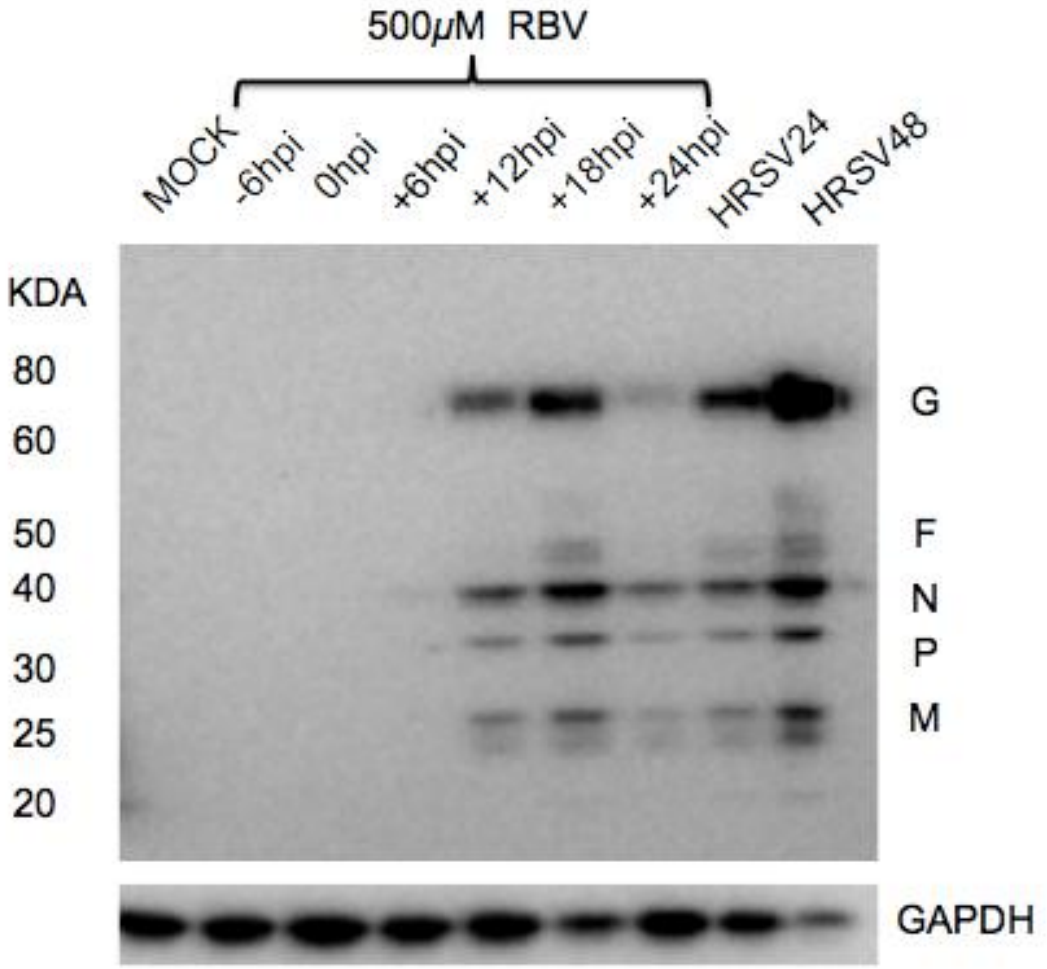


***Figure 3.5*** *Western blot with the selected assay time points in HEp-2 cells. Mock (cells only), -6 hr post-infection (treated 6 hr before infection), 0 hr post-infection (treated and infected at the same time), +6 hr post-infection (treated after 6 hr of infection), +12 hr post-infection (treated after 12 hr of infection), +18 hr post-infection (treated after 18 hr of infection), HRSV (positive control harvested at 24 hr post-infection), +24 hr post-infection (treated after 24 hr post infection) and HRSV 48 hr (positive control harvested at 48 hr post-infection). The HRSV infection was at MOI 0.5 and 500 μM of ribavirin treated. Primary antibody diluted was 1:1000 goat anti-HRSV antibody and 1:2500 rabbit anti-goat antibody and the products corresponding to the HRSV*

*proteins are labelled. GAPDH was probed after striping the membrane to confirm equal protein loading.*

All time points (in triplicates) that were tested by western blot (Figure 3.5); Mock (cells only), -6 hr post-infection (treated 6 hr before infection) as prophylaxis, 0 hr post-infection (treated and infected at the same), +6 hr post-infection (treated after 6 hr of infection), +12 hr post-infection (treated after 12 hr of infection), +18 hr post-infection (treated after 18 hr of infection), HRSV (positive control harvested at 24 hr post-infection), +24 hr post-infection (treated after 24 hr post-infection) and HRSV 48 hr (positive control harvested at 48 hr post-infection). 500 µM of ribavirin was used in all treated time points. As can be seen from Figure 3.5 adding ribavirin 6 hr before infection and at the same time of infection (0 hr post-infection) no viral proteins were observed indicating that growth of the virus was inhibited. Moreover, adding ribavirin 6 hr post-infection only the N protein could be visualised, suggesting an impairment of replication compared to the controls. However, at later time points; 12, 18, 24 hr post-infection, the G, F, N, P and M proteins were present. These results indicated that 500 µM ribavirin has an inhibitory affect when applied early in infection.

Progeny virus production was also assayed. $TCID_{50}$ (Figures 3.6 A and B) have demonstrated the average of viral progeny production from all time points in HEp-2 cells in triplicates. The data from both intra-cellular and extra-cellular virus indicated that 500 µM ribavirin significantly reduced progeny virus production by 24 hr post-infection when added at -6 hr post-infection, 0 hr post-infection, +6 hr post-infection and +12 hr post-infection when compared to progeny virus production in untreated infected cells. In infected

cells treated with 500 μM ribavirin at +24 hr post-infection and virus biology and progeny virus production determined at +48 hr post-infection, there was no significant difference in progeny virus, compared to untreated infected cells. Indicating that to be effective, ribavirin should be applied early in infection.

**A**

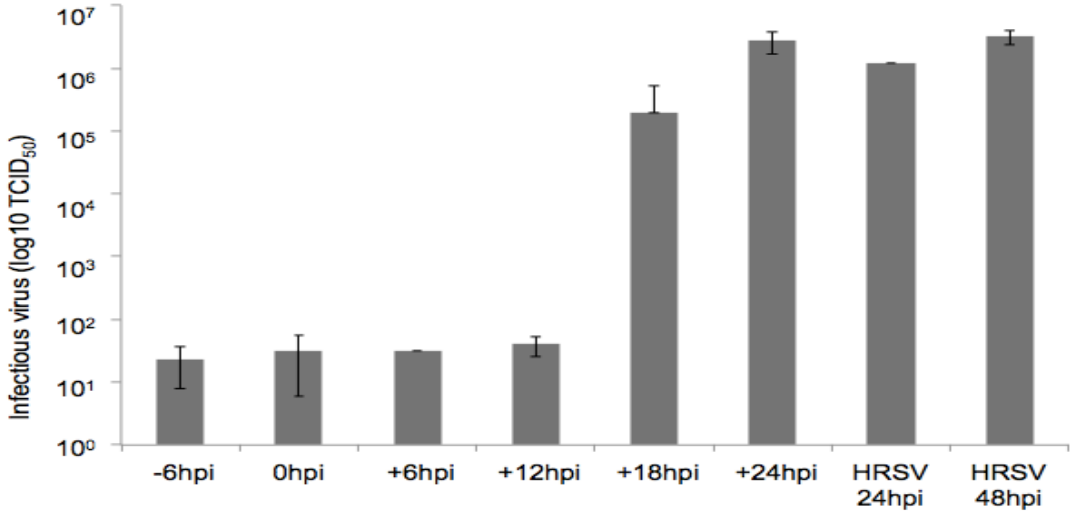


**B**

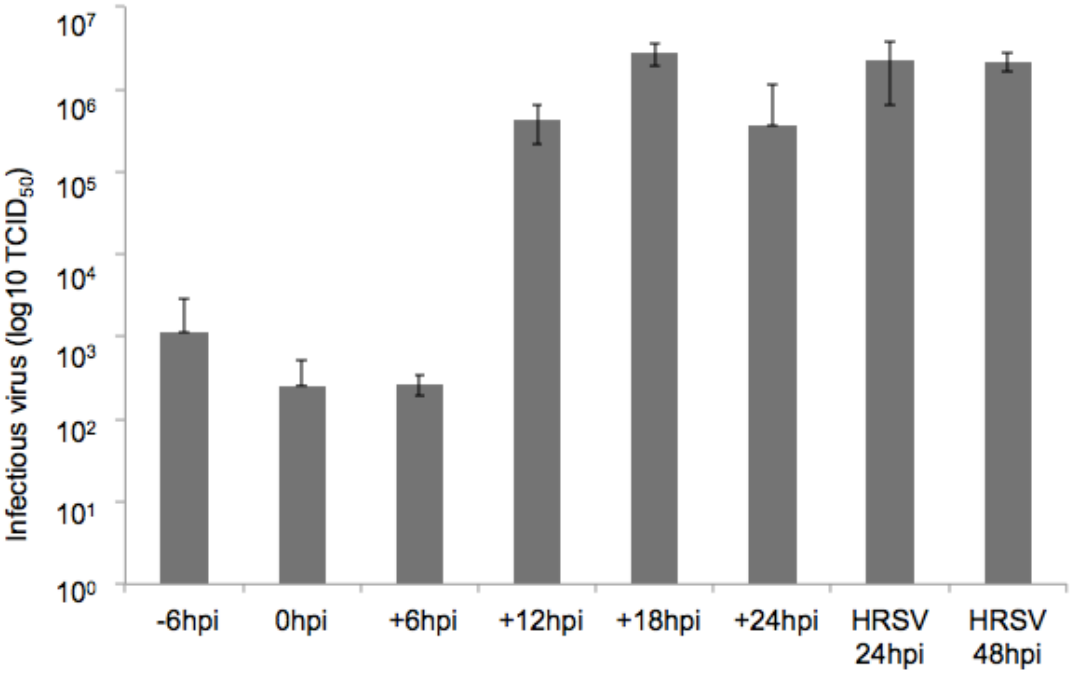


***Figure 3.6*** *Tissue culture Infectious dose, $TCID_{50}$, in both (A) intra-cellular and (B) extra-cellular showing all time points in HEp-2 cells; -6 hr post-*

*infection (treated 6 hr before infection), 0 hr post-infection (treated and infected at the same time), +6 hr post-infection (treated after 6 hr of infection), +12 hr post-infection (treated after 12 hr of infection), +18 hr post-infection (treated after 18 hr of infection), HRSV (positive control harvested at 24 hr post-infection), +24 hr post-infection (treated after 24 hr post-infection) and HRSV 48 hr (positive control harvested at 48 hr post-infection). 500 μM of ribavirin was used in all treated time points.*

All data by immunofluorescence, western blot and $TCID_{50}$ indicated that 500 µM ribavirin significantly reduced virus biology and progeny virus production by 24 hr post-infection when added at -6, 0, +6 and +12 hr post-infection when compared to progeny virus production in untreated infected cells. In infected cells treated with 500 µM ribavirin at +24 hr post-infection and virus biology and progeny virus production determined at +48 hr post-infection, there was no significant difference in progeny virus, compared to untreated infected cells (Figures 3.4, 3.5 and 3.6). Therefore application of ribavirin at +24 hr post-infection will be predicted to affect viral RNA and protein synthesis after this time point, and impinge on a second round of infection. This is indicated by a reduction in the abundance of viral proteins, reflected by both immunofluorescence and western blot analysis (Figures 3.4 and 3.5). From this analysis, two time points were selected for the investigation using high-resolution approaches; 500 µM ribavirin added at +6 and +24 hr post-infection, with an assay point of purifying cellular RNA and proteins at +24 hr post-infection and +48 hr post-infection, respectively.

### 3.2.4 THE EFFECT OF DMSO, AND RIBAVIRIN ON INFECTED CELLS

DMSO was added to dissolve the ribavirin stock. It is important to assess the potential effect of DMSO on the cells and also on the infected cells with HRSV, as this may impinge on the interpretation of the data. To assess the effect of DMSO: different experiments were performed to assess virus biology; $TCID_{50}$ – measuring and comparing the titre of progeny virus (Figure 3.7), western blot to compare viral protein abundance (Figure 3.8) and

immunofluorescence to provide an overall visual guide of the number of infected cells (Figure 3.9). The data indicated that there was no significant effect of DMSO on virus biology by measuring these three parameters, with the optimal MOI of 0.5 (Figures 3.7, 3.8, 3.9).

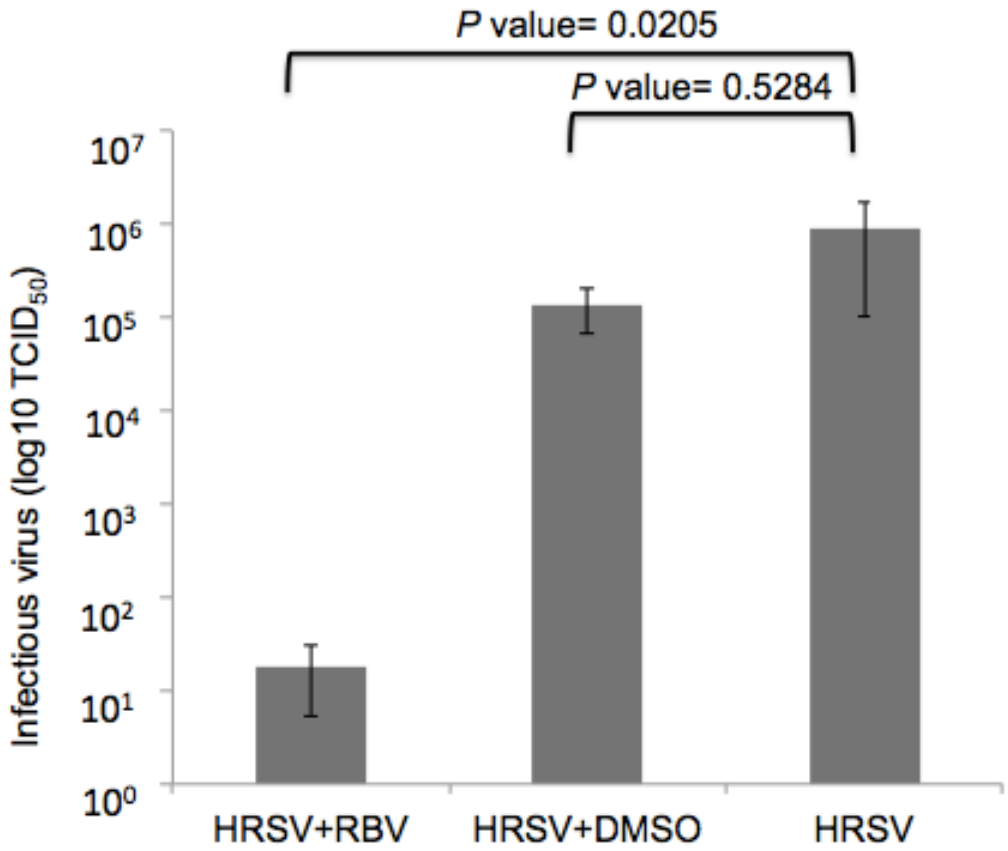


***Figure 3.7*** *Progeny virus production was compared in the presence and absence of RBV and DMSO only control. Tissue culture Infectious dose $TCID_{50}$ analysis of extra-cellular virus production been diluted on samples HRSV, HRSV+DMSO and HRSV+RBV in HEp-2 cells and syncytia counted in the day seven of the infection. All samples were infected with HRSV-A2, MOI 0.5. Ribavirin and DMSO were added after 6 hr post-infection and all samples have harvested after 24 hr post-infection and performed in serial dilution and added to 96 well plates that have cells already confluent. This graph indicates a statistically significant difference P<0.05 of log10 TCID50 titer mean between HRSV+RBV vs HRSV. However, there was no significant difference between HRSV+DMSO vs HRSV P>0.05. Statistical analysis was performed using Kruskal-Wallis test.*

There was no significant effect of DMSO on infected cells compared to cells infected only (*p* value=0.5284) on extra-cellular (progeny virus in the supernatant) by $TCID_{50}$. However, the data indicated that the amount of progeny HRSV, from cells infected with MOI of 0.5, was significantly reduced by approximately 5 logs in the presence of 500 μM ribavirin compared to either infected cells untreated or treated with the DMSO only.

Western blot (a semi-quantitative method) and immunofluorescence were used to study the effect of DMSO on the abundance of viral proteins and general infectivity (Figures 3.8 and 3.9, respectively) with the following conditions: Mock (cells only), DMSO (added to cells), +6hpi (treated after 6 h of infection), RBV (500 μM ribavirin added to cells), HRSV (positive control harvested at 24 hr post-infection), HRSV+DMSO (DMSO was added to infected cells at 6 hr post-infection), HRSV+RBV (500 μM ribavirin was added to infected cells at 6 hr post-infection). Taken together, these results indicated that adding DMSO on cells and on infected cells with HRSV MOI 0.5 resulted in stable affect compared to mock-untreated and infection with HRSV, respectively.

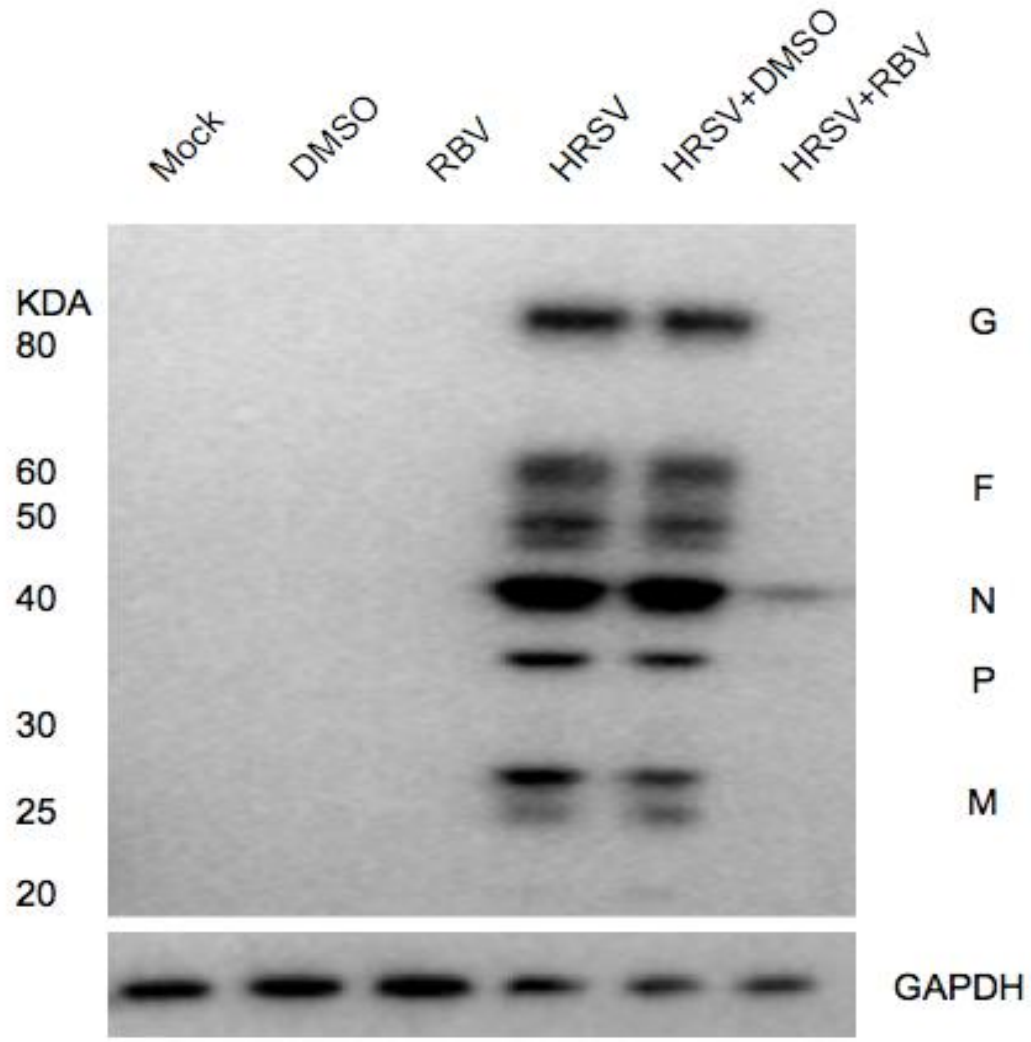


***Figure 3.8*** *Western blot analysis on 24 hr post-infection in continuous HEp-2 cells that infected with HRSV-A2 at an MOI 0.5. Cells lysates were examined by SDS-PAGE followed by western blot. The infections were confirmed using a (primary antibody) anti-HRSV 1:1000 goat anti-HRSV antibody (Abcam 20745) and (secondary antibody) 1:2500 rabbit anti-goat antibody and the bands corresponding to the HRSV proteins. Antibody specific for GAPDH (as indicator for equal protein load) mouse anti-GAPDH (primary antibody) 1:5000 (Abcam 8245) and (secondary antibody) 1:2500 mouse (Abcam 4116) was used after striping the membrane to test loading samples.*

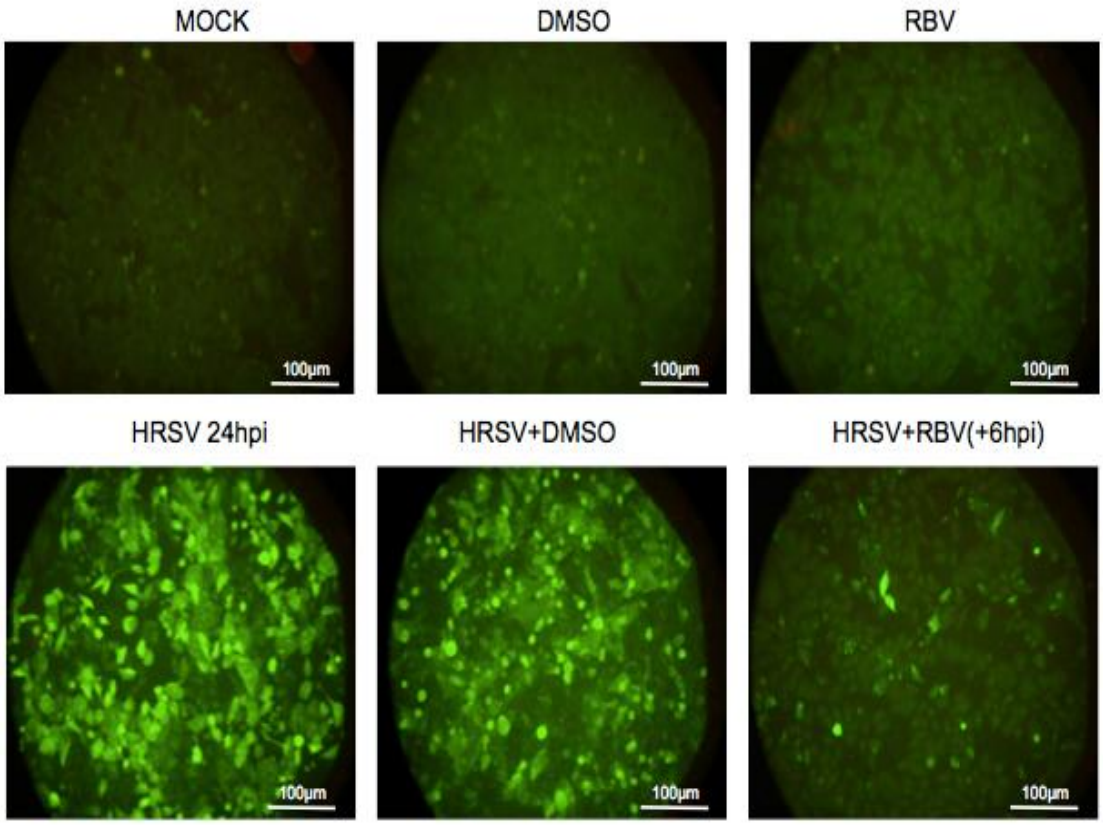


***Figure 3.9*** *Direct Immunofluorescence analysis in continuous cell culture HEp-2 in response to infection with HRSV-A2 at 24 hr post-infection. Mock (cells only), DMSO (added to cells), +6hpi (treated after 6 hr of infection), RBV (500 µM ribavirin added to cells), HRSV (positive control harvested at 24 hr post-infection), HRSV+DMSO (DMSO was added to infected cells at 6 hr post-infection), HRSV+RBV (500 µM ribavirin was added to infected cells at 6 hr post-infection). All samples after 24 hr post-infection were washed by PBS, fix by %4 PFA and permeabilised. FITC conjugated HRSV primary antibody (Abcam 20391) diluted 1:50 (v/v) and added on the top of coverslips (where cells there) for 1 hr at dark in the room temperature and mounted on slides microscopy. For each of the IF picture the scale bar is shown.*

Taken together these results suggested that there was no effect of DMSO on virus biology. Hence, DMSO was used to dissolve ribavirin; it is necessary to analyse any effect that might occurred.

## 3.3. DISCUSSION

The results of this chapter provided analysis data for the optimisation of the RNA-seq and proteomic to study the effect of ribavirin on the abundance of host and viral gene products and also the viral genome. The optimisation considered both infection of the virus and toxicity of ribavirin and the DMSO. HEp-2, a lung cell line, was used as a model system to study the effect of ribavirin in the presence and absence of infection. The continuous cell type HEp-2 has previously been used to study cell viability with anti-viral drugs and HRSV infection (Currie *et al.*, 2013; Donalisio *et al.*, 2012; Hughes *et al.*, 1988; Shah *et al.*, 2010). This study employed both quantitative and qualitative techniques to assess the concentrations of ribavirin, HRSV MOI and time points that could be used. The qualitative methods used involved direct immunofluorescence assay and western blot and $TCID_{50}$. These demonstrated the infection of cells by HRSV-A2 with/without ribavirin antiviral treatment, while no cells were infected in mock-infected/treated, thus providing a clear discriminator for the comparative techniques and demonstrating virological methodologies that have no cross contamination. The findings of these independent analyses also showed a significant reduction of infection when ribavirin was added, in line with previous literature and expected results (Debing *et al.*, 2014; Wyde *et al.*, 2003). The measurement of progeny virus using $TCID_{50,}$ as a quantitative approach, provides a direct measure of output virus and allows the comparison of ribavirin treatment on viral load.

As well as a quantitative methods, the MTT assay was also used with different concentrations of ribavirin for 24 hr post-treated on HEp-2 cells (Figure 3.1) in order to assess the viability of cells and optimise ribavirin treatment from the perspective of cell viability. The result indicated that at concentrations below 500 µM of ribavirin cells were more viable; however, any concentrations above 500 µM of ribavirin cells were less viable. Therefore, 500 µM of ribavirin was selected as the $EC_{50}$. This concentration of ribavirin has been used with other viruses to investigate its effects in cell culture models e.g. Vesicular Stomatitis virus and Sendai virus (Shah *et al*., 2010). For comparison of the ribavirin treatments, untreated cells were used to measure the total viable cell population, whereas, etoposide, which promotes apoptosis was used as a positive control for cell death, and hence for loss of cell viability. Multiplicity of infection (MOI) on the other hand, was used to determine the proportion of cells infected by immunofluorescence assay. Different MOIs (MOI 5, 0.5, 0.05 and 0.005) at 48 hr post-infection (Figure 3.2) were used to maximize cells infection. Moreover, the same MOIs were used and treated with 500 µM of ribavirin at 24 hr post-infection in order to confirm that this concentration of ribavirin was effective on disrupting virus biology in a measurable way. The data indicated that at MOI of 0.005 and 0.05, ribavirin 500 µM were effective in reducing the amount of HRSV, but only few cells were infected. Immunofluorescence analysis indicated that at MOI 5 majority of the cells were infected, but there was little apparent difference in infection with HRSV between the ribavirin treated or untreated cells. In contrast, at MOI of 0.5, majority of the cells were infected, but 500 µM ribavirin resulted in a decrease in the proportion of stained cells.

A time course assay was used to determine which time point was best to perform the 500 μM anti-viral ribavirin administration into infected cells with at an MOI of 0.5, in order to investigate the influence of ribavirin on infected cells. Several methods were established to investigate virus biology; namely indirect immunofluorescence, western blot and $TCID_{50}$ (Figures 3.4, 3.5, 3.6). Considering that ribavirin could be added before the infection as prophylaxis or after the infection as treatment (Zhang *et al.*, 2003), several different treatment options were used; -6 hr prior to infection and +6, +12, +18, and +24 hr post-infection. Also, in this study, two times points; 24 and 48 hr post-infection without treatment were included as a positive control. The findings of these independent analyses demonstrated that adding ribavirin 6 hr before infection was effective at preventing viral growth. However, there was a slight increase in viral growth when adding ribavirin at 6 hr post-infection. Only N protein of HRSV at 6 hr post-infection was detected by western blot, whereas, other late time points; 12, 18, 24 hr post-infection, viral proteins G, F, N, P and M were detected, indicating that 500 μM ribavirin was unable to prevent the infection and no significant difference in progeny virus, compared with untreated infected cells.

Therefore, taken together the following study design (Figure 3.10) was used to investigate the effects of ribavirin on cell and virus biology using the high-resolution approaches described in the subsequent chapters. Six condition samples; Mock (non-infected and non-treated cells), DMSO (uninfected cells but treated with DMSO only), ribavirin (uninfected cells but treated with 500

μM ribavirin), HRSV (infected but un-treated cells), HRSV+DMSO (infected but cells treated with DMSO) and HRSV+RBV (infected but cells treated with 500 μM ribavirin). The MOI was 0.5. The experiments were conducted in triplicate.

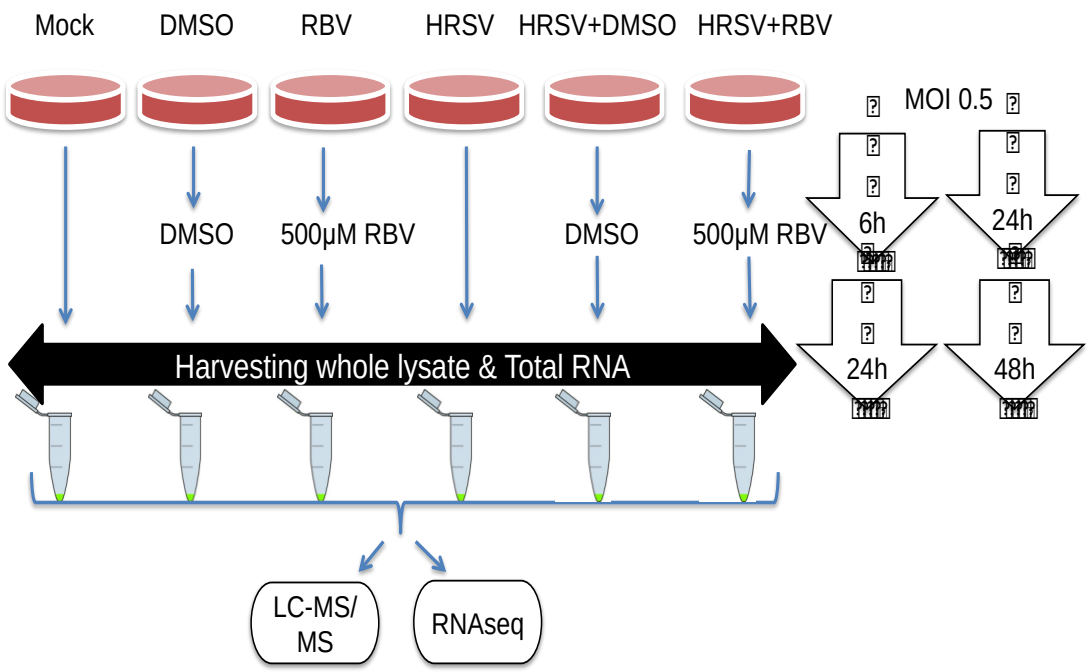


***Figure 3.10*** *Study design of the main experiments for label free quantitative proteomics and RNA-seq. This design shows all control samples (negative and positive) in all experiments; immunofluorescence, Western Blot, Proteomics and deep sequences. Mock (cells only, and no virus and no drug), DMSO only, RBV only 500 µM concentration, HRSV only, HRSV+DMSO, and HRSV+RBV adding 500 µM of ribavirin after 6 hr post-infection (early time point) and after 24 hr post-infection (late time point).*

# CHAPTER 4: INVESTIGATING THE EFFECT OF THE ANTI-VIRAL RIBAVIRIN ON CELLS INFECTED AND UNINFECTED WITH HRSV USING LABEL FREE PROTEOMICS AND TRANSCRIPTOMICS

## 4.1 INTRODUCTION

Human respiratory syncytial virus (HRSV) is one of the major lower respiratory tract pathogens and infants are infected at least once within the first two years of life (Collins & Graham, 2008). There is no vaccine for HRSV or general anti-viral therapy. In acute cases, HRSV infection is treated therapeutically with ribavirin, a broad spectrum anti-viral, whose mechanism of action is not clearly understood. Ribavirin is the only therapeutic approved by the Food and Drug Administration (FDA) for the treatment of HRSV (Chu *et al.*, 2013). Clinically ribavirin tends not to be used due to several factors including evidence of marginal efficacy and no difference in the length of stay in hospital for treated versus untreated patients. However, ribavirin may also be used in immune-compromised and/or transplant and acute high-risk groups infected with HRSV for example see (Waghmare *et al.*, 2013). Ribavirin has broad-spectrum antiviral properties and apart from HRSV is also used clinically in the treatment of hepatitis E virus (Kamar *et al.*, 2014) and hepatitis C virus (HCV), where the treatment has been shown to have mutagenic effect on the viral genome (Dietz *et al.*, 2013). Ribavirin is also used in the treatment of disease caused by hemorrhagic fever viruses (for example see (Soares-Weiser *et al.*, 2010). The drug has been described as a being active against a number of viruses with RNA and DNA genomes, and can be considered a broad-spectrum anti-viral inhibitor.

The mechanism of action of ribavirin in many cases is unknown. Several hypotheses for a mode of action have been advanced. Ribavirin treatment may cause loss of fitness in RNA virus genomes. Ribavirin is a base analog of either adenine or guanine and thus can base pair with cytosine or uracil. For RNA viruses, ribavirin might be incorporated into genomic RNA by the RNA-dependent RNA polymerase during replication. In terms of base, G→A mutations were predicated to be induced by incorporation of ribavirin triphosphate as a GTP nucleoside analog during positive strand RNA synthesis, however C→T mutations were predicated to be the result of ribavirin incorporation during negative strand synthesis. The result is termed hyper-mutation that can be lethal to virus biology through error catastrophe. This mechanism of action has been proposed and supported by experimental data *in vitro* for poliovirus (Crotty *et al.*, 2001) and HCV and *in vivo* for HCV (Dietz *et al.*, 2013). There are two types of DNA substitution mutations; transitions are a point mutation that changes purine/purine nucleotides (A↔G) or pyrimidine/pyrimidine nucleotides (C↔T) and transversions are interchanges of purine/ pyrimidine (A↔T, A↔C, C↔G, G↔T) (Figure 4.1) (Collins & Jukes, 1994).

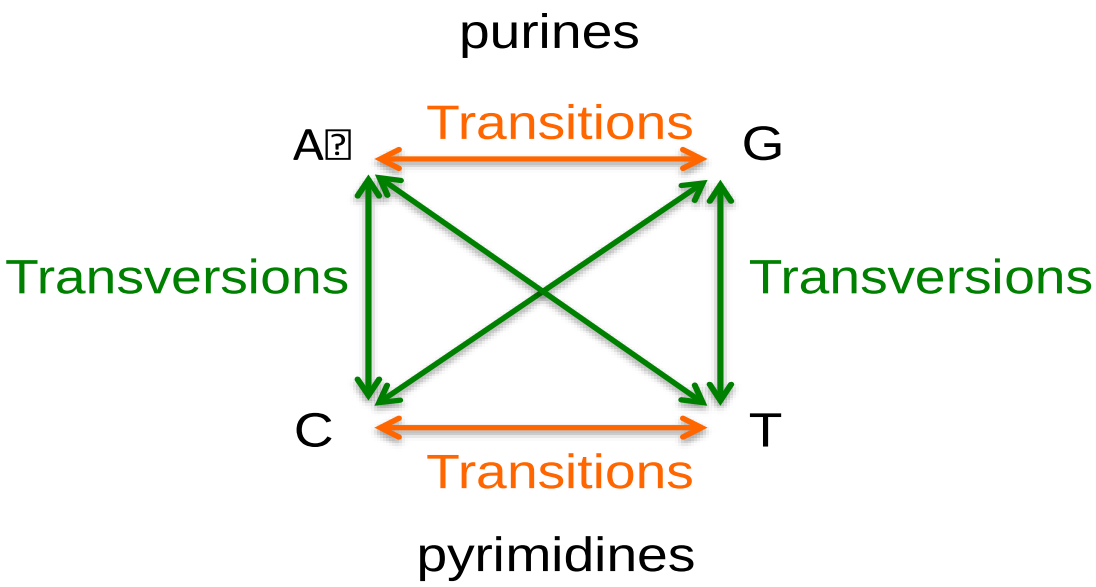


***Figure 4.1*** *Definition of transition and transversion mutations. Shows the purine/pyrimidine transversions, the purine/purine and pyrimidine/pyrimidine transitions.*

Ribavirin may cause up-regulation of anti-viral gene products inside the cell in the absence of infection. Micro-array analysis suggested that ribavirin can directly up-regulate antiviral gene expression including STAT-1α and STAT-1β in HRSV-infected cells (Zhang *et al.*, 2003). Intracellular pools of GTP have been shown to be depleted in ribavirin treated cells through inhibition of cellular inosine monophosphate dehydrogenase IMPDH. This has been suggested to be correlated with the inhibition of flavivirus (including yellow fever virus) and paramyxovirus replication (Leyssen *et al.*, 2005; Leyssen *et al.*, 2006). Ribavirin can also affect the translation of eukaryotic mRNAs and has been proposed as a therapeutic for acute myeloid leukemia (Tamburini *et al.*, 2009) and has been shown to act as a competitive inhibitor of the methyl 7-guanosine (m(7)G) cap, the natural ligand of the translation initiation factor eIF4E (Volpon *et al.*, 2013).

GTP depletion by ribavirin may act in concert to increase its incorporation into viral genomes thus increasing error prone replication as has been suggested for West Nile virus (Day *et al.*, 2005).

The objective of this chapter was to investigate the action of ribavirin on the host cell and HRSV biology in general, a combined high-resolution RNA-seq and deep discovery label free quantitative proteomics approach was used to analyze infected cells. The potential direct mutagenic effect of ribavirin on the HRSV genome is described in Chapter 5. Quantitative label free proteomics and RNA-seq were used to quantify changes in the abundance of cellular and viral proteins and genes, respectively. From the analysis in Chapter 3, two time points were selected for investigation using label free proteomics approaches; based upon the time course analysis several experimental conditions to assess the effects of 500 μM ribavirin on virus were set up at +6 hr post-infection (assay point +24 hr post-infection) and +24 hr post-infection (assay point +48 hr post-infection) (Figure 3.7).

The data indicated that the abundance of cellular mRNAs and proteins altered in the presence of ribavirin; antiviral response was the top pathway significantly increased in infected-cells and untreated with ribavirin. Whereas cell death and survival were the top molecular and cellular functions in infected and cells-treated. Also, the proteomics and transcriptomics data demonstrated the viral proteins and genes significantly decreased in the presence of ribavirin, confirming its antiviral mode of action.

Some of the work (mainly the chaperone proteins which were detected in mock vs HRSV infected cells) described in this chapter has recently been published in the Journal of Virology. Diane C. Munday, Weining Wu, Nikki Smith, Jenna Fix, Sarah Louise Noton, Marie Galloux, Olivier Touzelet, Stuart D. Armstrong, Jenna M. Dawson, **Waleed Aljabr**, Andrew J. Easton, Marie-Anne Rameix Welti, Andressa Peres de Oliveira, Fernando M. Simabuco, Armando M. Ventura, David J. Hughes, John N. Barr, Rachel Fearns, Paul Digard, Jean-François Eléouët, Julian A. Hiscox (2015) Interactome Analysis of the Human Respiratory Syncytial Virus RNA Polymerase Complex Identifies Protein Chaperones as Important Cofactors That Promote L-Protein Stability and RNA Synthesis J. Virol. vol. 89 (2): 917-930. (See appendix). Also, A manuscript is currently in preparation using the most data in this chapter.

The candidate confirms that the work submitted is his own, except where work which has formed part of jointly-authored publications has been included. The contribution of the candidate and the other authors to this work has been explicitly indicated below. The candidate confirms that appropriate credit has been given within the thesis where reference has been made to the work of others.

**Chapter 4** of this thesis was based on the work from jointly-authored publication:

- Diane Munday and Weining Wu planned the experiments, optimised and performed data analyses and subsequent immunoblot and

immunofluorescence confocal analyses, prepared tables and figures and jointly wrote the manuscript.

- Olivier Touzelet expertise regarding mice experiments.
- Stuart Armstrong run samples and helped on MS-proteomic analysis.
- Jenna M. Dawson helped on western blot.
- Waleed Aljabr prepared samples for MS-proteomics and performed data analysis the chaperone proteins which were detected in mock vs HRSV infected cells.
- Jenna Fix, Sarah Noton, Marie Galloux, Andrew Easton, Marie-Anne Welti, Andressa Peres de Oliveira, Fernando Simabuco, Armando Ventura and David Hughes provided expertise and advice.
- Nikki Smith and Paul Digard carried out pluse chase experiments with the mini genome system.
- Jean-François Eléouët provided the EGFP-L constructs, support plasmid and expertise.
- John N. Barr, Rachel Fearns and Julian A. Hiscox jointly wrote the manuscript.

## 4.2. RESULTS

Both RNA-seq and label free quantitative proteomics were used to identify and quantify cellular and viral RNA and proteins, respectively. These were in several experimental conditions; mock-infected and mock-treated cells; mock-infected cells treated with (DMSO) only; mock-infected cells treated with 500 μM ribavirin; HRSV-infected cells; HRSV-infected cells treated with the DMSO only; HRSV-infected cells treated with 500 μM ribavirin. These conditions were investigated in triplicate using the high-resolution approaches. Quantitative label free proteomics was used to identify and quantify proteins in whole cell lystates and this returned an average of 2616 proteins. Several selection criteria were used to improve the confidence in the identification of proteins. Individual ion scores > 13 indicated identity or extensive homology ($p < 0.05$) and using a criterion of two or more peptides pre-selected 1721 proteins and the abundance of these proteins was then compared across the six different treatment conditions. For the proteomic analysis, the data was presented as volcano plots, which allow the visualization of proteins that are significantly increased and decreased in abundance and points are plotted against abundance and *p*-value. For RNA-seq analysis, total RNA was prepared from cells with the different experimental conditions. It is important to mention that the *p*-value was used to standardize the analysis of RNA-seq data and proteomics data. Also, data presented in this chapter is based on the 24 hr post-infection assay point. This is because the effect of ribavirin at 48 hr post-infection, when the drug was added after 24 hr of virus replication, was limited and no apparent decrease in progeny virus production was noted.

### 4.2.1 THE EFFECT OF DMSO AND RIBAVIRIN ONLY ON THE HOST CELL

Ribavirin was added to cells in a DMSO. To assess the potential effect of DMSO on host cell biology, the proteomics datasets for mock-infected cells on both untreated and treated with DMSO were compared (Figure 4.1 A). Supplementary tables I and II (see appendix) respectively show the identified proteins that were decreased or increased significantly. The transcriptomics datasets for mock-infected cells of both untreated and treated with DMSO were also compared (Figure 4.2 B). Supplementary tables III and IV (see appendix) list the genes that were significantly decreased or increased in abundance. This data indicated, for the +6hpi (assay point +24hpi), that out of a total of 1720 proteins identified and quantified by 2 or more unique peptides, 6 cellular proteins increased in abundance and 2 cellular proteins decreased in abundance in the presence of DMSO (~0.4%).

There was a good correlation between the abundance of both proteins and mRNAs (Figure 4.2 B). RNA-seq comparison between untreated and cells treated with DMSO for the +6hpi (assay point +24hpi) treatment indicated that 13 transcripts were significantly increased in abundance greater than 2-fold in the presence of DMSO, whereas 50 transcripts significantly decreased in abundance (Figure 4.2). This indicated that out of 62844 surFit transcripts that DMSO had a slight effect (~0.1%) on host cell transcription, but the abundance of most transcripts and the corresponding proteins remained unchanged (Figure 4.2).

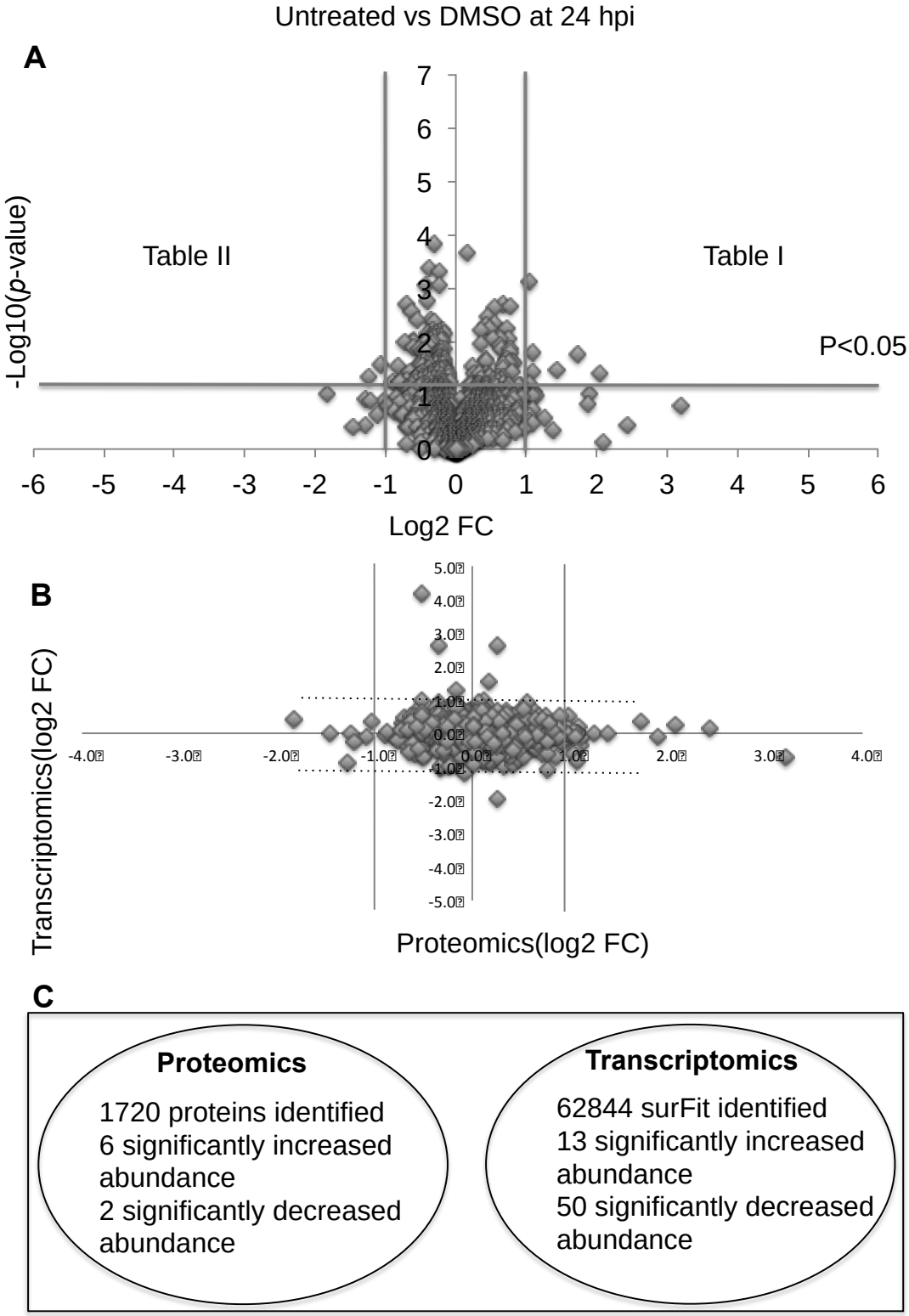


***Figure 4.2*** *(A) Volcano plot representing results of the label-free LC-MS/MS of mock-infected cells-untreated verses DMSO untreated at 24 hpi. The gray*

*line in the middle shows where p value of 0.05 with points above the line having a p value <0.05 and points below the line having a p value >0.05. Two cellular proteins increased in abundance and 6 cellular proteins decreased in abundance in the presence of DMSO. (B) Showing the match between transcript (y-axis) and protein (x-axis) abundance. The $log_2$ fold change identified was calculated for both transcript and protein. The corresponding values were then plotted on the histogram in similar fashion for each of the genes. (C) Venn diagram showing numbers of genes and proteins identified in mock-infected, untreated and treated with DMSO. The data indicates for the +6hpi (assay point +24hpi), that out of a total of 1716 proteins (identified and quantified by 2 or more unique peptides) 2 cellular proteins increased in abundance and 6 cellular proteins decreased in abundance in the presence of DMSO. Likewise, RNA-seq from 62844 surFit (identified and quantified by $log_2$ fold change) 13 significant genes increased in abundance and 51 significant genes decreased in abundance.*

The addition of ribavirin at +6hpi (assay point +24hpi) resulted in, based on filters that been used, 6 cellular proteins being increased in abundance and 4 cellular proteins being decreased in abundance (Figure 4.3). Tables 4.1 and 4.2 show proteins that were significantly decreased and increased in abundance, respectively). The proteomic data indicated that UTP14A, decreased in abundance by approximately 6-fold in cells treated with DMSO and ribavirin compared to cells treated with DMSO only. This protein is involved in RNA metabolism and is involved in ribosome biogenesis and 18S rRNA synthesis. From the proteomic data sets, SLC29A1, solute carrier family 29, (Equilibrative nucleoside transporter protein), was identified in both the analysis of cells treated with DMSO and the analysis of cells treated DMSO plus ribavirin, as being increased in abundance. This protein increased approximately 2-fold in abundance, in both cases, and may be attributed to the potential action of DMSO on cells.

For RNA-seq analysis at this time point and treatment condition, out of 62,844 surFit transcripts, 389 were shown to have a significant increase abundance greater than 2-fold in the presence of ribavirin, whereas 253 transcripts were decreased more than 2-fold. For transcripts that increased in abundance in the presence of ribavirin, these included connective tissue growth factor (CTGF) (8-fold), Cytochrome P450, family 1, subfamily A, polypeptide 1 (CYP1A1) (7-fold) (involved in drug metabolism), interleukin-6 (6 fold), Chemokine (C-X-C motif) ligand 2 (CXCL2) (6-fold) and interleukin-7 receptor (IL7R) (6-fold) (involved in the development of immune cells). The transcript encoding 2'-5' oligoadenylate synthetase (OAS) (OASL) was

decreased in abundance approximately -5 fold at +6hpi (assay point +24hpi). The encoded protein family can bind double stranded RNA and has been reported to have anti-viral activity. Analysis indicated changes in both the transcriptome and proteome in the presence of ribavirin (Figure 4.3). In addition, the transcriptomic data pointed to activation of the c-fos and c-jun and NFKB (*p*-value of $1.92x10^{13}$) transcription pathways in the presence of ribavirin.

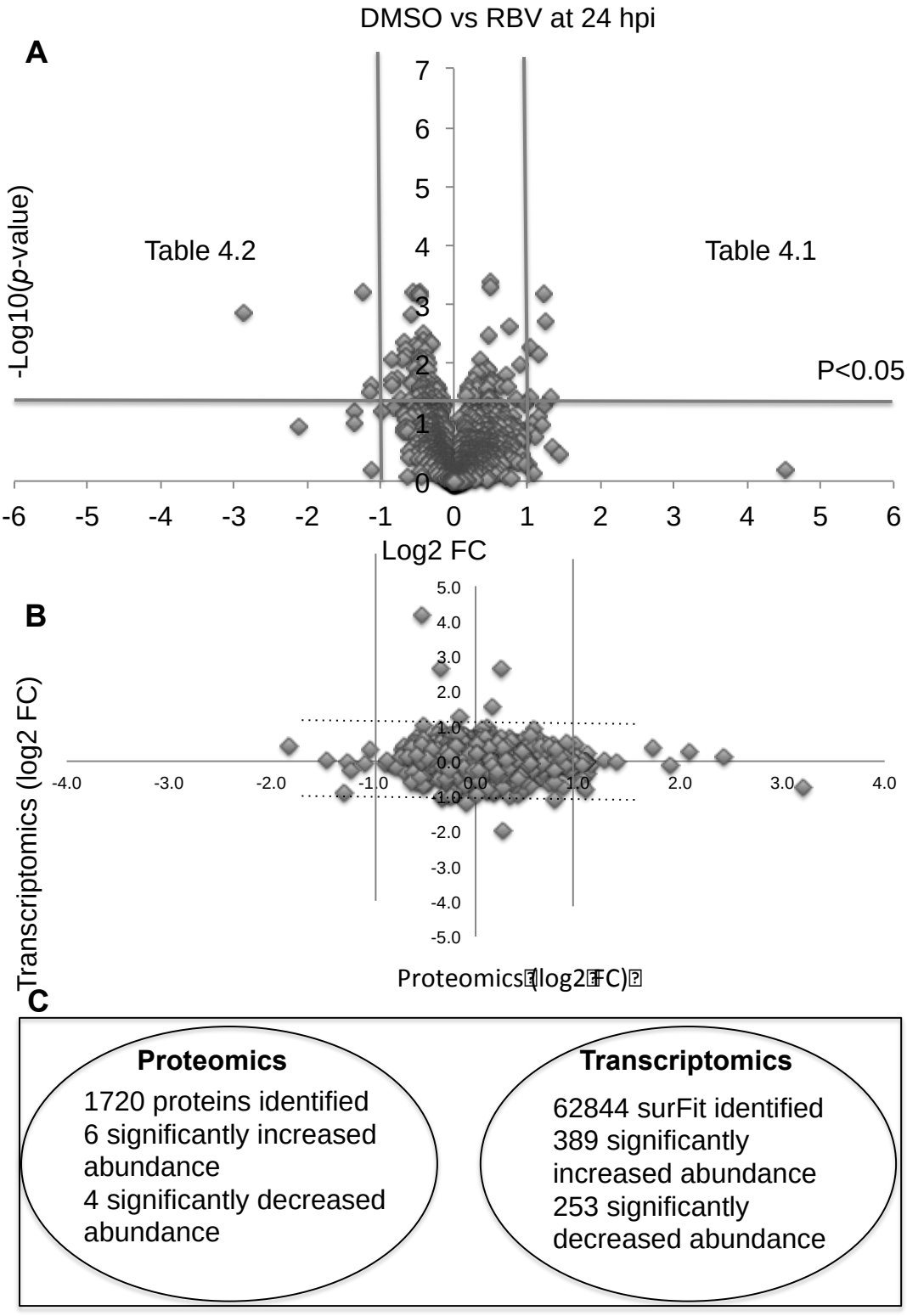


***Figure 4.3*** *(A) Volcano plot demonstrating the analysis of cells treated with DMSO and the analysis of cells treated with DMSO plus ribavirin at +6hpi (assay point +24hpi) resulted in 6 cellular proteins being increased in*

*abundance and 4 cellular proteins being decreased in abundance. (B) The match between transcript (y-axis) and protein (x-axis) abundance and the changes in the presence of ribavirin. The $log_2$ fold change identified was calculated for both transcript and protein. The corresponding values were then plotted on the histogram for the same each gene. (C) Venn diagram showing numbers of genes and proteins identified in mock-infected and untreated/ treated with DMSO. Analysis indicated changes in both the transcriptome and proteome in the presence of ribavirin but no significant matched. For RNA-seq analysis at this time point and treatment conditions, 389 mRNAs were shown to have a significant increase abundance greater than 2-fold in the presence of ribavirin, whereas 253 mRNAs were decreased more than 2-fold.*

**Table 4.1** Proteins increased in abundance in DMSO vs RBV (top right of Figure 4.3). Statistical analysis was based on observed fold change 2 or greater, and more than 2 peptides and a *p*-value less than 0.05. Proteins were identified and quantified by LC MS/MS.

| Gene name | Protein name | Peptide count | Peptides used for quantitation | $Log_2$ FC |
|---|---|---|---|---|
| SLC25A11 | Mitochondrial 2-oxoglutarate/malate carrier protein | 3 | 3 | 1.3 |
| TK1 | Thymidine kinase, cytosolic | 5 | 5 | 1.3 |
| SLC29A1 | Equilibrative nucleoside transporter 1 | 2 | 2 | 1.2 |
| TF1 | Protein ELYS | 2 | 2 | 1.2 |
| KIF11 | Kinesin-like protein KIF11 | 3 | 2 | 1.1 |
| PRPF6 | Pre-mRNA-processing factor 6 | 2 | 2 | 1.0 |

**Table 4.2** Proteins decreased in abundance in DMSO vs RBV (top left Figure 4.3). Statistical analysis was based on observed fold change 2 or greater, and more than 2 peptides and a *p*-value less than 0.05. Proteins were identified and quantified by LC MS/MS.

| Gene name | Protein name | Peptide count | Peptides used for quantitation | $Log_2$ FC |
|---|---|---|---|---|
| MRFAP1 | MORF4 family-associated protein 1 | 2 | 2 | -1.2 |

| | | | | |
|---|---|---|---|---|
| UTP14A | U3 small nucleolar RNA-associated protein 14 homolog A | 2 | 2 | -2.9 |
| RSL1D1 | Ribosomal L1 domain-containing protein 1 | 9 | 8 | -1.1 |
| BYSL | Bystin | 3 | 3 | -1.1 |

### 4.2.2 THE EFFECT OF HRSV WITH DMSO ON THE HOST CELL TRANSCRIPTOME AND PROTEOME

As would be predicted and has been previously characterized by both micro-array and proteomic analysis (Dave *et al.*, 2014; Hastie *et al.*, 2012; Martínez *et al.*, 2007; Munday *et al.*, 2010a; Ternette *et al.*, 2011; van Diepen *et al.*, 2010; Wu *et al.*, 2011), HRSV infection resulted in a number of changes in the abundance of host cell transcripts and proteins (e.g. for +6hpi (assay point +24hpi) Figure 4.3), with most changes reflecting an increased abundance of both transcripts and proteins. At this time point, out of 62,844 transcripts, 521 were increased in abundance more than 2-fold and these included those that encoded the C-C chemokine receptor-like 2 protein (CCRL2), interleukin 6 (IL6) and interferon-induced GTP-binding protein MX2. 127 transcripts were significantly decreased in abundance, for instance, DNA damage –inducible transcript 4 protein (DDIT4), NDRG4 and METTL7A. This transcriptome data was compared to a previously published analysis of the cellular transcriptome in HRSV infected cells using micro arrays (Martínez *et al.*, 2007). Although different cell types, times post-infection, viral strains and statistical analysis were used, there was generally

good agreement between the different datasets, for example in the increase in abundance of mRNAs encoding proteins associated with the immune response (data not shown). Taking this data from 24hpi, the transcriptomics analysis would suggest that gene expression is increased rather than decreased in HRSV-infected cells.

HRSV infection resulted in a number of changes in the abundance of host cell proteins at +6hpi (assay point +24hpi) resulted in 30 cellular proteins being significantly increased in abundance and 13 cellular proteins that significantly decreased in abundance (Figure 4.4). Supplementary tables V and VI demonstrated proteins that significantly decreased and increased in abundance, respectively. (See appendix).

There were 14 cellular genes that were significantly overlapped with cellular proteins in HRSV infected cells with DMSO (Figure 4.4). Interestingly, most of these significant overlapped genes and proteins are anti-viral response genes; DDX58, OAS3, IFIT1, IFIT2, IFIT3, OASL and ZC3HAV1, and both significantly increased abundance. These anti-viral proteins and genes have such agreement which all of them were significantly increased in abundance. In addition, there are some identified genes that play a key role in the innate immune response in viral infection such as ISG15 and KRT16. Overall, all of these genes and proteins were increased abundance except UAP1, which was significantly increased abundance in transcriptomics and significantly decreased abundance in protein (Figure 4.5).

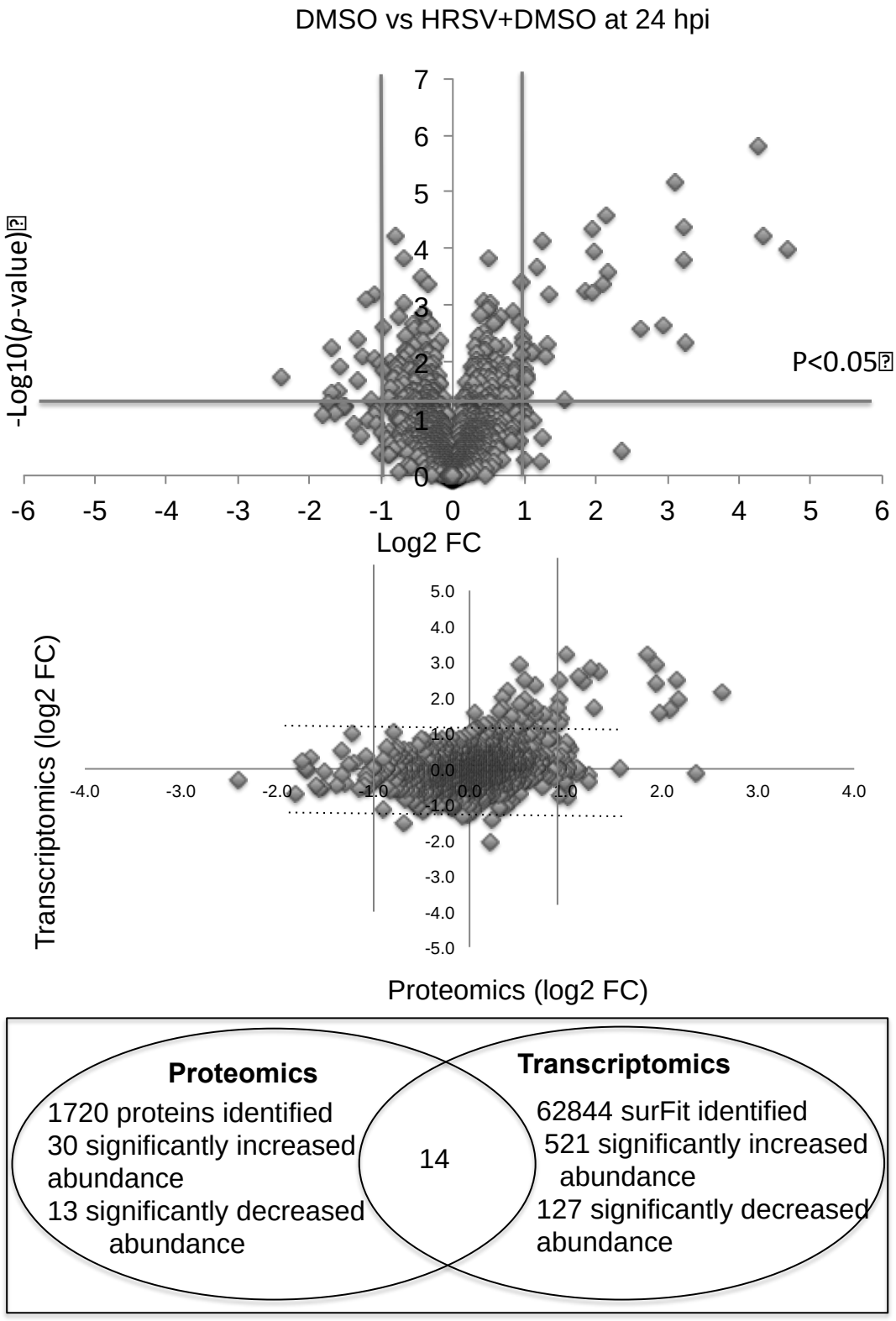


***Figure 4.4*** *(A) Volcano plot representing the effect of HRSV on cells plus DMSO by proteomics DMSO vs HRSV+DMSO. HRSV infection resulted in*

*increased abundance in viral proteins and in cellular proteins. (B) The match between transcript (y-axis) and protein (x-axis) abundance and the changes when infected with HRSV at MOI 0.5. The $log_2$ fold change identified was calculated for both transcript and protein. The most changes are reflecting an increased abundance of both mRNAs and proteins. (C) Venn diagram shows numbers of genes and proteins identified in infected cells. Out of a total of 62844 surFit identified, 555 mRNAs were significantly increased in abundance whereas 156 mRNAs were significantly decreased in abundance. However, out of a total 1720 proteins identified, 30 proteins were significantly increased in abundance and 13 proteins significantly decreased in abundance. 14 genes and proteins were significantly overlapped and their fold change more than 2.*

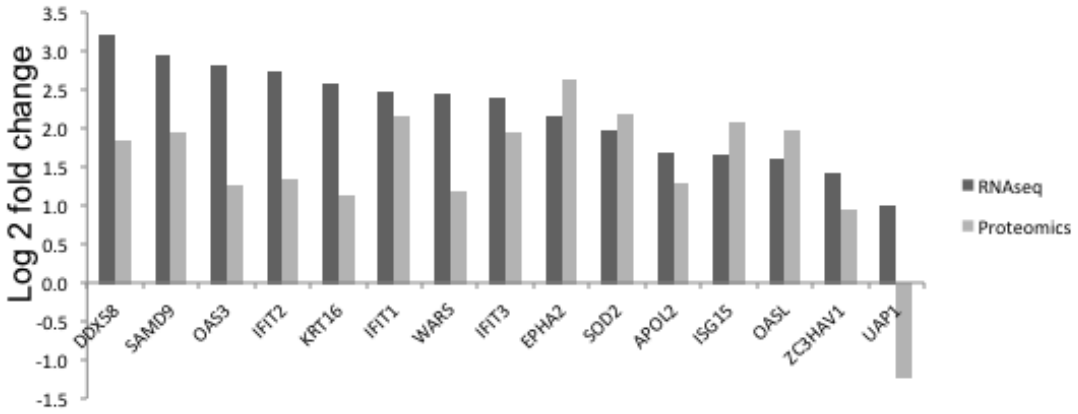


***Figure 4.5*** *Overlap fourteen proteins and genes in infected cells with HRSV vs DMSO were significantly increased in abundance. Most of these matched genes function as anti-viral response genes. DDX58 is the gene that is expressed the highest.*

Ingenuity Pathway Analysis of the proteomic data sets also highlighted several pathways and cellular processes that were affected by HRSV, including CXCR4 signalling (data not shown). These identified changes in the cellular proteome through virus-infection were in close agreement with previous proteomic based approaches to investigate the interaction between HRSV and the host cell (Dave *et al.*, 2014; Munday *et al.*, 2010a), placing confidence in this analysis. This included activation of interferon, NFKB and other pathways such as mitochondrial dysfunction, which has also been observed in a targeted analysis (Munday *et al.*, 2014a). Highlighted in the proteomic analysis was potential cell cycle disruption at the G2/M phase (p-value $1.62x10^{-7}$). This again, has been observed in HRSV-infected cells (Wu *et al.*, 2011), validating the high throughput approach.

There appeared to be little affect of the DMSO on either the cellular and viral transcriptome or proteome in HRSV-infected cells either untreated or treated with DMSO only (~0.5) (Figure 4.2). This is evident in the close correlation of the mRNA and protein abundance in the untreated-infected cells versus the DMSO only treated infected cells (~3.5) (Figure 4.4). Thus the data indicated that DMSO did not have an apparent affect on HRSV biology. This is reflected in the fact that there was no significant difference in HRSV progeny virus production between infected cells either untreated or treated with DMSO (Chapter 5), and was underlined by no apparent difference in the abundance of viral proteins as determined by western blot (data not shown).

### 4.2.3 THE ABUNDANCE OF PROTEOME IS NOT PRESENT AS A LINEAR GRADIENT IN VIRUS INFECTED CELLS

Several studies have previously analysed the abundance of viral proteins in HRSV-infected cells using various quantitative approaches (Dave *et al.*, 2014; Munday *et al.*, 2010a; Munday *et al.*, 2010c). All of these studies found that the viral protein abundance did not correspond to a linear gradient as would be predicted if the protein abundance matched the predicted viral mRNA profile. The most robust approach, by Dave *et al*., also used a label free quantitative approach (Dave *et al.*, 2014) and found that the abundance of viral proteins from highest to lowest abundance was P, N, M, F, M2-1, NS1, NS2, G and L, and noted that this profile did not match the expected profile (Dave *et al.*, 2014). The authors discussed that deriving relative viral protein abundance from mass spectrometry is difficult. As an example they noted that the G protein was not very abundant possibly due to its heavy glycosylation negatively influencing its ability to be identified and quantified by mass spectrometry (Dave *et al.*, 2014).

The proteomics analysis in this study indicated that the abundance of viral proteins in HEp-2 cells infected with HRSV at 24hpi from highest to lowest was P, M, N, M2-1, F, SH, NS1, G and NS2. The L protein was not detected (Figure 4.6). The abundance of viral proteins at 48hpi in HEp-2 cells infected with HRSV from highest to lowest was P, M, N, M2-1, SH, F, NS1, G, NS2 and the L protein (data not shown). Thus taken together with previous proteomic studies (Dave *et al.*, 2014; Munday *et al.*, 2010a; Munday *et al.*,

2010c) the current data would suggest that the abundance of viral mRNAs and proteins does not follow the profile that would be predicted if the abundance was related to the order of the gene along the genome.

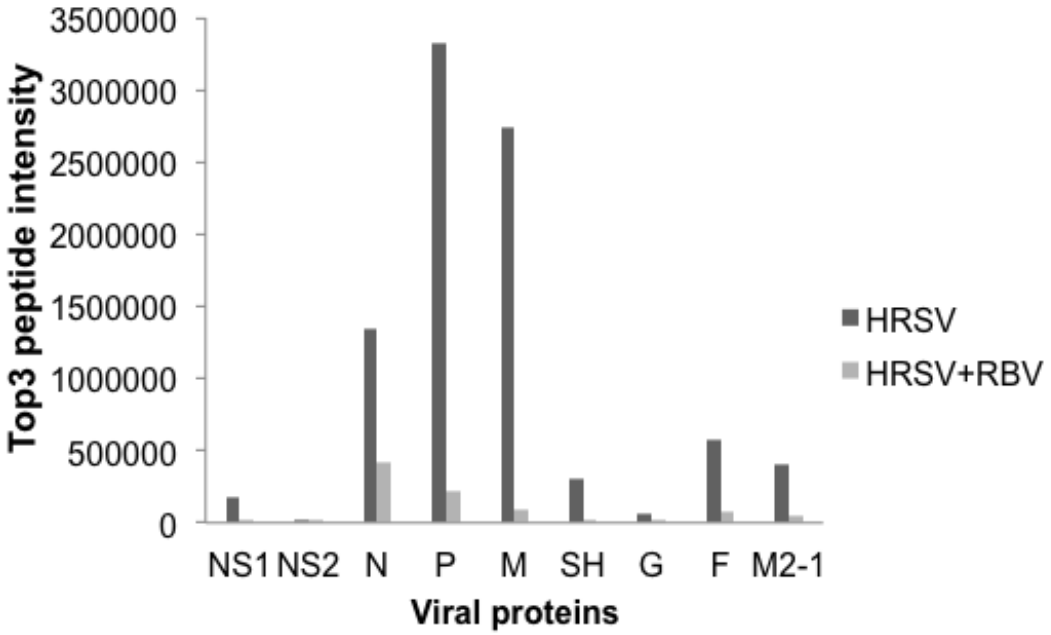


***Figure 4.6*** *Abundance of HRSV proteins after ribavirin treatment. The relative abundance of individual viral proteins was measured before and after ribavirin treatment with a Hi-N approach using the proteome quantitation software Progenesis QI (Nonlinear Dynamics). Briefly, the abundance of the top 3 most intense peptides obtained via LC-MS/MS were averaged to provide a reading for the protein signal. This reading allows relative quantitation of the same protein across LC-MS/MS runs.*

### 4.2.4 THE AFFECT OF INFECTED-CELL ON UNTREATED WITH RIBAVIRIN BY TRANSCRIPTOME AND PROTEOME

In order to study the affect of ribavirin on the host cells, it is important to study the effect HRSV on cells without treatment with ribavirin and do comparison for each sample condition separately. This will allow us to see the difference between infected only and infected plus ribavirin treated. HRSV infection resulted in a number of changes in the abundance of host cell transcripts and proteins (e.g. for +6hpi (assay point +24hpi) Figure 4.7), with most changes reflecting an increased abundance of both transcripts and proteins. At this time point, out of 62,844 surFit transcripts, 426 were increased in abundance more than 2-fold change, whereas, 136 transcripts were significantly decreased in abundance more than 2-fold change. This data also indicated, for the +6hpi (assay point +24hpi), that out of a total of 1716 proteins identified and quantified by 2 or more unique peptides, 77 cellular proteins increased in abundance and 15 cellular proteins decreased in abundance in the infected cells (Supplementary Tables VII, VIII) see appendix.

There were 21 overlap significant matched genes and proteins in HRSV infected cells (Figure 4.8). All of these matched genes and proteins were increased abundance and many of them reflect the antiviral response. DDX58 had the largest change in abundance and the $\log_2$ fold change was 3.2. However, other anti-viral response genes (IFIT1, OAS1, IFIT3, IFIT2 and OAS3) were almost the same fold change 2.7.

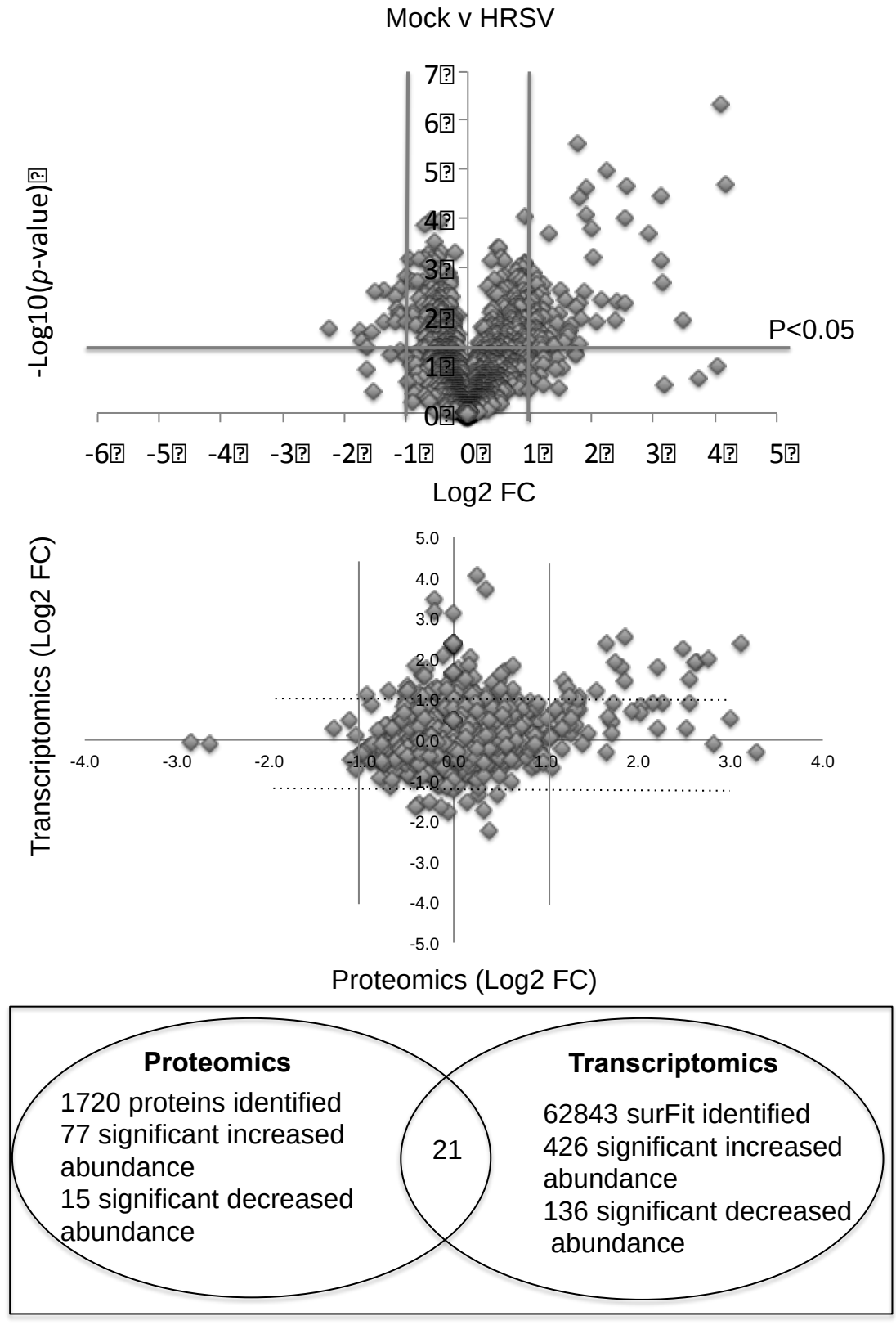


***Figure 4.7*** *(A) Volcano plot of proteomics data showing the effect of HRSV on cells. There were 77 and 15 significant cellular proteins increased and*

*decreased in abundance, respectively. (B) The histogram demonstrated the correlation data between proteomics and transcriptomics.* Out of 62,844 surFit transcripts, 426 was increased in abundance more than 2-fold change, whereas, 136 transcripts were significantly decreased in abundance. This data also indicated that out of a total of 1716 proteins identified and quantified by 2 or more unique peptides, 77 cellular proteins increased in abundance and 15 cellular proteins decreased in abundance in the infected cells*. (C) Venn diagram demonstrating the RNA-seq and proteomics analysis. At this point, 21 significant overlap proteins and genes which their abundance greater than 2-fold.*

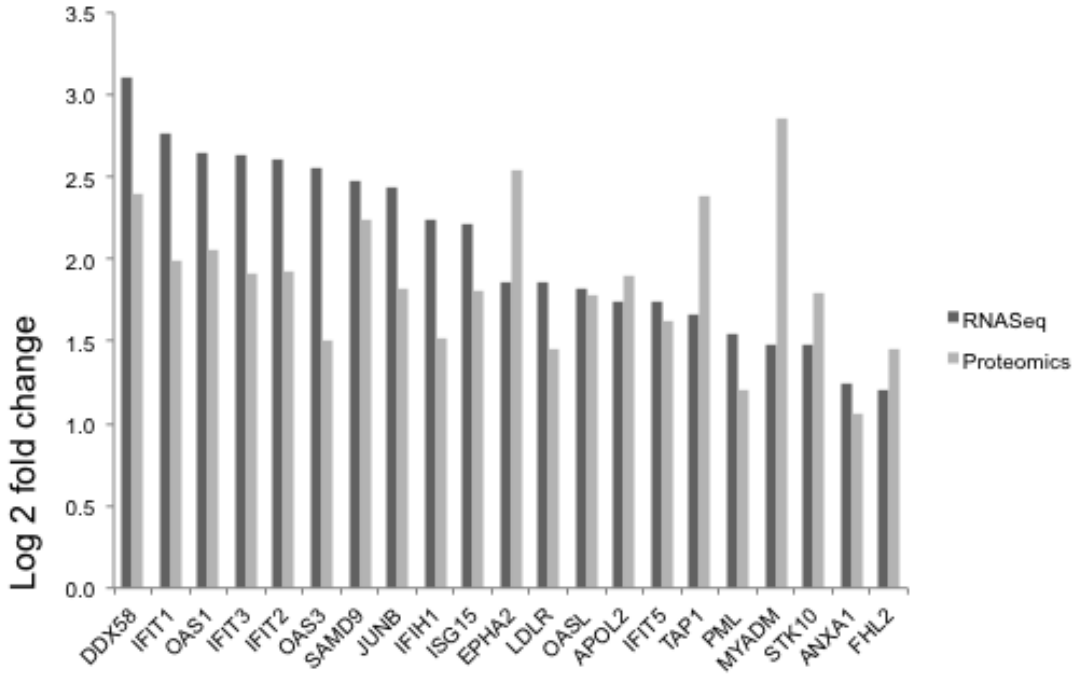


***Figure 4.8*** *Overlap proteins and genes significantly increased in abundance in HRSV vs mock at 24 hr post-infection. DDX58 including anti-viral response were the largest change in abundance.*

### 4.2.5 TREATMENT OF HRSV-INFECTED CELLS WITH RIBAVIRIN

HRSV infected cells were treated with ribavirin at 6 hr post-infection with cellular mRNAs and proteins analyzed at 24 hr post-infection, with 5-fold decrease in progeny virus (Chapter 3). The data indicated that for infected cells treated at 6 hr post-infection with ribavirin and cellular mRNAs and proteins analyzed at 24 hr post-infection there was a reversal in the abundance of cellular and viral proteins that had been increased in untreated DMSO only infected cells (Figure 4.7). This was also generally reflected in the comparison of the cellular transcriptome and proteome (Figure 4.9). As an example, in HRSV-infected cells, the DDX58 pathway (anti-viral response) contains many proteins that are increased in abundance (Figure 4.8). In contrast in HRSV-infected cells treated with ribavirin, in this pathway, the same proteins were decreased in abundance compared to HRSV-infected cells only (Figure 4.10). Thus reversing the effects of the virus on this host cell pathway.

At this time point (at 24 hr post-infection), out of 62,844 surFit transcripts, 480 were increased in abundance more than 2-fold, whereas, 533 transcripts were significantly decreased in abundance with more than a 2-fold change. This data also indicated, for the +6hpi (assay point +24hpi), that out of a total of 1720 proteins identified and quantified by 2 or more unique peptides, 90 cellular proteins increased in abundance and 23 cellular proteins decreased in abundance in the infected cells (Figure 4.9) (Tables 4.3 and 4.4). There were 83 genes significantly overlapped with proteins and most of them matched with the increased and decreased abundance between genes and proteins (Figure 4.10).

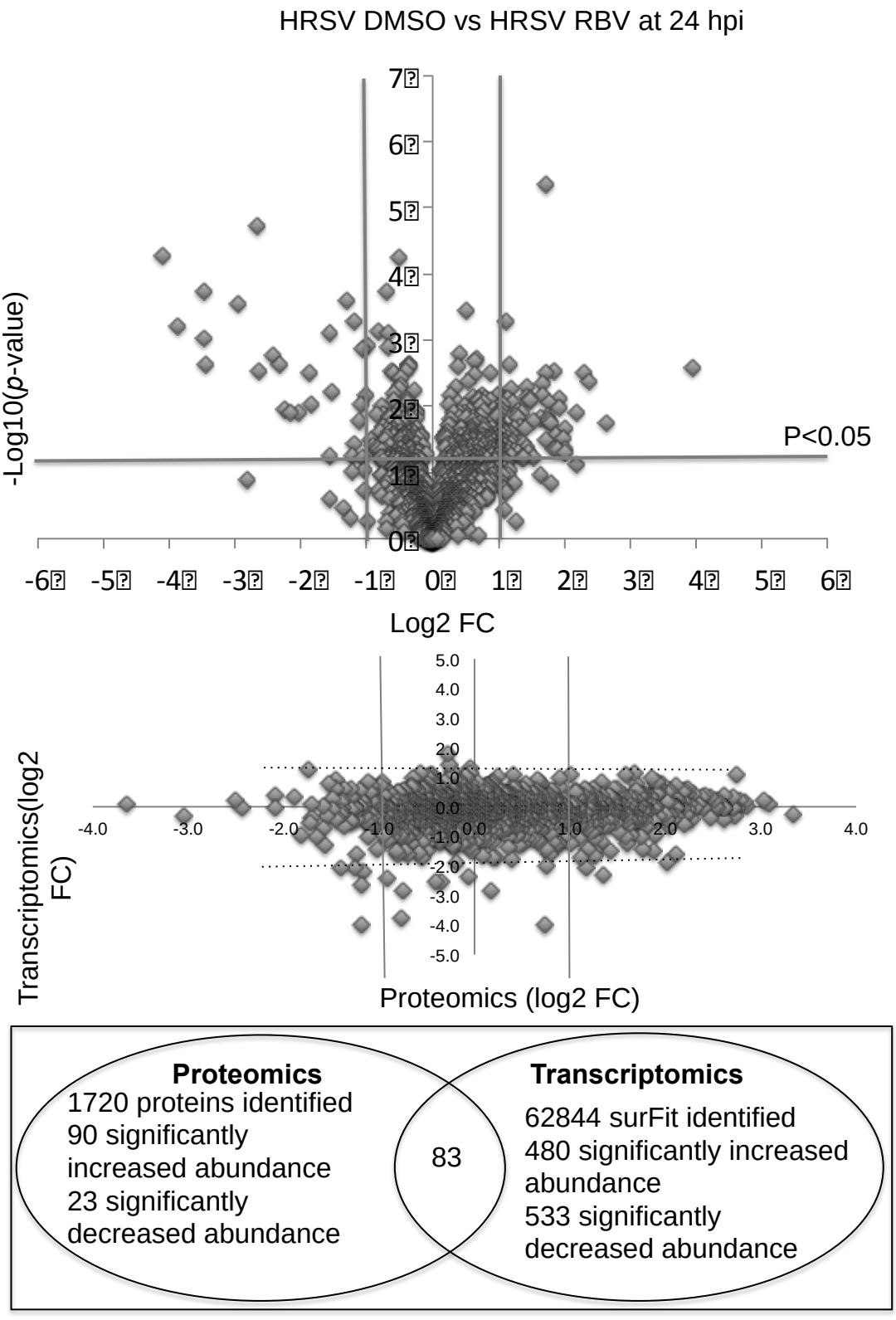


***Figure 4.9*** *(A) Volcano plot representing the affect of ribavirin on infected cells. Decreased abundance in the top left which viral proteins where there,*

*whereas, increased abundance in the top right. (B) The histogram shows the vibration of RNA-seq and proteomics of each gene. (C) Venn diagram shows the significant transcript and proteomics and there are 83 significant matched.*

**Table 4.3** Proteins increased in abundance in HRSV DMSO vs HRSV RBV (top right of Figure 4.9). Statistical analysis was based on observed fold change 2 or greater, and more than 2 peptides and a *p*-value less than 0.05. These proteins were identified and quantified by LC MS/MS.

| Gene name | Protein name | Peptide identification | Peptides used for quantitation | $Log_2$ FC |
|---|---|---|---|---|
| MRPL16 | 39S ribosomal protein L16, mitochondrial | 2 | 2 | 3.9 |
| SYNE2 | Nesprin-2 | 2 | 2 | 2.6 |
| HIST1H4A-L, HIST2H4A,B,HISR4H4 | Histone H4 | 13 | 13 | 2.4 |
| H2AFY | Core histone macro-H2A.1 | 7 | 7 | 2.3 |
| HMGN2 | Non-histone chromosomal protein HMG-17 | 2 | 2 | 2.2 |
| DFFA | DNA fragmentation factor subunit alpha | 3 | 3 | 2 |
| HMGA1 | High mobility group protein HMG-I/HMG-Y | 2 | 2 | 2 |
| ANXA11 | Annexin A11 | 2 | 2 | 2 |
| CISD1 | CDGSH iron-sulfur domain- | 3 | 3 | 1.9 |

| | | | | |
|---|---|---|---|---|
| | containing protein 1 | | | |
| HIST1H2BM | Histone H2B type 1-M | 10 | 2 | 1.9 |
| CHD1 | Chromodomain-helicase-DNA-binding protein 1 | 2 | 2 | 1.9 |
| C2orf47 | Uncharacterized protein C2orf47, mitochondrial | 2 | 2 | 1.9 |
| TMPO | Lamina-associated polypeptide 2, isoforms beta/gamma | 9 | 3 | 1.8 |
| PSIP1 | PC4 and SFRS1-interacting protein | 5 | 3 | 1.8 |
| TOP2B | DNA topoisomerase 2-beta | 8 | 2 | 1.8 |
| MDC1 | Mediator of DNA damage checkpoint protein 1 | 4 | 4 | 1.8 |
| RBMX | RNA-binding motif protein, X chromosome | 14 | 4 | 1.8 |
| NDUFB10 | NADH dehydrogenase [ubiquinone] 1 beta subcomplex subunit 10 | 3 | 3 | 1.7 |
| CCDC86 | Coiled-coil domain-containing protein 86 | 3 | 3 | 1.7 |
| SPCS3 | Signal peptidase complex subunit 3 | 2 | 2 | 1.7 |
| LEPRE1 | Prolyl 3-hydroxylase 1 | 2 | 2 | 1.7 |
| CYB5R1 | NADH-cytochrome b5 reductase 1 | 3 | 3 | 1.7 |
| H2AFX | Histone H2AX | 5 | 2 | 1.7 |
| RPS29 | 40S ribosomal protein S29 | 2 | 2 | 1.7 |
| COX6C | Cytochrome c oxidase subunit 6C | 3 | 3 | 1.6 |
| TOP2A | DNA topoisomerase 2-alpha | 18 | 12 | 1.5 |

| | | | | |
|---|---|---|---|---|
| MLEC | Malectin | 2 | 2 | 1.5 |
| HIST1H2BO | Histone H2B type 1-O | 10 | 2 | 1.5 |
| TMEM126A | Transmembrane protein 126A | 2 | 2 | 1.4 |
| LUC7L3 | Luc7-like protein 3 | 2 | 2 | 1.4 |
| SNRPA | U1 small nuclear ribonucleoprotein A | 3 | 2 | 1.4 |
| RECQL | ATP-dependent DNA helicase Q1 | 4 | 4 | 1.4 |
| PODXL | Podocalyxin | 2 | 2 | 1.4 |
| ITPR3 | Inositol 1,4,5-trisphosphate receptor type 3 | 5 | 4 | 1.3 |
| SLC25A3 | Phosphate carrier protein, mitochondria | 11 | 11 | 1.3 |
| SLC25A11 | Mitochondrial 2-oxoglutarate/malate carrier protein | 3 | 3 | 1.3 |
| NDUFS8 | NADH dehydrogenase [ubiquinone] iron-sulfur protein 8, mitochondrial | 3 | 3 | 1.3 |
| CBX5 | Chromobox protein homolog 5 | 3 | 3 | 1.3 |
| CD59 | CD59 glycoprotein | 3 | 3 | 1.3 |
| DEK | Protein DEK | 3 | 3 | 1.3 |
| PELP1 | Proline-, glutamic acid- and leucine-rich protein 1 | 2 | 2 | 1.3 |
| CAV1 | Caveolin-1 | 3 | 2 | 1.2 |
| ATP5F1 | ATP synthase F(0) complex subunit B1, mitochondrial | 4 | 4 | 1.2 |
| ZNF326 | DBIRD complex subunit ZNF326 | 3 | 3 | 1.2 |

| | | | | |
|---|---|---|---|---|
| HNRNPM | Heterogeneous nuclear ribonucleoprotein M | 30 | 29 | 1.2 |
| RCC1 | Regulator of chromosome condensation | 6 | 6 | 1.2 |
| NCBP1 | Nuclear cap-binding protein subunit 1 | 4 | 4 | 1.2 |
| S100A10 | Protein S100-A10 | 5 | 5 | 1.2 |
| MTA2 | Metastasis-associated protein MTA2 | 3 | 3 | 1.2 |
| NNT | NAD(P) transhydrogenase, mitochondrial | 11 | 10 | 1.1 |
| EGFR | Epidermal growth factor receptor | 9 | 9 | 1.1 |
| ANLN | Actin-binding protein anillin | 3 | 3 | 1.1 |
| LMNA | Prelamin-A/C | 41 | 40 | 1.1 |
| ATP5C1 | ATP synthase subunit gamma, mitochondrial | 5 | 5 | 1.1 |
| PTGES | Prostaglandin E synthase | 2 | 2 | 1.1 |
| NAA10 | N-alpha-acetyltransferase 10 | 6 | 5 | 1.1 |
| SLC25A5 | ADP/ATP translocase 2 | 14 | 6 | 1.1 |
| P20073 | Annexin A7 | 6 | 6 | 1.1 |
| EMD | Emerin | 6 | 6 | 1.1 |
| MFF | Mitochondrial fission factor | 4 | 4 | 1.1 |
| SLTM | SAFB-like transcription modulator | 3 | 3 | 1.1 |
| SAFB | Scaffold attachment factor B1 | 5 | 3 | 1.1 |
| PDS5A | Sister chromatid cohesion protein PDS5 homolog A | 5 | 5 | 1.1 |
| UHRF1 | E3 ubiquitin-protein ligase UHRF1 | 2 | 2 | 1.1 |

| | | | | |
|---|---|---|---|---|
| STT3B | Dolichyl-diphosphooligosaccharide--protein glycosyltransferase subunit STT3B | 2 | 2 | 1.1 |
| TFRC | Transferrin receptor protein 1 | 19 | 19 | 1 |
| MT-CO2 | Cytochrome c oxidase subunit 2 | 3 | 3 | 1 |
| FUBP3 | Far upstream element-binding protein 3 | 9 | 6 | 1 |
| PARP1 | Poly [ADP-ribose] polymerase 1 | 25 | 25 | 1 |
| POR | NADPH--cytochrome P450 reductase | 4 | 4 | 1 |
| FBL | rRNA 2'-O-methyltransferase fibrillarin | 5 | 5 | 1 |
| YBX3 | Y-box-binding protein 3 | 3 | 2 | 1 |
| UQCRC2 | Cytochrome b-c1 complex subunit 2, mitochondria | 5 | 5 | 1 |
| PHF6 | PHD finger protein 6 | 2 | 2 | 1 |
| LBR | Lamin-B receptor | 2 | 2 | 1 |
| VDAC2 | Voltage-dependent anion-selective channel protein 2 | 11 | 11 | 1 |
| GPRC5A | Retinoic acid-induced protein 3 | 2 | 2 | 1 |
| MPDU1 | Mannose-P-dolichol utilization defect 1 protein | 2 | 2 | 1 |
| RRP1 | Ribosomal RNA processing protein 1 homolog A | 2 | 2 | 1 |

**Table 4.4** Proteins decreased in abundance in Mock vs HRSV (top left of Figure 4.9). Statistical analysis was based on observed fold change 2 or greater, and more than 2 peptides and a *p*-value less than 0.05. Proteins were identified and quantified by LC MS/MS. Those with a red colour are viral proteins.

| Gene name | Protein name | Peptide count | Peptides used for quantitation | $Log_2$ FC |
|---|---|---|---|---|
| TUBA1C | Tubulin alpha-1C chain | 25 | 2 | -1.0 |
| PMPCA | Mitochondrial-processing peptidase subunit alpha | 3 | 3 | -1.1 |
| CDC123 | Cell division cycle protein 123 homolog | 2 | 2 | -1.1 |
| CLIC4 | Chloride intracellular channel protein 4 | 2 | 2 | -1.1 |
| WARS | Tryptophan--tRNA ligase, cytoplasmic | 21 | 21 | -1.2 |
| WNK1 | Serine/threonine-protein kinase WNK1 | 3 | 3 | -1.2 |
| MRFAP1 | MORF4 family-associated protein 1 | 2 | 2 | -1.3 |
| RSL1D1 | Ribosomal L1 domain-containing protein 1 | 9 | 8 | -1.5 |
| SOD2 | Superoxide dismutase [Mn], mitochondrial | 2 | 2 | -1.6 |
| KRT1 | Keratin, type II cytoskeletal 1 | 30 | 24 | -1.9 |
| KRT14 | Keratin, type I cytoskeletal 14 | 23 | 4 | -1.9 |
| KRT2 | Keratin, type II cytoskeletal 2 epidermal | 17 | 7 | -2.0 |
| KRT10 | Keratin, type I cytoskeletal 10 | 24 | 19 | -2.2 |

| | | | | |
|---|---|---|---|---|
| HRNR | Hornerin | 3 | 3 | -2.3 |
| N | Nucleoprotein | 18 | 18 | -2.4 |
| G | Major surface glycoprotein G | 2 | 2 | -2.6 |
| M2-1 | Matrix M2-1 | 14 | 14 | -2.7 |
| F | Fusion glycoprotein F0 | 11 | 11 | -3.0 |
| NS2 | Non-structural protein 2 | 2 | 2 | -3.5 |
| P | Phosphoprotein | 12 | 12 | -3.5 |
| UTP14A | U3 small nucleolar RNA-associated protein 14 homolog A | 2 | 2 | -3.5 |
| NS1 | Non-structural protein 1 | 3 | 3 | -3.9 |
| M | Matrix protein | 17 | 16 | -4.1 |

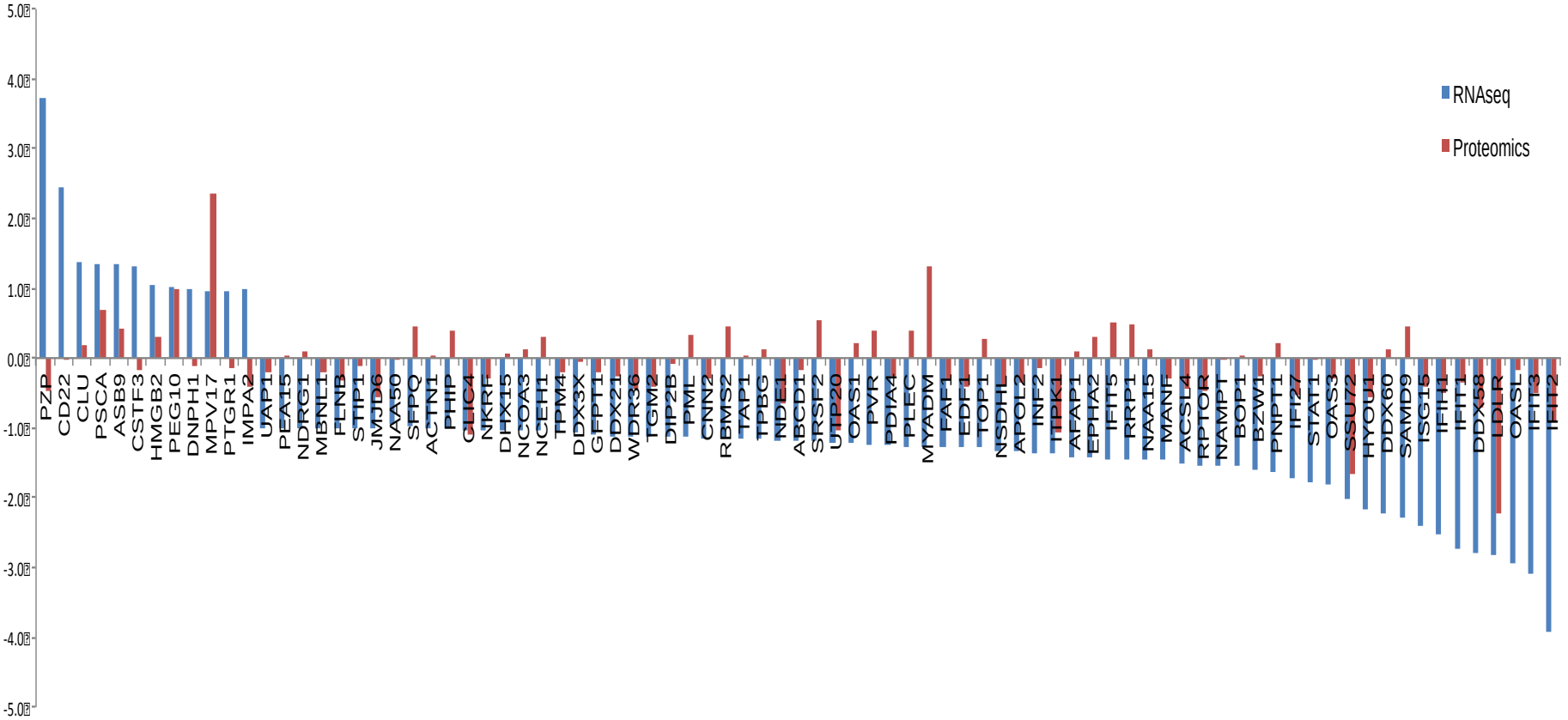


***Figure 4.10*** *This figure demonstrates 83 genes significantly overlapped with proteins on infected cells verse infected plus treated with ribavirin at 24 hr post-infection. Anti-viral ribavirin has a clear effect on infected cells when added after 6 hr post-infection.*

## 4.2.6. BIOINFORMATIC ANALYSIS OF PROTEOMICS AND TRANSCRIPTOMICS DATASET

Proteomics and RNA-seq data were further analyzed using Ingenuity Pathway Analysis (IPA) software (Ingenuity Systems), this helped to build the relationships of a large number of proteins and genes and understand their potential functions. In infected cells without treatment with ribavirin (Mock vs HRSV), there was significant increased in abundance in proteins and genes at 24 hr post-infection. These proteins and genes were classified in terms of subcellular localization (Table 4.5). Antimicrobial response, inflammatory response and cell signalling were the functional categories containing the largest number of 52 significant proteins and 35 significant genes. The network of these proteins was analysed using the Core Analysis function on IPA (Figure 4.11). It was important to know what the antiviral response and viral infection genes that were increased in abundance during infection were, as this study focused on the antiviral drug, ribavirin. These genes were identified using IPA and a network analysis was made (Figure 4.12 A).

As expected, when samples infected and treated with ribavirin at 6 hr post-infection (DMSO HRSV vs HRSV RBV), both cellular proteins and genes were significantly decreased in abundance (Figure 4.12 B). Interesting, the decrease almost was among those proteins and genes that had increased in abundance in infected cells without treatment. Data analyses using IPA, infectious diseases, cell-to-cell signalling and interaction, and cellular movement were the top network function at infection and treated cells with

ribavirin. Proteins and genes that were significantly increased and decreased in abundance at this condition, were classified in terms of subcellular localization (Table 4.5). Moreover, as a big picture for the effect of antiviral ribavirin on different condition, heat map and relative clustering (Figure 4.13) was created by Gene-E. The analyses indicate that the effect of ribavirin when added into infected cells made a significant decreased in abundance.

**Table 4.5** Subcellular localization of proteins and genes identified in MOCK vs HRSV and HRSV DMSO vs HRSV RBV samples showing a $\log_2$ fold or greater relative increase or decrease in abundance. The localization was determined using Ingenuity Pathway Analysis software.

| Subcellular localization | Number of proteins & genes | | | |
|---|---|---|---|---|
| | MOCK vs HRSV | | HRSV DMSO vs HRSV RBV | |
| | Proteins | Genes | Proteins | Genes |
| Nucleus | 38 | 134 | 32 | 220 |
| Cytoplasm | 26 | 191 | 14 | 279 |
| Plasma membrane | 10 | 96 | 8 | 144 |
| Other | 9 | 141 | 48 | 370 |

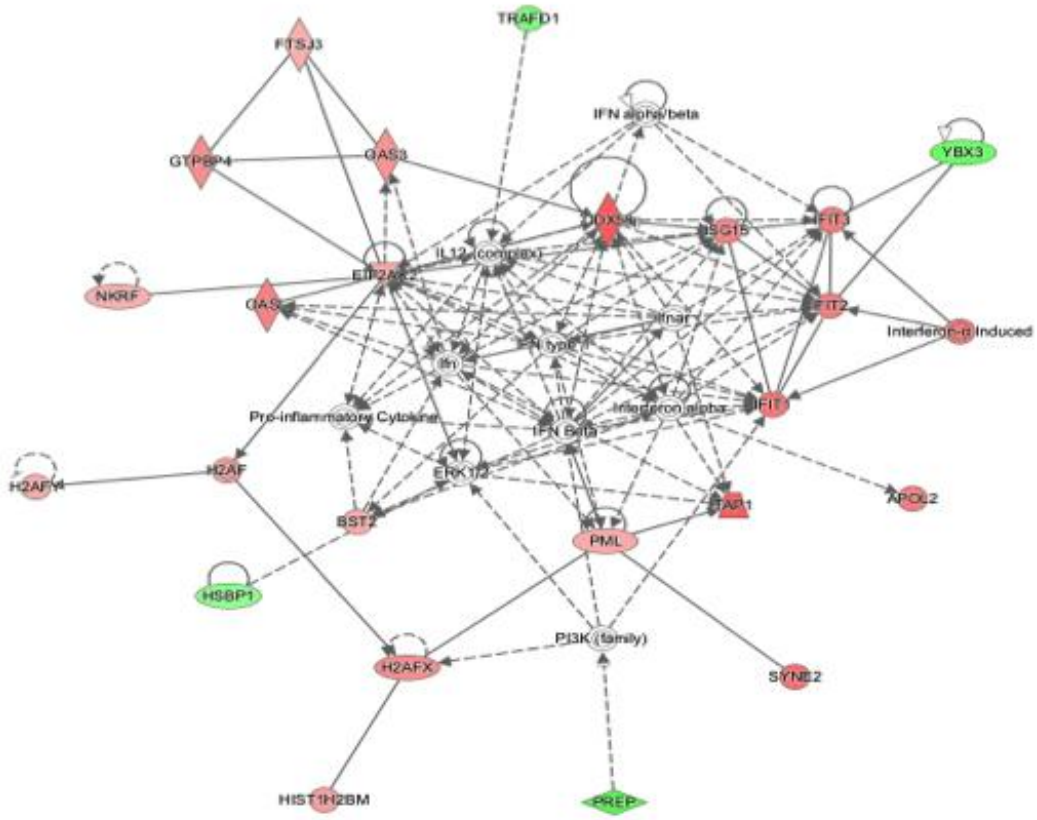


***Figure 4.11*** *Network pathway analyses of 52 significant genes that function as antimicrobial response, inflammatory response and cell signalling using IPA. Genes shaded in red corresponded to a 2-fold or greater increase in abundance and the colour intensity indicated the degree of gene abundance. Genes shaded in green corresponded to a 2-fold or lesser decreased in abundance. The shapes donated the molecular class of the gene.*

**A**

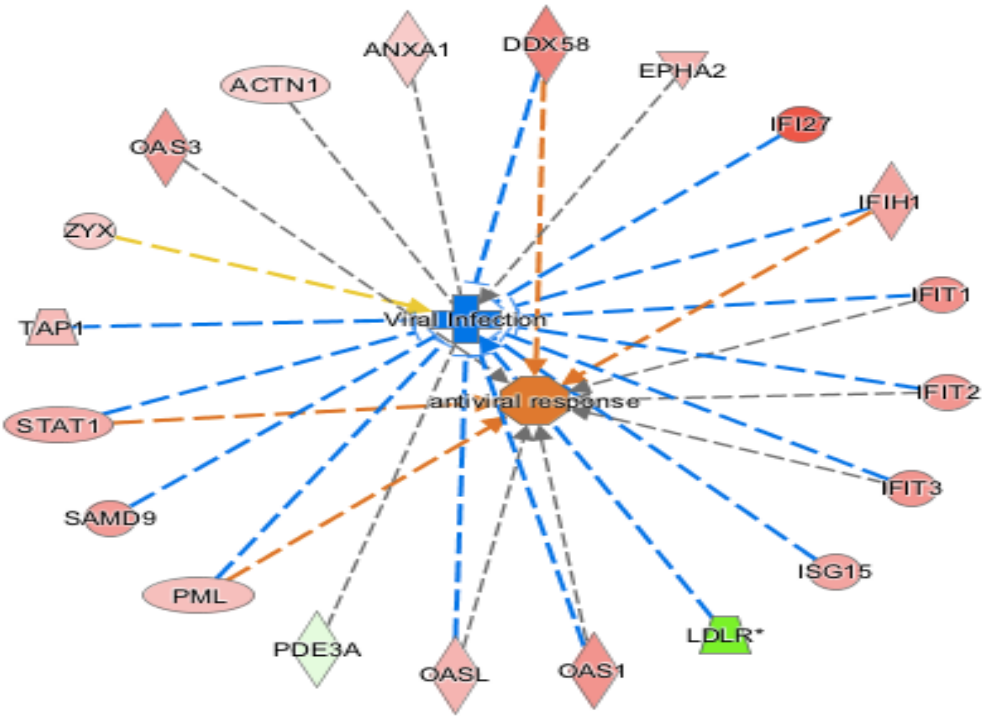
ANXA1
DDX58
EPHA2
ACTN1
IFI27
OAS3
IFIH1
ZYX
IFIT1
TAP1
Viral Infection
antiviral response
IFIT2
STAT1
IFIT3
SAMD9
ISG15
PML
LDLR
PDE3A
OASL
OAS1

**B**

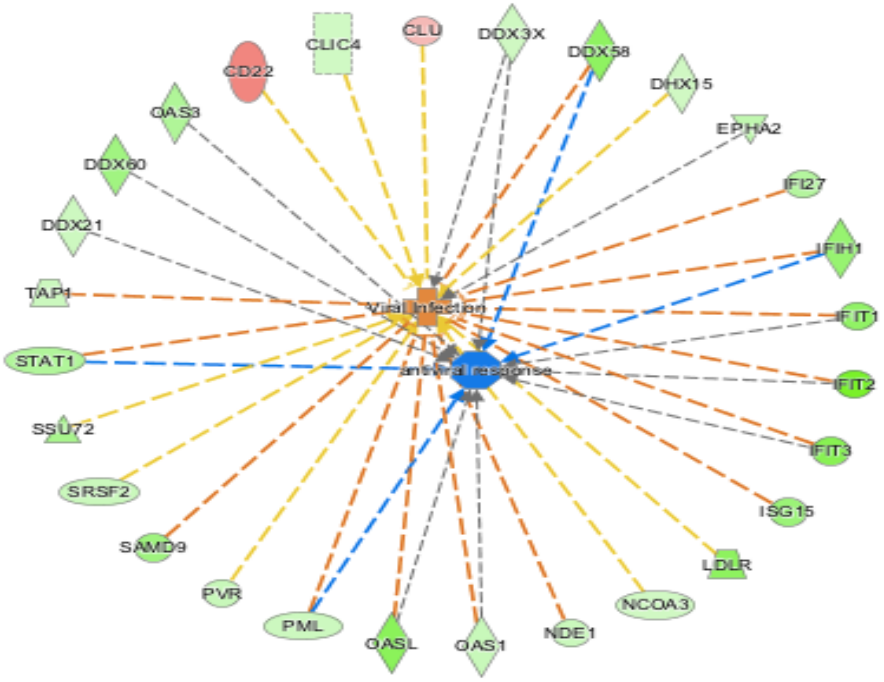
CLIC4
CLU
DDX3X
DDX58
CD22
DHX15
OAS3
EPHA2
DDX60
IFI27
DDX21
IFIH1
TAP1
Viral Infection
IFIT1
STAT1
antiviral response
IFIT2
SSU72
IFIT3
SRSF2
ISG15
SAMD9
LDLR
PVR
NCOA3
PML
OASL
OAS1
NDE1

***Figure 4.12*** *Network pathway analyses of RNA-seq data on* ***(A)*** *Mock vs HRSV. All genes shaded in red corresponded to a 2-fold or greater increased in abundance at 6 hr post-infection. All of these genes significantly increased abundance during HRSV infection except LDLR and PDE3A.* ***(B)*** *(HRSV DMSO vs HRSV+RBV), viral infection overlapped with antiviral response of using IPA. Genes shaded in green corresponded to a 2-fold or greater decreased in abundance at 6 hr post-infection.*

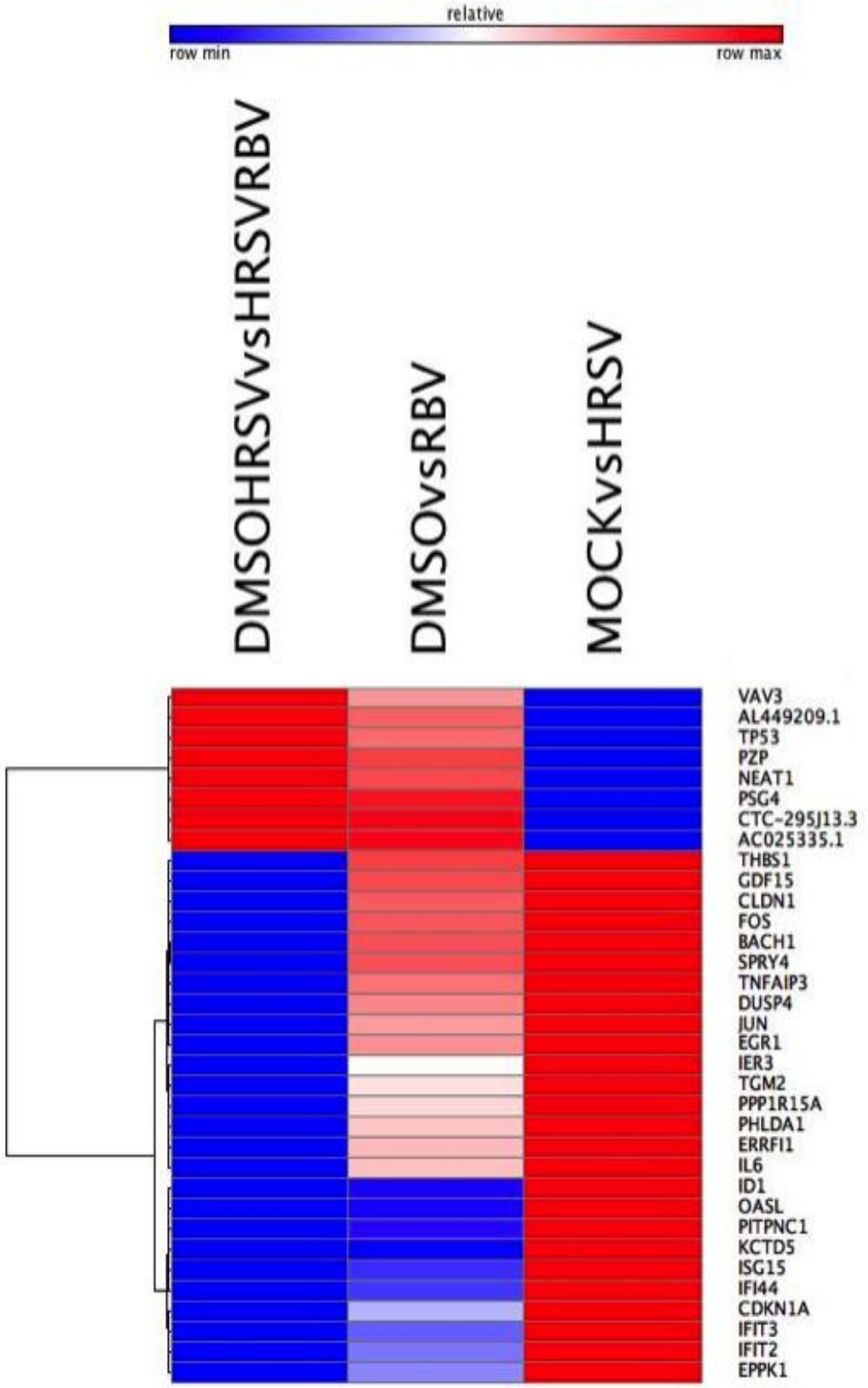


***Figure 4.13*** *Heat map represent genes expression that significantly changed in abundance at different conditions. The heat map based on the estimated*

*relative abundance. Colour intensity represents gene abundance with red indicating significant increased abundance and blue indicating significant decreased abundance. The analyses indicate that the effect of ribavirin when added into infected cells made a significant decreased in abundance.*

## 4.3 DISCUSSION

For the first time two high-resolution approaches have been used, RNA-seq and quantitative proteomics, to analyse the effect of a widely used and reportedly broad spectrum antiviral drug, ribavirin, on the host cell, to determine whether the drug causes any effects on host cellular mRNA and proteins in the presence and absence of infection. Further, these approaches were allowed to simultaneously explore the potential effect of the drug on virus biology using HRSV as a model pathogen. Ribavirin is the only licensed therapeutic treatment for HRSV infection, yet its mechanism of action remains largely uncharacterized and for many viruses, it is thought to promote hyper mutation and error catastrophe in the viral genome (Cameron & Castro, 2001; Crotty *et al.*, 2002). Thus leading to a decrease in viral load. The effect of ribavirin on the host cell was examined, at an active concentration that disrupted virus biology, and caused a significant decrease in progeny virus production. This study was focused on whether treatment of cells with ribavirin resulted in a difference in abundance of either cellular mRNAs or proteins using the transcriptomic and proteomic approaches. In this case, the transcriptomic approach identified more specific gene products than the proteomic approach (Figure 4.3). The data indicated that the abundance of several hundred cellular mRNAs was affected by treatment with ribavirin and also the abundance of several cellular proteins that were detected was altered. This suggests that ribavirin can have a direct effect on the host cell, which becomes obvious in terms of the decrease in cell viability as the concentration of ribavirin is increased (Chapter 3). A number of cellular mRNAs increased in abundance in the presence of ribavirin and

these included transcripts associated with the innate immune response and also pathways activated as part of anti-viral signalling cascades. This may have a direct effect on HRSV-infection, perhaps by activating these responses in bystander cells that may be infected during viral spread and secondary rounds of infection.

Interestingly, the analysis indicated that there were not many cellular mRNA and proteins increased or decreased in the presence and absence of DMSO with and without ribavirin (Figures 4.4, 4.5). In terms of viral mRNA and proteins, there were a significant increase in infected cells un-treated and significant decreased in infected plus treated. Proteomic analysis of cells infected with either HRSV or cells infected with HRSV and treated with the DMSO, recapitulated many of the previously reported effects of viral infection on the host cell (Dave *et al.*, 2014; Munday *et al.*, 2010c). This established the robustness and reproducibility of the analysis. The transcriptomic approach allowed us not only to examine global gene expression analysis of cellular genes in virus-infected cells but also to examine the effect of ribavirin treatment on virus RNA by building consensus genomes and mapping minor variants (Chapter 5).

What both experimental approaches indicated and agree upon was that the mRNA encoding the G gene was the most abundant (Chapter 5), however, the P protein was the most abundant. The abundance of the other viral mRNAs did not conform to a pattern if their abundance reflected transcription

by a linear gradient, at least under the conditions that were used in the experiment. Such observations can be supported by the data in this study and previous analysis of viral protein abundance using quantitative proteomics in different cell types infected with HRSV (Dave *et al.*, 2014; Munday *et al.*, 2010b). Here, the abundance of viral proteins did not correspond to a profile if their abundance was solely determined by mRNA abundance - assuming a linear gradient expression profile. As noted by Dave *et al*., 2014, care should be taken when interpreting the relative abundance of viral proteins using quantitative proteomics as not all proteins may be refractive to the steps used in mass spectrometry identification and quantification. This is reflected in the western blot analysis of viral proteins (Chapter 3). Taken at face value, the G protein would appear to be more abundant, and then the N, P and M proteins. However, this data was generated using polyclonal sera raised against viral proteins derived from infected cell lysate and several different factors can affect antigen and epitope selection. However, these findings, if correct, do not rule out a model in which the abundance of viral transcripts is related to their order and position along the viral genome. Other factors such as mRNA stability may play a significant role in determining the relative levels of abundance for HRSV transcripts.

These results investigated the effect of ribavirin on HRSV-infected cells using a combination of RNA-seq and quantitative label free proteomics. This study was able to demonstrate that treatment of cells with ribavirin resulting in increase transcription of selected cellular mRNAs including those involved in

mediating anti-viral signalling. Additionally, ribavirin treatment caused a decrease in the viral mRNA and proteins. Clearly by using IPA that in the infected cells the most significant pathway was antiviral response that is a natural response to fight the virus that attacking cells (Martínez *et al.*, 2007). Therefore, the concentration of ribavirin on HRSV infection has clearly shown the reduction of viral proteins and other cellular proteins.

These combined approaches; RNA-seq and label free quantitative proteomics, have not been used before to study HRSV biology and can be readily applied to the investigation of virus host interactions and the effects of therapeutics on the host. This study indicated that ribavirin affected only a subset of cellular mRNA and proteins.

# CHAPTER 5: INVESTIGATING THE INFLUENCE OF RIBAVIRIN ON HUMAN RESPIRATORY SYNCYTIAL VIRUS RNA SYNTHESIS USING A HIGH-RESOLUTION RNA-SEQ APPROACH

## 5.1. INTRODUCTION

Ribavirin can be used in children who are extremely ill to reduce the amount of HRSV and lower the burden of disease (Everard *et al.*, 2001; Ventre & Randolph, 2007). Ribavirin is also used as an experimental therapy with other viruses (Paeshuyse *et al.*, 2011; Sparrelid *et al.*, 1997). However, the mechanism of action of ribavirin in HRSV is not well understood, although it is thought to increase the mutation rate of the viral polymerase during replication (Graci & Cameron, 2006). Previous studies have investigated the effect of inosin monophosphate dehydrogenase (IMPDH) inhibition during HRSV infection (Leyssen *et al.*, 2005; Smee & Matthews, 1986). Other mechanism have been studied; loss of fitness of RNA virus genomes (Crotty *et al.*, 2001; Dietz *et al.*, 2013), up-regulation of anti-viral gene products (Zhang *et al.*, 2003), Inefficient translation (Tamburini *et al.*, 2009; Volpon *et al.*, 2013) and Multiple mechanisms of action (Day *et al.*, 2005), but the effect that ribavirin might have on fidelity of HRSV RNAs, or the stability of resulting mRNA transcripts has not previously been examined. To investigate the effect of ribavirin on HRSV RNA synthesis, high-resolution RNA-seq was used. Minor variant analysis (location of nucleotides mapped along the genome of HRSV) helped to assess the effect of ribavirin on the frequency of mutations in the HRSV genome. The addition of ribavirin resulted in a

decrease in the abundance of viral RNA and a modest increase in the frequency of transition, but not transversion, mutations, suggesting direct influence on polymerase fidelity. In addition, that been found in both the absence and presence of ribavirin, the cumulative abundance of viral mRNA at the two time points (24 and 48 hr post-infection) analysed did not follow the transcription gradient of mRNA synthesis, contrary to what was anticipated.

Various studies have revealed the inhibitory nature of ribavirin on HRSV *in vitro*. For example, addition of ribavirin at -2, 0 and 1 hr post-infection resulted in a 95% plaque reduction (Hruska *et al.*, 1980), however the mechanism of this inhibition is unclear. In the published literature RNA-seq has not been applied at high read depth to study HRSV replication and transcription and it provides an ideal approach to study the potential mutagenic effect of ribavirin on HRSV genome biology. A recent study described a pipeline (based on the Galaxy platform) that was used to generate consensus genomes and maps of minor variants to study Ebola virus evolution in a guinea pig model (Dowall *et al.*, 2014) and in patient samples taken from the 2014-2015 West African outbreak (Carroll *et al.*, 2015). These studies indicated that a greater read depth during RNA-seq provided more accurate base calling on the consensus genome and provided maps of minor variants.

To provide sufficient viral RNA for sequencing and to balance this with infectivity and cell viability (through both treatment with ribavirin and infection with HRSV) several optimization experiments were performed (Chapter 3). The concentration of ribavirin used was based on previous literature (Shah *et al.*, 2010; Zhang *et al.*, 2003), and an MTT assay was used to establish cell viability versus toxicity in HEp-2 cells (Figure 3.1). These analyses, together with concentrations previously used in the literature, suggested that a concentration of 500 μM would be tolerated by the cells in culture and provide anti-viral activity. Also, different optimizations were performed to identify the best viral MOI in the absence and presence of 500 μM of ribavirin (Chapter 3). The data indicated that at a MOI of 0.5 and in the presence of 500 μM ribavirin, there was a visible decrease in the number of infected cells compared to untreated cells (Figure 3.2). Ribavirin treatment at different time points on HRSV infected cells were studied in Chapter 3. The data indicated that two time points were chosen for this study; ribavirin added at +6 hr post-infection and RNA harvested at 24 hr post-infection and ribavirin added at +24 hr post-infection and RNA harvested at 48 hr post-infection. The aim of this study is to investigate the effect of ribavirin on the HRSV infected cells.

The work described in this chapter has recently been published in the Journal of Virology. **Waleed Aljabr**, Olivier Touzelet, Georgios Pollakis, Weining Wu, Diane C. Munday, Margaret Hughes, Christiane Hertz-Fowler, John Kenny, Rachel Fearns, John N. Barr, David A. Matthews and Julian A. Hiscox, (2015) Investigating the influence of ribavirin on human respiratory

syncytial virus RNA synthesis using a high-resolution RNA-seq approach 10.1128/JVI.02349-15. (See appendix)

The candidate confirms that the work submitted is his own, except where work which has formed part of jointly-authored publications has been included. The contribution of the candidate and the other authors to this work has been explicitly indicated below. The candidate confirms that appropriate credit has been given within the thesis where reference has been made to the work of others.

**Chapter 5** of this thesis was based on the work from jointly-authored publication:

- Waleed Aljabr planned and performed all experiments, prepared samples for RNA-seq, western blot, immunofluorescence, data analyses, and jointly wrote the manuscript.
- Rachel Fearns and John Barr provided advice regarding manuscript structure.
- Oliver Touzelet, Weining Wu and Diane Munday provided technical support.
- Georgios Pollakis provided minor variant analysis.
- John Kenny, Margaret Hughes and Christiane Hertz-Fowler run RNA-seq.
- David Matthews provided viral transcriptomic analysis.
- Julian Hiscox provided supervision and jointly wrote the manuscript.

Also, some of this work in this chapter has been published in Virology. Sarah L. Noton, **Waleed Aljabr**, Julian A. Hiscox, David A. Matthews, Rachel Fearns, (2014) Factors affecting *de novo* RNA synthesis and back-priming by the respiratory syncytial virus polymerase. Virology, 462-463:318-327. (See appendix)

The candidate confirms that the work submitted is his own, except where work which has formed part of jointy-authored publications has been included. The contribution of the candidate and the other authors to this work has been explicitly indicated below. The candidate confirms that appropriate credit has been given within the thesis where reference has been made to the work of others.

**Chapter 5** of this thesis was based on the work from jointly-authored publication:

- Sarah Noton and Rachel Fearns planned the experiments, prepared figures, performed data analyses and jointly wrote the manuscript.
- Waleed Aljabr planned and performed all experiments and prepared samples for RNA-seq.
- Julian Hiscox and David Matthews prepared transcriptomics analysis.

## 5.2 RESULTS

### 5.2.1 DETERMINING THE ABUNDANCE OF VIRAL MRNAS IN HRSV INFECTED CELLS USING RNA-SEQ

RNA-seq was used to measure the abundance of poly A selected viral mRNAs under the two different time points in both untreated and ribavirin treated HEp-2 cells. RNA-seq analysis of the two different time points indicated that in untreated HEp-2 cells at 24 and 48 hr post-infection, 19.8% and 10.53% of total reads mapped to HRSV RNA (Table 5.1), corresponding to 6,162,832 and 3,810,092 reads at each time point, respectively. HRSV transcripts also reached a high level in A549 cells, in this case representing 34.72% of the total reads (Table 5.1), a total of 14,105,224 reads.

From the RNA-seq data, the relative abundance of each viral mRNA at 24 and 48 hr post-infection in the absence and presence of ribavirin treatment was calculated using the number of reads mapping to each gene. This approach was unable to discriminate monocistronic viral mRNA from polycistronic RNAs, although the abundances of polycistronic read-through products are generally low in HRSV infections (Cartee *et al.*, 2003). The data indicated that as a proportion of total reads, the amount of viral RNA decreased in the presence of ribavirin (Table 5.1).

**Table 5.1** Number and proportion of sequence reads mapping to the HRSV genome out of the total number of sequence reads.

| Cell lines | Conditions | Reads mapping to the HRSV genome | Total number of reads | % of total reads |
|---|---|---|---|---|
| HEp-2 | HRSV at 24hpi | 6162832 | 31118416 | 19.8 |
| | HRSV+RIBAVIRIN at 24hpi | 21350 | 32769666 | 0.07 |
| | HRSV at 48hpi | 3810092 | 36182362 | 10.53 |
| | HRSV+RIBAVIRIN at 48hpi | 436172 | 44545058 | 0.98 |
| A549 | HRSV at 24hpi | 14105224 | 40622791 | 34.72 |
| | HRSV+17-AAG at 24hpi | 1549050 | 37493536 | 4.13 |

The accumulation of each viral mRNA in an infected cell, if this follows the pattern postulated for other *mononegavirales*, might be expected to reflect the order of genes on the genome, so that the relative abundance of different gene transcripts would correlate with gene position relative to the 3' end (Lim & Yin, 2009; Pagán *et al.*, 2012). However, for the two time points examined, the data showed that, whilst there was a general trend of abundance

correlating with gene order, there were exceptions (Figure 5.1 A). For example, as expected the L mRNA was the least abundant transcription product (Figure 5.1 A), however, the mRNA encoding the G protein appeared to be the most abundant mRNA at both time points in both the absence and presence of ribavirin. This observation suggests that factors other than gene order may be able to influence HRSV mRNA abundance in cells, in particular for the G mRNA. Importantly, the profile of relative viral mRNA abundance was equivalent in untreated versus ribavirin treated infected HEp-2 cells, suggesting that ribavirin did not impinge upon the overall program of HRSV transcription per se.

If viral mRNA transcript levels are governed in part by mRNA stability, the profile of relative levels might be different in different cell types. Therefore, the abundance of viral mRNA in HRSV infected A549 cells at 24 hr post-infection was investigated. In this instance 34.72% of the total reads mapped to the HRSV mRNA (Table 5.1), a total of 14,105,224 reads. Again, the data indicated that the abundance of viral mRNAs at this time point and in this cell type did not correspond to the predicated linear gradient (Figure 5.1 A).

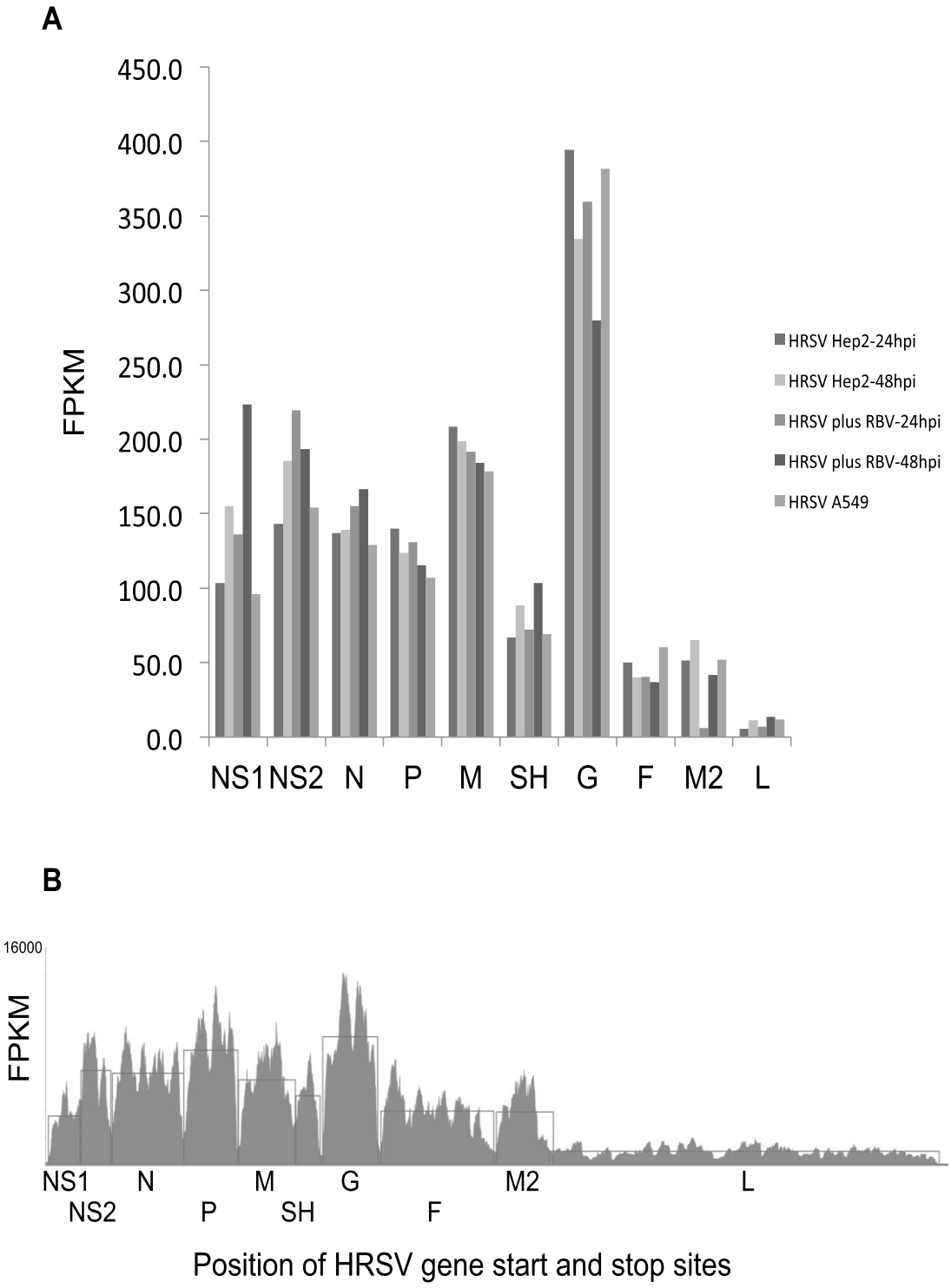
A
450.0
400.0
350.0
300.0
250.0
200.0
150.0
100.0
50.0
0.0
FPKM
HRSV Hep2-24hpi
HRSV Hep2-48hpi
HRSV plus RBV-24hpi
HRSV plus RBV-48hpi
HRSV A549
NS1 NS2 N P M SH G F M2 L
B
16000
FPKM
NS1 N M G M2 L
NS2 P SH F
Position of HRSV gene start and stop sites

***Figure 5.1*** *(A) Analysis of the abundance of viral mRNAs HE-p2 or A549 cells infected with HRSV at different time points and for HEp-2 cells in the absence or presence of ribavirin. The viral mRNA abundance is shown in order of the particular gene along the HRSV genome, from 3' to 5', and also the order in which the particular gene is transcribed. The abundance is shown in fragments per kilobase of exon per million fragments mapped (FPKM). (B) RNA-seq data from HEp-2 cells at 24 hpi was further processed to include only proper mate pair reads, where both reads were mapped and correctly orientated with respect to each other. The seed length was increased from 28 to 35. The maximum number of miss matches was reduced to 1. The horizontal line traces the average abundance of the mapped reads for each gene.*

To investigate this further, as an exemplar, the RNA-seq data for HRSV in HEp-2 cells at 24 hr post-infection was further processed to include only proper mate pair reads, where both reads were mapped and correctly orientated with respect to each other. The seed length was increased from 28 to 35. The maximum number of miss matches was reduced to 1. One effect of this is to bias the reads to those that match the consensus sequence. This data again indicated that the L mRNA was the least abundant HRSV transcript (Figure 5.1 B), however the difference in the other gene products was less pronounced, with P and G transcripts being almost equivalent (Figure 5.1 B).

### 5.2.2. READ THROUGH AT GENE JUNCTIONS CORRELATES WITH PREVIOUS SUBGENOMIC REPLICON DATA

The data also provided a measurement of read-through, which allowed a direct comparison to previously published results, and allowed validation of the RNA-seq approach to quantify viral RNA. This was determined by comparing the average Fragments Per Kilobase Million (FPKM) in the intergenic region to the total virus FPKM (Table 5.2). From this, the % read through between adjacent genes was calculated, with those for NS1/NS2=30%, NS2/N=13%, N/P=10%, P/M=4%, M/SH=21%, SH/G=4%, G/F=8% and F/M2=11%. For the gene junctions examined, this pattern of relative read through efficiency correlates with data examining the transcription termination efficiency of gene junctions in the context of subgenomic replicons (Cartee *et al.*, 2003). For example, in both studies, data indicated that the SH/G gene junction terminated transcriptions with the

greatest efficiency and produced low levels of read-through transcripts, whereas the NS1/NS2 gene junction had the highest level of read through (Cartee *et al.*, 2003).

**Table 5.2** Percentage read through between adjacent genes along the HRSV genome.

| Read-through | Average FPKM | % Total virus FPKM | % Between adjacent genes |
|---|---|---|---|
| Leader | 122 | 0.17 | - |
| Non-structural protein 1 (NS1) | 3578 | 5.11 | - |
| Intergenic region | 4500 | 6.43 | 30 |
| Non-structural protein 2 (NS2) | 6952 | 9.94 | - |
| Intergenic region | 2070 | 2.96 | 13 |
| Nucleoprotein (N) | 6740 | 9.63 | - |
| Intergenic region | 1838 | 2.63 | 11 |
| Phosphoprotein (P) | 8446 | 12.07 | - |
| Intergenic region | 671 | 0.96 | 4 |
| Matrix protein (M) | 6255 | 8.94 | - |
| Intergenic region | 3098 | 4.43 | 21 |
| Small hydrophobic protein (SH) | 5072 | 7.25 | - |
| Intergenic region | 662 | 0.95 | 4 |
| Glycoprotein (G) | 9444 | 13.5 | - |
| Intergenic region | 1177 | 1.68 | 8 |

| | | | |
|---|---|---|---|
| Fusion protein (F) | 3544 | 5.07 | - |
| Intergenic region | 929 | 1.33 | 11 |
| M2 protein | 3877 | 5.54 | - |
| Large polymerase protein (L) | 968 | 1.38 | - |
| Trailer | 25 | 0.04 | - |
| Total | 69968 | 100 | - |

### 5.2.3 RNA-SEQ ANALYSIS REVEALED AN INCREASE IN THE FREQUENCY OF TRANSITION BUT NOT TRANSVERSION MUTATIONS IN THE PRESENCE OF RIBAVIRIN

To access the frequency of potential nucleotide substitution in these different populations, the QuasiRecomb algorithm (Töpfer *et al.*, 2013) was used to obtain coverage and data on the proportion of each nucleotide used at any given location on the genome. The results were further processed by an in-house script to determine which nucleotide was the most abundant at each nucleotide position, and how frequently any of the other three nucleotides were used at that position. A similar approach was used to derive consensus genomes and examine nucleotide variation that corresponded with increase in virulence with Ebola virus in a guinea pig model of infection (Dowall *et al.*, 2014), to measure Ebola virus evolution during the 2014-2015 West African outbreak (Carroll *et al.*, 2015) and to investigate infection of human and bat cells with Hendra virus (Wynne *et al.*, 2014). These data were displayed as frequency of use of minor nucleotides along the genome (Figure 5.2). For example, in the case of HRSV assayed at +24 hr post-infection, there were

13 nucleotide positions that had a substitution in 30% or more of the sequence reads that mapped across that location (Figure 5.2 A). On first inspection, the nucleotide substitution frequency in HRSV RNA isolated from cells that had been treated with ribavirin at +6 hr post-infection (assay point +24 hr post- infection), seemed large, especially in the L gene sequence (Figure 5.2 B). However, further inspection of the data revealed that given the 166-fold decrease in mappable reads at this assay point, there were relatively few quality reads, and the apparent nucleotide frequency variation decreased when lower quality reads were removed (Figure 5.2 C). Also, the number of mapped reads obtained without ribavirin was artificially reduced to the level seen when examined cells were treated with ribavirin at +6 hr post-infection (data not shown). This dataset was examined for minor variants and a similar pattern of nucleotide variation was seen (data not shown) confirming the supposition that compared to the higher number of mappable reads (Figure 5.2 D), the low number of mappable reads (Figure 5.2 E) led to an apparent increase in variation and this cannot be attributed to be the ribavirin treatment.

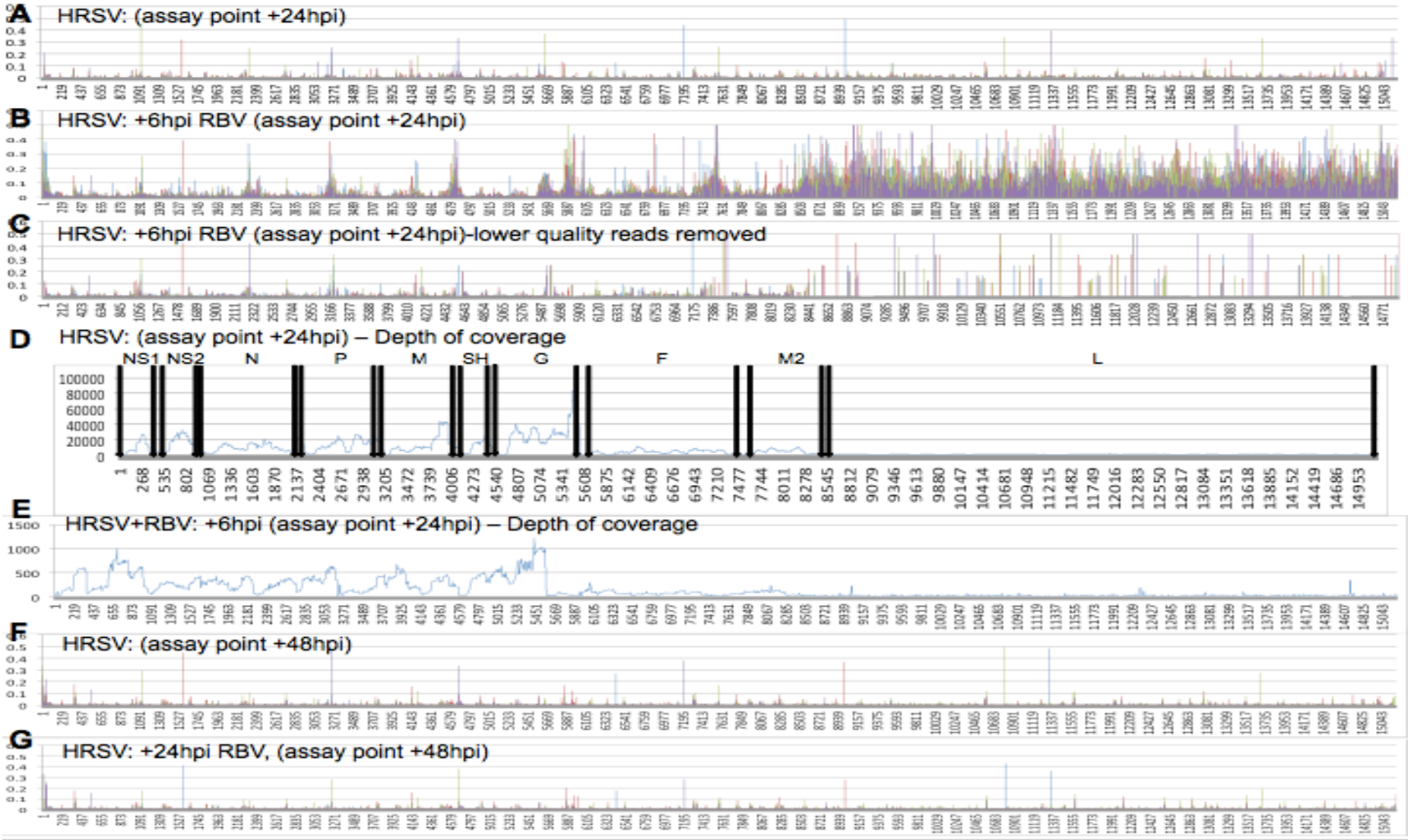
A
HRSV: (assay point +24hpi)
B
HRSV: +6hpi RBV (assay point +24hpi)
C
HRSV: +6hpi RBV (assay point +24hpi)-lower quality reads removed
D
HRSV: (assay point +24hpi) – Depth of coverage
NS1 NS2 N P M SH G F M2 L
E
HRSV+RBV: +6hpi (assay point +24hpi) – Depth of coverage
F
HRSV: (assay point +48hpi)
G
HRSV: +24hpi RBV, (assay point +48hpi)

***Figure 5.2*** *Analysis of depth of coverage and minor variation along the HRSV genome in the presence or absence of HRSV. In each part, the nucleotide position is indicated along the x axis. Charts illustrating the minor variation show the proportion of minor nucleotide calls at each nucleotide as a fraction of 1, thus a bar height of 0.4 indicates that at that nucleotide position some 40% of the sequence reads indicated an alternate base from the consensus. Charts illustrating coverage depth are a simple plot of the depth of sequence coverage at each nucleotide position. (A) Shows the location of minor variant base calls for HRSV mRNA mapped to the HRSV genome at 24 hours post- infection. (B) Shows the location of minor variant base calls for HRSV mRNA mapped to the HRSV genome at 24 hours post-infection when ribavirin has been added to the media at 6 hours post-infection using the same mapping pipeline as used in part A. (C) Shows an analysis of the same raw sequence data as in (B) but with low quality sequence reads removed (e.g. all reads with MAPQ less than 11 and mapped read length less than 50 bases). (D) Depth of coverage of sequence data for HRSV mRNA mapped to the HRSV genome at 24 hours post-infection with the location of HRSV genes indicated. (E) Depth of coverage of sequence data for HRSV mRNA mapped to the HRSV genome at 24 hours post-infection with ribavirin added at 6 hours post- infection, note the change in scale on the Y axis. (F) Shows the location of minor variant base calls for HRSV mRNA mapped to the HRSV genome at 48 hours post-infection. (G) Shows the location of minor variant base calls for HRSV mRNA mapped to the HRSV genome at 48 hours post-infection when ribavirin has been added*

*to the media at 24 hours post-infection using the same mapping pipeline as used in (A).*

Analysis of the sequence data when ribavirin was added at +24 hr post-infection and viral RNA analysed at 48 hr post-infection provided higher quality reads. For the control untreated HRSV infection there were 8 nucleotide positions that had a substitution in 30% or more of the sequence reads that mapped across that location (Figure 5.2 F). For HRSV infection in which ribavirin was added at +24 hr post-infection and nucleotide sequence analysed at 48 hr post-infection there were 5 nucleotide substitutions that were present in 30% or more of the sequence reads that mapped across that location (Figure 5.2 G).

As described in the introduction, ribavirin treatment might be expected to result in an increase in transition mutations specifically. To distinguish this effect, analysis of mutations was performed using the Bioedit Textpad and Excel software. Initially all transitions and transversions were scored and given a binary identification. Transversions were also analysed as an internal control to investigate whether the frequency of any mutation increased in the presence of ribavirin. Subsequently a sliding window of 500 nucleotides, was arbitrarily chosen, and was moved across the full length of the reference sequence by increments of 500 nucleotides. In each step, the number of transversion and transitions was determined among the minor sequence quasispecies (Figure 5.3). The data indicated that transition mutations significantly increased in the presence of ribavirin compared to the untreated control. The frequency of transversions was not significantly different. Reflecting this, the ratio of transitions to transversions was significantly

higher in ribavirin treated infected cells compared to untreated infected cells. There was greater experimental noise associated with the analysis of transitions in cells treated with ribavirin at +6 hr post-infection (assay point 24 hr post-infection) compared to ribavirin added at +24 hr post-infection (assay point 48 hr post-infection). This was attributed to the lower quality sequence reads, and the comparative data shown in Figure 5.3 is based on sequence reads obtained with the more abundant transcripts produced from the first half of the genome.

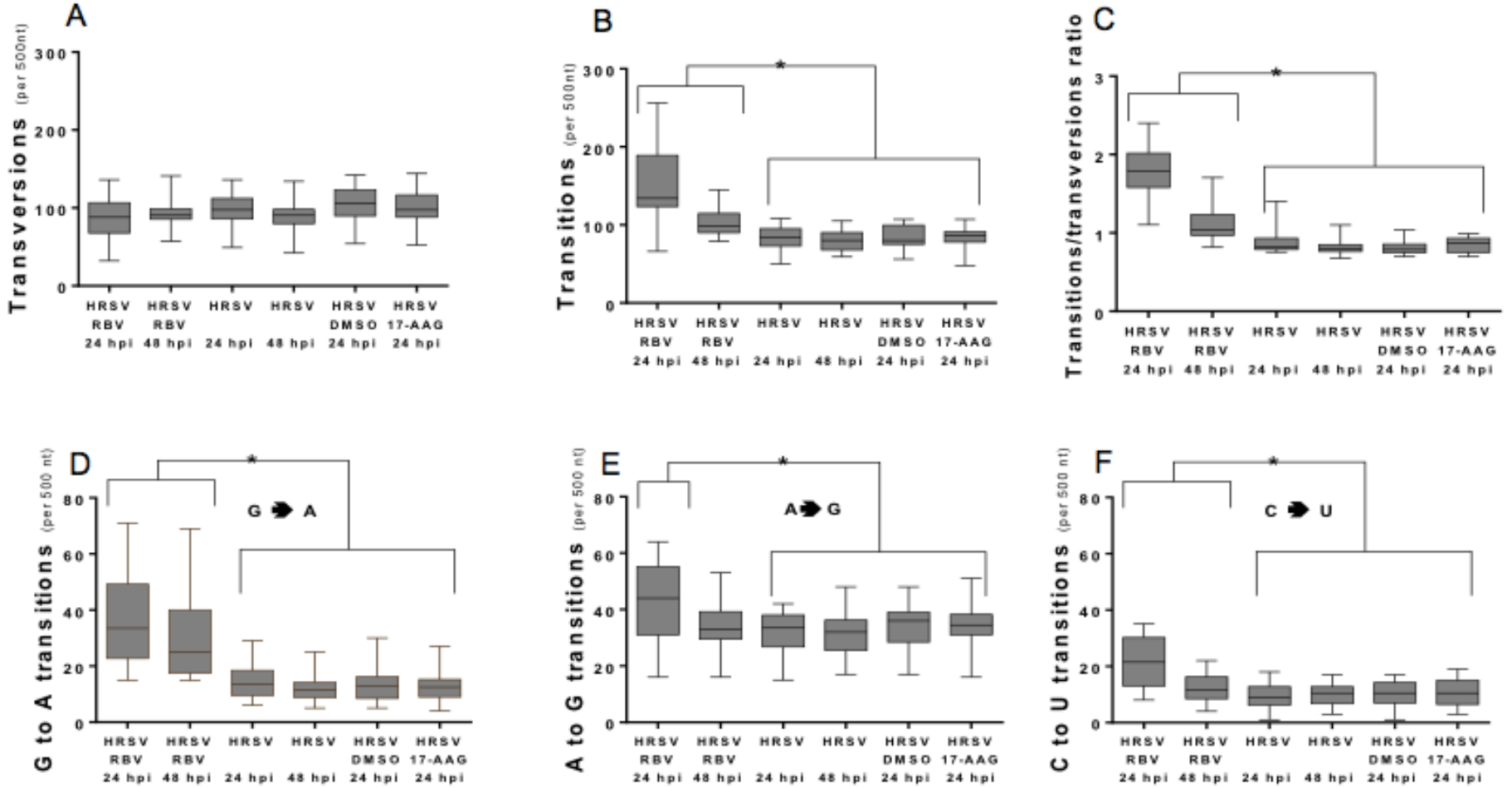
A
Transversions (per 500nt)
300
200
100
0
HRSV RBV 24 hpi
HRSV RBV 48 hpi
HRSV 24 hpi
HRSV 48 hpi
HRSV DMSO 24 hpi
HRSV 17-AAG 24 hpi
B
Transitions (per 500nt)
*
C
Transitions/transversions ratio
3
2
1
D
G to A transitions (per 500 nt)
G ➔ A
80
60
40
20
E
A to G transitions (per 500 nt)
A ➔ G
F
C to U transitions (per 500 nt)
C ➔ U

***Figure 5.3*** *Transition and transversion analyses for each of the culture conditions. The analysis was implemented, using a 500 hundred nucleotide sliding window across the genome. The area coding for the polymerase gene was not included in the analysis since the sequencing depth for this genomic region was much lower. The box-plot indicates the mean value, the 25 and 75 percentiles and the 95% CI of mean. For comparisons the paired t-test was implemented using the Prism software package (http://www.graphpad.com/scientific-software/prism.htm). (A) Shows the purine/pyrimidine transversions (B) the purine/purine and pyrimidine/pyrimidine transitions (C) shows transitions and tranversions (D) shows the G to A (E) the A to G and (F) the C to U permutations. The analysis was also performed using a 100 hundred nucleotide sliding window (data not shown) and results were similar.*

These results were also compared to data obtained from cells treated with 17-AAG as a control. Treatment of infected cells with 17-AAG inhibits the chaperone activity of HSP90, and results in destabilization of the HRSV L protein and concomitant reduction in viral mRNA and protein levels (Munday *et al.*, 2014b). Thus, 17-AAG acts indirectly as an inhibitor of RdRp accumulation (rather than activity) and has been shown to have an antiviral affect for HRSV (Geller *et al.*, 2013; Munday *et al.*, 2014b; Radhakrishnan *et al.*, 2010) and other negative strand RNA viruses (Connor *et al.*, 2007). Here, nucleotide substitution frequency was analysed at 24 hr post-infection. At this time, there were 8 nucleotide positions that had a substitution in 30% or more of the sequence reads that mapped across that location in the untreated control (Figure 5.4). For HRSV infection treated with 17-AAG at +6 hr post-infection and HRSV sequence analysed at 24 hr post-infection, this resulted in a 9-fold decrease in mappable reads to the HRSV genome (Table 5.1). There were 9 nucleotide positions that had a substitution in 30% or more of the sequence reads that mapped across that location (Figure 5.4). There was no evidence that 17-AAG caused an increase in the frequency of transition or transversions in HRSV-infected cells (Figure 5.3).

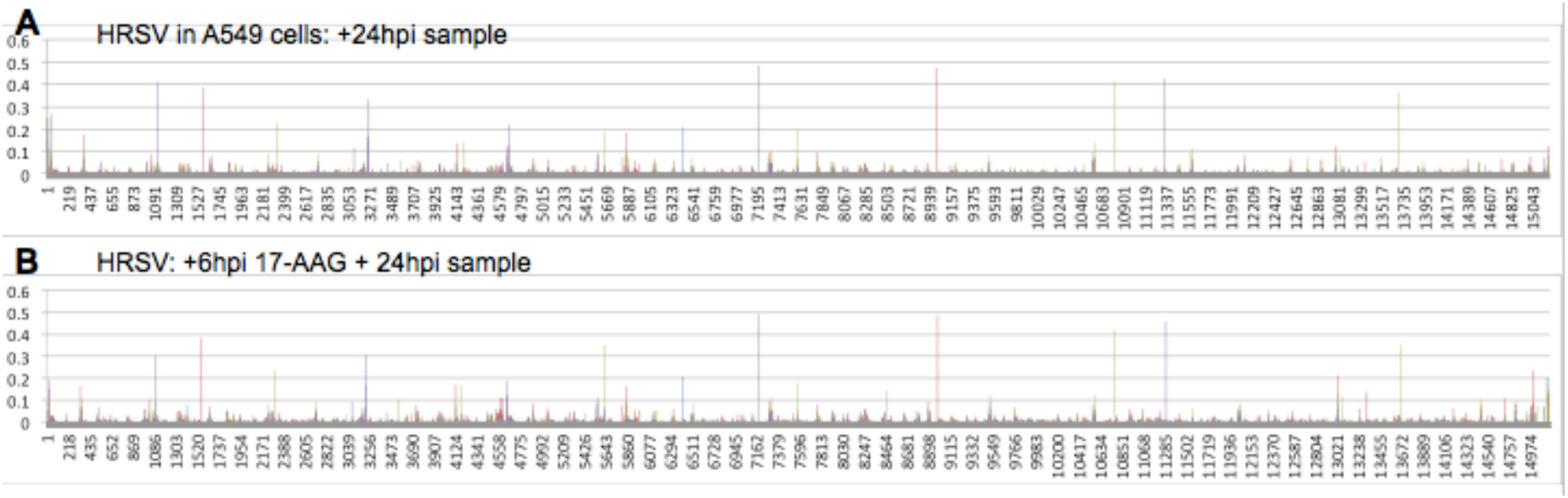


***Figure 5.4*** *Analysis of minor variation along the HRSV genome in the presence or absence of 17-AAG. In each part, the nucleotide position is indicated along the x axis. As before, the minor variation shows the proportion of minor nucleotide calls at each nucleotide as a fraction of 1, thus a bar height of 0.4 indicates that at that nucleotide position some 40% of the sequence reads indicated an alternate base from the consensus. (A) Shows the location of minor variant base calls for HRSV mRNA mapped to the HRSV genome at 24 hours post-infection in A549 cells. (B) Shows the location of minor variant base calls for HRSV mRNA mapped to the HRSV genome at 24 hours post-infection when 17-AAG has been added to the media at 6 hours post-infection in A549 cells using the same mapping pipeline as used in part A. Both data sets were generated independently of those analysed in Figure 5.2.*

### 5.2.4 TRANSITION AND TRANSVERSION SUBSTITUTIONS POTENTIALLY OCCUR IN CLUSTERS ALONG THE HRSV RNA GENOME

Interestingly, analysis of the position and frequency of the transition and transversion mutations along the HRSV genome, either untreated or treated with ribavirin suggested that these background substitutions did not occur with an even distribution and instead clustered in discrete hotspots (e.g. Figure 5.5). These hotspots were equivalent for HRSV grown in either HEp-2 or A549 cells, indicating that this observation was not dependent in these two cell types. Some of these hotspots are located at the intergenic regions but were also found in coding regions. There was no significant increase in transition or transversion substitutions in HRSV-infected cells treated with DMSO (e.g. Figure 5.3), which was the ribavirin solvent. However, there was an increase in transition mutations between (and within) hotspots with ribavirin treatment. From this analysis, it is clear that nucleotide changes in the viral genome due to the action of ribavirin then occur both in these clusters and between these clusters (Figure 5.5). The data also indicated that, in general, there was a greater frequency of transition and transversion substitutions within non-coding regions compared to coding regions (Figure 5.6).

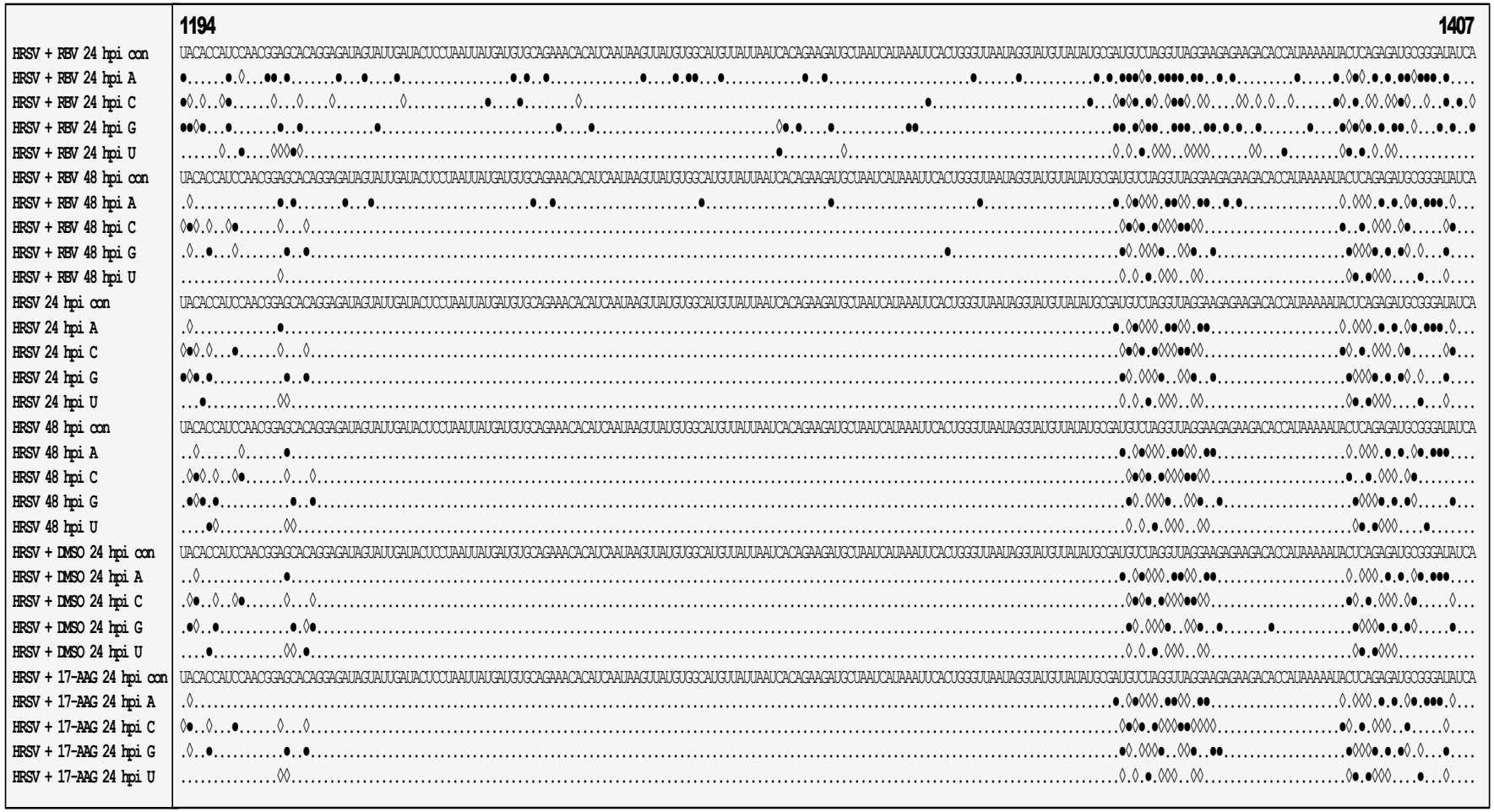
1194
1407
HRSV + RBV 24 hpi con
HRSV + RBV 24 hpi A
HRSV + RBV 24 hpi C
HRSV + RBV 24 hpi G
HRSV + RBV 24 hpi U
HRSV + RBV 48 hpi con
HRSV + RBV 48 hpi A
HRSV + RBV 48 hpi C
HRSV + RBV 48 hpi G
HRSV + RBV 48 hpi U
HRSV 24 hpi con
HRSV 24 hpi A
HRSV 24 hpi C
HRSV 24 hpi G
HRSV 24 hpi U
HRSV 48 hpi con
HRSV 48 hpi A
HRSV 48 hpi C
HRSV 48 hpi G
HRSV 48 hpi U
HRSV + DMSO 24 hpi con
HRSV + DMSO 24 hpi A
HRSV + DMSO 24 hpi C
HRSV + DMSO 24 hpi G
HRSV + DMSO 24 hpi U
HRSV + 17-AAG 24 hpi con
HRSV + 17-AAG 24 hpi A
HRSV + 17-AAG 24 hpi C
HRSV + 17-AAG 24 hpi G
HRSV + 17-AAG 24 hpi U

***Figure 5.5*** *Representative analysis of transitions (full circle) and transversions (open rombe) resulting the minor nucleotide variants at each position of HRSV genome with the different treatment regimes. For each condition, the consensus sequence is shown on the first line. The following four lines represent each of the four nucleotides found as a minor variant. The cut off value was 0.5% and the region of the genome shown is indicated by the bold numbers on top.*

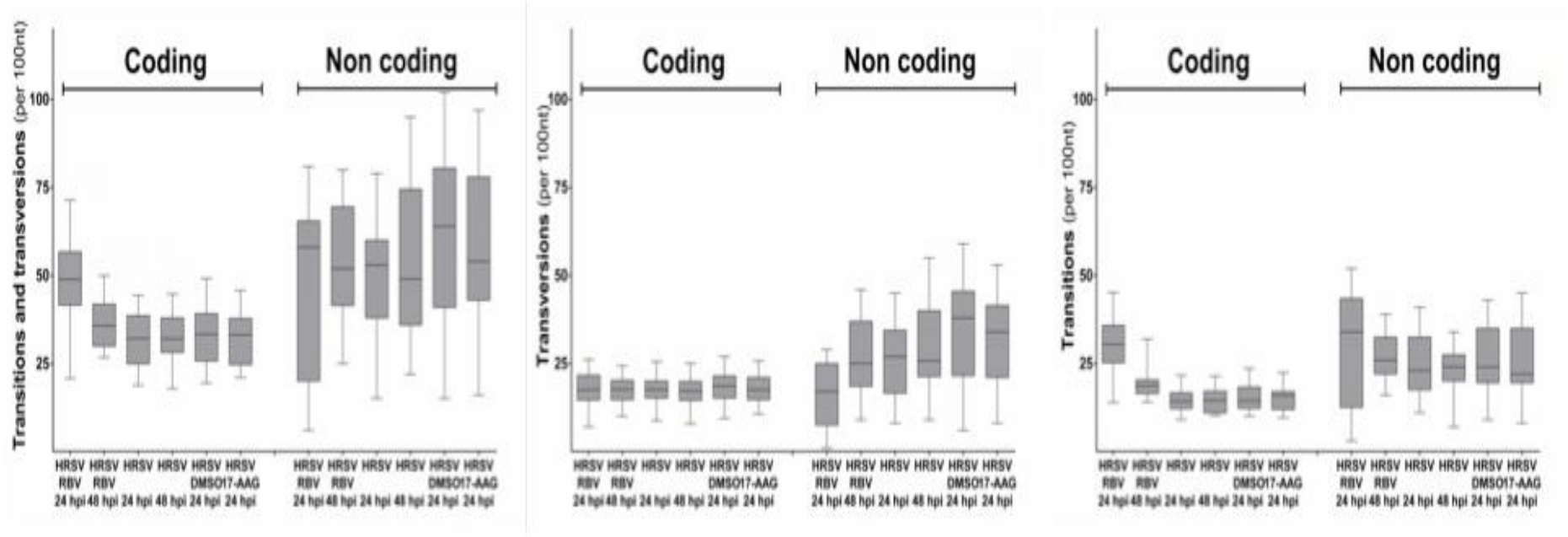


***Figure 5.6*** *Analysis of transitions and transversions in coding and non-coding regions of the HRSV genome with the different treatment regimes.*

## 5.3 DISCUSSION

For the first time, RNA-seq at high-resolution has been used to investigate HRSV RNA synthesis and to analyse the effect of a widely used and reportedly broad spectrum antiviral drug, ribavirin, on infected cell RNA accumulation and viral RNA mutation frequency. In the absence of ribavirin, RNA-seq analysis revealed that HRSV-specific RNAs formed up to one third of all RNA reads, suggesting a remarkable domination of the cellular RNA pool, at least in cell culture models. Indeed the analysis of sequencing data to generate minor variants was capped at 1 million reads mapping to the HRSV genome.

Ribavirin treatment of HRSV-infected cells resulted in decreases in progeny virus and overall levels of viral RNA as determined by the number of sequence reads that mapped to the HRSV genome (Table 5.1). Whilst this reduction in reads mapping to the HRSV genome in proportion to the total of reads obtained could be explained by an increase in cellular mRNA levels caused by ribavirin treatment, the data available does not support this conclusion. This would require a significant (~10 fold) and across the board increase (and in just the same genes detected in the ribavirin only control samples) in the total amount of mRNA in the cell. This would be unusual for either ribavirin treatment or HRSV infection. In addition, no evidence of increases in total RNA extracted from the cells treated solely with ribavirin was seen.

The analysis indicated that the frequency of transitions but not transversions in the HRSV genome were significantly different between infected cells treated with ribavirin versus untreated infected cells. No increase in nucleotide transitions or transversions in HRSV sequence was associated with treatment of infected cells with 17-AAG, an inhibitor of HSP90 (Figure 5.3) and HRSV polymerase accumulation and function (Munday *et al.*, 2014b). There was an approximately 1.5-fold increase in the recorded frequency of transitions on HRSV RNA in infected cells treated with ribavirin at 24 hr post-infection compared to the untreated control (Figure 5.3). This is less than the 4.4-fold increase in the frequency of transitions associated with the treatment of poliovirus-infected cells with 400 μM ribavirin (Crotty *et al.*, 2001), and the reasons for this are unclear. In the poliovirus study, cells were pretreated with ribavirin and the drug was maintained throughout the six-hour infection, whereas in this study, ribavirin was not added to the HRSV infected cells until either 6 or 24 hr post-infection. Alternatively, or in addition, it might be that the HRSV RdRp is more stringent than that of poliovirus, possibly due to the two-fold longer length of the HRSV genome. In this scenario, the HRSV RdRp might better discriminate against ribavirin triphosphate, resulting in reduced incorporation and thus a lower mutation rate. Regardless, elevations in mutation frequencies by as low as two-fold have been proposed to lead to fitness losses and extinctions of large RNA virus populations in cell culture and animal models of infection (Anderson *et al.*, 2004), and so the 1.5-fold increase in mutation frequency observed here could explain why ribavirin treatment resulted in reduced HRSV-specific RNA levels and progeny virus (Figures 3.8 and 3.11). While these results strongly suggest

the anti-HRSV action of ribavirin is through direct incorporation into nascent RNA by the viral polymerase, it cannot exclude the possibility that other proposed activities such as reduction of the GTP pool also contribute to reduced viral growth and HRSV-specific RNAs, although ribavirin did not affect the overall levels of cellular mRNA (Table 5.1).

As noted, the read depth of viral RNA was much lower when infected cells were treated with ribavirin at +6 hr post-infection compared to when infected cells were treated with ribavirin at +24 hr post-infection. In order to compare the nucleotide substitution frequency between these two experimental conditions, data from 3' proximal portion half of the HRSV genome was used. This is because the majority of the 5' proximal portion of the genome encodes the L mRNA, and this is the least abundant transcript, and subsequently has even fewer sequence reads mapping to it. The error rate of viral RdRp is estimated to be between $1.5\times10^{-3}$ $bp^{-1}$ (bacteriophage Q *β*) and $7.2\times10^{-5}bp^{-1}$ (influenza virus) (Drake, 1993). This relaxed fidelity of RdRp activity is an important feature of RNA virus biology, providing a source of sequence diversity that can allow virus quasispecies to form, enabling the virus to adapt successfully to changing environments. However, this inherent RdRp error rate can also be detrimental to virus biology and lead to the generation of non-viable templates that reduce overall viral fitness. The term rate 'error catastrophe' has been used to describe the outcome of a RdRp error rate at which too many non-viable templates are generated and a virus population becomes unsustainable, and it is believed that many viral RdRps

operate close to this threshold (Crotty & Andino, 2002; Crotty *et al.*, 2002). Although the length of the HRSV genome is only ~1.5 x longer than HCV or poliovirus, a 50% increase in the frequency of transition mutations appears to be sufficient to cause a loss in viable virus.

Interestingly the analysis indicated that transitions and transversions occurred in clusters along the HRSV RNA genome (Figure 5.5), and this was the same for viruses grown in different cell lines (e.g. HEp-2 and A549) and under a variety of different treatment conditions (e.g. in the presence of 17-AAG). Some of these clusters localized to the intergenic regions, and one possibility for this is the known tolerance for sequence changes within this region of the HRSV genome, and this is reflected in the difference between transition and transversion events between the coding and non-coding sequence (Figure 5.6). It is worth noting that these are the positions where such minor variants can occur, but these do not reflect the average consensus sequence. Analysis indicated that treatment with ribavirin increased the frequency of transition mutations in both the coding and non-coding regions (Figure 5.6).

The data also indicated a preponderance of A to G changes in the minor variants, which is a characteristic of adenosine deaminases acting on RNA (ADAR) modification, which depending on the virus, has been reported to have both anti-viral and pro-viral activity (Samuel, 2011). Genome wide association studies have shown an increase in ADAR transcripts during

HRSV infection in a mouse model (Stark *et al.*, 2010). Escape mutant analysis with antibodies specific for the G protein suggested that the G gene could potentially be modified by ADAR activity (Martínez & Melero, 2002).

Analysis of the abundance of HRSV mRNA, at the two time points analysed, indicated that they did not reflect a linear gradient that is predicated by the generally accepted and long-standing model for polar and sequential transcription of negative stranded RNA viruses (Figure 5.1). Several different algorithms were used to analyse the RNA-seq data and each of these indicated that the abundance of viral mRNAs in the cell at these specific time points did not follow a precise linear gradient. For the final data analysis shown in Figure 5.1, fragments per kilobase of gene per million bases mapped were manually calculated. Even a very conservative analysis of the RNA-seq data indicated a non-polar abundance of viral transcripts (Figure 5.1B). Given that there are very strong data to show that the HRSV RdRp cannot enter the template internally (Dickens *et al.*, 1984) and that in an *in vitro* transcription assay the amount of each transcript reflects the position of the gene on the genome (Barik, 1992), this result indicates that while gene order is a principle determinant of transcript abundance, it is not the only factor, with mRNA stability likely making an important contribution to relative mRNA levels. Importantly with respect to this study, ribavirin had no effect on the relative abundance of the ten sequentially transcribed HRSV transcripts (Figure 5.1). This current finding also suggests ribavirin has no detectable influence on RNA synthesis processes that could affect transcript stability.

These include RNA processing events such as 5' capping and poly (A) tail addition. The RNA-seq approach may provide a bias towards the recording of different mRNA abundances, although the data indicated that the % read through of HRSV transcripts followed the same pattern as that described using alternative approaches (Cartee *et al.*, 2003).

Using RNA-seq to measure viral mRNA abundance, a similar result has been recently described in the analysis of Hendra virus mRNA in infected human or bat cells (Wynne *et al.*, 2014). Similar to HRSV, Hendra virus is a member of the *Paramyxoviridae* family and both viruses share a similar genome architecture, replication and expression strategy. The order of genes along the Hendra virus genome (3' to 5') is N, P, M, F, G and L. In the analysis of either human or bat cells infected Hendra virus, there was a steep decline in the abundance of transcripts at the M-F gene boundary and the mRNA encoding the G protein was more abundant than the preceding mRNA encoding the F protein (Wynne *et al.*, 2014).

In summary, RNA-seq analysis was used to investigate HRSV RNA synthesis in infected cells and cells treated with ribavirin. This indicated that both transition and transversion mutations occurred in clusters along the HRSV genome. The frequency of transitions was increased in HRSV-infected cells treated with ribavirin and correlated with a reduction in the abundance of viral RNA and progeny virus, consistent with a loss of viral fitness.

# CHAPTER 6: GENERAL DISCUSSION AND FUTURE WORK

HRSV is mainly a paediatric infection and one of the major lower respiratory tract pathogens in infants - which are usually infected at least once within the first two years of life (Collins & Graham, 2008). Elderly patients, patients with chronic heart and lung conditions and immunocompromised patients are also at risk (Falsey *et al.*, 2005). There is no vaccine for HRSV or general anti-viral therapy. In acute cases, HRSV infection is treated therapeutically with ribavirin whose mechanism of action is not clearly understood. Ribavirin is the only therapeutic approved by the Food and Drug Administration (FDA) for the treatment of HRSV (Chu & Englund, 2013). In addition, ribavirin may also be used in immune-compromised and/or transplant and acute high-risk groups infected with HRSV. However, one postulated mechanism of action is to cause hyper-mutation of the target viral genome, which leads to error catastrophe during virus replication. Other mechanisms may include effects on host cell biology such as capping of mRNAs and activation of anti-viral gene expression. Therefore, studies in this field are necessary for a better understanding the action of ribavirin in HRSV infection and its wider application as anti-viral for the treatment of Crimean Congo Haemorrhagic fever virus and hepatitis C virus.

This thesis focused on the investigation of the effect of the antiviral, ribavirin on the cell biology of infected and un-infected cells and virus biology in an *in vitro* cell culture model using a combined high-resolution RNA-seq and deep

discovery label free quantitative proteomics approach. These approaches had not been applied before to investigate the effect of ribavirin as an anti-viral. Three aspects were studied, involving optimising the conditions for ribavirin treatment and viral infection in the cell culture model (Chapter 3), investigating the effect of ribavirin on host cells infected and uninfected with HRSV (Chapter 4) and analysis of the effect of ribavirin on HRSV infection (Chapter 5). Thus investigating both host cell biology and virus biology. The mechanisms of ribavirin on HRSV and infection of other viruses have been studied previously, however they are conflicting and may reflect different experimental conditions and viruses. To investigate the potential mechanism of action on HRSV, a combined high-resolution RNA-seq and deep discovery label free quantitative proteomics approach was used in this thesis. These combined approaches have not been used before to study HRSV biology and provides an opportunity to capture the maximum amount of data concerning the mechanism of action of this therapeutic. This includes investigating potential mechanisms of action of viral mutation rate, activation of host gene expression in anti-viral pathways and a reduction in the stability of mRNAs in general. In addition, several time points and treatment conditions were examined and these focused on early and late events during virus infection. This was to investigate and potentially model when ribavirin is used during infection *in vivo*. In general, ribavirin is not given as prophylactic and if treatment is giving too late in infection, then it is ineffective. This is also similar to influenza virus, when antivirals have to be given within the first 48 hr of infection, or viral loads become to high for the anti-viral to be effective (Monto *et al.*, 1999; Whitley *et al.*, 2001).

The effect of ribavirin on the host cell was examined and caused a significant decrease in progeny virus production. This study was focused on whether treatment of cells with ribavirin resulted in a difference in abundance of either cellular mRNAs or proteins. The transcriptomic approach identified more specific gene products than the proteomic approach, probably due to its higher sensitivity for detecting low abundance products. Potentially the mass spectrometry could be conducted under more sensitive conditions by increasing both sample run time and also pre-fractionation of the sample by gel electrophoresis to reduce the complexity of the sample being analysed.

The data indicated that the abundance of several hundred cellular mRNAs was affected by treatment with ribavirin and also the abundance of several cellular proteins were altered. This suggests that ribavirin can have a direct effect on the host cell. A number of cellular mRNAs increased in abundance in the presence of ribavirin and these included transcripts associated with the innate immune response and also pathways activated as part of anti-viral signalling cascades, confirming that ribavirin can directly activate host anti-viral gene transcripts – in the absence of viral infection. This may have a direct effect on HRSV-infection, perhaps by activating these responses in bystander cells that may subsequently be infected during viral spread and secondary rounds of infection. This has previously been observed before for HRSV in cell culture using microarrays to quantify host cell mRNAs (Martínez *et al.*, 2007; Zhang *et al.*, 2003). The RNA-seq based approach had the greater advantage of identifying many more transcripts – both in terms of

mRNA species that were unchanged and also those that were altered in abundance.

Additionally, ribavirin treatment caused a dramatic decrease in the viral mRNA abundance which then affected viral protein abundance (detected in the mass spectrometry) and also viral load (assayed by plaque assay). Most interestingly the data indicated that the transcription/abundance profile of viral mRNAs inside the infected cells did not conform to established literature. The potential of negative strand RNA virus mRNA transcription or at least mRNA abundance not to follow a linear gradient was also recently described for Hendra virus (Wynne *et al.*, 2014) and follows unpublished data from our own laboratory examining the replication of Ebola virus. Overall, the data suggested that both virological and cell factors (affecting RNA stability) influence the relative abundance of viral mRNA.

The analysis indicated that the frequency of transitions but not transversions in the HRSV genome were significantly different between infected cells treated with ribavirin versus untreated infected cells. There was an approximately 1.5-fold increase in the recorded frequency of transitions on HRSV RNA in infected cells treated with ribavirin at 24 hr post-infection compared to the untreated control. This is less than the 4.4-fold increase in the frequency of transitions associated with the treatment of poliovirus-infected cells with 400 μM ribavirin (Crotty *et al.*, 2001), and the reasons for this are unclear. Alternatively, or in addition, it might be that the HRSV RdRp

is more stringent than that of poliovirus, possibly due to the two-fold longer length of the HRSV genome. In this scenario, the HRSV RdRp might better discriminate against ribavirin triphosphate, resulting in reduced incorporation and thus a lower mutation rate. Regardless, elevations in mutation frequencies by as low as two-fold have been proposed to lead to fitness losses and extinctions of large RNA virus populations in cell culture and animal models of infection (Anderson *et al.*, 2004), and so the 1.5-fold increase in mutation frequency observed here could explain why ribavirin treatment resulted in reduced HRSV-specific RNA levels and progeny virus. While these results strongly suggest the anti-HRSV action of ribavirin is through direct incorporation into nascent RNA by the viral polymerase, it cannot exclude the possibility that other proposed activities such as reduction of the GTP pool also contribute to reduced viral growth and HRSV-specific RNAs, although ribavirin did not affect the overall levels of cellular mRNA. It would be interesting to use these datasets to analyse whether there are any potential errors in cellular mRNA transcripts e.g. the mutational frequency increases. However, this might be predicted to adversely affect cellular protein synthesis or abundance either due to incomplete translation or protein mis-folding. However, in general no overall decrease in the levels of cellular proteins were observed.

From five primary mechanisms of action suggested for ribavirin; inhibition of the viral polymerase, inhibition of RNA capping activity, loss of fitness of RNA virus genomes, immunomodulation effect and inhibition of IMPDH activity;

the novel data in this thesis strongly supports two out of these five potential mechanisms of action. These are the loss of fitness of viral RNA genomes and activation of innate/intrinsic anti-viral genes. Together these factors are likely to promote an anti-viral in both infected and bystander cells – that mediates the mechanism of action of ribavirin. There was no evidence in the RNAseq and proteomic data that overall levels of cellular mRNAs or cellular proteins were affected by ribavirin thus eliminating other mechanisms such as disruption of RNA capping as a potential route by which ribavirin works. However, these maybe viral specific as disruption of human parainfluenza virus acitivity *in vitro* is based on inhibition of IMPDH activity (Leyssen *et al.*, 2005). One of the future implementation plans from this study is to perform high-resolution approaches on human primary cells infected with HRSV and do some experiments to investigate whether the nucleotide mutations can cause amino acid changes and this causes redaction in viral biology. Such as the use of replicon or reverse genetic systems to evaluate the function of the polymerase under higher mutational frequency. Additionally, nasal aspirates from patients infected with and hospitalized due to HRSV could be analysed using deep sequencing – particularly if the patients have been treated with ribavirin and longitudinal samples taken.

In future, as the application of RNA-seq and label free proteomics provided powerful tools for investigating the mechanism of action of ribavirin and for better understanding of mutation in HRSV infection, this will allow further studies into the effect of ribavirin on other viruses as mechanisms differ from

virus to virus (Crotty *et al.*, 2002). Further studies could then compare the *in vitro* and *in vivo* data and study transcripts that are up/down-regulated in the presence of antiviral ribavirin. This general combined approach of RNAseq and proteomics could be used to rapidly study and characterize new viruses and measure the effect of therapeutics. For example, to study Middle East Respiratory Syndrome coronavirus MERS-CoV, which is a new strain of a coronavirus that was discovered in late 2012. This would also identifying biomarkers within a patient that will act as predictors of disease severity and inform treatment options. Also, potential cellular targets that the virus uses to enhance infection will be identified. These potentially could be targeted with repurposed therapeutics to reduce viral load and clinical symptoms by using high-resolution approaches; RNA-seq and proteomics to study MERS-CoV in respiratory epithelial cells.

In conclusion, this thesis and resulting publications have given a new insight into the action of the antiviral ribavirin with/without HRSV by using high-resolution approaches RNA-seq and label free proteomics. The data analysis indicated that ribavirin had a direct mutagenic effect on the HRSV genome and the frequency of transition mutations were increased in HRSV-infected cells treated with ribavirin and correlated with a reduction in the abundance of viral RNA and progeny virus, consistent with a loss of viral fitness. The findings of this study have increased our understanding of mechanism of ribavirin for HRSV supporting its direct role in increasing the mutation rate in the viral genome and activation of intrinsic/innate anti-viral signalling.

# CHAPTER 7: REFERENCES

**ALFSON KJ, W. G., CARRION R JR, GRIFFITHS A (2015). DETERMINATION AND THERAPEUTIC EXPLOITATION OF EBOLA VIRUS SPONTANEOUS MUTATION FREQUENCY. *JOURNAL OF VIROLOGY*.**

**AMAYA, M., BAER, A., VOSS, K., CAMPBELL, C., MUELLER, C., BAILEY, C., KEHN-HALL, K., PETRICOIN, E., 3RD & NARAYANAN, A. (2014). PROTEOMIC STRATEGIES FOR THE DISCOVERY OF NOVEL DIAGNOSTIC AND THERAPEUTIC TARGETS FOR INFECTIOUS DISEASES. *PATHOG DIS* 71, 177-189.**

**ANDERSON, J. P., DAIFUKU, R. & LOEB, L. A. (2004). VIRAL ERROR CATASTROPHE BY MUTAGENIC NUCLEOSIDES. *ANNUAL REVIEW OF MICROBIOLOGY* 58, 183-205.**

**ASENJO, A., CALVO, E. & VILLANUEVA, N. (2006). PHOSPHORYLATION OF HUMAN RESPIRATORY SYNCYTIAL VIRUS P PROTEIN AT THREONINE 108 CONTROLS ITS INTERACTION WITH THE M2-1 PROTEIN IN THE VIRAL RNA POLYMERASE COMPLEX. *JOURNAL OF GENERAL VIROLOGY* 87, 3637-3642.**

**ASENJO, A., GONZÁLEZ-ARMAS, J. C. & VILLANUEVA, N. (2008). PHOSPHORYLATION OF HUMAN RESPIRATORY SYNCYTIAL VIRUS P PROTEIN AT SERINE 54 REGULATES VIRAL UNCOATING. *VIROLOGY* 380, 26-33.**

**BACHI, T. & HOWE, C. (1973). MORPHOGENESIS AND ULTRASTRUCTURE OF RESPIRATORY SYNCYTIAL VIRUS. *JOURNAL OF VIROLOGY* 12, 1173-1180.**

**BAKRE, A., WU, W., HISCOX, J., SPANN, K., TENG, M. N. & TRIPP, R. A. (2015). HUMAN RESPIRATORY SYNCYTIAL VIRUS NON-STRUCTURAL PROTEIN NS1 MODIFIES MIR-24 EXPRESSION VIA TRANSFORMING GROWTH FACTOR-B. *JOURNAL OF GENERAL VIROLOGY* 96, 3179-3191.**

**BALTIMORE, D. (1971). EXPRESSION OF ANIMAL VIRUS GENOMES. *BACTERIOL REV* 35, 235-241.**

**BANTSCHEFF, M., SCHIRLE, M., SWEETMAN, G., RICK, J. & KUSTER, B. (2007). QUANTITATIVE MASS SPECTROMETRY IN PROTEOMICS: A CRITICAL REVIEW. *ANALYTICAL AND BIOANALYTICAL CHEMISTRY* 389, 1017-1031.**

**BARIK, S. (1992). TRANSCRIPTION OF HUMAN RESPIRATORY SYNCYTIAL VIRUS GENOME RNA IN VITRO: REQUIREMENT OF CELLULAR FACTOR(S). *JOURNAL OF VIROLOGY* 66, 6813-6818.**

**BARRY, M. A., REYNOLDS, J. E. & EASTMAN, A. (1993). ETOPOSIDE-INDUCED APOPTOSIS IN HUMAN HL-60 CELLS IS ASSOCIATED WITH INTRACELLULAR ACIDIFICATION. *CANCER RESEARCH* 53, 2349-2357.**

**BEHERA, A. K., MATSUSE, H., KUMAR, M., KONG, X., LOCKEY, R. F. & MOHAPATRA, S. S. (2001). BLOCKING INTERCELLULAR ADHESION**

MOLECULE-1 ON HUMAN EPITHELIAL CELLS DECREASES RESPIRATORY SYNCYTIAL VIRUS INFECTION. *BIOCHEMICAL AND BIOPHYSICAL RESEARCH COMMUNICATIONS* 280, 188-195.

BERMINGHAM, A. & COLLINS, P. L. (1999). THE M2-2 PROTEIN OF HUMAN RESPIRATORY SYNCYTIAL VIRUS IS A REGULATORY FACTOR INVOLVED IN THE BALANCE BETWEEN RNA REPLICATION AND TRANSCRIPTION. *PROCEEDINGS OF THE NATIONAL ACADEMY OF SCIENCES OF THE UNITED STATES OF AMERICA* 96, 11259-11264.

BHOJ, V. G., SUN, Q., BHOJ, E. J., SOMERS, C., CHEN, X., TORRES, J. P., MEJIAS, A., GOMEZ, A. M., JAFRI, H., RAMILO, O. & CHEN, Z. J. (2008). MAVS AND MYD88 ARE ESSENTIAL FOR INNATE IMMUNITY BUT NOT CYTOTOXIC T LYMPHOCYTE RESPONSE AGAINST RESPIRATORY SYNCYTIAL VIRUS. *PROCEEDINGS OF THE NATIONAL ACADEMY OF SCIENCES OF THE UNITED STATES OF AMERICA* 105, 14046-14051.

BITKO, V., SHULYAYEVA, O., MAZUMDER, B., MUSIYENKO, A., RAMASWAMY, M., LOOK, D. C. & BARIK, S. (2007). NONSTRUCTURAL PROTEINS OF RESPIRATORY SYNCYTIAL VIRUS SUPPRESS PREMATURE APOPTOSIS BY AN NF-KB-DEPENDENT, INTERFERON-INDEPENDENT MECHANISM AND FACILITATE VIRUS GROWTH. *JOURNAL OF VIROLOGY* 81, 1786-1795.

BLOUNT JR, R. E., MORRIS, J. A. & SAVAGE, R. E. (1956). RECOVERY OF CYTOPATHOGENIC AGENT FROM CHIMPANZEES WITH CORYZA. *PROC SOC EXP BIOL MED* 92, 544-549.

BOCCHINI JR, J. A., BERNSTEIN, H. H., BRADLEY, J. S., BRADY, M. T., BYINGTON, C. L., FISHER, M. C., GLODE, M. P., JACKSON, M. A., KEYSERLING, H. L., KIMBERLIN, D. W., ORENSTEIN, W. A., SCHUTZE, G. E., WILLOUGHBY, R. E., DENNEHY, P. H., FRENCK JR, R. W., BELL, B., BORTOLUSSI, R., CLOVER, R. D., FISCHER, M. A., GELLIN, B., GORMAN, R. L., PRATT, R. D., LEE, L., READ, J. S., STARKE, J. R., SWANSON, J., BAKER, C. J., LONG, S. S., PICKERING, L. K., LEDBETTER, E. O., MEISSNER, H. C., RUBIN, L. G., HALL, C. & FRANTZ, J. (2009). POLICY STATEMENT - MODIFIED RECOMMENDATIONS FOR USE OF PALIVIZUMAB FOR PREVENTION OF RESPIRATORY SYNCYTIAL VIRUS INFECTIONS. *PEDIATRICS* 124, 1694-1701.

BOECKH, M., BERREY, M. M., BOWDEN, R. A., CRAWFORD, S. W., BALSLEY, J. & COREY, L. (2001). PHASE 1 EVALUATION OF THE RESPIRATORY SYNCYTIAL VIRUS-SPECIFIC MONOCLONAL ANTIBODY PALIVIZUMAB IN RECIPIENTS OF HEMATOPOIETIC STEM CELL TRANSPLANTS. *JOURNAL OF INFECTIOUS DISEASES* 184, 350-354.

BORCHERS, A. T., CHANG, C., GERSHWIN, M. E. & GERSHWIN, L. J. (2013). RESPIRATORY SYNCYTIAL VIRUS - A COMPREHENSIVE REVIEW. *CLINICAL REVIEWS IN ALLERGY AND IMMUNOLOGY* 45, 331-379.

BRADLEY, J. P., BACHARIER, L. B., BONFIGLIO, J., SCHECHTMAN, K. B., STRUNK, R., STORCH, G. & CASTRO, M. (2005). SEVERITY OF RESPIRATORY SYNCYTIAL VIRUS BRONCHIOLITIS IS AFFECTED BY CIGARETTE SMOKE EXPOSURE AND ATOPY. *PEDIATRICS* 115, E7-E14.

**BRONZE, M. S. & GREENFIELD, R. A. (2003). THERAPEUTIC OPTIONS FOR DISEASES DUE TO POTENTIAL VIRAL AGENTS OF BIOTERRORISM. *CURRENT OPINION IN INVESTIGATIONAL DRUGS* 4, 172-178.**

**BROWN, G., RIXON, H. W. M. & SUGRUE, R. J. (2002). RESPIRATORY SYNCYTIAL VIRUS ASSEMBLY OCCURS IN GM1-RICH REGIONS OF THE HOST-CELL MEMBRANE AND ALTERS THE CELLULAR DISTRIBUTION OF TYROSINE PHOSPHORYLATED CAVEOLIN-1. *JOURNAL OF GENERAL VIROLOGY* 83, 1841-1850.**

**BUKREYEV, A., WHITEHEAD, S. S., MURPHY, B. R. & COLLINS, P. L. (1997). RECOMBINANT RESPIRATORY SYNCYTIAL VIRUS FROM WHICH THE ENTIRE SH GENE HAS BEEN DELETED GROWS EFFICIENTLY IN CELL CULTURE AND EXHIBITS SITE-SPECIFIC ATTENUATION IN THE RESPIRATORY IN TRACT OF THE MOUSE. *JOURNAL OF VIROLOGY* 71, 8973-8982.**

**BURKE, E., DUPUY, L., WALL, C. & BARIK, S. (1998). ROLE OF CELLULAR ACTIN IN THE GENE EXPRESSION AND MORPHOGENESIS OF HUMAN RESPIRATORY SYNCYTIAL VIRUS. *VIROLOGY* 252, 137-148.**

**BURKE, E., MAHONEY, N. M., ALMO, S. C. & BARIK, S. (2000). PROFILIN IS REQUIRED FOR OPTIMAL ACTIN-DEPENDENT TRANSCRIPTION OF RESPIRATORY SYNCYTIAL VIRUS GENOME RNA. *JOURNAL OF VIROLOGY* 74, 669-675.**

**CAMERON, C. E. & CASTRO, C. (2001). THE MECHANISM OF ACTION OF RIBAVIRIN: LETHAL MUTAGENESIS OF RNA VIRUS GENOMES MEDIATED BY THE VIRAL RNA-DEPENDENT RNA POLYMERASE. *CURRENT OPINION IN INFECTIOUS DISEASES* 14, 757-764.**

**CANE, P. A., MATTHEWS, D. A. & PRINGLE, C. R. (1991). IDENTIFICATION OF VARIABLE DOMAINS OF THE ATTACHMENT (G) PROTEIN OF SUBGROUP A RESPIRATORY SYNCYTIAL VIRUSES. *JOURNAL OF GENERAL VIROLOGY* 72, 2091-2096.**

**CARROLL, M. W., MATTHEWS, D. A., HISCOX, J. A., ELMORE, M. J., POLLAKIS, G., RAMBAUT, A., HEWSON, R., GARCÍA-DORIVAL, I., BORE, J. A., KOUNDOUNO, R., ABDELLATI, S., AFROUGH, B., AIYEPADA, J., AKHILOMEN, P., ASOGUN, D., ATKINSON, B., BADUSCHE, M., BAH, A., BATE, S., BAUMANN, J., BECKER, D., BECKER-ZIAJA, B., BOCQUIN, A., BORREMANS, B., BOSWORTH, A., BOETTCHER, J. P., CANNAS, A., CARLETTI, F., CASTILLETTI, C., CLARK, S., COLAVITA, F., DIEDERICH, S., DONATUS, A., DURAFFOUR, S., EHICHIOYA, D., ELLERBROK, H., FERNANDEZ-GARCIA, M. D., FIZET, A., FLEISCHMANN, E., GRYSEELS, S., HERMELINK, A., HINZMANN, J., HOPF-GUEVARA, U., IGHODALO, Y., JAMESON, L., KELTERBAUM, A., KIS, Z., KLOTH, S., KOHL, C., KORVA, M., KRAUS, A., KUISMA, E., KURTH, A., LIEDIGK, B., LOGUE, C. H., LÜDTKE, A., MAES, P., MCCOWEN, J., MÉLY, S., MERTENS, M., MESCHI, S., MEYER, B., MICHEL, J., MOLKENTHIN, P., MUÑOZ-FONTELA, C., MUTH, D., NEWMAN, E. N. C., NGABO, D., OESTEREICH, L., OKOSUN, J., OLOKOR, T., OMIUNU, R., OMOMOH, E., PALLASCH, E., PÁLYI, B., PORTMANN, J., POTTAGE, T., PRATT, C., PRIESNITZ, S., QUARTU, S., RAPPE, J., REPITS, J., RICHTER, M., RUDOLF,**

**M., SACHSE, A., SCHMIDT, K. M., SCHUDT, G., STRECKER, T., THOM, R., THOMAS, S., TOBIN, E., TOLLEY, H., TRAUTNER, J., VERMOESEN, T., VITORIANO, I., WAGNER, M., WOLFF, S., YUE, C., CAPOBIANCHI, M. R., KRETSCHMER, B., HALL, Y., KENNY, J. G., RICKETT, N. Y., DUDAS, G., COLTART, C. E. M., KERBER, R., STEER, D., WRIGHT, C., SENYAH, F., KEITA, S., DRURY, P., DIALLO, B., DE CLERCK, H., VAN HERP, M., SPRECHER, A., TRAORE, A., DIAKITE, M., KONDE, M. K., KOIVOGUI, L., MAGASSOUBA, N., AVŠIÄ-AUPANC, T., NITSCHE, A., STRASSER, M., IPPOLITO, G., BECKER, S., STOECKER, K., GABRIEL, M., RAOUL, H., DI CARO, A., WÖLFEL, R., FORMENTY, P. & GÜNTHER, S. (2015). TEMPORAL AND SPATIAL ANALYSIS OF THE 2014-2015 EBOLA VIRUS OUTBREAK IN WEST AFRICA. *NATURE* 524, 97-101.**

**CARTEE, T. L., MEGAW, A. G., OOMENS, A. G. P. & WERTZ, G. W. (2003). IDENTIFICATION OF A SINGLE AMINO ACID CHANGE IN THE HUMAN RESPIRATORY SYNCYTIAL VIRUS L PROTEIN THAT AFFECTS TRANSCRIPTIONAL TERMINATION. *JOURNAL OF VIROLOGY* 77, 7352-7360.**

**CARTEE, T. L. & WERTZ, G. W. (2001). RESPIRATORY SYNCYTIAL VIRUS M2-1 PROTEIN REQUIRES PHOSPHORYLATION FOR EFFICIENT FUNCTION AND BINDS VIRAL RNA DURING INFECTION. *JOURNAL OF VIROLOGY* 75, 12188-12197.**

**CARTER, S. D., DENT, K. C., ATKINS, E., FOSTER, T. L., VEROW, M., GORNY, P., HARRIS, M., HISCOX, J. A., RANSON, N. A., GRIFFIN, S. & BARR, J. N. (2010). DIRECT VISUALIZATION OF THE SMALL HYDROPHOBIC PROTEIN OF HUMAN RESPIRATORY SYNCYTIAL VIRUS REVEALS THE STRUCTURAL BASIS FOR MEMBRANE PERMEABILITY. *FEBS LETTERS* 584, 2786-2790.**

**CHU, H. Y. & ENGLUND, J. A. (2013). RESPIRATORY SYNCYTIAL VIRUS DISEASE: PREVENTION AND TREATMENT. *CURRENT TOPICS IN MICROBIOLOGY AND IMMUNOLOGY* 372, 235-258.**

**CHU, H. Y., KUYPERS, J., RENAUD, C., WALD, A., MARTIN, E., FAIRCHOK, M., MAGARET, A., SARANCINO, M. & ENGLUND, J. A. (2013). MOLECULAR EPIDEMIOLOGY OF RESPIRATORY SYNCYTIAL VIRUS TRANSMISSION IN CHILDCARE. *JOURNAL OF CLINICAL VIROLOGY* 57, 343-350.**

**CHUNG, R. T., GALE JR, M., POLYAK, S. J., LEMON, S. M., LIANG, T. J. & HOOFNAGLE, J. H. (2008). MECHANISMS OF ACTION OF INTERFERON AND RIBAVIRIN IN CHRONIC HEPATITIS C: SUMMARY OF A WORKSHOP. *HEPATOLOGY* 47, 306-320.**

**COLLINS, D. W. & JUKES, T. H. (1994). RATES OF TRANSITION AND TRANSVERSION IN CODING SEQUENCES SINCE THE HUMAN- RODENT DIVERGENCE. *GENOMICS* 20, 386-396.**

**COLLINS, P. L., AND J. JAMES E. CROWE (2007). *RESPIRATORY SYNCYTIAL VIRUS AND METAPNEUMOVIRUS, FIELDS VIROLOGY, 5TH EDITION 2, 14*.**

**COLLINS, P. L., CAMARGO, E. & HILL, M. G. (1999). SUPPORT PLASMIDS AND SUPPORT PROTEINS REQUIRED FOR RECOVERY OF RECOMBINANT RESPIRATORY SYNCYTIAL VIRUS. *VIROLOGY* 259, 251-255.**

**COLLINS, P. L. & GRAHAM, B. S. (2008). VIRAL AND HOST FACTORS IN HUMAN RESPIRATORY SYNCYTIAL VIRUS PATHOGENESIS. *JOURNAL OF VIROLOGY* 82, 2040-2055.**

**COLLINS, P. L., HILL, M. G., CAMARGO, E., GROSFELD, H., CHANOCK, R. M. & MURPHY, B. R. (1995). PRODUCTION OF INFECTIOUS HUMAN RESPIRATORY SYNCYTIAL VIRUS FROM CLONED CDNA CONFIRMS AN ESSENTIAL ROLE FOR THE TRANSCRIPTION ELONGATION FACTOR FROM THE 5′ PROXIMAL OPEN READING FRAME OF THE M2 MRNA IN GENE EXPRESSION AND PROVIDES A CAPABILITY FOR VACCINE DEVELOPMENT. *PROCEEDINGS OF THE NATIONAL ACADEMY OF SCIENCES OF THE UNITED STATES OF AMERICA* 92, 11563-11567.**

**COLLINS, P. L., HILL, M. G., CRISTINA, J. & GROSFELD, H. (1996). TRANSCRIPTION ELONGATION FACTOR OF RESPIRATORY SYNCYTIAL VIRUS, A NONSEGMENTED NEGATIVE-STRAND RNA VIRUS. *PROCEEDINGS OF THE NATIONAL ACADEMY OF SCIENCES OF THE UNITED STATES OF AMERICA* 93, 81-85.**

**COLLINS, P. L., KARRON,R.A. (2013). RESPIRATORY SYNCYTIAL VIRUS AND METAPNEUMOVIRUS. IN *FIELDS VIROLOGY*, 6TH ED EDN, PP. 1086-1123. EDITED BY D. M. KNIPE, HOWLEY, P.M. PHILADELPHIA: WOLTERS KLUWER/ LIPPINCOTT WILLIAMS & WILKINS.**

**COLLINS, P. L. & MELERO, J. A. (2011). PROGRESS IN UNDERSTANDING AND CONTROLLING RESPIRATORY SYNCYTIAL VIRUS: STILL CRAZY AFTER ALL THESE YEARS. *VIRUS RESEARCH* 162, 80-99.**

**COLLINS, P. L., MINK, M. A. & STEC, D. S. (1991). RESCUE OF SYNTHETIC ANALOGS OF RESPIRATORY SYNCYTIAL VIRUS GENOMIC RNA AND EFFECT OF TRUNCATIONS AND MUTATIONS ON THE EXPRESSION OF A FOREIGN REPORTER GENE. *PROCEEDINGS OF THE NATIONAL ACADEMY OF SCIENCES OF THE UNITED STATES OF AMERICA* 88, 9663-9667.**

**COLLINS, P. L. & MOTTET, G. (1991). POST-TRANSLATIONAL PROCESSING AND OLIGOMERIZATION OF THE FUSION GLYCOPROTEIN OF HUMAN RESPIRATORY SYNCYTIAL VIRUS. *JOURNAL OF GENERAL VIROLOGY* 72, 3095-3101.**

**COLLINS, P. L. & MOTTET, G. (1993). MEMBRANE ORIENTATION AND OLIGOMERIZATION OF THE SMALL HYDROPHOBIC PROTEIN OF HUMAN RESPIRATORY SYNCYTIAL VIRUS. *JOURNAL OF GENERAL VIROLOGY* 74, 1445-1450.**

**COLLINS, P. L. & WERTZ, G. W. (1983). CDNA CLONING AND TRANSCRIPTIONAL MAPPING OF NINE POLYADENYLYLATED RNAS ENCODED BY THE GENOME OF HUMAN RESPIRATORY SYNCYTIAL VIRUS. *PROCEEDINGS OF THE NATIONAL ACADEMY OF SCIENCES OF THE UNITED STATES OF AMERICA* 80, 3208-3212.**

**CONNOR, E. M. (1998). PALIVIZUMAB, A HUMANIZED RESPIRATORY SYNCYTIAL VIRUS MONOCLONAL ANTIBODY, REDUCES HOSPITALIZATION FROM RESPIRATORY SYNCYTIAL VIRUS INFECTION IN HIGH-RISK INFANTS. *PEDIATRICS* 102, 531-537.**

**CONNOR, J. H., MCKENZIE, M. O., PARKS, G. D. & LYLES, D. S. (2007). ANTIVIRAL ACTIVITY AND RNA POLYMERASE DEGRADATION FOLLOWING HSP90 INHIBITION IN A RANGE OF NEGATIVE STRAND VIRUSES. *VIROLOGY* 362, 109-119.**

**COOMBS, K. M., BERARD, A., XU, W., KROKHIN, O., MENG, X., CORTENS, J. P., KOBASA, D., WILKINS, J. & BROWN, E. G. (2010). QUANTITATIVE PROTEOMIC ANALYSES OF INFLUENZA VIRUS-INFECTED CULTURED HUMAN LUNG CELLS. *JOURNAL OF VIROLOGY* 84, 10888-10906.**

**COX, J., HEIN, M. Y., LUBER, C. A., PARON, I., NAGARAJ, N. & MANN, M. (2014). ACCURATE PROTEOME-WIDE LABEL-FREE QUANTIFICATION BY DELAYED NORMALIZATION AND MAXIMAL PEPTIDE RATIO EXTRACTION, TERMED MAXLFQ. *MOLECULAR AND CELLULAR PROTEOMICS* 13, 2513-2526.**

**COX, J. & MANN, M. (2011). QUANTITATIVE, HIGH-RESOLUTION PROTEOMICS FOR DATA-DRIVEN SYSTEMS BIOLOGY. IN *ANNUAL REVIEW OF BIOCHEMISTRY*, PP. 273-299.**

**CROTTY, S. & ANDINO, R. (2002). IMPLICATIONS OF HIGH RNA VIRUS MUTATION RATES: LETHAL MUTAGENESIS AND THE ANTIVIRAL DRUG RIBAVIRIN. *MICROBES AND INFECTION* 4, 1301-1307.**

**CROTTY, S., CAMERON, C. & ANDINO, R. (2002). RIBAVIRIN'S ANTIVIRAL MECHANISM OF ACTION: LETHAL MUTAGENESIS? *J MOL MED* 80, 86-95.**

**CROTTY, S., CAMERON, C. E. & ANDINO, R. (2001). RNA VIRUS ERROR CATASTROPHE: DIRECT MOLECULAR TEST BY USING RIBAVIRIN. *PROCEEDINGS OF THE NATIONAL ACADEMY OF SCIENCES OF THE UNITED STATES OF AMERICA* 98, 6895-6900.**

**CURRIE, S. M., FINDLAY, E. G., MCHUGH, B. J., MACKELLAR, A., MAN, T., MACMILLAN, D., WANG, H., FITCH, P. M., SCHWARZE, J. & DAVIDSON, D. J. (2013). THE HUMAN CATHELICIDIN LL-37 HAS ANTIVIRAL ACTIVITY AGAINST RESPIRATORY SYNCYTIAL VIRUS. *PLOS ONE* 8.**

**DAPAT, C. & OSHITANI, H. (2016). NOVEL INSIGHTS INTO HUMAN RESPIRATORY SYNCYTIAL VIRUS-HOST FACTOR INTERACTIONS THROUGH INTEGRATED PROTEOMICS AND TRANSCRIPTOMICS ANALYSIS. *EXPERT REVIEW OF ANTI-INFECTIVE THERAPY* 14, 285-297.**

**DAVE, K. A., NORRIS, E. L., BUKREYEV, A. A., HEADLAM, M. J., BUCHHOLZ, U. J., SINGH, T., COLLINS, P. L. & GORMAN, J. J. (2014). A COMPREHENSIVE PROTEOMIC VIEW OF RESPONSES OF A549 TYPE II ALVEOLAR EPITHELIAL CELLS TO HUMAN RESPIRATORY SYNCYTIAL VIRUS INFECTION. *MOLECULAR AND CELLULAR PROTEOMICS* 13, 3250-3269.**

**DAY, C. W., SMEE, D. F., JULANDER, J. G., YAMSHCHIKOV, V. F., SIDWELL, R. W. & MORREY, J. D. (2005). ERROR-PRONE REPLICATION OF WEST NILE VIRUS CAUSED BY RIBAVIRIN. *ANTIVIRAL RESEARCH* 67, 38-45.**

**DAY, T. W., WU, C. H. & SAFA, A. R. (2009). ETOPOSIDE INDUCES PROTEIN KINASE CΔ- AND CASPASE-3-DEPENDENT APOPTOSIS IN NEUROBLASTOMA CANCER CELLS. *MOLECULAR PHARMACOLOGY* 76, 632-640.**

**DAYON, L. & SANCHEZ, J. C. (2012). RELATIVE PROTEIN QUANTIFICATION BY MS/MS USING THE TANDEM MASS TAG TECHNOLOGY. IN *METHODS IN MOLECULAR BIOLOGY*, PP. 115-127. EDITED BY M. KATRIN.**

**DEBING, Y., EMERSON, S. U., WANG, Y., PAN, Q., BALZARINI, J., DALLMEIER, K. & NEYTS, J. (2014). RIBAVIRIN INHIBITS IN VITRO HEPATITIS E VIRUS REPLICATION THROUGH DEPLETION OF CELLULAR GTP POOLS AND IS MODERATELY SYNERGISTIC WITH ALPHA INTERFERON. *ANTIMICROBIAL AGENTS AND CHEMOTHERAPY* 58, 267-273.**

**DEVINCENZO, J. P. (2000). THERAPY OF RESPIRATORY SYNCYTIAL VIRUS INFECTION. *PEDIATRIC INFECTIOUS DISEASE JOURNAL* 19, 786-790.**

**DICKENS, L. E., COLLINS, P. L. & WERTZ, G. W. (1984). TRANSCRIPTIONAL MAPPING OF HUMAN RESPIRATORY SYNCYTIAL VIRUS. *JOURNAL OF VIROLOGY* 52, 364-369.**

**DIETZ, J., SCHELHORN, S. E., FITTING, D., MIHM, U., SUSSER, S., WELKER, M. W., FULLER, C., DAUMER, M., TEUBER, G., WEDEMEYER, H., BERG, T., LENGAUER, T., ZEUZEM, S., HERRMANN, E. & SARRAZIN, C. (2013). DEEP SEQUENCING REVEALS MUTAGENIC EFFECTS OF RIBAVIRIN DURING MONOTHERAPY OF HEPATITIS C VIRUS GENOTYPE 1-INFECTED PATIENTS. *JOURNAL OF VIROLOGY* 87, 6172-6181.**

**DONALISIO, M., RUSNATI, M., CAGNO, V., CIVRA, A., BUGATTI, A., GIULIANI, A., PIRRI, G., VOLANTE, M., PAPOTTI, M., LANDOLFO, S. & LEMBO, D. (2012). INHIBITION OF HUMAN RESPIRATORY SYNCYTIAL VIRUS INFECTIVITY BY A DENDRIMERIC HEPARAN SULFATE-BINDING PEPTIDE. *ANTIMICROBIAL AGENTS AND CHEMOTHERAPY* 56, 5278-5288.**

**DONG, Z. C. & CHEN, Y. (2013). TRANSCRIPTOMICS: ADVANCES AND APPROACHES. *SCI CHINA LIFE SCI* 56, 960-967.**

**DOVE, B. K., SURTEES, R., BEAN, T. J. H., MUNDAY, D., WISE, H. M., DIGARD, P., CARROLL, M. W., AJUH, P., BARR, J. N. & HISCOX, J. A. (2012). A QUANTITATIVE PROTEOMIC ANALYSIS OF LUNG EPITHELIAL (A549) CELLS INFECTED WITH 2009 PANDEMIC INFLUENZA A VIRUS USING STABLE ISOTOPE LABELLING WITH AMINO ACIDS IN CELL CULTURE. *PROTEOMICS* 12, 1431-1436.**

**DOWALL, S. D., MATTHEWS, D. A., GARCIA-DORIVAL, I., TAYLOR, I., KENNY, J., HERTZ-FOWLER, C., HALL, N., CORBIN-LICKFETT, K., EMPIG, C., SCHLUNEGGER, K., BARR, J. N., CARROLL, M. W., HEWSON, R. & HISCOX,**

**J. A. (2014). ELUCIDATING VARIATIONS IN THE NUCLEOTIDE SEQUENCE OF EBOLA VIRUS ASSOCIATED WITH INCREASING PATHOGENICITY. *GENOME BIOLOGY* 15, 540.**

**DRAKE, J. W. (1993). RATES OF SPONTANEOUS MUTATION AMONG RNA VIRUSES. *PROCEEDINGS OF THE NATIONAL ACADEMY OF SCIENCES OF THE UNITED STATES OF AMERICA* 90, 4171-4175.**

**DUPUY, L. C., DOBSON, S., BITKO, V. & BARIK, S. (1999). CASEIN KINASE 2-MEDIATED PHOSPHORYLATION OF RESPIRATORY SYNCYTIAL VIRUS PHOSPHOPROTEIN P IS ESSENTIAL FOR THE TRANSCRIPTION ELONGATION ACTIVITY OF THE VIRAL POLYMERASE; PHOSPHORYLATION BY CASEIN KINASE 1 OCCURS MAINLY AT SER215 AND IS WITHOUT EFFECT. *JOURNAL OF VIROLOGY* 73, 8384-8392.**

**ECKARDT-MICHEL, J., LOREK, M., BAXMANN, D., GRUNWALD, T., KEIL, G. M. & ZIMMER, G. (2008). THE FUSION PROTEIN OF RESPIRATORY SYNCYTIAL VIRUS TRIGGERS P53-DEPENDENT APOPTOSIS. *JOURNAL OF VIROLOGY* 82, 3236-3249.**

**EL SALEEBY, C. M., BUSH, A. J., HARRISON, L. M., AITKEN, J. A. & DEVINCENZO, J. P. (2011). RESPIRATORY SYNCYTIAL VIRUS LOAD, VIRAL DYNAMICS, AND DISEASE SEVERITY IN PREVIOUSLY HEALTHY NATURALLY INFECTED CHILDREN. *JOURNAL OF INFECTIOUS DISEASES* 204, 996-1002.**

**ENDERS, G. (1996). *MEDICAL MICROBIOLOGY, PARAMYXOVIRUSES, 4TH EDITION, 59.***

**ERIKSSON, B., HELGSTRAND, E., JOHANSSON, N. G., LARSSON, A., MISIORNY, A., NORÉN, J. O., PHILIPSON, L., STENBERG, K., STENING, G., STRIDH, S. & OBERG, B. (1977). INHIBITION OF INFLUENZA VIRUS RIBONUCLEIC ACID POLYMERASE BY RIBAVIRIN TRIPHOSPHATE. *ANTIMICROBIAL AGENTS AND CHEMOTHERAPY* 11, 946-951.**

**EVANS, V. C., BARKER, G., HEESOM, K. J., FAN, J., BESSANT, C. & MATTHEWS, D. A. (2012). DE NOVO DERIVATION OF PROTEOMES FROM TRANSCRIPTOMES FOR TRANSCRIPT AND PROTEIN IDENTIFICATION. *NAT METHODS* 9, 1207-1211.**

**EVERARD, M. L., SWARBRICK, A., RIGBY, A. S. & MILNER, A. D. (2001). THE EFFECT OF RIBAVIRIN TO TREAT PREVIOUSLY HEALTHY INFANTS ADMITTED WITH ACUTE BRONCHIOLITIS ON ACUTE AND CHRONIC RESPIRATORY MORBIDITY. *RESPIRATORY MEDICINE* 95, 275-280.**

**FALSEY, A. R., HENNESSEY, P. A., FORMICA, M. A., COX, C. & WALSH, E. E. (2005). RESPIRATORY SYNCYTIAL VIRUS INFECTION IN ELDERLY AND HIGH-RISK ADULTS. *N ENGL J MED* 352, 1749-1759.**

**FANG, S. H., HWANG, L. H., CHEN, D. S. & CHIANG, B. L. (2000). RIBAVIRIN ENHANCEMENT OF HEPATITIS C VIRUS CORE ANTIGEN-SPECIFIC TYPE 1 T**

HELPER CELL RESPONSE CORRELATES WITH THE INCREASED IL-12 LEVEL. *JOURNAL OF HEPATOLOGY* 33, 791-798.

FEARNS, R. & COLLINS, P. L. (1999). ROLE OF THE M2-1 TRANSCRIPTION ANTITERMINATION PROTEIN OF RESPIRATORY SYNCYTIAL VIRUS IN SEQUENTIAL TRANSCRIPTION. *JOURNAL OF VIROLOGY* 73, 5852-5864.

FELTES, T. F., CABALKA, A. K., MEISSNER, H. C., PIAZZA, F. M., CARLIN, D. A., TOP JR, F. H., CONNOR, E. M. & SONDHEIMER, H. M. (2003). PALIVIZUMAB PROPHYLAXIS REDUCES HOSPITALIZATION DUE TO RESPIRATORY SYNCYTIAL VIRUS IN YOUNG CHILDREN WITH HEMODYNAMICALLY SIGNIFICANT CONGENITAL HEART DISEASE. *JOURNAL OF PEDIATRICS* 143, 532-540.

FERNANDEZ-LARSSON, R. & PATTERSON, J. L. (1990). RIBAVIRIN IS AN INHIBITOR OF HUMAN IMMUNODEFICIENCY VIRUS REVERSE TRANSCRIPTASE. *MOLECULAR PHARMACOLOGY* 38, 766-770.

FÖRSTER, A., MAERTENS, G. N., FARRELL, P. J. & BAJOREK, M. (2015). DIMERIZATION OF MATRIX PROTEIN IS REQUIRED FOR BUDDING OF RESPIRATORY SYNCYTIAL VIRUS. *JOURNAL OF VIROLOGY* 89, 4624-4635.

GELLER, R., ANDINO, R. & FRYDMAN, J. (2013). HSP90 INHIBITORS EXHIBIT RESISTANCE-FREE ANTIVIRAL ACTIVITY AGAINST RESPIRATORY SYNCYTIAL VIRUS. *PLOS ONE* 8, E56762.

GHILDYAL, R., BAULCH-BROWN, C., MILLS, J. & MEANGER, J. (2003). THE MATRIX PROTEIN OF HUMAN RESPIRATORY SYNCYTIAL VIRUS LOCALISES TO THE NUCLEUS OF INFECTED CELLS AND INHIBITS TRANSCRIPTION. *ARCHIVES OF VIROLOGY* 148, 1419-1429.

GILCA, R., DE SERRES, G., TREMBLAY, M., VACHON, M. L., LEBLANC, E., BERGERON, M. G., DÉRY, P. & BOIVIN, G. (2006). DISTRIBUTION AND CLINICAL IMPACT OF HUMAN RESPIRATORY SYNCYTIAL VIRUS GENOTYPES IN HOSPITALIZED CHILDREN OVER 2 WINTER SEASONS. *JOURNAL OF INFECTIOUS DISEASES* 193, 54-58.

GOMAA, M. A., GALAL, O. & MAHMOUD, M. S. (2012). RISK OF ACUTE OTITIS MEDIA IN RELATION TO ACUTE BRONCHIOLITIS IN CHILDREN. *INTERNATIONAL JOURNAL OF PEDIATRIC OTORHINOLARYNGOLOGY* 76, 49-51.

GOMEZ, R. S., GUISLE-MARSOLLIER, I., BOHMWALD, K., BUENO, S. M. & KALERGIS, A. M. (2014). RESPIRATORY SYNCYTIAL VIRUS: PATHOLOGY, THERAPEUTIC DRUGS AND PROPHYLAXIS. *IMMUNOLOGY LETTERS* 162, 237-247.

GOWER, T. L., PASTEY, M. K., PEEPLES, M. E., COLLINS, P. L., MCCURDY, L. H., HART, T. K., GUTH, A., JOHNSON, T. R. & GRAHAM, B. S. (2005). RHOA SIGNALING IS REQUIRED FOR RESPIRATORY SYNCYTIAL VIRUS-INDUCED SYNCYTIUM FORMATION AND FILAMENTOUS VIRION MORPHOLOGY. *JOURNAL OF VIROLOGY* 79, 5326-5336.

**GRACI, J. D. & CAMERON, C. E. (2006). MECHANISMS OF ACTION OF RIBAVIRIN AGAINST DISTINCT VIRUSES. *REVIEWS IN MEDICAL VIROLOGY* 16, 37-48.**

**GRADA, A. & WEINBRECHT, K. (2013). NEXT-GENERATION SEQUENCING: METHODOLOGY AND APPLICATION. *J INVEST DERMATOL* 133.**

**GROOTHUIS, J. R., HOOPES, J. M. & JESSIE, V. G. H. (2011). PREVENTION OF SERIOUS RESPIRATORY SYNCYTIAL VIRUS-RELATED ILLNESS. I: DISEASE PATHOGENESIS AND EARLY ATTEMPTS AT PREVENTION. *ADVANCES IN THERAPY* 28, 91-109.**

**HALL, C. B., WEINBERG, G. A., IWANE, M. K., BLUMKIN, A. K., EDWARDS, K. M., STAAT, M. A., AUINGER, P., GRIFFIN, M. R., POEHLING, K. A., ERDMAN, D., GRIJALVA, C. G., ZHU, Y. & SZILAGYI, P. (2009). THE BURDEN OF RESPIRATORY SYNCYTIAL VIRUS INFECTION IN YOUNG CHILDREN. *NEW ENGLAND JOURNAL OF MEDICINE* 360, 588-598.**

**HALLAK, L. K., SPILLMANN, D., COLLINS, P. L. & PEEPLES, M. E. (2000). GLYCOSAMINOGLYCAN SULFATION REQUIREMENTS FOR RESPIRATORY SYNCYTIAL VIRUS INFECTION. *JOURNAL OF VIROLOGY* 74, 10508-10513.**

**HARDY, R. W. & WERTZ, G. W. (1998). THE PRODUCT OF THE RESPIRATORY SYNCYTIAL VIRUS M2 GENE ORF1 ENHANCES READTHROUGH OF INTERGENIC JUNCTIONS DURING VIRAL TRANSCRIPTION. *JOURNAL OF VIROLOGY* 72, 520-526.**

**HARMON, S. B. & WERTZ, G. W. (2002). TRANSCRIPTIONAL TERMINATION MODULATED BY NUCLEOTIDES OUTSIDE THE CHARACTERIZED GENE END SEQUENCE OF RESPIRATORY SYNCYTIAL VIRUS. *VIROLOGY* 300, 304-315.**

**HASTIE, M. L., HEADLAM, M. J., PATEL, N. B., BUKREYEV, A. A., BUCHHOLZ, U. J., DAVE, K. A., NORRIS, E. L., WRIGHT, C. L., SPANN, K. M., COLLINS, P. L. & GORMAN, J. J. (2012). THE HUMAN RESPIRATORY SYNCYTIAL VIRUS NONSTRUCTURAL PROTEIN 1 REGULATES TYPE I AND TYPE II INTERFERON PATHWAYS. *MOLECULAR & CELLULAR PROTEOMICS : MCP* 11, 108-127.**

**HEMINWAY, B. R., YU, Y., TANAKA, Y., PERRINE, K. G., GUSTAFSON, E., BERNSTEIN, J. M. & GALINSKI, M. S. (1994). ANALYSIS OF RESPIRATORY SYNCYTIAL VIRUS F, G, AND SH PROTEINS IN CELL FUSION. *VIROLOGY* 200, 801-805.**

**HENDERSON, G., MURRAY, J. & YEO, R. P. (2002). SORTING OF THE RESPIRATORY SYNCYTIAL VIRUS MATRIX PROTEIN INTO DETERGENT-RESISTANT STRUCTURES IS DEPENDENT ON CELL-SURFACE EXPRESSION OF THE GLYCOPROTEINS. *VIROLOGY* 300, 244-254.**

**HENDRICKS, D. A., BARADARAN, K., MCINTOSH, K. & PATTERSON, J. L. (1987). APPEARANCE OF A SOLUBLE FORM OF THE G PROTEIN OF RESPIRATORY SYNCYTIAL VIRUS IN FLUIDS OF INFECTED CELLS. *JOURNAL OF GENERAL VIROLOGY* 68, 1705-1714.**

**HENDRICKS, D. A., MCINTOSCH, K. & PATTERSON, J. L. (1988). FURTHER CHARACTERIZATION OF THE SOLUBLE FORM OF THE G GLYCOPROTEIN OF RESPIRATORY SYNCYTIAL VIRUS. *JOURNAL OF VIROLOGY* 62, 2228-2233.**

**HOFMANN, W. P., HERRMANN, E., SARRAZIN, C. & ZEUZEM, S. (2008). RIBAVIRIN MODE OF ACTION IN CHRONIC HEPATITIS C: FROM CLINICAL USE BACK TO MOLECULAR MECHANISMS. *LIVER INT* 28, 1332-1343.**

**HRUSKA, J. F., BERNSTEIN, J. M., DOUGLAS JR, R. G. & HALL, C. B. (1980). EFFECTS OF RIBAVIRIN ON RESPIRATORY SYNCYTIAL VIRUS IN VITRO. *ANTIMICROBIAL AGENTS AND CHEMOTHERAPY* 17, 770-775.**

**HUANG, Y. T., COLLINS, P. L. & WERTZ, G. W. (1985). CHARACTERIZATION OF THE 10 PROTEINS OF HUMAN RESPIRATORY SYNCYTIAL VIRUS: IDENTIFICATION OF A FOURTH ENVELOPE-ASSOCIATED PROTEIN. *VIRUS RESEARCH* 2, 157-173.**

**HUGHES, J. H., MANN, D. R. & HAMPARIAN, V. V. (1988). DETECTION OF RESPIRATORY SYNCYTIAL VIRUS IN CLINICAL SPECIMENS BY VIRAL CULTURE, DIRECT AND INDIRECT IMMUNOFLUORESCENCE, AND ENZYME IMMUNOASSAY. *JOURNAL OF CLINICAL MICROBIOLOGY* 26, 588-591.**

**IMAZ, M. S., SEQUEIRA, M. D., VIDELA, C., VERONESSI, I., COCIGLIO, R., ZERBINI, E. & CARBALLAL, G. (2000). CLINICAL AND EPIDEMIOLOGIC CHARACTERISTICS OF RESPIRATORY SYNCYTIAL VIRUS SUBGROUPS A AND B INFECTIONS IN SANTA FE, ARGENTINA. *JOURNAL OF MEDICAL VIROLOGY* 61, 76-80.**

**JAFRI, H. S. (2003). TREATMENT OF RESPIRATORY SYNCYTIAL VIRUS: ANTIVIRAL THERAPIES. *PEDIATRIC INFECTIOUS DISEASE JOURNAL* 22, S89-S93.**

**JAIRATH, S., BROWN VARGAS, P., HAMLIN, H. A., FIELD, A. K. & KILKUSKIE, R. E. (1997). INHIBITION OF RESPIRATORY SYNCYTIAL VIRUS REPLICATION BY ANTISENSE OLIGODEOXYRIBONUCLEOTIDES. *ANTIVIRAL RESEARCH* 33, 201-213.**

**JOHNSON, J. E., GONZALES, R. A., OLSON, S. J., WRIGHT, P. F. & GRAHAM, B. S. (2007). THE HISTOPATHOLOGY OF FATAL UNTREATED HUMAN RESPIRATORY SYNCYTIAL VIRUS INFECTION. *MODERN PATHOLOGY* 20, 108-119.**

**JOHNSON, P. R., SPRIGGS, M. K., OLMSTED, R. A. & COLLINS, P. L. (1987). THE G GLYCOPROTEIN OF HUMAN RESPIRATORY SYNCYTIAL VIRUSES OF SUBGROUPS A AND B: EXTENSIVE SEQUENCE DIVERGENCE BETWEEN ANTIGENICALLY RELATED PROTEINS. *PROCEEDINGS OF THE NATIONAL ACADEMY OF SCIENCES OF THE UNITED STATES OF AMERICA* 84, 5625-5629.**

**KAMAR, N., IZOPET, J., TRIPON, S., BISMUTH, M., HILLAIRE, S., DUMORTIER, J., RADENNE, S., COILLY, A., GARRIGUE, V., D'ALTEROCHE, L., BUCHLER, M., COUZI, L., LEBRAY, P., DHARANCY, S., MINELLO, A., HOURMANT, M., ROQUE-AFONSO, A. M., ABRAVANEL, F., POL, S., ROSTAING, L. & MALLET, V. (2014). RIBAVIRIN FOR CHRONIC HEPATITIS E VIRUS INFECTION IN**

TRANSPLANT RECIPIENTS. *THE NEW ENGLAND JOURNAL OF MEDICINE* 370, 1111-1120.

KARRON, R. A., WRIGHT, P. F., BELSHE, R. B., THUMAR, B., CASEY, R., NEWMAN, F., POLACK, F. P., RANDOLPH, V. B., DEATLY, A., HACKELL, J., GRUBER, W., MURPHY, B. R. & COLLINS, P. L. (2005). IDENTIFICATION OF A RECOMBINANT LIVE ATTENUATED RESPIRATORY SYNCYTIAL VIRUS VACCINE CANDIDATE THAT IS HIGHLY ATTENUATED IN INFANTS. *JOURNAL OF INFECTIOUS DISEASES* 191, 1093-1104.

KHATTAR, S. K., YUNUS, A. S. & SAMAL, S. K. (2001). MAPPING THE DOMAINS ON THE PHOSPHOPROTEIN OF BOVINE RESPIRATORY SYNCYTIAL VIRUS REQUIRED FOR N-P AND P-L INTERACTIONS USING A MINIGENOME SYSTEM. *JOURNAL OF GENERAL VIROLOGY* 82, 775-779.

KOLOKOLTSOV, A. A., DENIGER, D., FLEMING, E. H., ROBERTS JR, N. J., KARPILOW, J. M. & DAVEY, R. A. (2007). SMALL INTERFERING RNA PROFILING REVEALS KEY ROLE OF CLATHRIN-MEDIATED ENDOCYTOSIS AND EARLY ENDOSOME FORMATION FOR INFECTION BY RESPIRATORY SYNCYTIAL VIRUS. *JOURNAL OF VIROLOGY* 81, 7786-7800.

KREMPL, C., MURPHY, B. R. & COLLINS, P. L. (2002). RECOMBINANT RESPIRATORY SYNCYTIAL VIRUS WITH THE G AND F GENES SHIFTED TO THE PROMOTER-PROXIMAL POSITIONS. *JOURNAL OF VIROLOGY* 76, 11931-11942.

KRISTENSEN, K., HJULER, T., RAVN, H., SIMOëS, E. A. F. & STENSBALLE, L. G. (2012). CHRONIC DISEASES, CHROMOSOMAL ABNORMALITIES, AND CONGENITAL MALFORMATIONS AS RISK FACTORS FOR RESPIRATORY SYNCYTIAL VIRUS HOSPITALIZATION: A POPULATION-BASED COHORT STUDY. *CLINICAL INFECTIOUS DISEASES* 54, 810-817.

KURT-JONES, E. A., POPOVA, L., KWINN, L., HAYNES, L. M., JONES, L. P., TRIPP, R. A., WALSH, E. E., FREEMAN, M. W., GOLENBOCK, D. T., ANDERSON, L. J. & FINBERG, R. W. (2000). PATTERN RECOGNITION RECEPTORS TLR4 AND CD14 MEDIATE RESPONSE TO RESPIRATORY SYNCYTIAL VIRUS. *NAT IMMUNOL* 1, 398-401.

LAM, Y. W., EVANS, V. C., HEESOM, K. J., LAMOND, A. I. & MATTHEWS, D. A. (2010). PROTEOMICS ANALYSIS OF THE NUCLEOLUS IN ADENOVIRUS-INFECTED CELLS. *MOLECULAR AND CELLULAR PROTEOMICS* 9, 117-130.

LAMB, R. L., PARKS, G.D. (2013). PARAMYXOVIRIDAE. IN *FIELDS VIROLOGY*, 6TH ED EDN, PP. 957-995. EDITED BY D. M. KNIPE, HOWLEY, P.M. PHILADELPHIA: WOLTERS KLUWER/ LIPPINCOTT WILLIAMS & WILKINS.

LEYSSEN, P., BALZARINI, J., DE CLERCQ, E. & NEYTS, J. (2005). THE PREDOMINANT MECHANISM BY WHICH RIBAVIRIN EXERTS ITS ANTIVIRAL ACTIVITY IN VITRO AGAINST FLAVIVIRUSES AND PARAMYXOVIRUSES IS MEDIATED BY INHIBITION OF IMP DEHYDROGENASE. *JOURNAL OF VIROLOGY* 79, 1943-1947.

**LEYSSEN, P., DE CLERCQ, E. & NEYTS, J. (2006). THE ANTI-YELLOW FEVER VIRUS ACTIVITY OF RIBAVIRIN IS INDEPENDENT OF ERROR-PRONE REPLICATION. *MOLECULAR PHARMACOLOGY* 69, 1461-1467.**

**LIEBERTHAL, A. S., BAUCHNER, H., HALL, C. B., JOHNSON, D. W., KOTAGAL, U., LIGHT, M. J., MASON, W., MEISSNER, H. C., PHELAN, K. J., ZORC, J. J., BROWN, M. A., CLOVER, R. D., NATHANSON, I. T., KORPPI, M., SHIFFMAN, R. N., STANKO-LOPP, D. & DAVIDSON, C. (2006). DIAGNOSIS AND MANAGEMENT OF BRONCHIOLITIS. *PEDIATRICS* 118, 1774-1793.**

**LIETZÉN, N., ÖHMAN, T., RINTAHAKA, J., JULKUNEN, I., AITTOKALLIO, T., MATIKAINEN, S. & NYMAN, T. A. (2011). QUANTITATIVE SUBCELLULAR PROTEOME AND SECRETOME PROFILING OF INFLUENZA A VIRUS-INFECTED HUMAN PRIMARY MACROPHAGES. *PLOS PATHOG* 7.**

**LILJEROOS, L., KRZYZANIAK, M. A., HELENIUS, A. & BUTCHER, S. J. (2013). ARCHITECTURE OF RESPIRATORY SYNCYTIAL VIRUS REVEALED BY ELECTRON CRYOTOMOGRAPHY. *PROCEEDINGS OF THE NATIONAL ACADEMY OF SCIENCES OF THE UNITED STATES OF AMERICA* 110, 11133-11138.**

**LIM, K. I. & YIN, J. (2009). COMPUTATIONAL FITNESS LANDSCAPE FOR ALL GENE-ORDER PERMUTATIONS OF AN RNA VIRUS. *PLOS COMPUT BIOL* 5.**

**LIU, Y., ZHOU, J. & WHITE, K. P. (2014). RNA-SEQ DIFFERENTIAL EXPRESSION STUDIES: MORE SEQUENCE OR MORE REPLICATION? *BIOINFORMATICS* 30, 301-304.**

**MACLELLAN, K., LONEY, C., YEO, R. P. & BHELLA, D. (2007). THE 24-ANGSTROM STRUCTURE OF RESPIRATORY SYNCYTIAL VIRUS NUCLEOCAPSID PROTEIN-RNA DECAMERIC RINGS. *JOURNAL OF VIROLOGY* 81, 9519-9524.**

**MAILAPARAMBIL, B., GRYCHTOL, R. & HEINZMANN, A. (2009). RESPIRATORY SYNCYTIAL VIRUS BRONCHIOLITIS AND ASTHMA - INSIGHTS FROM RECENT STUDIES AND IMPLICATIONS FOR THERAPY. *INFLAMMATION AND ALLERGY - DRUG TARGETS* 8, 202-207.**

**MALHOTRA, R., WARD, M., BRIGHT, H., PRIEST, R., FOSTER, M. R., HURLE, M., BLAIR, E. & BIRD, M. (2003). ISOLATION AND CHARACTERISATION OF POTENTIAL RESPIRATORY SYNCYTIAL VIRUS RECEPTOR(S) ON EPITHELIAL CELLS. *MICROBES AND INFECTION* 5, 123-133.**

**MALINOSKI, F. & STOLLAR, V. (1981). INHIBITORS OF IMP DEHYDROGENASE PREVENT SINDBIS VIRUS REPLICATION AND REDUCE GTP LEVELS IN AEDES ALBOPICTUS CELLS. *VIROLOGY* 110, 281-291.**

**MANTIONE, K. J., KREAM, R. M., KUZELOVA, H., PTACEK, R., RABOCH, J., SAMUEL, J. M. & STEFANO, G. B. (2014). COMPARING BIOINFORMATIC GENE EXPRESSION PROFILING METHODS: MICROARRAY AND RNA-SEQ. *MED SCI MONIT BASIC RES* 20, 138-142.**

**MARIONI, J. C., MASON, C. E., MANE, S. M., STEPHENS, M. & GILAD, Y. (2008). RNA-SEQ: AN ASSESSMENT OF TECHNICAL REPRODUCIBILITY AND COMPARISON WITH GENE EXPRESSION ARRAYS. *GENOME RES* 18, 1509-1517.**

**MARTÍNEZ, I., LOMBARDÍA, L., GARCÍA-BARRENO, B., DOMÍNGUEZ, O. & MELERO, J. A. (2007). DISTINCT GENE SUBSETS ARE INDUCED AT DIFFERENT TIME POINTS AFTER HUMAN RESPIRATORY SYNCYTIAL VIRUS INFECTION OF A549 CELLS. *JOURNAL OF GENERAL VIROLOGY* 88, 570-581.**

**MARTÍNEZ, I. & MELERO, J. A. (2002). A MODEL FOR THE GENERATION OF MULTIPLE A TO G TRANSITIONS IN THE HUMAN RESPIRATORY SYNCYTIAL VIRUS GENOME: PREDICTED RNA SECONDARY STRUCTURES AS SUBSTRATES FOR ADENOSINE DEAMINASES THAT ACT ON RNA. *JOURNAL OF GENERAL VIROLOGY* 83, 1445-1455.**

**MARTY, A., MEANGER, J., MILLS, J., SHIELDS, B. & GHILDYAL, R. (2004). ASSOCIATION OF MATRIX PROTEIN OF RESPIRATORY SYNCYTIAL VIRUS WITH THE HOST CELL MEMBRANE OF INFECTED CELLS. *ARCHIVES OF VIROLOGY* 149, 199-210.**

**MCCORMICK, J. B., KING, I. J., WEBB, P. A., SCRIBNER, C. L., CRAVEN, R. B., JOHNSON, K. M., ELLIOTT, L. H. & BELMONT-WILLIAMS, R. (1986). LASSA FEVER: EFFECTIVE THERAPY WITH RIBAVIRIN. *NEW ENGLAND JOURNAL OF MEDICINE* 314, 20-26.**

**MCGETTIGAN, P. A. (2013). TRANSCRIPTOMICS IN THE RNA-SEQ ERA. *CURR OPIN CHEM BIOL* 17, 4-11.**

**MCNAMARA, P. S., FLANAGAN, B. F., HART, C. A. & SMYTH, R. L. (2005). PRODUCTION OF CHEMOKINES IN THE LUNGS OF INFANTS WITH SEVERE RESPIRATORY SYNCYTIAL VIRUS BRONCHIOLITIS. *JOURNAL OF INFECTIOUS DISEASES* 191, 1225-1232.**

**MCNAMARA, P. S. & SMYTH, R. L. (2002). THE PATHOGENESIS OF RESPIRATORY SYNCYTIAL VIRUS DISEASE IN CHILDHOOD. *BRITISH MEDICAL BULLETIN* 61, 13-28.**

**MELERO, J. A. (2007). *MOLECULAR BIOLOGY OF HUMAN RESPIRATORY SYNCYTIAL VIRUS. RESPIRATORY SYNCYTIAL VIRUS. FIRST EDITION, 1- 42***

**MIYAIRI, I. & DEVINCENZO, J. P. (2008). HUMAN GENETIC FACTORS AND RESPIRATORY SYNCYTIAL VIRUS DISEASE SEVERITY. *CLINICAL MICROBIOLOGY REVIEWS* 21, 686-703.**

**MONTO, A. S., FLEMING, D. M., HENRY, D., DE GROOT, R., MAKELA, M., KLEIN, T., ELLIOTT, M., KEENE, O. N. & MAN, C. Y. (1999). EFFICACY AND SAFETY OF THE NEURAMINIDASE INHIBITOR ZANAMIVIR IN THE TREATMENT OF INFLUENZA A AND B VIRUS INFECTIONS. *JOURNAL OF INFECTIOUS DISEASES* 180, 254-261.**

**MORFIN, F., DUPUIS-GIROD, S., MUNDWEILER, S., FALCON, D., CARRINGTON, D., SEDLACEK, P., BIERINGS, M., CETKOVSKY, P., KROES, A. C. M., VAN TOL, M. J. D. & THOUVENOT, D. (2005). IN VITRO SUSCEPTIBILITY OF ADENOVIRUS TO ANTIVIRAL DRUGS IS SPECIES-DEPENDENT. *ANTIVIRAL THERAPY* 10, 225-229.**

**MOSMANN, T. (1983). RAPID COLORIMETRIC ASSAY FOR CELLULAR GROWTH AND SURVIVAL: APPLICATION TO PROLIFERATION AND CYTOTOXICITY ASSAYS. *J IMMUNOL METHODS* 65, 55-63.**

**MOUDY, R. M., SULLENDER, W. M. & WERTZ, G. W. (2004). VARIATIONS IN INTERGENIC REGION SEQUENCES OF HUMAN RESPIRATORY SYNCYTIAL VIRUS CLINICAL ISOLATES: ANALYSIS OF EFFECTS ON TRANSCRIPTIONAL REGULATION. *VIROLOGY* 327, 121-133.**

**MUNDAY, D. C., EMMOTT, E., SURTEES, R., LARDEAU, C. H., WU, W., DUPREX, W. P., DOVE, B. K., BARR, J. N. & HISCOX, J. A. (2010A). QUANTITATIVE PROTEOMIC ANALYSIS OF A549 CELLS INFECTED WITH HUMAN RESPIRATORY SYNCYTIAL VIRUS. *MOLECULAR AND CELLULAR PROTEOMICS* 9, 2438-2459.**

**MUNDAY, D. C., EMMOTT, E., SURTEES, R., LARDEAU, C. H., WU, W., DUPREX, W. P., DOVE, B. K., BARR, J. N. & HISCOX, J. A. (2010B). QUANTITATIVE PROTEOMIC ANALYSIS OF A549 CELLS INFECTED WITH HUMAN RESPIRATORY SYNCYTIAL VIRUS. *MOLECULAR & CELLULAR PROTEOMICS : MCP* 9, 2438-2459.**

**MUNDAY, D. C., HISCOX, J. A. & BARR, J. N. (2010C). QUANTITATIVE PROTEOMIC ANALYSIS OF A549 CELLS INFECTED WITH HUMAN RESPIRATORY SYNCYTIAL VIRUS SUBGROUP B USING SILAC COUPLED TO LC-MS/MS. *PROTEOMICS* 10, 4320-4334.**

**MUNDAY, D. C., HOWELL, G., BARR, J. N. & HISCOX, J. A. (2014A). PROTEOMIC ANALYSIS OF MITOCHONDRIA IN RESPIRATORY EPITHELIAL CELLS INFECTED WITH HUMAN RESPIRATORY SYNCYTIAL VIRUS AND FUNCTIONAL IMPLICATIONS FOR VIRUS AND CELL BIOLOGY. *THE JOURNAL OF PHARMACY AND PHARMACOLOGY*.**

**MUNDAY, D. C., SURTEES, R., EMMOTT, E., DOVE, B. K., DIGARD, P., BARR, J. N., WHITEHOUSE, A., MATTHEWS, D. & HISCOX, J. A. (2012A). USING SILAC AND QUANTITATIVE PROTEOMICS TO INVESTIGATE THE INTERACTIONS BETWEEN VIRAL AND HOST PROTEOMES. *PROTEOMICS* 12, 666-672.**

**MUNDAY, D. C., SURTEES, R., EMMOTT, E., DOVE, B. K., DIGARD, P., BARR, J. N., WHITEHOUSE, A., MATTHEWS, D. & HISCOX, J. A. (2012B). USING SILAC AND QUANTITATIVE PROTEOMICS TO INVESTIGATE THE INTERACTIONS BETWEEN VIRAL AND HOST PROTEOMES. *PROTEOMICS* 12, 666-672.**

**MUNDAY, D. C., WU, W., SMITH, N., FIX, J., NOTON, S. L., GALLOUX, M., TOUZELET, O., ARMSTRONG, S. D., DAWSON, J. M., ALJABR, W., EASTON, A. J., RAMEIX-WELTI, M. A., DE OLIVEIRA, A. P., SIMABUCO, F., VENTURA, A. M., HUGHES, D. J., BARR, J. N., FEARNS, R., DIGARD, P., ELEOUET, J. F.**

**& HISCOX, J. A. (2014B). INTERACTOME ANALYSIS OF THE HUMAN RESPIRATORY SYNCYTIAL VIRUS RNA POLYMERASE COMPLEX IDENTIFIES PROTEIN CHAPERONES AS IMPORTANT CO-FACTORS THAT PROMOTE L PROTEIN STABILITY AND RNA SYNTHESIS. *JOURNAL OF VIROLOGY*.**

**MUNDAY, D. C., WU, W., SMITH, N., FIX, J., NOTON, S. L., GALLOUX, M., TOUZELET, O., ARMSTRONG, S. D., DAWSON, J. M., ALJABR, W., EASTON, A. J., RAMEIX-WELTI, M. A., DE OLIVEIRA, A. P., SIMABUCO, F. M., VENTURA, A. M., HUGHES, D. J., BARR, J. N., FEARNS, R., DIGARD, P., ELÉOUËT, J. F. & HISCOX, J. A. (2015). INTERACTOME ANALYSIS OF THE HUMAN RESPIRATORY SYNCYTIAL VIRUS RNA POLYMERASE COMPLEX IDENTIFIES PROTEIN CHAPERONES AS IMPORTANT COFACTORS THAT PROMOTE L-PROTEIN STABILITY AND RNA SYNTHESIS. *JOURNAL OF VIROLOGY* 89, 917-930.**

**NAIR, H., NOKES, D. J., GESSNER, B. D., DHERANI, M., MADHI, S. A., SINGLETON, R. J., O'BRIEN, K. L., ROCA, A., WRIGHT, P. F., BRUCE, N., CHANDRAN, A., THEODORATOU, E., SUTANTO, A., SEDYANINGSIH, E. R., NGAMA, M., MUNYWOKI, P. K., KARTASASMITA, C., SIMÕES, E. A., RUDAN, I., WEBER, M. W. & CAMPBELL, H. (2010). GLOBAL BURDEN OF ACUTE LOWER RESPIRATORY INFECTIONS DUE TO RESPIRATORY SYNCYTIAL VIRUS IN YOUNG CHILDREN: A SYSTEMATIC REVIEW AND META-ANALYSIS. *THE LANCET* 375, 1545-1555.**

**NAVAS, L., WANG, E., DE CARVALHO, V. & ROBINSON, J. (1992). IMPROVED OUTCOME OF RESPIRATORY SYNCYTIAL VIRUS INFECTION IN A HIGH-RISK HOSPITALIZED POPULATION OF CANADIAN CHILDREN. *JOURNAL OF PEDIATRICS* 121, 348-354.**

**OTTO, A., BECHER, D. & SCHMIDT, F. (2014). QUANTITATIVE PROTEOMICS IN THE FIELD OF MICROBIOLOGY. *PROTEOMICS* 14, 547-565.**

**OZSOLAK, F. & MILOS, P. M. (2011). RNA SEQUENCING: ADVANCES, CHALLENGES AND OPPORTUNITIES. *NAT REV GEN* 12, 87-98.**

**PAESHUYSE, J., DALLMEIER, K. & NEYTS, J. (2011). RIBAVIRIN FOR THE TREATMENT OF CHRONIC HEPATITIS C VIRUS INFECTION: A REVIEW OF THE PROPOSED MECHANISMS OF ACTION. *CURRENT OPINION IN VIROLOGY* 1, 590-598.**

**PAGÁN, I., HOLMES, E. C. & SIMON-LORIERE, E. (2012). LEVEL OF GENE EXPRESSION IS A MAJOR DETERMINANT OF PROTEIN EVOLUTION IN THE VIRAL ORDER MONONEGAVIRALES. *JOURNAL OF VIROLOGY* 86, 5253-5263.**

**PASTEY, M. K., CROWE JR, J. E. & GRAHAM, B. S. (1999). RHOA INTERACTS WITH THE FUSION GLYCOPROTEIN OF RESPIRATORY SYNCYTIAL VIRUS AND FACILITATES VIRUS-INDUCED SYNCYTIUM FORMATION. *JOURNAL OF VIROLOGY* 73, 7262-7270.**

**PAWLOTSKY, J. M. (2003). MECHANISMS OF ANTIVIRAL TREATMENT EFFICACY AND FAILURE IN CHRONIC HEPATITIS C. *ANTIVIRAL RESEARCH* 59, 1-11.**

**PLAYER, M. R., BARNARD, D. L. & TORRENCE, P. F. (1998). POTENT INHIBITION OF RESPIRATORY SYNCYTIAL VIRUS REPLICATION USING A 2-5A-ANTISENSE CHIMERA TARGETED TO SIGNALS WITHIN THE VIRUS GENOMIC RNA. *PROCEEDINGS OF THE NATIONAL ACADEMY OF SCIENCES OF THE UNITED STATES OF AMERICA* 95, 8874-8879.**

**PODWOJSKI, K., STEPHAN, C. & EISENACHER, M. (2012). IMPORTANT ISSUES IN PLANNING A PROTEOMICS EXPERIMENT: STATISTICAL CONSIDERATIONS OF QUANTITATIVE PROTEOMIC DATA. IN *METHODS IN MOLECULAR BIOLOGY*, PP. 3-21.**

**POLACK, F. P., IRUSTA, P. M., HOFFMAN, S. J., SCHIATTI, M. P., MELENDI, G. A., DELGADO, M. F., LAHAM, F. R., THUMAR, B., HENDRY, R. M., MELERO, J. A., KARRON, R. A., COLLINS, P. L. & KLEEBERGER, S. R. (2005). THE CYSTEINE-RICH REGION OF RESPIRATORY SYNCYTIAL VIRUS ATTACHMENT PROTEIN INHIBITS INNATE IMMUNITY ELICITED BY THE VIRUS AND ENDOTOXIN. *PROCEEDINGS OF THE NATIONAL ACADEMY OF SCIENCES OF THE UNITED STATES OF AMERICA* 102, 8996-9001.**

**QIAN, F., CHUNG, L., ZHENG, W., BRUNO, V., ALEXANDER, R. P., WANG, Z., WANG, X., KURSCHEID, S., ZHAO, H., FIKRIG, E., GERSTEIN, M., SNYDER, M. & MONTGOMERY, R. R. (2013). IDENTIFICATION OF GENES CRITICAL FOR RESISTANCE TO INFECTION BY WEST NILE VIRUS USING RNA-SEQ ANALYSIS. *VIRUSES* 5, 1664-1681.**

**RADHAKRISHNAN, A., YEO, D., BROWN, G., MYAING, M. Z., IYER, L. R., FLECK, R., TAN, B. H., AITKEN, J., SANMUN, D., TANG, K., YARWOOD, A., BRINK, J. & SUGRUE, R. J. (2010). PROTEIN ANALYSIS OF PURIFIED RESPIRATORY SYNCYTIAL VIRUS PARTICLES REVEALS AN IMPORTANT ROLE FOR HEAT SHOCK PROTEIN 90 IN VIRUS PARTICLE ASSEMBLY. *MOLECULAR & CELLULAR PROTEOMICS : MCP* 9, 1829-1848.**

**RAMASWAMY, M., SHI, L., MONICK, M. M., HUNNINGHAKE, G. W. & LOOK, D. C. (2004). SPECIFIC INHIBITION OF TYPE I INTERFERON SIGNAL TRANSDUCTION BY RESPIRATORY SYNCYTIAL VIRUS. *AMERICAN JOURNAL OF RESPIRATORY CELL AND MOLECULAR BIOLOGY* 30, 893-900.**

**RANKIN JR, J. T., EPPES, S. B., ANTCZAK, J. B. & JOKLIK, W. K. (1989). STUDIES ON THE MECHANISM OF THE ANTIVIRAL ACTIVITY OF RIBAVIRIN AGAINST REOVIRUS. *VIROLOGY* 168, 147-158.**

**REHERMANN, B. (2009). HEPATITIS C VIRUS VERSUS INNATE AND ADAPTIVE IMMUNE RESPONSES: A TALE OF COEVOLUTION AND COEXISTENCE. *J CLIN INVEST* 119, 1745-1754.**

**REHERMANN, B. & NASCIMBENI, M. (2005). IMMUNOLOGY OF HEPATITIS B VIRUS AND HEPATITIS C VIRUS INFECTION. *NATURE REVIEWS IMMUNOLOGY* 5, 215-229.**

**RESCH, B., GUSENLEITNER, W. & MÜLLER, W. (2002). THE IMPACT OF RESPIRATORY SYNCYTIAL VIRUS INFECTION: A PROSPECTIVE STUDY IN HOSPITALIZED INFANTS YOUNGER THAN 2 YEARS. *INFECTION* 30, 193-197.**

**RODRÍGUEZ, L., CUESTA, I., ASENJO, A. & VILLANUEVA, N. (2004). HUMAN RESPIRATORY SYNCYTIAL VIRUS MATRIX PROTEIN IS AN RNA-BINDING PROTEIN: BINDING PROPERTIES, LOCATION AND IDENTITY OF THE RNA CONTACT RESIDUES. *JOURNAL OF GENERAL VIROLOGY* 85, 709-719.**

**SAMPALIS, J. S., LANGLEY, J., CARBONELL-ESTRANY, X., PAES, B., O'BRIEN, K., ALLEN, U., MITCHELL, I., FIGUERAS ALOY, J., PEDRAZ, C. & MICHALISZYN, A. F. (2008). DEVELOPMENT AND VALIDATION OF A RISK SCORING TOOL TO PREDICT RESPIRATORY SYNCYTIAL VIRUS HOSPITALIZATION IN PREMATURE INFANTS BORN AT 33 THROUGH 35 COMPLETED WEEKS OF GESTATION. *MED DECIS MAK* 28, 471-480.**

**SAMUEL, C. E. (2011). ADENOSINE DEAMINASES ACTING ON RNA (ADARS) ARE BOTH ANTIVIRAL AND PROVIRAL. *VIROLOGY* 411, 180-193.**

**SHAH, N. R., SUNDERLAND, A. & GRDZELISHVILI, V. Z. (2010). CELL TYPE MEDIATED RESISTANCE OF VESICULAR STOMATITIS VIRUS AND SENDAI VIRUS TO RIBAVIRIN. *PLOS ONE* 5.**

**SHU, Q. & NAIR, V. (2008). INOSINE MONOPHOSPHATE DEHYDROGENASE (IMPDH) AS A TARGET IN DRUG DISCOVERY. *MED RES REV* 28, 219-232.**

**SIDWELL, R. W., HUFFMAN, J. H., KHARE, G. P., ALLEN, L. B., WITKOWSKI, J. T. & ROBINS, R. K. (1972). BROAD-SPECTRUM ANTIVIRAL ACTIVITY OF VIRAZOLE: 1-B-D-RIBOFURANOSYL-1, 2,4-TRIAZOLE-3-CARBOXAMIDE. *SCIENCE* 177, 705-706.**

**SIMÕES, E. A. F., CARBONELL-ESTRANY, X., FULLARTON, J. R., LIESE, J. G., FIGUERAS-ALOY, J., DOERING, G. & GUZMAN, J. (2008). A PREDICTIVE MODEL FOR RESPIRATORY SYNCYTIAL VIRUS (RSV) HOSPITALISATION OF PREMATURE INFANTS BORN AT 33-35 WEEKS OF GESTATIONAL AGE, BASED ON DATA FROM THE SPANISH FLIP STUDY. *RESPIR RES* 9.**

**SMEE, D. F. & MATTHEWS, T. R. (1986). METABOLISM OF RIBAVIRIN IN RESPIRATORY SYNCYTIAL VIRUS-INFECTED AND UNINFECTED CELLS. *ANTIMICROBIAL AGENTS AND CHEMOTHERAPY* 30, 117-121.**

**SOARES-WEISER, K., THOMAS, S., THOMSON, G. & GARNER, P. (2010). RIBAVIRIN FOR CRIMEAN-CONGO HEMORRHAGIC FEVER: SYSTEMATIC REVIEW AND META-ANALYSIS. *BMC INFECTIOUS DISEASES* 10, 207.**

**SPANN, K. M., TRAN, K. C. & COLLINS, P. L. (2005). EFFECTS OF NONSTRUCTURAL PROTEINS NS1 AND NS2 OF HUMAN RESPIRATORY SYNCYTIAL VIRUS ON INTERFERON REGULATORY FACTOR 3, NF-ΚB, AND PROINFLAMMATORY CYTOKINES. *JOURNAL OF VIROLOGY* 79, 5353-5362.**

**SPARRELID, E., LJUNGMAN, P., EKELÖF-ANDSTRÖM, E., ASCHAN, J., RINGDÉN, O., WINIARSKI, J., WÅHLIN, B. & ANDERSSON, J. (1997). RIBAVIRIN THERAPY IN BONE MARROW TRANSPLANT RECIPIENTS WITH VIRAL RESPIRATORY TRACT INFECTIONS. *BONE MARROW TRANSPLANTATION* 19, 905-908.**

**SRINIVASAKUMAR, N., OGRA, P. L. & FLANAGAN, T. D. (1991). CHARACTERISTICS OF FUSION OF RESPIRATORY SYNCYTIAL VIRUS WITH HEP-2 CELLS AS MEASURED BY R18 FLUORESCENCE DEQUENCHING ASSAY. *JOURNAL OF VIROLOGY* 65, 4063-4069.**

**STARK, J. M., BARMADA, M. M., WINTERBERG, A. V., MAJUMBER, N., GIBBONS JR, W. J., STARK, M. A., SARTOR, M. A., MEDVEDOVIC, M., KOLLS, J., BEIN, K., MAILAPARAMBIL, B., KRUEGER, M., HEINZMANN, A., LEIKAUF, G. D. & PROWS, D. R. (2010). GENOMEWIDE ASSOCIATION ANALYSIS OF RESPIRATORY SYNCYTIAL VIRUS INFECTION IN MICE. *JOURNAL OF VIROLOGY* 84, 2257-2269.**

**STEC, D. S., HILL III, M. G. & COLLINS, P. L. (1991). SEQUENCE ANALYSIS OF THE POLYMERASE L GENE OF HUMAN RESPIRATORY SYNCYTIAL VIRUS AND PREDICTED PHYLOGENY OF NONSEGMENTED NEGATIVE-STRAND VIRUSES. *VIROLOGY* 183, 273-287.**

**STENSBALLE, L. G., DEVASUNDARAM, J. K. & SIMOES, E. A. F. (2003). RESPIRATORY SYNCYTIAL VIRUS EPIDEMICS: THE UPS AND DOWNS OF A SEASONAL VIRUS. *PEDIATRIC INFECTIOUS DISEASE JOURNAL* 22, S21-S32.**

**STREETER, D. G., WITKOWSKI, J. T., KHARE, G. P., SIDWELL, R. W., BAUER, R. J., ROBINS, R. K. & SIMON, L. N. (1973). MECHANISM OF ACTION OF 1- -D-RIBOFURANOSYL-1,2,4-TRIAZOLE-3-CARBOXAMIDE (VIRAZOLE), A NEW BROAD-SPECTRUM ANTIVIRAL AGENT. *PROCEEDINGS OF THE NATIONAL ACADEMY OF SCIENCES OF THE UNITED STATES OF AMERICA* 70, 1174-1178.**

**TAMBURINI, J., GREEN, A. S., CHAPUIS, N., BARDET, V., LACOMBE, C., MAYEUX, P. & BOUSCARY, D. (2009). TARGETING TRANSLATION IN ACUTE MYELOID LEUKEMIA: A NEW PARADIGM FOR THERAPY? *CELL CYCLE* 8, 3893-3899.**

**TAWAR, R. G., DUQUERROY, S., VONRHEIN, C., VARELA, P. F., DAMIER-PIOLLE, L., CASTAGNE, N., MACLELLAN, K., BEDOUELLE, H., BRICOGNE, G., BHELLA, D., ELÉOUËT, J. F. & REY, F. A. (2009). CRYSTAL STRUCTURE OF A NUCLEOCAPSID-LIKE NUCLEOPROTEIN-RNA COMPLEX OF RESPIRATORY SYNCYTIAL VIRUS. *SCIENCE* 326, 1279-1283.**

**TECHAARPORNKUL, S., BARRETTO, N. & PEEPLES, M. E. (2001). FUNCTIONAL ANALYSIS OF RECOMBINANT RESPIRATORY SYNCYTIAL VIRUS DELETION MUTANTS LACKING THE SMALL HYDROPHOBIC AND/OR ATTACHMENT GLYCOPROTEIN GENE. *JOURNAL OF VIROLOGY* 75, 6825-6834.**

**TECHAARPORNKUL, S., COLLINS, P. L. & PEEPLES, M. E. (2002). RESPIRATORY SYNCYTIAL VIRUS WITH THE FUSION PROTEIN AS ITS ONLY VIRAL**

GLYCOPROTEIN IS LESS DEPENDENT ON CELLULAR GLYCOSAMINOGLYCANS FOR ATTACHMENT THAN COMPLETE VIRUS. *VIROLOGY* 294, 296-304.

TENG, M. N. & COLLINS, P. L. (1998). IDENTIFICATION OF THE RESPIRATORY SYNCYTIAL VIRUS PROTEINS REQUIRED FOR FORMATION AND PASSAGE OF HELPER-DEPENDENT INFECTIOUS PARTICLES. *JOURNAL OF VIROLOGY* 72, 5707-5716.

TENG, M. N., WHITEHEAD, S. S. & COLLINS, P. L. (2001). CONTRIBUTION OF THE RESPIRATORY SYNCYTIAL VIRUS G GLYCOPROTEIN AND ITS SECRETED AND MEMBRANE-BOUND FORMS TO VIRUS REPLICATION IN VITRO AND IN VIVO. *VIROLOGY* 289, 283-296.

TENGT, M. N. & COLLINS, P. L. (2002). THE CENTRAL CONSERVED CYSTINE NOOSE OF THE ATTACHMENT G PROTEIN OF HUMAN RESPIRATORY SYNCYTIAL VIRUS IS NOT REQUIRED FOR EFFICIENT VIRAL INFECTION IN VITRO OR IN VIVO. *JOURNAL OF VIROLOGY* 76, 6164-6171.

TERNETTE, N., WRIGHT, C., KRAMER, H. B., ALTUN, M. & KESSLER, B. M. (2011). LABEL-FREE QUANTITATIVE PROTEOMICS REVEALS REGULATION OF INTERFERON-INDUCED PROTEIN WITH TETRATRICOPEPTIDE REPEATS 3 (IFIT3) AND 5'-3'-EXORIBONUCLEASE 2 (XRN2) DURING RESPIRATORY SYNCYTIAL VIRUS INFECTION. *VIROL J* 8, 442.

TOLTZIS, P., O'CONNELL, K. & PATTERSON, J. L. (1988). EFFECT OF PHOSPHORYLATED RIBAVIRIN ON VESICULAR STOMATITIS VIRUS TRANSCRIPTION. *ANTIMICROBIAL AGENTS AND CHEMOTHERAPY* 32, 492-497.

TÖPFER, A., ZAGORDI, O., PRABHAKARAN, S., ROTH, V., HALPERIN, E. & BEERENWINKEL, N. (2013). PROBABILISTIC INFERENCE OF VIRAL QUASISPECIES SUBJECT TO RECOMBINATION. *J COMPUT BIOL* 20, 113-123.

TRAN, T. L., CASTAGNÉ, N., DUBOSCLARD, V., NOINVILLE, S., KOCH, E., MOUDJOU, M., HENRY, C., BERNARD, J., YEO, R. P. & ELÉOUËT, J. F. (2009). THE RESPIRATORY SYNCYTIAL VIRUS M2-1 PROTEIN FORMS TETRAMERS AND INTERACTS WITH RNA AND P IN A COMPETITIVE MANNER. *JOURNAL OF VIROLOGY* 83, 6363-6374.

TRIPP, R. A., JONES, L. P., HAYNES, L. M., ZHENG, H., MURPHY, P. M. & ANDERSON, L. J. (2001). CX3C CHEMOKINE MIMICRY BY RESPIRATORY SYNCYTIAL VIRUS G GLYCOPROTEIN. *NAT IMMUNOL* 2, 732-738.

TURNER, T. L., KOPP, B. T., PAUL, G., LANDGRAVE, L. C., HAYES JR, D. & THOMPSON, R. (2014). RESPIRATORY SYNCYTIAL VIRUS: CURRENT AND EMERGING TREATMENT OPTIONS. *CLIN OUTCOMES RES* 6, 217-225.

VAN DIEPEN, A., BRAND, H. K., SAMA, I., LAMBOOY, L. H. J., VAN DEN HEUVEL, L. P., VAN DER WELL, L., HUYNEN, M., OSTERHAUS, A. D. M. E., ANDEWEG, A. C. & HERMANS, P. W. M. (2010). QUANTITATIVE PROTEOME PROFILING OF RESPIRATORY VIRUS-INFECTED LUNG EPITHELIAL CELLS. *J PROTEOMICS* 73, 1680-1693.

**VAN DRUNEN LITTEL-VAN DEN HURK, S. & WATKISS, E. R. (2012). PATHOGENESIS OF RESPIRATORY SYNCYTIAL VIRUS. *CURRENT OPINION IN VIROLOGY* 2, 300-305.**

**VENTRE, K. & RANDOLPH, A. G. (2007). RIBAVIRIN FOR RESPIRATORY SYNCYTIAL VIRUS INFECTION OF THE LOWER RESPIRATORY TRACT IN INFANTS AND YOUNG CHILDREN. *COCHRANE DATABASE OF SYSTEMATIC REVIEWS*.**

**VOLPON, L., OSBORNE, M. J., ZAHREDDINE, H., ROMEO, A. A. & BORDEN, K. L. (2013). CONFORMATIONAL CHANGES INDUCED IN THE EUKARYOTIC TRANSLATION INITIATION FACTOR EIF4E BY A CLINICALLY RELEVANT INHIBITOR, RIBAVIRIN TRIPHOSPHATE. *BIOCHEMICAL AND BIOPHYSICAL RESEARCH COMMUNICATIONS* 434, 614-619.**

**WAGHMARE, A., CAMPBELL, A. P., XIE, H., SEO, S., KUYPERS, J., LEISENRING, W., JEROME, K. R., ENGLUND, J. A. & BOECKH, M. (2013). RESPIRATORY SYNCYTIAL VIRUS LOWER RESPIRATORY DISEASE IN HEMATOPOIETIC CELL TRANSPLANT RECIPIENTS: VIRAL RNA DETECTION IN BLOOD, ANTIVIRAL TREATMENT, AND CLINICAL OUTCOMES. *CLINICAL INFECTIOUS DISEASES : AN OFFICIAL PUBLICATION OF THE INFECTIOUS DISEASES SOCIETY OF AMERICA* 57, 1731-1741.**

**WANG, Z., GERSTEIN, M. & SNYDER, M. (2009). RNA-SEQ: A REVOLUTIONARY TOOL FOR TRANSCRIPTOMICS. *NAT REV GEN* 10, 57-63.**

**WHITLEY, R. J., HAYDEN, F. G., REISINGER, K. S., YOUNG, N., DUTKOWSKI, R., IPE, D., MILLS, R. G. & WARD, P. (2001). ORAL OSELTAMIVIR TREATMENT OF INFLUENZA IN CHILDREN. *PEDIATRIC INFECTIOUS DISEASE JOURNAL* 20, 127-133.**

**WIESE, S., REIDEGELD, K. A., MEYER, H. E. & WARSCHEID, B. (2007). PROTEIN LABELING BY ITRAQ: A NEW TOOL FOR QUANTITATIVE MASS SPECTROMETRY IN PROTEOME RESEARCH. *PROTEOMICS* 7, 340-350.**

**WRAY, S. K., GILBERT, B. E., NOALL, M. W. & KNIGHT, V. (1985). MODE OF ACTION OF RIBAVIRIN: EFFECT OF NUCLEOTIDE POOL ALTERATIONS ON INFLUENZA VIRUS RIBONUCLEOPROTEIN SYNTHESIS. *ANTIVIRAL RESEARCH* 5, 29-37.**

**WRIGHT, M. & PIEDIMONTE, G. (2011). RESPIRATORY SYNCYTIAL VIRUS PREVENTION AND THERAPY: PAST, PRESENT, AND FUTURE. *PEDIATRIC PULMONOLOGY* 46, 324-347.**

**WRIGHT, P. F., IKIZLER, M. R., GONZALES, R. A., CARROLL, K. N., JOHNSON, J. E. & WERKHAVEN, J. A. (2005). GROWTH OF RESPIRATORY SYNCYTIAL VIRUS IN PRIMARY EPITHELIAL CELLS FROM THE HUMAN RESPIRATORY TRACT. *JOURNAL OF VIROLOGY* 79, 8651-8654.**

**WU, W., MUNDAY, D. C., HOWELL, G., PLATT, G., BARR, J. N. & HISCOX, J. A. (2011). CHARACTERIZATION OF THE INTERACTION BETWEEN HUMAN RESPIRATORY SYNCYTIAL VIRUS AND THE CELL CYCLE IN CONTINUOUS CELL**

CULTURE AND PRIMARY HUMAN AIRWAY EPITHELIAL CELLS. *JOURNAL OF VIROLOGY* 85, 10300-10309.

WU, W., TRAN, K. C., TENG, M. N., HEESOM, K. J., MATTHEWS, D. A., BARR, J. N. & HISCOX, J. A. (2012). THE INTERACTOME OF THE HUMAN RESPIRATORY SYNCYTIAL VIRUS NS1 PROTEIN HIGHLIGHTS MULTIPLE EFFECTS ON HOST CELL BIOLOGY. *JOURNAL OF VIROLOGY* 86, 7777-7789.

WYDE, P. R., CHETTY, S. N., JEWELL, A. M., BOIVIN, G. & PIEDRA, P. A. (2003). COMPARISON OF THE INHIBITION OF HUMAN METAPNEUMOVIRUS AND RESPIRATORY SYNCYTIAL VIRUS BY RIBAVIRIN AND IMMUNE SERUM GLOBULIN IN VITRO. *ANTIVIRAL RESEARCH* 60, 51-59.

WYNNE, J. W., SHIELL, B. J., MARSH, G. A., BOYD, V., HARPER, J. A., HEESOM, K., MONAGHAN, P., ZHOU, P., PAYNE, J., KLEIN, R., TODD, S., MOK, L., GREEN, D., BINGHAM, J., TACHEDJIAN, M., BAKER, M. L., MATTHEWS, D. & WANG, L. F. (2014). PROTEOMICS INFORMED BY TRANSCRIPTOMICS REVEALS HENDRA VIRUS SENSITIZES BAT CELLS TO TRAIL MEDIATED APOPTOSIS. *GENOME BIOLOGY* 15, 532.

XATZIPSALTI, M. & PAPADOPOULOS, N. (2007). CELLULAR AND ANIMALS MODELS FOR RHINOVIRUS INFECTION IN ASTHMA. IN *CONTRIBUTIONS TO MICROBIOLOGY*, PP. 33-41. EDITED BY U. SJOBRING & J. D. TAYLOR.

ZHANG, L., PEEPLES, M. E., BOUCHER, R. C., COLLINS, P. L. & PICKLES, R. J. (2002). RESPIRATORY SYNCYTIAL VIRUS INFECTION OF HUMAN AIRWAY EPITHELIAL CELLS IS POLARIZED, SPECIFIC TO CILIATED CELLS, AND WITHOUT OBVIOUS CYTOPATHOLOGY. *JOURNAL OF VIROLOGY* 76, 5654-5666.

ZHANG, Y., JAMALUDDIN, M., WANG, S., TIAN, B., GAROFALO, R. P., CASOLA, A. & BRASIER, A. R. (2003). RIBAVIRIN TREATMENT UP-REGULATES ANTIVIRAL GENE EXPRESSION VIA THE INTERFERON-STIMULATED RESPONSE ELEMENT IN RESPIRATORY SYNCYTIAL VIRUS-INFECTED EPITHELIAL CELLS. *JOURNAL OF VIROLOGY* 77, 5933-5947.

ZHU, Q., MCAULIFFE, J. M., PATEL, N. K., PALMER-HILL, F. J., YANG, C. F., LIANG, B., SU, L., ZHU, W., WACHTER, L., WILSON, S., MACGILL, R. S., KRISHNAN, S., MCCARTHY, M. P., LOSONSKY, G. A. & SUZICH, J. A. (2011). ANALYSIS OF RESPIRATORY SYNCYTIAL VIRUS PRECLINICAL AND CLINICAL VARIANTS RESISTANT TO NEUTRALIZATION BY MONOCLONAL ANTIBODIES PALIVIZUMAB AND/OR MOTAVIZUMAB. *JOURNAL OF INFECTIOUS DISEASES* 203, 674-682.

# CHAPTER 8: APPENDIX

**Table I** Proteins increased in abundance in untreated verses DMSO (top right of Figure 4.1) identified and quantified by LC MS/MS. Statistical analysis was based on observed fold change 2 or greater, and more than 2 peptides and a *p*-value less than 0.05.

| Gene name | Protein name | Peptide count | Peptides used for quantitation | $Log_2$ FC |
|---|---|---|---|---|
| HIST1H3A-J | Histone H3.1 | 5 | 2 | 2.1 |
| TMEM126A | Transmembrane protein 126A | 2 | 2 | 1.7 |
| CBX1 | Chromobox protein homolog 1 | 4 | 3 | 1.4 |
| TOR1AIP1 | Torsin-1A-interacting protein 1 | 4 | 3 | 1.1 |
| SLC29A1 | Equilibrative nucleoside transporter 1 | 2 | 2 | 1.1 |
| RIF1 | Telomere-associated protein RIF1 | 2 | 2 | 1.0 |

**Table II** Proteins decreased in abundance in untreated verses DMSO (top left of Figure 4.1) identified and quantified by LC MS/MS. Statistical analysis was based on observed fold change 2 or greater, and more than 2 peptides and a *p*-value less than 0.05.

| Gene name | Protein name | Peptide count | Peptides used for quantitation | $Log_2$ FC |
|---|---|---|---|---|
| SNAP29 | Synaptosomal-associated protein 29 | 2 | 2 | -1.1 |
| S100A7 | Protein S100-A7 | 3 | 3 | -1.3 |

**Table III** Genes increased in abundance in untreated vs DMSO (Figure 4.1 C). Statistical analysis was based on observed fold change 2 or greater, and more than 2 peptides and a *p*-value less than 0.05. Genes were identified and quantified by RNA-seq.

| gene_id | Gene | $log_2$ FC | p_value | q_value |
|---|---|---|---|---|
| ENSG00000171858 | RPS21 | 1.0 | 0.0109 | 0.561336 |
| ENSG00000159335 | PTMS | 1.0 | 0.01815 | 0.712119 |
| ENSG00000184831 | APOO | 1.1 | 0.0396 | 0.976553 |
| ENSG00000226958 | RNA28S5 | 1.1 | 0.0222 | 0.784769 |
| ENSG00000228974 | AC006483.5 | 1.2 | 0.0071 | 0.456032 |
| ENSG00000227034 | RP11-234N17.1 | 1.2 | 0.0429 | 0.99965 |
| ENSG00000188243 | COMMD6 | 1.2 | 0.03615 | 0.943075 |
| ENSG00000230679 | ENO1-AS1 | 1.3 | 0.0202 | 0.750345 |

| | | | | |
|---|---|---|---|---|
| ENSG00000149499 | EML3 | 1.3 | 0.0495 | 0.99965 |
| ENSG00000256167 | ATF4P4 | 1.6 | 0.03545 | 0.935561 |
| ENSG00000140931 | CMTM3 | 1.8 | 0.0386 | 0.968004 |
| ENSG00000166922 | SCG5 | 3.9 | 0.03115 | 0.892923 |
| ENSG00000230259 | AC008738.1 | 10.5 | 0.0465 | 0.99965 |

**Table IV** Genes decreased in abundance in untreated vs DMSO (Figure 4.1 C) identified and quantified by RNA-seq. Statistical analysis was based on observed fold change 2 or greater, and more than 2 peptides and a *p*-value less than 0.05.

| Gene_id | Gene | $log_2$ FC | p_value | q_value |
|---|---|---|---|---|
| ENSG00000269922 | DKFZP547B0914 | -12.3 | 0.009 | 0.511812 |
| ENSG00000189157 | FAM47E | -3.5 | 0.02575 | 0.82978 |
| ENSG00000134121 | CHL1 | -3.4 | 0.0184 | 0.71603 |
| ENSG00000130822 | PNCK | -3.2 | 0.04285 | 0.99965 |
| ENSG00000155465 | SLC7A7 | -2.8 | 0.0061 | 0.42248 |
| ENSG00000196876 | SCN8A | -2.5 | 0.02265 | 0.789101 |
| ENSG00000253686 | CTB-43E15.3 | -2.4 | 0.04305 | 0.99965 |
| ENSG00000136895 | GARNL3 | -2.3 | 0.00915 | 0.516982 |
| ENSG00000233280 | CRYBG3 | -2.1 | 0.00745 | 0.46535 |

| | | | | |
|---|---|---|---|---|
| ENSG00000163596 | ICA1L | -2.1 | 0.0137 | 0.626684 |
| ENSG00000018236 | CNTN1 | -2 | 0.0468 | 0.99965 |
| ENSG00000198265 | HELZ | -1.8 | 0.01785 | 0.708638 |
| ENSG00000118596 | SLC16A7 | -1.7 | 0.0009 | 0.137934 |
| ENSG00000198315 | ZKSCAN8 | -1.7 | 0.00195 | 0.220881 |
| ENSG00000008086 | CDKL5 | -1.6 | 0.0219 | 0.780472 |
| ENSG00000109756 | RAPGEF2 | -1.6 | 0.0262 | 0.836745 |
| ENSG00000226121 | AHCTF1P1 | -1.6 | 0.0039 | 0.330727 |
| ENSG00000176994 | SMCR8 | -1.6 | 0.0059 | 0.414956 |
| ENSG00000248109 | CTC-295J13.3 | -1.5 | 0.0499 | 0.99965 |
| ENSG00000240618 | RP11-206L10.5 | -1.4 | 0.02275 | 0.790719 |
| ENSG00000135913 | USP37 | -1.4 | 0.02815 | 0.861175 |
| ENSG00000105855 | ITGB8 | -1.4 | 0.0229 | 0.791738 |
| ENSG00000177888 | ZBTB41 | -1.4 | 0.02265 | 0.789101 |
| ENSG00000196159 | FAT4 | -1.3 | 0.02965 | 0.875645 |
| ENSG00000157106 | SMG1 | -1.3 | 0.0147 | 0.644706 |
| ENSG00000103222 | ABCC1 | -1.3 | 0.0465 | 0.99965 |
| ENSG00000158987 | RAPGEF6 | -1.3 | 0.03895 | 0.970352 |
| ENSG00000090857 | PDPR | -1.3 | 0.04225 | 0.99965 |
| ENSG00000188211 | NCR3LG1 | -1.2 | 0.041 | 0.989687 |
| ENSG00000106692 | FKTN | -1.2 | 0.04685 | 0.99965 |
| ENSG00000177034 | MTX3 | -1.2 | 0.0478 | 0.99965 |

| | | | | |
|---|---|---|---|---|
| ENSG00000144460 | NYAP2 | -1.1 | 0.04295 | 0.99965 |
| ENSG00000165895 | ARHGAP42 | -1.1 | 0.0477 | 0.99965 |
| ENSG00000170153 | RNF150 | -1.1 | 0.0307 | 0.886371 |
| ENSG00000174197 | MGA | -1.1 | 0.01045 | 0.550158 |
| ENSG00000114127 | XRN1 | -1.1 | 0.03105 | 0.891679 |
| ENSG00000168143 | FAM83B | -1.1 | 0.04625 | 0.99965 |
| ENSG00000103994 | ZNF106 | -1.1 | 0.0321 | 0.902411 |
| ENSG00000100697 | DICER1 | -1.1 | 0.04 | 0.981294 |
| ENSG00000111371 | SLC38A1 | -1.1 | 0.0202 | 0.750345 |
| ENSG00000152104 | PTPN14 | -1.1 | 0.0201 | 0.748632 |
| ENSG00000095564 | BTAF1 | -1.1 | 0.02215 | 0.784528 |
| ENSG00000160551 | TAOK1 | -1 | 0.0107 | 0.556374 |
| ENSG00000166128 | RAB8B | -1 | 0.03325 | 0.914493 |
| ENSG00000116984 | MTR | -1 | 0.03375 | 0.918511 |
| ENSG00000157540 | DYRK1A | -1 | 0.04675 | 0.99965 |
| ENSG00000076770 | MBNL3 | -1 | 0.0334 | 0.915952 |
| ENSG00000138829 | FBN2 | -1 | 0.0119 | 0.586857 |
| ENSG00000139496 | NUPL1 | -1 | 0.0269 | 0.843251 |
| ENSG00000140563 | MCTP2 | -1 | 0.0458 | 0.99965 |
| ENSG00000145495 | Mar-06 | -1 | 0.02345 | 0.801484 |

**Table V** Proteins increased in abundance in DMSO vs HRSV+DMSO (top right of Figure 4.3). Statistical analysis was based on observed fold change 2 or greater, and more than 2 peptides and a *p*-value less than 0.05. Proteins were identified and quantified by LC MS/MS. Those with a red color are viral proteins.

| Gene name | Protein name | Peptide count | Peptides used for quantitation | $Log_2$ FC |
|---|---|---|---|---|
| NS1 | Non-structural protein 1 | 3 | 3 | 4.7 |
| P | Phosphoprotein | 12 | 12 | 4.3 |
| M | Matrix protein | 17 | 16 | 4.3 |
| NS2 | Non-structural protein 2 | 2 | 2 | 3.3 |
| N | Nucleoprotein | 18 | 18 | 3.2 |
| F | Fusion glycoprotein F0 | 11 | 11 | 3.2 |
| M2-1 | Matrix M2-1 | 14 | 14 | 3.1 |
| G | Major surface glycoprotein G | 2 | 2 | 2.9 |
| EPHA2 | Ephrin type-A receptor 2 | 2 | 2 | 2.6 |
| SOD2 | Superoxide dismutase [Mn], mitochondrial | 2 | 2 | 2.2 |

| | | | | |
|---|---|---|---|---|
| IFIT1 | Interferon-induced protein with tetratricopeptide repeats 1 | 9 | 9 | 2.2 |
| ISG15 | Ubiquitin-like protein ISG15 | 9 | 8 | 2.1 |
| OASL | 2'-5'-oligoadenylate synthase-like protein | 6 | 6 | 2.0 |
| SAMD9 | Sterile alpha motif domain-containing protein 9 | 6 | 5 | 1.9 |
| IFIT3 | Interferon-induced protein with tetratricopeptide repeats 3 | 13 | 13 | 1.9 |
| DDX58 | Probable ATP-dependent RNA helicase DDX58 | 4 | 4 | 1.8 |
| S100A7 | Protein S100-A7 | 3 | 3 | 1.6 |
| IFIT2 | Interferon-induced protein with tetratricopeptide repeats 2 | 3 | 3 | 1.4 |
| | Trypsin | 5 | 5 | 1.3 |
| APOL2 | Apolipoprotein L2 | 4 | 3 | 1.3 |

| | | | | |
|---|---|---|---|---|
| OAS3 | 2'-5'-oligoadenylate synthase 3 | 2 | 2 | 1.3 |
| WARS | Tryptophan—tRNA ligase, cytoplasmic | 21 | 21 | 1.2 |
| CYP51A1 | Lanosterol 14-alpha demethylase | 2 | 2 | 1.1 |
| BAZ1B | Tyrosine-protein kinase BAZ1B | 5 | 4 | 1.1 |
| KPNA4 | Importin subunit alpha-3 | 4 | 3 | 1.0 |
| PITRM1 | Preseq uence protease, mitochondria | 2 | 2 | 1.0 |
| NUP62 | Nuclear pore glycoprotein p62 | 2 | 2 | 1.0 |
| GLRX | Glutaredoxin-1 | 3 | 3 | 1.0 |
| RRS1 | Ribosome biogenesis regulatory protein homolog | 2 | 2 | 1.0 |
| NHP2L1 | NHP2-like protein 1 | 2 | 2 | 1.0 |

**Table VI** Proteins decreased in abundance in DMSO vs HRSV DMSO (top left of Figure 4.3) identified and quantified by LC MS/MS. Statistical analysis was based on observed fold change 2 or greater, and more than 2 peptides and a *p*-value less than 0.05.

| Gene name | Protein name | Peptide count | Peptides used for quantitation | $Log_2$ FC |
|---|---|---|---|---|
| BLMH | Bleomycin hydrolase | 4 | 4 | -1.0 |
| GSS | Glutathione synthetase | 2 | 2 | -1.1 |
| TRAFD1 | TRAF-type zinc finger domain-containing protein 1 | 3 | 3 | -1.1 |
| SNCG | Gamma-synuclein | 3 | 3 | -1.1 |
| UAP1 | UDP-N-acetylhexosamine pyrophosphorylase | 7 | 7 | -1.2 |
| YBX3 | Y-box-binding protein 3 | 3 | 2 | -1.3 |
| PFKL | 6-phosphofructokinase, liver type | 4 | 3 | -1.3 |
| HDAC2 | Histone deacetylase 2 | 3 | 2 | -1.3 |
| ACACA | Acetyl-CoA carboxylase 1 | 4 | 3 | -1.6 |

| | | | | |
|---|---|---|---|---|
| DTYMK | Thymidylate kinase | 2 | 2 | -1.6 |
| LEPRE1 | Prolyl 3-hydroxylase 1 | 2 | 2 | -1.7 |
| DFFA | DNA fragmentation factor subunit alpha | 3 | 3 | -1.7 |
| MRPL16 | 39S ribosomal protein L16, mitochondrial | 2 | 2 | -2.4 |

**Table VII** Proteins increased in abundance in DMSO vs HRSV+DMSO (top right of Figure 4.6) identified and quantified by LC MS/MS. Statistical analysis was based on observed fold change 2 or greater, and more than 2 peptides and a *p*-value less than 0.05.

| Gene name | Protein name | Peptide identification | Peptides used for quantitation | $Log_2$ FC |
|---|---|---|---|---|
| P | Phosphoprotein | 12 | 12 | 4.2 |
| M | Matrix protein | 17 | 16 | 4.1 |
| RPL7L1 | 60S ribosomal protein L7-like 1 | 2 | 2 | 3.5 |
| NS1 | Non-structural protein 1 | 3 | 3 | 3.2 |
| HIST1H3A,B,C, | Histone H3.1 | 5 | 2 | 3.1 |

| | | | | |
|---|---|---|---|---|
| D,E,F,G,F,H,I,J | | | | |
| N | Nucleoprotein | 18 | 18 | 3.1 |
| M2-1 | Matrix M2-1 | 14 | 14 | 2.9 |
| F | Fusion glycoprotein F0 | 11 | 11 | 2.6 |
| G | Major surface glycoprotein G | 2 | 2 | 2.6 |
| EPHA2 | Ephrin type-A receptor 2 | 2 | 2 | 2.5 |
| DDX58 | Probable ATP-dependent RNA helicase DDX58 | 4 | 4 | 2.4 |
| TAP1 | Antigen peptide transporter 1 | 2 | 2 | 2.4 |
| SAMD9 | Sterile alpha motif domain-containing protein 9 | 6 | 5 | 2.2 |
| NS2 | Non-structural protein 2 | 2 | 2 | 2.2 |
| SYNE2 | Nesprin-2 | 2 | 2 | 2.1 |
| TOR1AIP1 | Torsin-1A-interacting protein 1 | 4 | 3 | 2 |
| IFIT1 | Interferon-induced protein with tetratricopeptide repeats 1 | 9 | 9 | 2 |
| IFIT2 | Interferon-induced protein with tetratricopeptide repeats 2 | 3 | 3 | 1.9 |
| IFIT3 | Interferon-induced protein with tetratricopeptide repeats 3 | 13 | 13 | 1.9 |

| | | | | |
|---|---|---|---|---|
| APOL2 | Apolipoprotein L2 | 4 | 3 | 1.9 |
| SLC29A1 | Equilibrative nucleoside transporter 1 | 2 | 2 | 1.8 |
| CBX1 | Chromobox protein homolog 1 | 4 | 3 | 1.8 |
| C19orf43 | Uncharacterized protein C19orf43 | 2 | 2 | 1.8 |
| ISG15 | Ubiquitin-like protein ISG15 | 9 | 8 | 1.8 |
| OASL | 2'-5'-oligoadenylate synthase-like protein | 6 | 6 | 1.8 |
| TMEM126A | Transmembrane protein 126A | 2 | 2 | 1.8 |
| HIST1H4A-L, HIST2H4A,B, HIST4H4 | Histone H4 | 13 | 13 | 1.7 |
| HEATR1 | HEAT repeat-containing protein 1 | 8 | 8 | 1.6 |
| GTPBP4 | Nucleolar GTP-binding protein 1 | 3 | 3 | 1.6 |
| HIST2H | Histone H3.2 | 5 | 2 | 1.6 |

| | | | | |
|---|---|---|---|---|
| 3A,C,D | | | | |
| H2AFX | Histone H2AX | 5 | 2 | 1.6 |
| WDR36 | WD repeat-containing protein 36 | 2 | 2 | 1.6 |
| OAS3 | 2'-5'-oligoadenylate synthase 3 | 2 | 2 | 1.5 |
| ANXA11 | Annexin A11 | 2 | 2 | 1.5 |
| FHL2 | Four and a half LIM domains protein 2 | 3 | 3 | 1.5 |
| HIST1H2BM | Histone H2B type 1-M | 10 | 2 | 1.4 |
| CYP51A1 | Lanosterol 14-alpha demethylase | 2 | 2 | 1.4 |
| TCERG1 | Transcription elongation regulator 1 | 3 | 3 | 1.4 |
| TMPO | Lamina-associated polypeptide 2, isoforms beta/gamma | 9 | 3 | 1.3 |
| EIF2AK2 | Interferon-induced, double-stranded RNA-activated protein kinase | 6 | 6 | 1.3 |
| RIF1 | Telomere-associated protein RIF1 | 2 | 2 | 1.3 |
| PELP1 | Proline-, glutamic acid- and leucine-rich protein 1 | 2 | 2 | 1.3 |
| SMCHD | Structural maintenance of chromosomes flexible hinge | 2 | 2 | 1.3 |

| | | | | |
|---|---|---|---|---|
| 1 | domain-containing protein 1 | | | |
| AHCTF1 | Protein ELYS | 2 | 2 | 1.3 |
| COMTD1 | Catechol O-methyltransferase domain-containing protein 1 | 2 | 2 | 1.2 |
| NOLC1 | Nucleolar and coiled-body phosphoprotein 1 | 8 | 8 | 1.2 |
| ATAD1 | ATPase family AAA domain-containing protein 1 | 3 | 3 | 1.2 |
| H2AFY | Core histone macro-H2A.1 | 7 | 7 | 1.2 |
| ANXA2 | Annexin A2 | 26 | 26 | 1.2 |
| FBL | rRNA 2'-O-methyltransferase fibrillarin | 5 | 5 | 1.2 |
| PML | Protein PML | 2 | 2 | 1.2 |
| EXOSC10 | Exosome component 1 | 2 | 2 | 1.2 |
| BST2 | Bone marrow stromal antigen 2 | 3 | 3 | 1.2 |
| DR1 | Protein Dr1 | 2 | 2 | 1.2 |
| MDC1 | Mediator of DNA damage checkpoint protein 1 | 4 | 4 | 1.2 |
| CISD1 | CDGSH iron-sulfur domain-containing protein 1 | 3 | 3 | 1.2 |
| SLC25A | Mitochondrial 2-oxoglutarate/malate carrier protein | 3 | 3 | 1.2 |

| | | | | |
|---|---|---|---|---|
| 11 | | | | |
| MYO1B | Unconventional myosin-Ib | 5 | 5 | 1.1 |
| HIST1H2BO | Histone H2B type 1-O | 10 | 2 | 1.1 |
| NOL6 | Nucleolar protein 6 | 3 | 3 | 1.1 |
| BMS1 | Ribosome biogenesis protein BMS1 homolog | 2 | 2 | 1.1 |
| CELF1 | CUGBP Elav-like family member 1 | 2 | 2 | 1.1 |
| NKRF | NF-kappa-B-repressing factor | 2 | 2 | 1.1 |
| TSPO | Translocator protein | 2 | 2 | 1.1 |
| FTSJ3 | pre-rRNA processing protein FTSJ3 | 5 | 5 | 1.1 |
| PHF5A | PHD finger-like domain-containing protein 5A | 4 | 4 | 1.1 |
| WDR12 | Ribosome biogenesis protein WDR12 | 4 | 4 | 1.1 |
| NHP2 | H/ACA ribonucleoprotein complex subunit 2 | 2 | 2 | 1.1 |
| GPRC5A | Retinoic acid-induced protein 3 | 2 | 2 | 1.1 |
| HIST2H2AA3 | Histone H2A type 2-A | 7 | 2 | 1.1 |

| | | | | |
|---|---|---|---|---|
| GNAI3 | Guanine nucleotide-binding protein G(k) subunit alpha | 4 | 2 | 1.1 |
| ANXA4 | Annexin A4 | 5 | 4 | 1.1 |
| MLEC | Malectin | 2 | 2 | 1.1 |
| ANXA1 | Annexin A1 | 21 | 21 | 1.1 |
| RRP9 | U3 small nucleolar RNA-interacting protein 2 | 4 | 4 | 1.1 |
| BOP1 | Ribosome biogenesis protein BOP1 | 3 | 3 | 1 |
| NOP58 | Nucleolar protein 58 | 7 | 7 | 1 |

**Table VIII** Proteins decreased in abundance in Mock vs HRSV (top left of Figure 4.6) identified and quantified by LC MS/MS. Statistical analysis was based on observed fold change 2 or greater, and more than 2 peptides and a *p*-value less than 0.05.

| Gene name | Protein name | Peptide identification | Peptides used for quantitation | $Log_2$ FC |
|---|---|---|---|---|
| HSBP1 | Heat shock factor-binding protein 1 | 3 | 3 | -1.0 |
| PTPN11 | Tyrosine-protein phosphatase non-receptor | 2 | 2 | -1.1 |

| | | | | |
|---|---|---|---|---|
| | type 11 | | | |
| SKP1 | S-phase kinase-associated protein 1 | 8 | 7 | -1.1 |
| CAP2 | Adenylyl cyclase-associated protein 2 | 3 | 3 | -1.1 |
| ADI1 | 1,2-dihydroxy-3-keto-5-methylthiopentene dioxygenase | 3 | 3 | -1.1 |
| TRAFD1 | TRAF-type zinc finger domain-containing protein 1 | 3 | 3 | -1.2 |
| CKB | Creatine kinase B-type | 9 | 8 | -1.2 |
| YBX3 | Y-box-binding protein 3 | 3 | 2 | -1.4 |
| CLPP | Putative ATP-dependent Clp protease proteolytic subunit, mitochondrial | 2 | 2 | -1.4 |
| MRFAP1 | MORF4 family-associated protein 1 | 2 | 2 | -1.5 |
| PPP1R2 | Protein phosphatase inhibitor 2 | 3 | 3 | -1.5 |

| | | | | |
|---|---|---|---|---|
| PEX19 | Peroxisomal biogenesis factor 19 | 2 | 2 | -1.6 |
| PREP | Prolyl endopeptidase | 2 | 2 | -1.7 |
| SNAP29 | Synaptosomal-associated protein 29 | 2 | 2 | -1.8 |
| NT5C2 | Cytosolic purine 5'-nucleotidase | 5 | 5 | -2.3 |

## List of publications